

5th European IRPA Congress
4 - 8 June 2018
The Hague, The Netherlands

Encouraging Sustainability
in Radiation Protection

POSTERS

Volume 3

- Medical
- Occupational



IRPA 2018 Posters
Volume 3:
Medical and Occupational

7 January 2019 - Version 1
Editor: Ronald Smetsers

IRPA 2018 Posters - Volume 3

Table of Contents

Medical	1
Occupational	27

Medical

5th European IRPA Congress
4 - 8 June 2018
The Hague, The Netherlands

Encouraging Sustainability
in Radiation Protection



A study of scatter radiation in diagnostic X-ray rooms and radiation protection

Nataša Todorović, Jovana Nikolov, Nemanja Golubovac, Miodrag Krmar

University of Novi Sad, Faculty of Sciences, Department of Physics, Novi Sad, Serbia

INTRODUCTION

The purpose of radiation shielding is to limit radiation exposures to employees and members of the public to an acceptable level. The objective of a shielding calculation is to determine the thickness of the barrier that is sufficient to reduce the air KERMA in an occupied area to a value $\leq P/T$, the weekly shielding design goal modified by the occupancy factor for the area to be shielded. A method for determining the thickness requirements for barriers against scatter and leaking radiation in a radiographic room is presented. The measurements were performed by RTI Barracuda equipment and R100B detector (Fig 1.) which are very suitable for scattered radiation measurements because of the high sensitivity and the minimal energy dependence. Obtained thickness of the barriers were compared with calculated values according to NCRP report No. 147 which contains recommendation and technical information related to the design and installation of structural shielding for facilities that use X-rays for diagnostic imaging.



(Fig 1.) RTI Barracuda and R100B detector

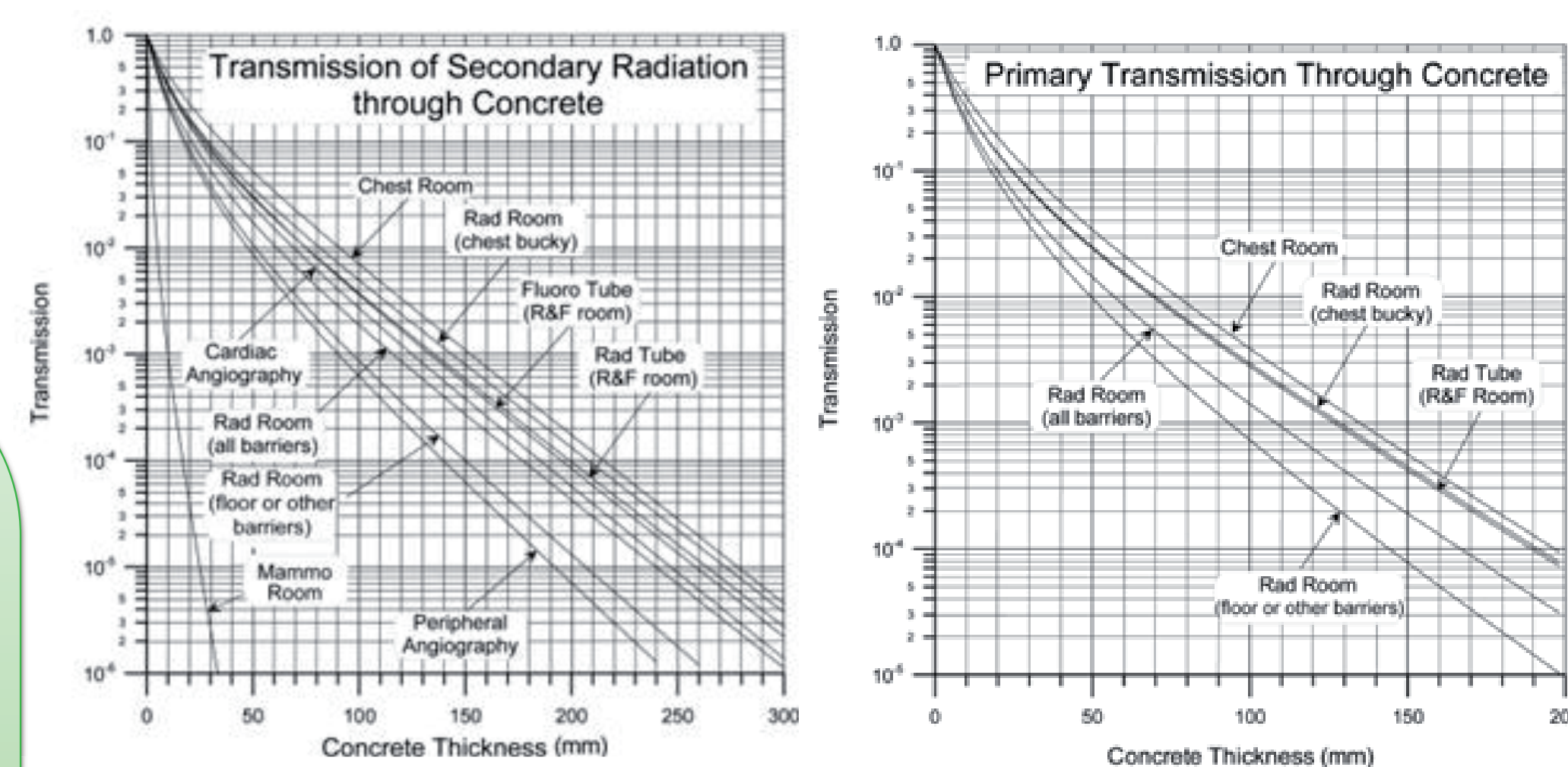


(Fig 2.) Transmission of Primary and Secondary Radiation through Concrete (NCRP 147)

Measurements and methods

The most common NCRP protocol calculation were performed to obtain transmission coefficient. Transmission coefficient is defined as ratio of background KERMA and calculated KERMA for given RTG tube type multiplied with occupancy factor for shielded area. From transmission coefficient, barrier thickness of the basic radiographic room can easily be calculated or read manually from the graphics (Fig.2).

To measure transmission coefficient R100B detector must be attached to the wall and measure air KERMA. From air KERMA, transmission coefficient is calculated as the ratio of background KERMA and measured air KERMA multiplied with occupancy factor for shielded area. Barracuda detector system used for the measurements is connected to the Ocean software from where, using correct template, air KERMA can be obtained, and used in further calculations. To measure difference between leakage and scattered radiation detector is attached at the height of 79 cm, and 163 cm from the floor level. Blueprints of the radiographic room and wall distances from the RTG tube, which were used in calculations and measurements are shown in Fig.3. Protection goal is to reduce the KERMA to the background KERMA level, in all shielded areas, even for the controlled areas. Mean working time of the tube is 50 ms for one exposition. The weekly number of patients is 120, and the weekly number of patients taken for calculations of primary barrier for chest bucky is 60.



(Fig 3.) Blueprints of the Radiographic room

Results

Shielded area	Occupancy factor	Measured air KERMA rate at 79 cm ($\mu\text{Gy/s}$)	Measured weekly air KERMA At 79 cm ($\mu\text{Gy/week}$)	Transmission coefficient (measured at 79 cm)	Measured air KERMA rate at 163 cm ($\mu\text{Gy/s}$)	Measured weekly air KERMA At 163 cm ($\mu\text{Gy/week}$)	Transmission coefficient (measured at 163 cm)	Calculated weekly air KERMA (NCRP) (mGy/week)	Transmission coefficient (calculated)	Proposition of shield thickness (primary barrier) (mm)	Proposition of shield thickness (secondary barrier) (mm)
Control room	1	13.65	81.90	0,24	16.82	100.92	0.20	0.90	0.02	No primary barriers	Plate Glass (calc.)= 60 Plate Glass (meas.) = 15 Concrete (calc.)= 60 Concrete (meas.)= 10
Waiting room	1/5	13.65	81.90	0.24	16.82	100.92	0.20	0.90	0.02	No primary barriers	Lead (calc.)= 0.5 Lead (meas.)=0.1 Concrete (calc.)= 60 Concrete (meas.)=10
Hall	1/5	3.67	22.02	0.91	13.80	82.80	0.24	0.81	0.02	No primary barriers	Lead (calc.)= 0.5 Lead (meas.)=0.1 Concrete (calc.)= 60 Concrete (meas.)=10
Staircases	1/40	23.88	143.28	0,14	25.77	154.62	0.13	1.40	0.01	No primary barriers	Concrete (calc.)= 100 Concrete (meas.)= 25
Parking lot (primary barrier for chest bucky)	1/40	5.39	32.34	0,62	8.35	50.10	0.40	Primary: 11.94 Secondary: 0.51	Prim: 0.002 Sec: 0.04	Concrete (calc.) = 80	Concrete (calc.)= 30 Concrete (meas.)= 5

Conclusion

- ✓ Comparing transmission coefficient results obtained from calculating NCRP method and results obtained from measuring with R100B detector, measured values are for one magnitude higher than the calculated values. Barrier thickness is growing exponentially with the reduce of the transmission coefficient. Barrier thickness obtained in calculated method is four to six times greater than barrier thickness obtained from measured method. Knowing this, one can say that NCRP protocol is conservative method and fully according to ALARA principle. Note that occupancy factors aren't included in the calculations, which would only increase transmission coefficient results obtained from both methods, and reduce barrier thickness.
- ✓ Measurements of scattered and leakage radiation is easy and quick on site quality assurance method that barriers are designed properly, following NCRP recommendations.
- ✓ With air KERMA measured at two heights from the floor level, one can compare air KERMA rate of leakage and scatter radiation. In NCRP protocol leakage radiation is greater than scatter which can be confirmed from these results. At 163 cm from the floor level, detector is at the shorter distance from the RTG tube, and thus leakage radiation have greater influence on the outcome of the air KERMA rate. At 79 cm from the floor level, which is the level of the phantom, scatter radiation have the main influence at the outcome of the air KERMA rate.

An Assessment of Radiation Doses for Breast, Ovaries and Uterus while Investigating the Head, Chest, and Abdomen- Pelvis Using CT.

Corina Mariana Pera^{1,2}, Elena Dădulescu³, Florentin Mihail Niculescu³, Daniela Mossang³, Malaescu Iosif¹, Elisabeta Antonescu⁴

¹West University of Timisoara, Romania

²County Emergency Hospital Resita, Romania

³Laboratory for the Hygiene of Radiations, Public Health Authority of Dolj County, Romania

⁴Lucian Blaga University of Sibiu, Romania

INTRODUCTION

The Computerised Tomography (CT) has changed the medical imagery by providing a tridimensional image of the organs or places of interest. An increase in the frequency of applying this diagnosis means has a great impact on the patients and the population in general. Medical exposures through CT represent about 14% of the total radiological investigations used for diagnosis. The distribution of CT examinations in Romania is balanced as regards the gender of patients (50.1 for men and 49.9 for women). In women's case, the most frequent examinations were for pelvis (56.1%), abdomen and chest (51.8%).



OBJECTIVES AND METHODOLOGY

The aim of the study is to assess the organ dose in women for the radio-sensitive organs (breast, ovaries, and uterus) through three CT procedures (head, chest, and abdomen-pelvis). The study was carried out on two types of CT, both with 64 rows on a number of 60 patients for each CT (20 patients for each procedure). Following the data about the patient's identity, the exposure parameters, the CTDI and DLP values for each patient, the organ doses were estimated both by using the calculation model published in RP 154 and the Impact Dose software.

THE RESULTS

In the medical exposure for the head, the value of the average dose on breast was of about 0.036 ± 0.012 mSv, 0.001 mSv for ovaries, and 0.000 mSv for the uterus. In the medical exposure for the chest, the value of the average dose was of about 28.86 ± 11.79 mSv for breasts, 0.365 ± 0.27 mSv for ovaries, and 0.310 ± 0.28 for the uterus. In the abdomen-pelvis investigation, the average values of the doses varied like this: 12.74 ± 6.98 for breasts, 59.94 ± 7.72 mSv for ovaries, and 60.38 ± 7.43 for the uterus. The estimated values for the two CTs were comparable.

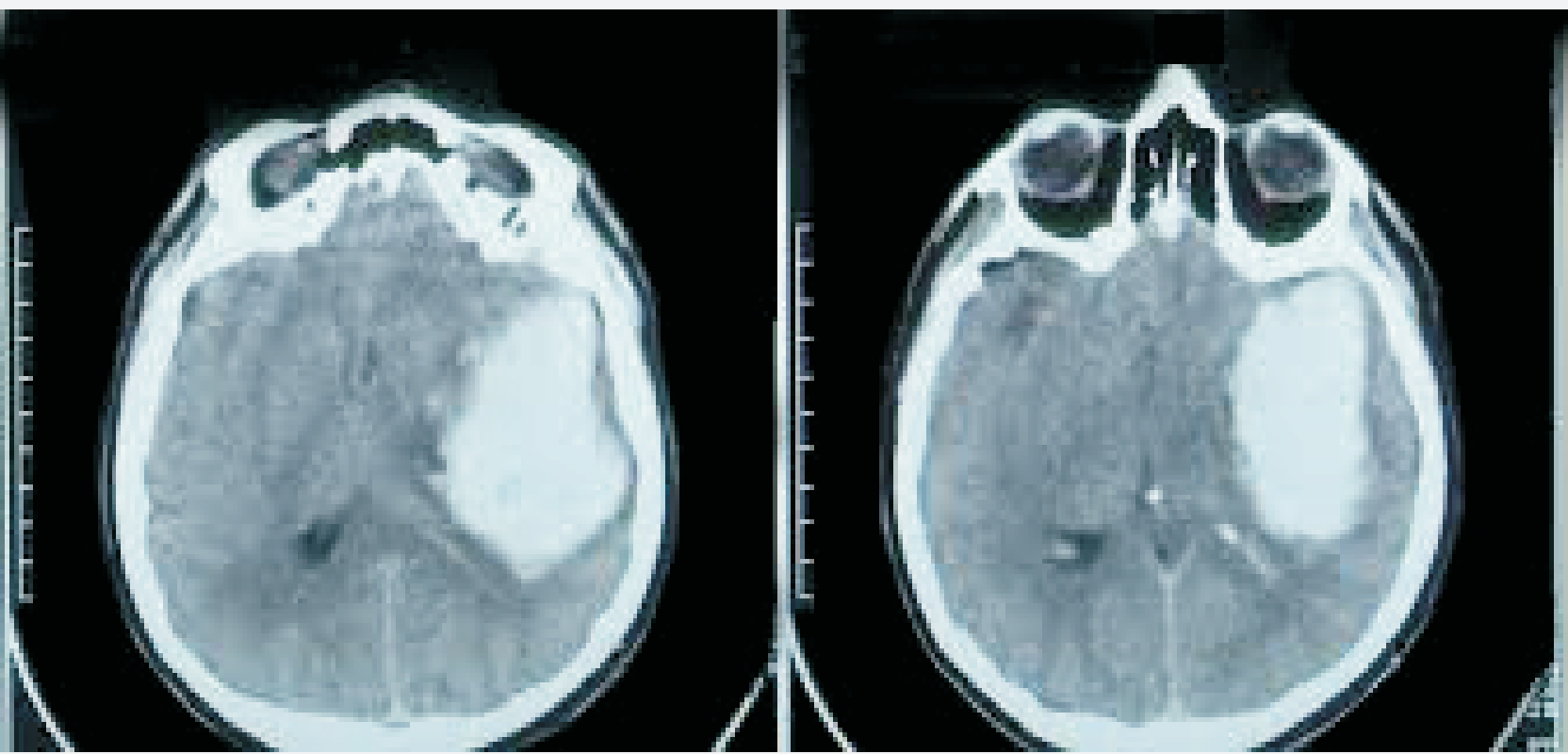
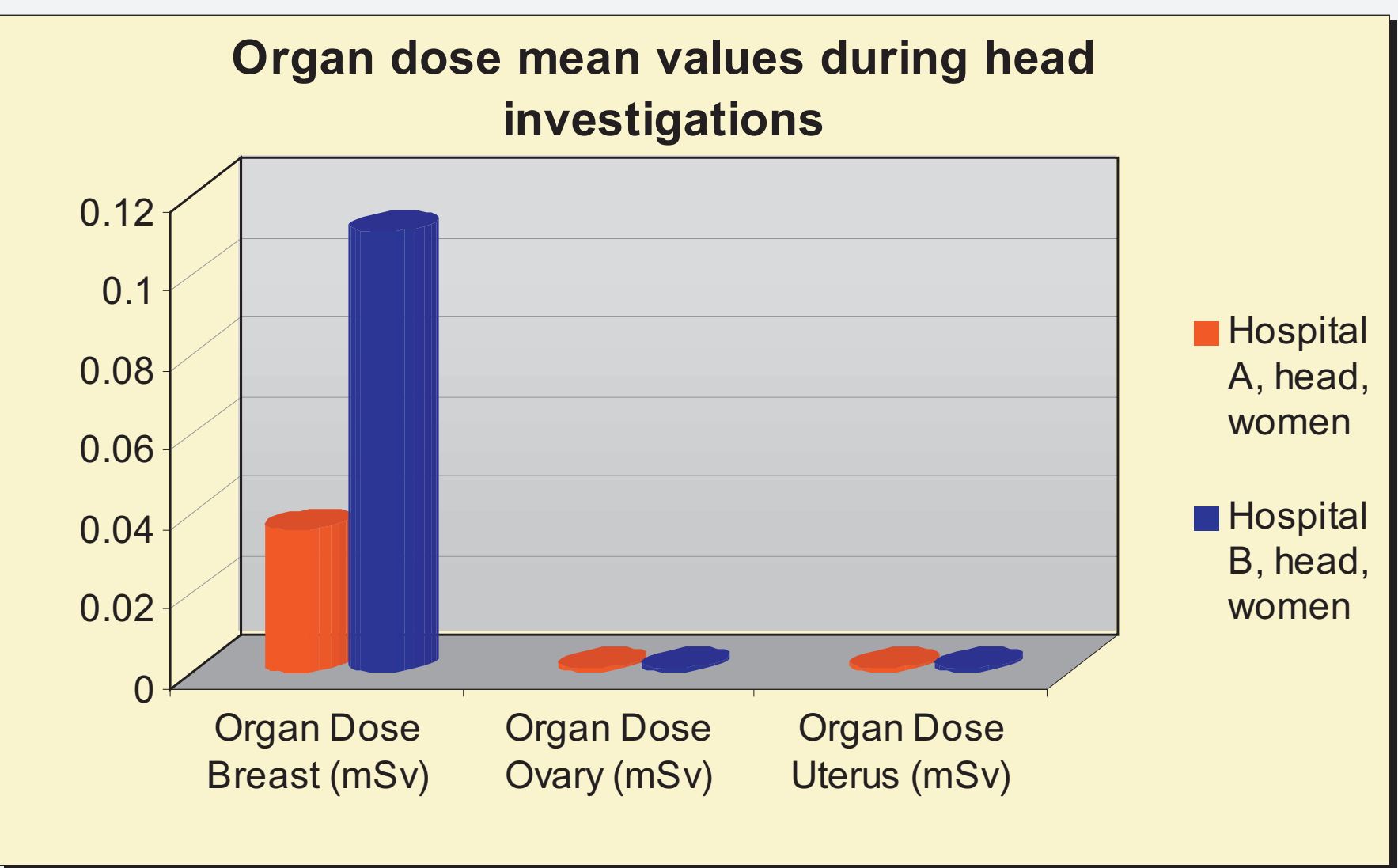
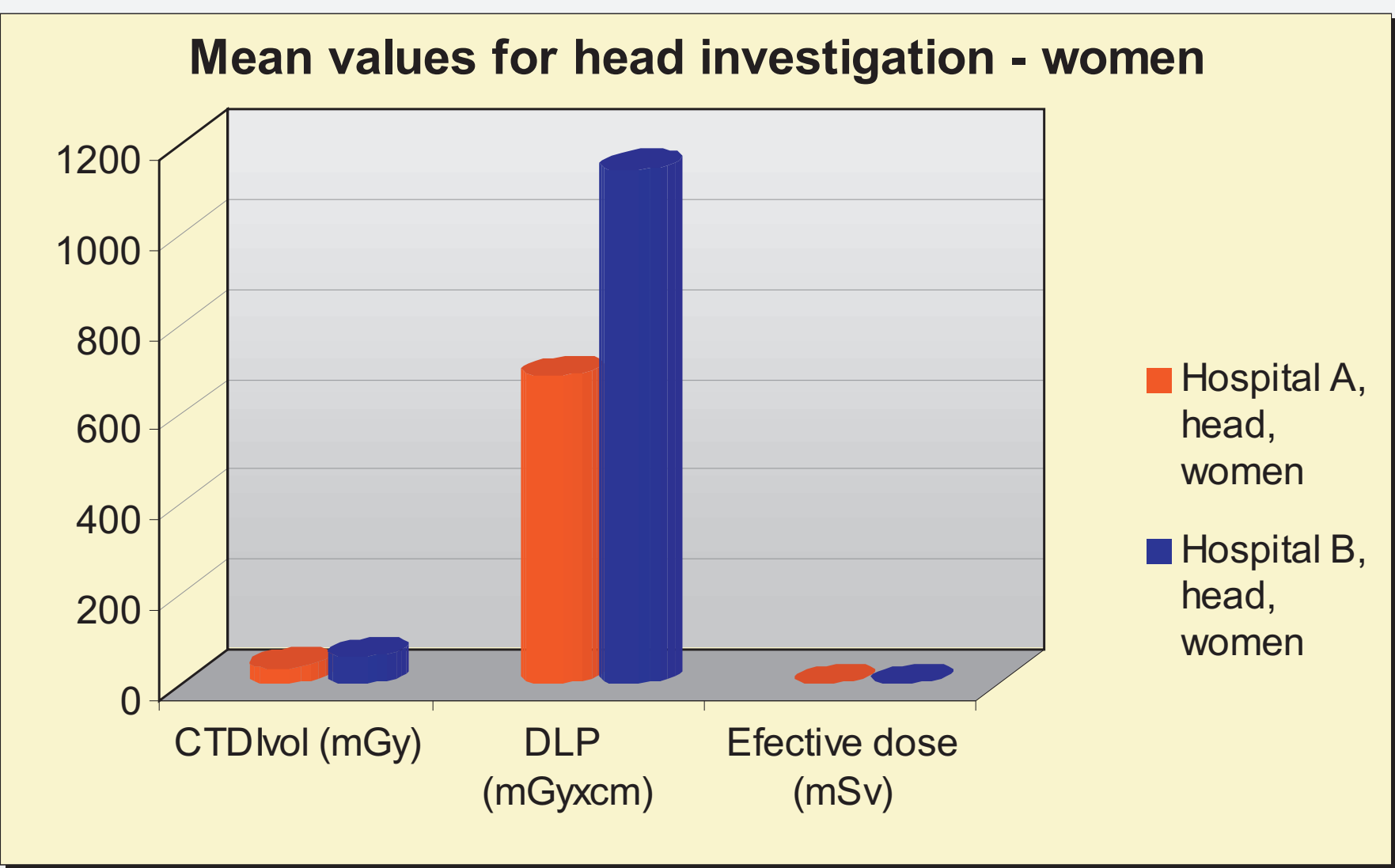


Fig. 1, 2 Mean values during head investigation - women

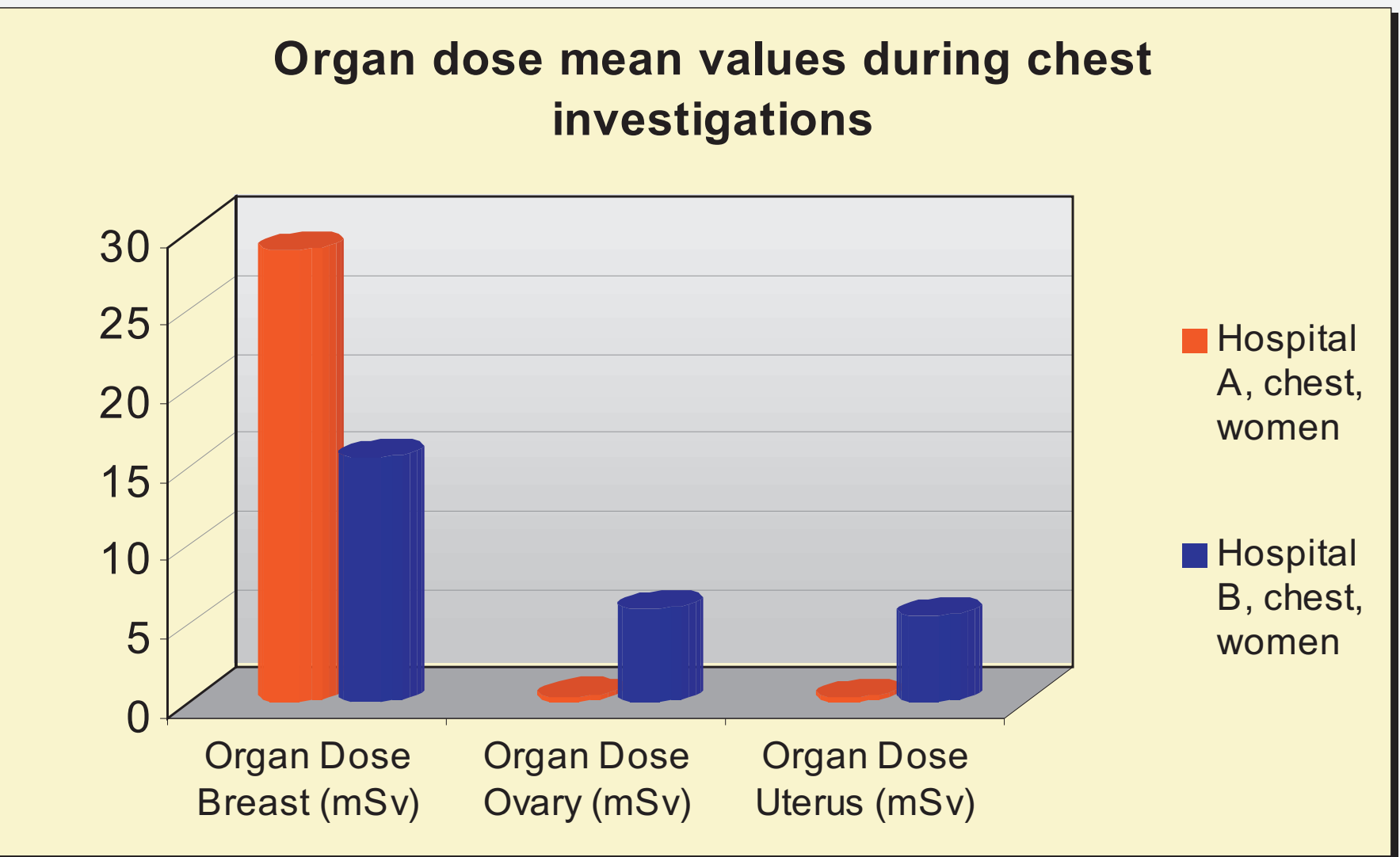
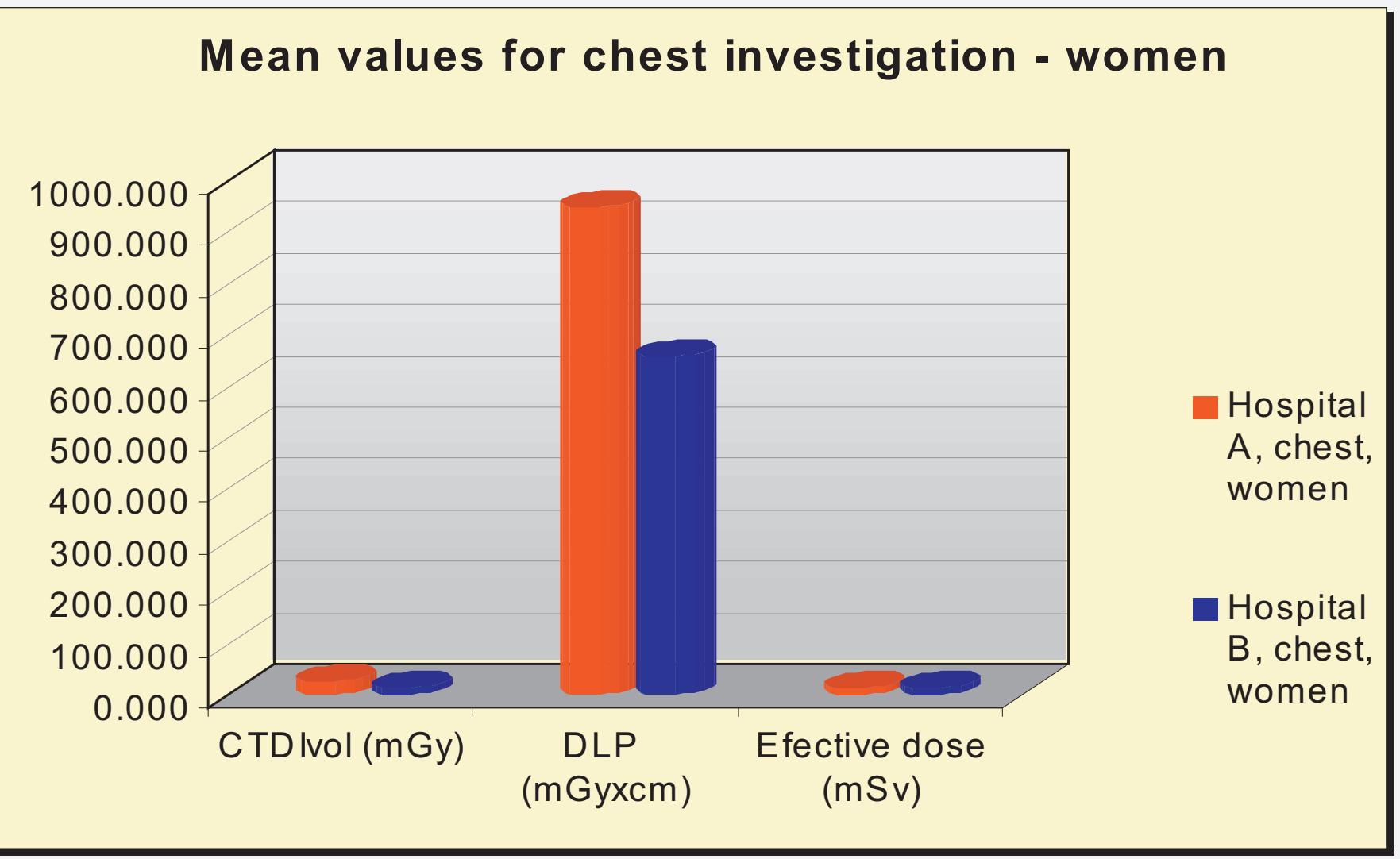


Fig. 3, 4 Mean values during chest investigation – women

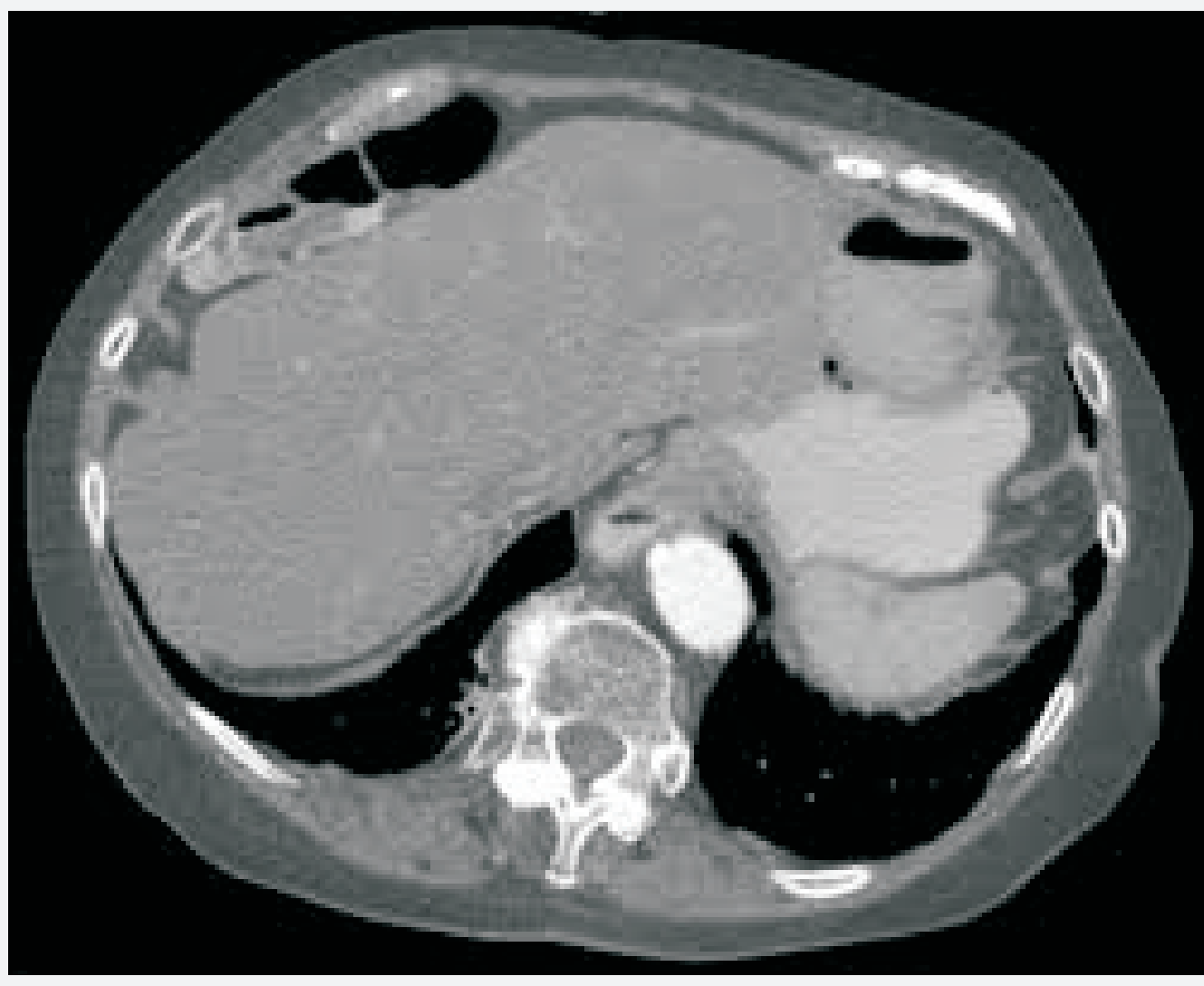
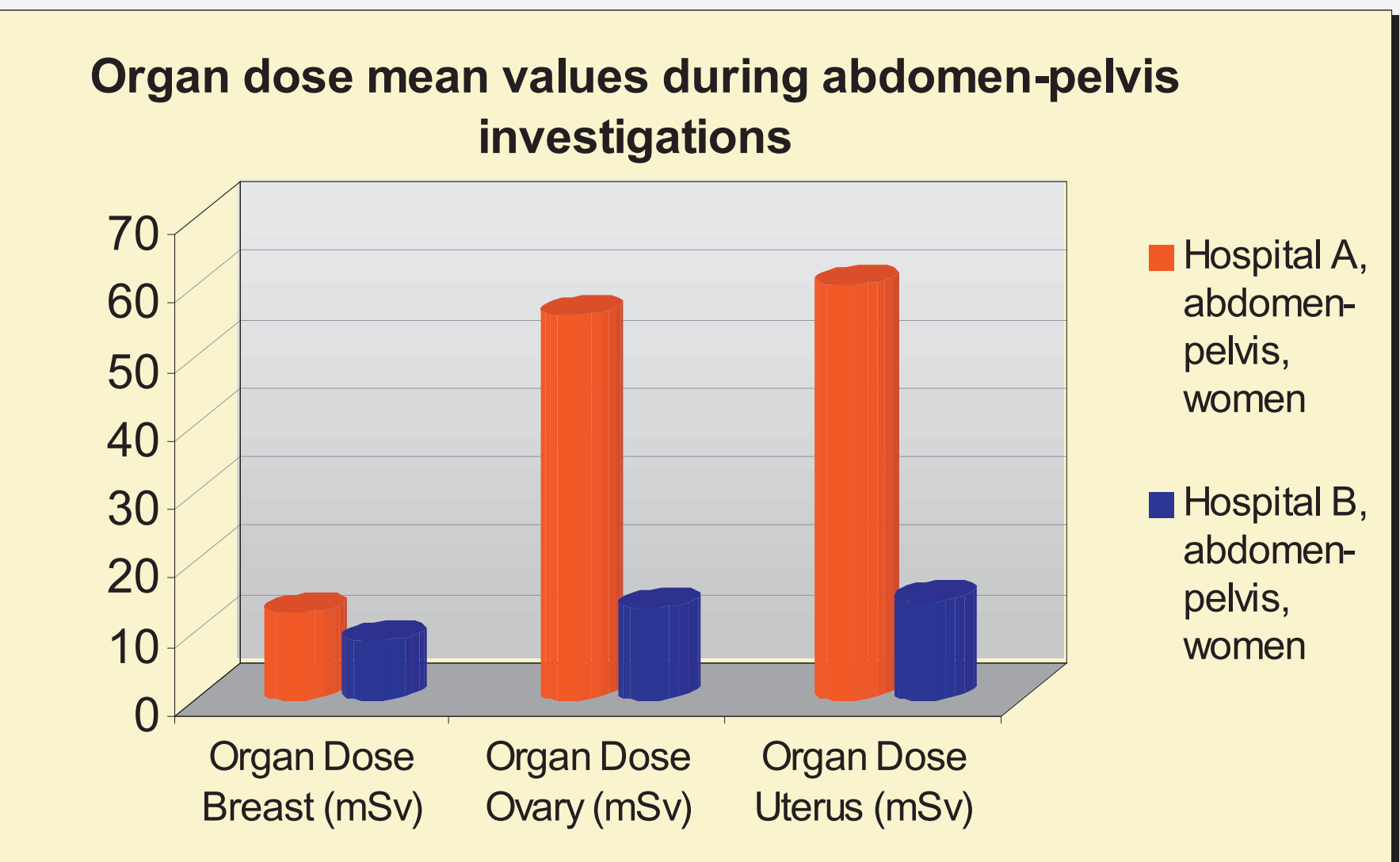
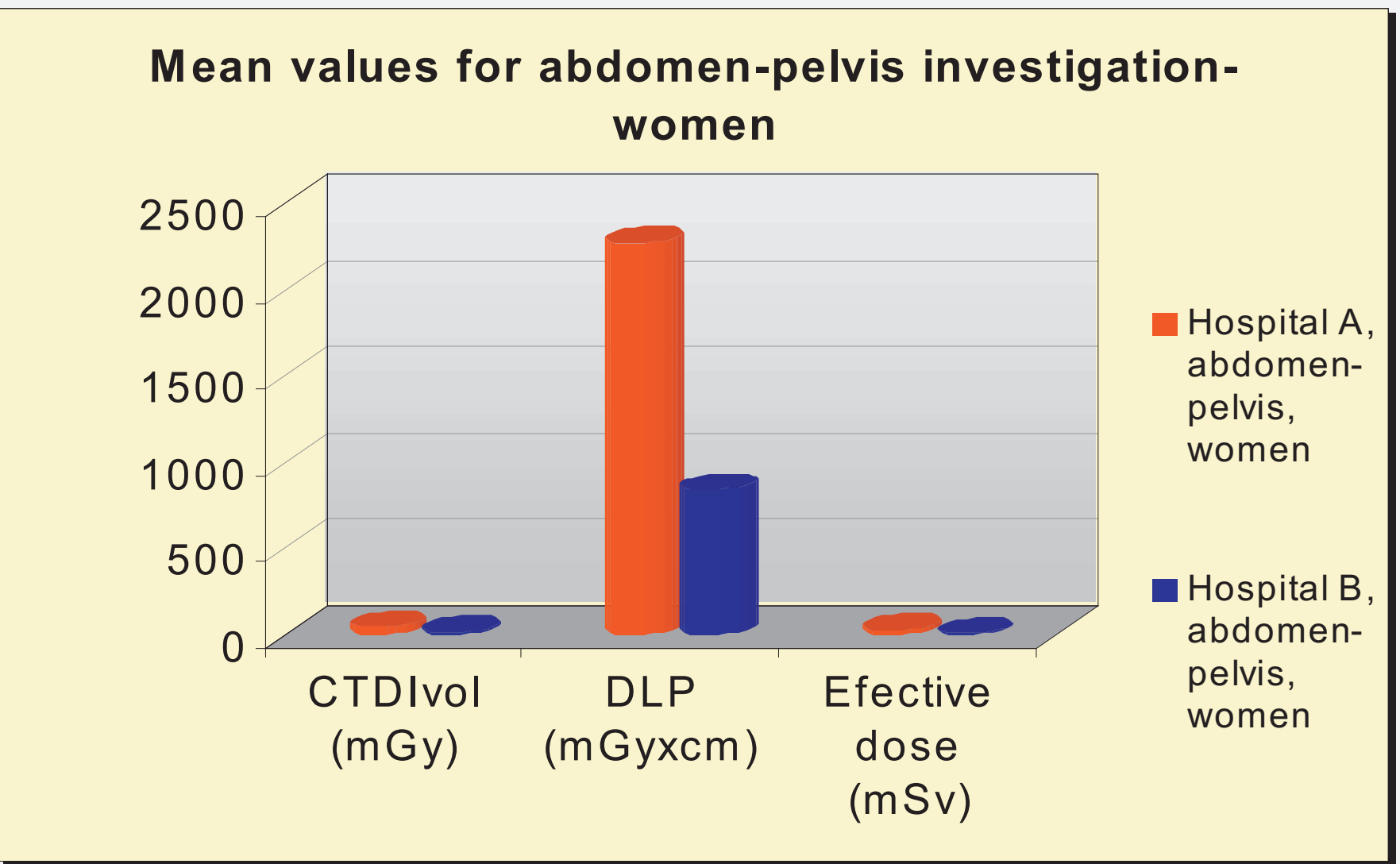


Fig. 5, 6 Mean values during chest investigation – women

CONCLUSIONS

The organ doses were higher in all the investigation procedures compared to other studies carried out in countries such as Germany and England. We found a variation of the organ dose depending on more factors, such as the investigation parameters, the radioprotection measures for patients, and the radioprotection training of the technologist. It is necessary an increased attention in optimising protocols leading to a decrease of doses especially in the organs with a high radio-sensitivity. We must also pay special attention to the team-work of all the specialists implied in these procedures.

Key words: computer tomography, organ dose, breasts, ovaries, and uterus.

The culture of radiological safety must be improved for all the members of the staff, including those who order radiological procedures. There are also necessary measures of a better sanitary education of the population regarding the risk of medical exposures in excess.

Applications of a solid state dose profile meter in a fluoroscopic system

María E. Pérez Álvarez, Desiderio González Moreno, Joaquín Tomás García
Servicio de Radiofísica y Protección Radiológica. Hospital General Universitario de Ciudad Real

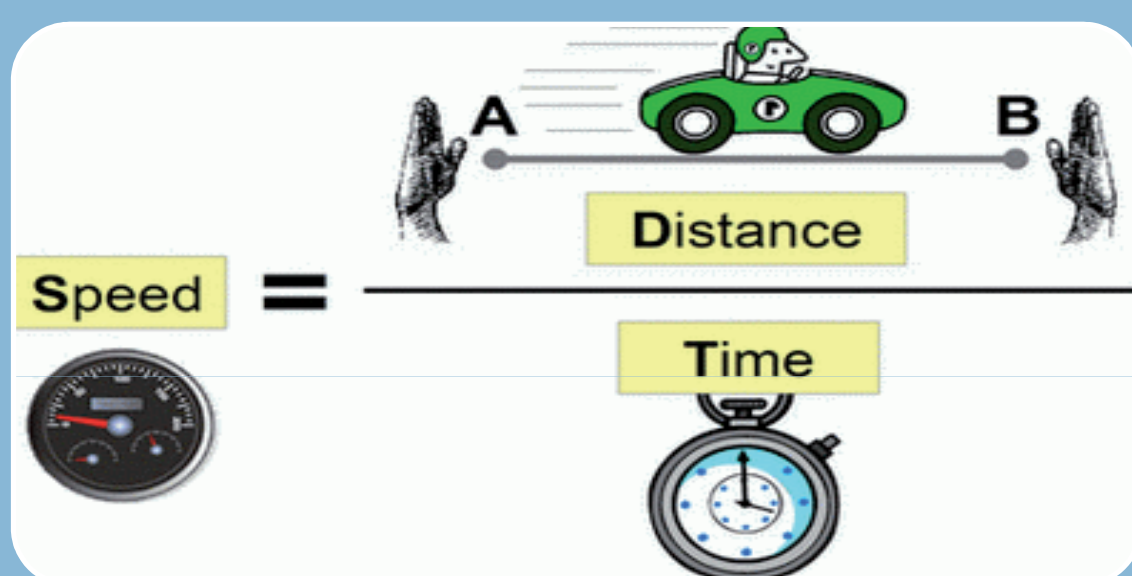
INTRODUCTION

Until now, computed radiography system and radiographic films are commonly accepted for field size determination. But as digital systems are here to stay, in time CR will become obsolete and radiographic film is very costly in a long term. A new methodology for measuring field size of a X-ray machine is described using as a dose profiler the CT Dose Profiler of RTI based on solid-state technology. With Black Piranha it can be achieved sensitivity for dose rate of 40nGy/s-760mGy/s and a spatial resolution of 0,25mm. We compare our method against CR method.

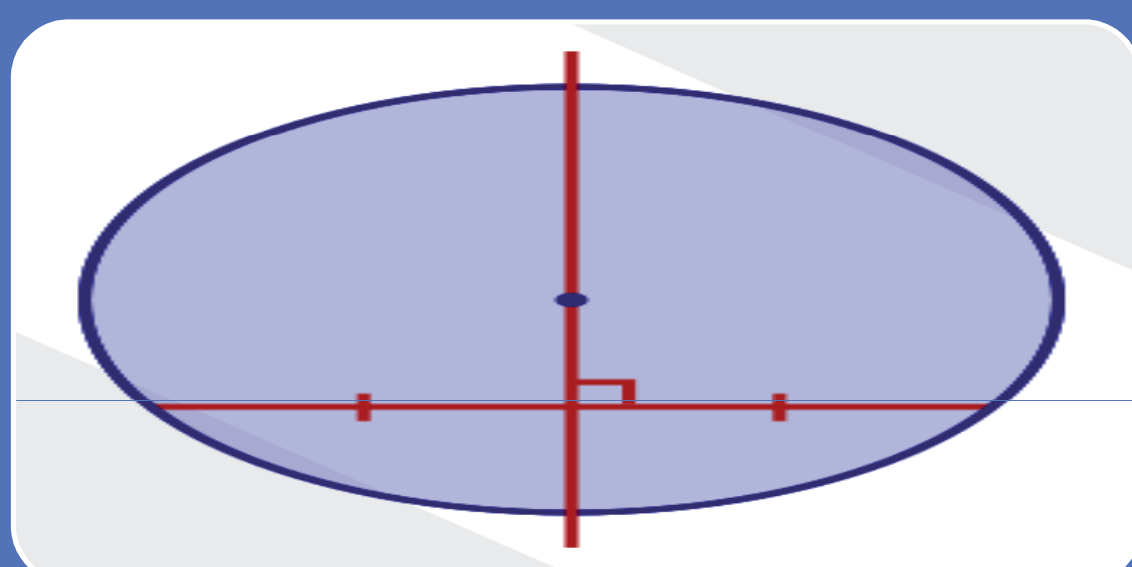
Method



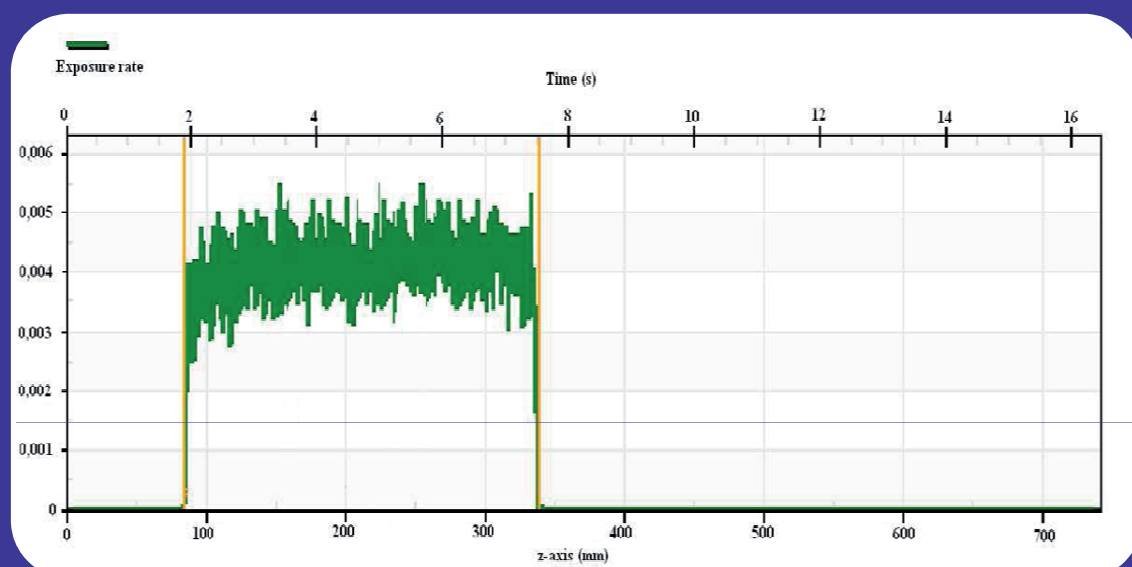
Multifunction X-ray machine was chosen, allowing us to control the dose profiler moving the table remotely for scanning the x-ray field size.



With the speed of the table and the time of measurement, we are capable to obtain the dimensions of the radiation field. In the following measurements we could use this characterization of the speed table for our measurements.



It requires perform one measurement where we obtain a chord of the circumference. The following measurements will be made on the bisector of this chord. Therefore we assure the dose profile is passing through the center of the radiation field.



Finally, we can measure all the field sizes of our multifunction X-ray machine.

Results

The differences between diameter field measured with CR and measurements with dose profiler are not higher to 4mm.

Speed of table (mm/s)	Field size (mm)	Light field size (mm)	CR field size (mm)	Measured field size (mm)	Diference CR-measured size (mm)
45.08	N	320	321	317	-4
45.08	1	260	257	257	0
45.08	1	260	257	257	0
45.08	1	260	257	255	-2
45.08	2	195	196	196	0
45.08	3	150	145	148	3

Conclusions

The results of this study demonstrate our method is comparable to the CR method.

The main advantages are that outdated and more expensive methods requiring read-out after each scan can be avoided.

In addition, measurements are stored with the other control data.

The main disadvantage is careful placement of the dose profiler is required and it only gives diameter information instead of the whole field.

ASSESSMENT OF PATIENT DOSES FROM PET/CT EXAMINATIONS IN THE RUSSIAN FEDERATION

L.A. CHIPIGA*
St-Petersburg Research Institute of Radiation Hygiene
National Almazov Medical Research Centre, St. Petersburg, Russian Federation

A.V. VODOVATOV, I.A. ZVONOVA
St-Petersburg Research Institute of Radiation Hygiene St. Petersburg, Russian Federation
C. BERNHARDSSON
Medical Radiation Physics, Department of Translational Medicine, Skåne University Hospital Malmö, Sweden

INTRODUCTION

Positron emission tomography is developing and expanding in Russian Federation. Due to the rapid increase in the number of PET units, and the increasing availability of PET examinations in Russia, there is a growing need for optimization within this field in order to avoid overexposure of the patients and to improve the diagnostic information. The aim of the current study was to determine the structure of PET diagnostics by performing a patient dose survey in PET/CT departments and to suggest possible methods for optimization in PET diagnostics in the Russian Federation.

MATERIAL AND METHODS

Table 1. Diagnostic equipment in investigated PET departments and period of data collection.

Region	Scanner model	Year of data collection	Region	Scanner model	Year of data collection
St-Petersburg	Discovery 690	2017	Moscow	Biograph mCT 128	2017
	Biograph mCT 128	2017		Biograph mCT 128	2017
	Biograph mCT 40	2017		Biograph mCT 20	2016
	Ecat Exact	2017		Biograph mCT 20	2016
	Gemini	2017		Gemini TF 64	2016
	Discovery 710	2017		Discovery 610	2016
	Biograph 16	2013	Orel region	Discovery 610	2016
	Discovery 710	2016	Sverdlovsk region	Discovery 610	2016
	Biograph 6	2014	Bashkortostan	Optima 560	2016
	Biograph DUO	2014	Belgorod region	Discovery 610	2016
Kazan region	Discovery 600	2014	Tambov region	Optima 560	2016
	Discovery 690	2014	Kursk region	Discovery 710	2016
Tumen region	Biograph 64 True Point	2012	Lipetsk region	Discovery 710	2016
Primorsky krai	Gemini	2016			

* PET centers that have own radiopharmaceutical production

RESULTS AND DISCUSSION

Table 2. PET examinations types, radiopharmaceuticals and statistics of administered activities

Examination type	Radiopharmaceutical	Administered activity, MBq		
		Mean	Min	Max
Brain	¹⁸ F-FDG	170	130	200
	¹¹ C-methionine	530	250	800
	¹⁸ F-tyrosine	200	200	200
	¹⁸ F-choline	190	175	225
Myocardial perfusion	¹³ N-ammonie	775	750	800
Whole body (WB)	¹⁸ F-FDG	280	200	390
	⁶⁸ Ga- PSMA	105	-	-
	⁶⁸ Ga- DOTATATE/ ⁶⁸ Ga- DOTANOC	105	-	-
WB/Pelvis	¹⁸ F-choline	310	255	350
	¹¹ C-choline	380	210	550

Table 3. Anatomical regions and type of CT scans in PET/CT examinations, statistics of DLP.

Anatomical region	№ of PET units	DLP, mGy·cm		
		Mean	Min	Max
Whole body	27	890	400	1700
WB + Chest	4	1000	950	1100
Multiphase WB	10	1880	1300	2400
Brain	18	440	40	1700
Chest (myocardium)	3	70	50	100
Pelvis	2	500	500	500

Table 4. Typical administered activities and patient doses for whole-body PET/CT with ¹⁸F-FDG in Russia, and comparison with other countries

Value	This study	England	Austria	Germany	Finland	France	Ireland	Switzerland	Korea
Administrated activity, MBq	280	400	400	370	370	300 – 350	375	350	310
DLP, mGy·cm	890	-	-	-	-	630	-	-	430
Total patient dose, mSv	20	18	-	-	-	14	-	-	12

CONCLUSION

A patient dose survey was performed in Russian PET/CT departments in 2012-2017. For whole-body examinations, the highest dose was about 20 mSv. The patient dose is increased by a factor of two with multiphase as compared to standard CT scans. The patient doses in the Russian departments studied are high, as compared to a selection of other countries. The CT scan composes 70-90% of the total patient dose in whole body PET/CT examinations. For reducing the patient dose in PET/CT examinations it is recommended to use low-dose CT protocols and justification of diagnostic and multiphase CT.

CALCULATION OF ORGAN DOSES FOR COMPUTED TOMOGRAPHY : A SOFTWARE COMPARISON

Fouad Maaloul¹ (fouad.maaloul@biomediqa.com) – Aya Al masri^{1,2} – Laura Guerini¹ – Stéphanie Battini¹ – Thibault Julien¹

INTRODUCTION

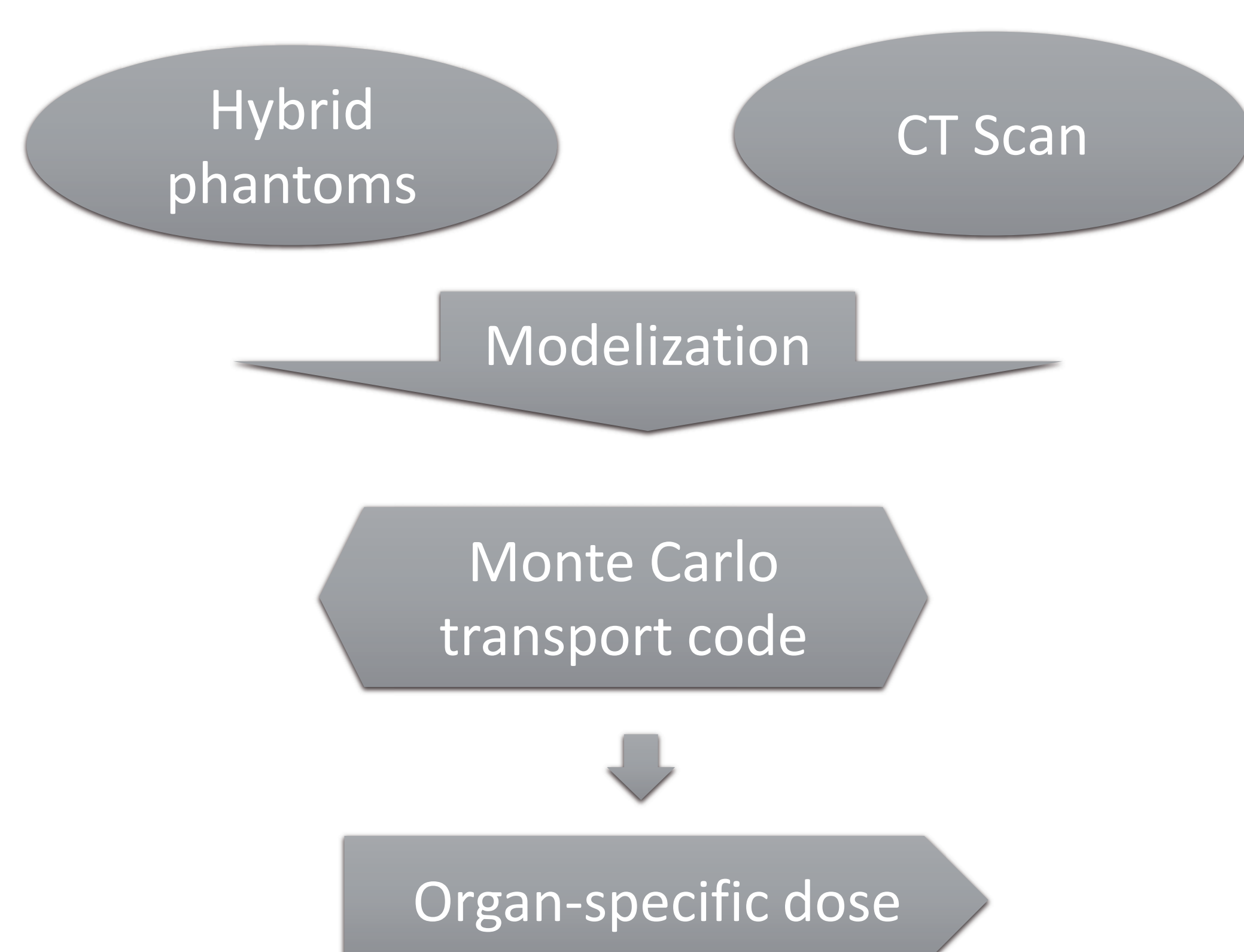
- ‘Computed tomography (CT)’ use increases rapidly worldwide.
- CT examinations deliver a relatively large radiation dose.
- The available dosimetric quantities did not account for the tissue differences or the organs location.
- It is essential to have an organ-specific dose estimation tool that reflects the average damage to the organ per unit of its mass and consequently the appearance of deterministic effects.

CONTEXT

- Developed since the year 2010, by BIOMEDIQA Group, **DOSITRACE** is a solution to optimize patient dose in medical imaging that uses ionizing radiations.
- DOSITRACE is a Dose Archiving and Communication System that collects exam settings from multi-imaging modalities, archives and analyzes them to return different patient dose indexes : Organ Dose, Effective dose and Skin dose-mapping.
- It insures patient dose history and traceability and can generate justified alerts for dosimetric optimization.
- CT organ doses given by DOSITRACE were compared with those given by a Hybrid-based software called “VirtualDose”.

MATERIALS AND METHODS

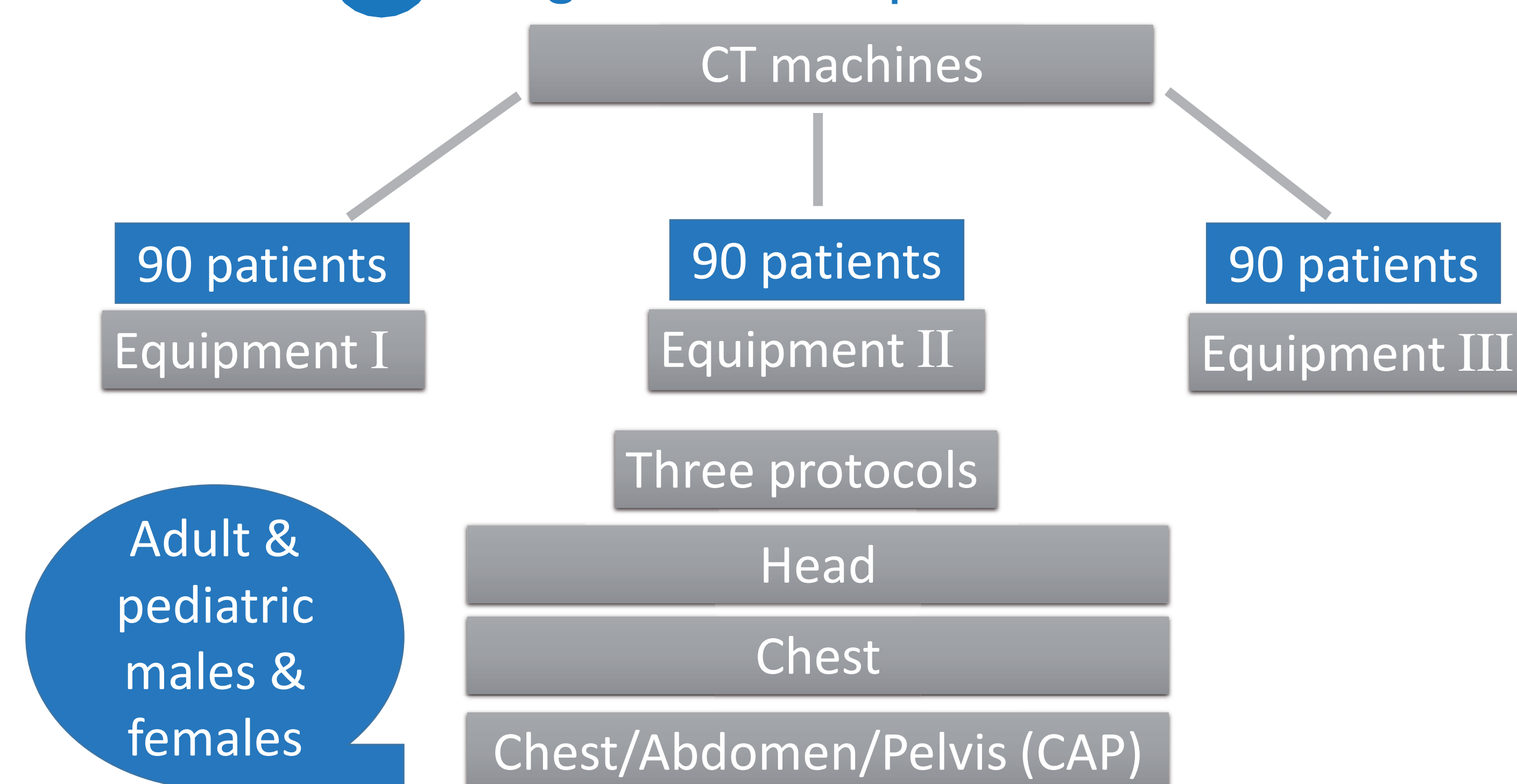
1 Organ dose calculation method



For any CT scan, organ dose can be calculated :

$$DH = (NF)E, T \times (D_{simulated})E, T \times \frac{((CTDI_{vol})E, T)_{Non-Validated CT}}{((CTDI_{vol})E, T)_{Validated CT}} \times \frac{Total\ mAs}{Utilized\ mAs}$$

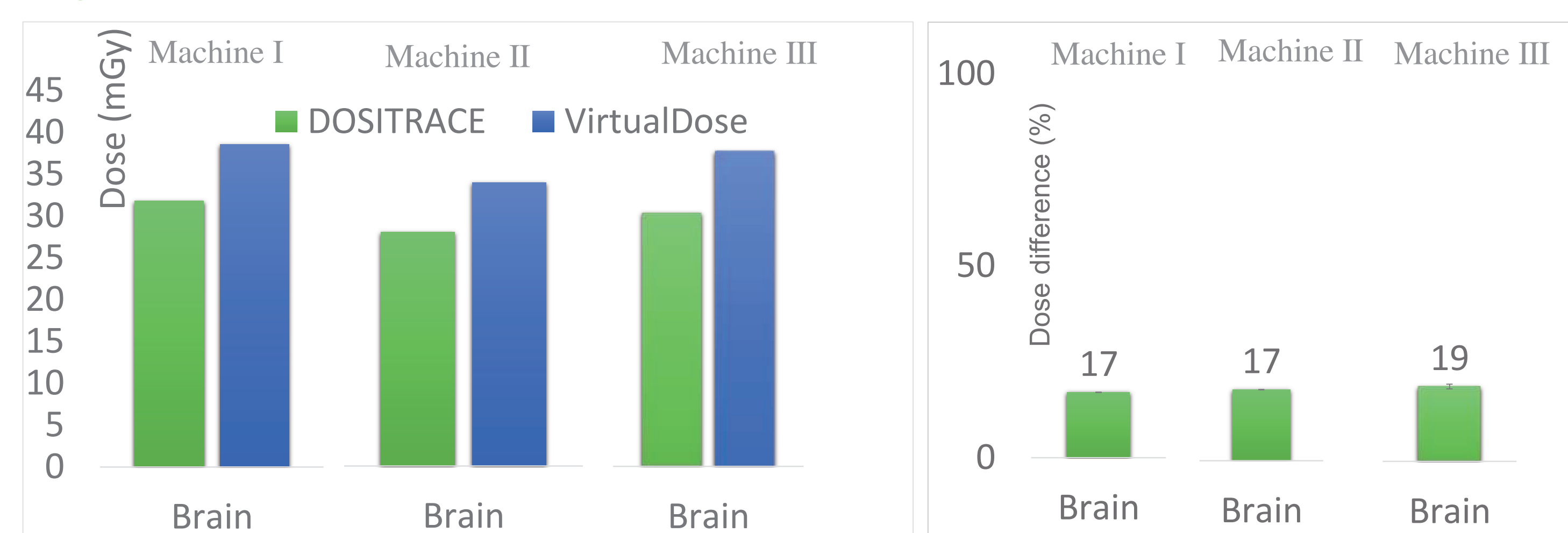
2 Organ dose comparison datasets



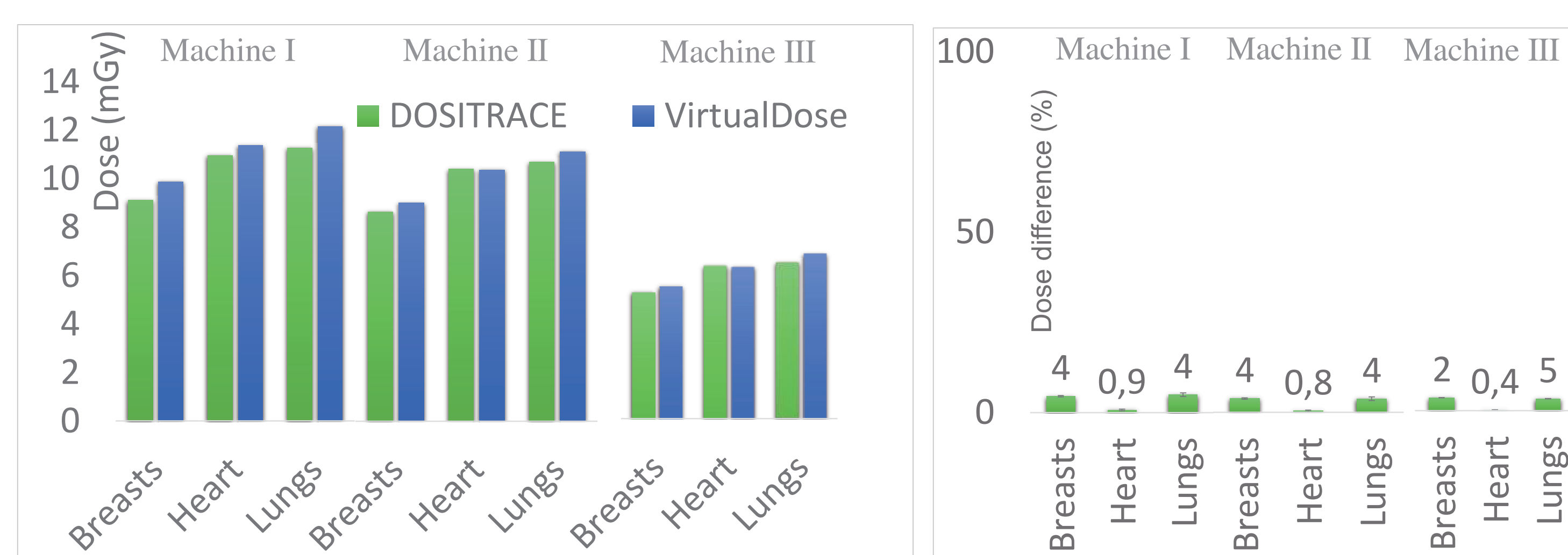
RESULTS

Organs that received 80% of the maximal dose are shown
We focus on Adult Females – Equivalent results were obtained for Adult males and pediatrics

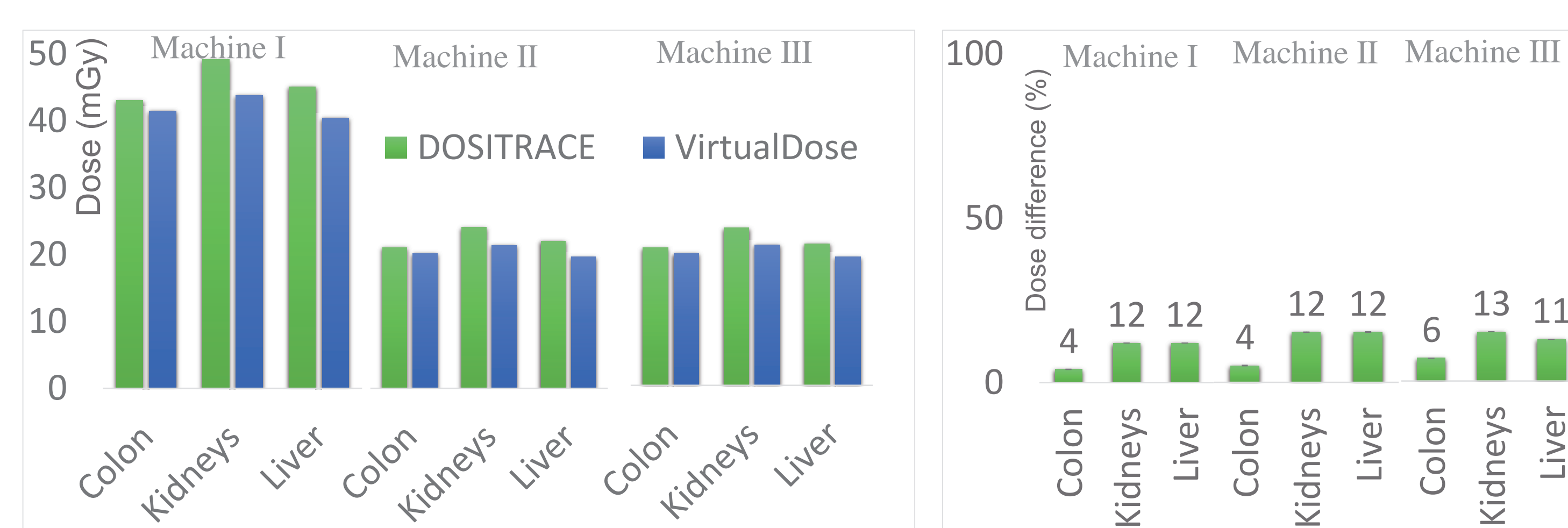
1 Head Protocol -> Obtained doses and percentage of difference



2 Chest Protocol -> Obtained doses and percentage of difference



3 CAP Protocol -> Obtained doses and percentage of difference



CONCLUSION

- The percentage of the dose difference between “DOSITRACE” and “VirtualDose” did not exceed 20%.
- It is independent of the CT machine, but varies slightly with the beam energy & collimation width.

COMPARISON OF ORGAN DOSES FOR WHOLE-BODY CT-EXAMINATION FOR PEDIATRIC AND ADULT PATIENTS ESTIMATED BY DIFFERENT METHODS

L.A. CHIPIGA*
St-Petersburg Research Institute of Radiation Hygiene
National Almazov Medical Research Centre, St. Petersburg, Russian Federation
*Corresponding author: larisa.chipiga@gmail.com

A.V. VODOVATOV, V.YU. GOLIKOV
St-Petersburg Research Institute of Radiation Hygiene St. Petersburg, Russian Federation
C. BERNHARDSSON
Medical Radiation Physics, Department of Translational Medicine, Skåne University Hospital
Malmö, Sweden

INTRODUCTION

Various MC-based organ dose calculators can be currently acquired, allowing quick dose calculations for medical physicists and physicians. However, they incorporate different computational models, which results in significant variations (up to an order of magnitude) in the estimated organ doses. The aim of the current study was to validate most common and available software , incorporating mathematical adult and pediatric human phantoms, comparing the calculated organ doses with the results of direct measurements in physical phantoms for different age categories (1 year-old, 5 years-old and adult).

MATERIAL AND METHODS

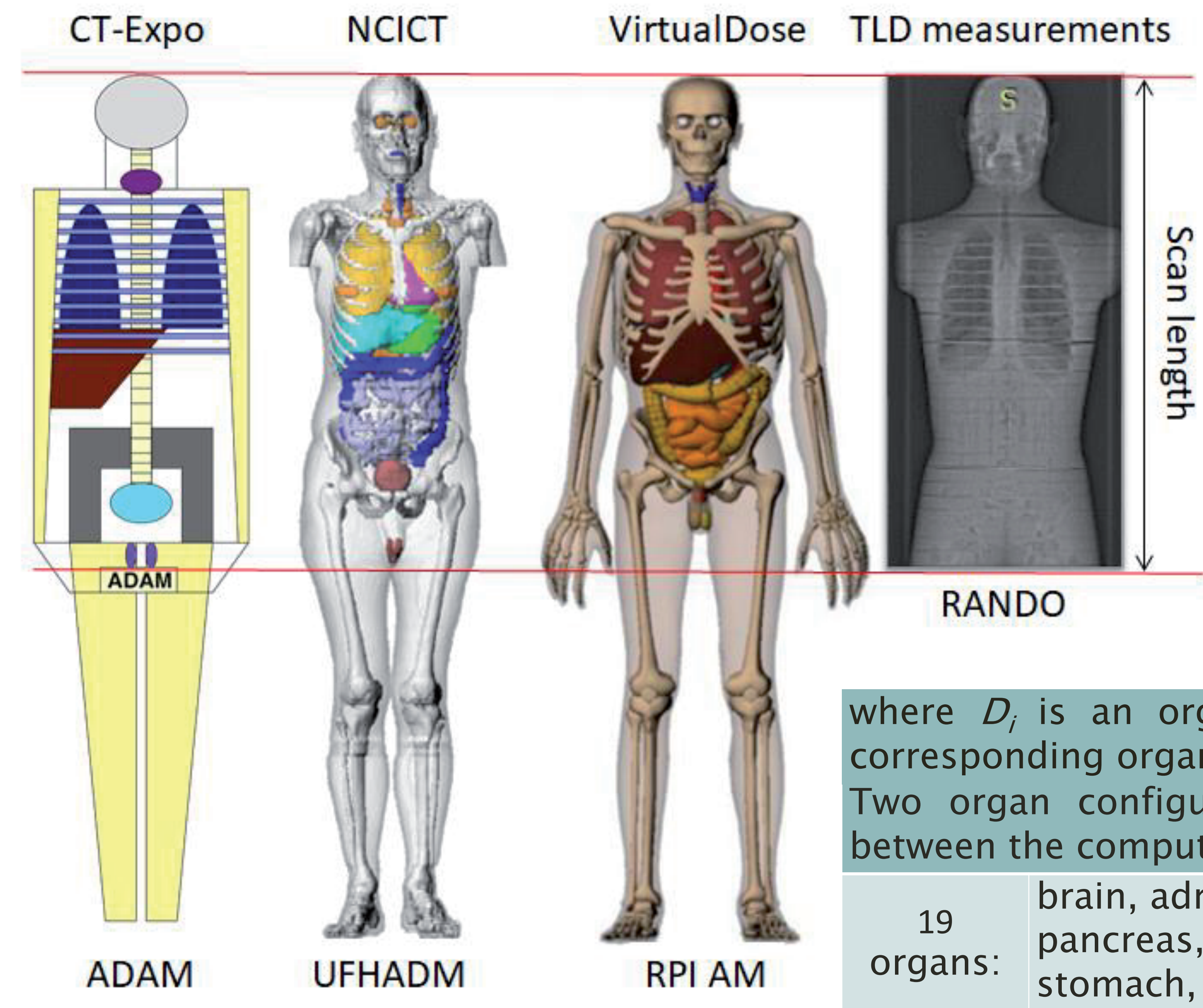


Table 1. Pediatric and adult CT protocols used in this study			
Parameter	1-y.o.	5-y.o.	Adult
Tube voltage (kV)	80	100	120
mAs (TCM was off)	95	95	200
Collimation (mm)	64×0.625	64×0.625	64×0.6
Time per tube rotation (s)	0.4	0.4	0.5
Pitch	1.015	1.015	1
Scan length (mm)	519	623	985
CTDI _{vol} (mGy)	1.8	3.7	13.5
DLP (mGy·cm)	106	233	1361

The relative difference, Δ , between the organ doses computed by the software programs and measured by TLDs was determined considering two organ configurations: 19 and 12 radiosensitive organs, using equation:
$$\Delta = \frac{D_i - D_{TLD}}{D_{TLD}} \cdot 100\%$$

where D_i is an organ dose as calculated by the software programs; D_{TLD} is the corresponding organ absorbed doses as measured by TLDs.

Two organ configurations: 19 and 12 radiosensitive organs for the comparison between the computational and direct measurement methods:

19 organs:	brain, adrenals, lung, urinary bladder, liver, esophagus, salivary glands, pancreas, kidneys, spleen, prostate, gall bladder, testes, thyroid, ovaries, stomach, uterus, colon, small intestine
12 organs:	organs with variation in location or shape (testes, thyroid, ovaries, stomach, uterus, colon, small intestine) were excluded

Figure 1. Methods of dose estimation and human phantoms used in each method.

RESULTS AND DISCUSSION

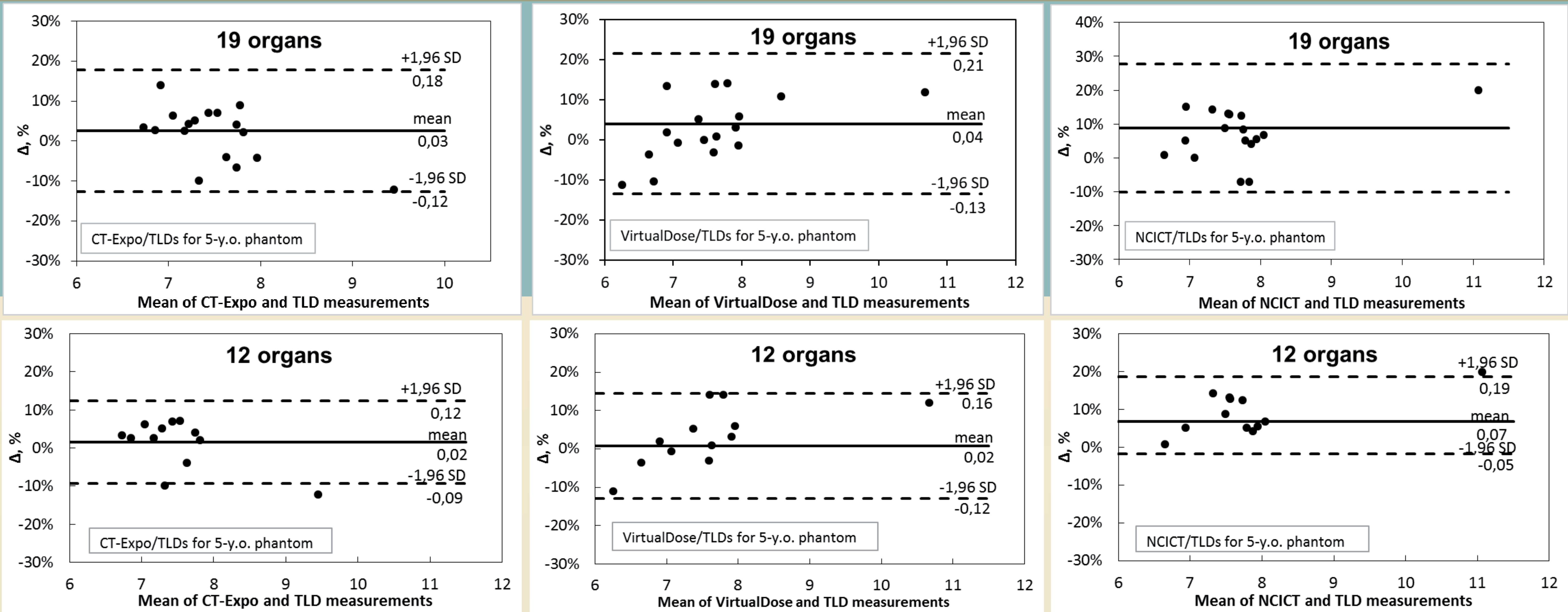


Figure 2. Bland–Altman plots presenting the relative difference (Δ) between doses of 19 and 12 radiosensitive organs estimated by software programs and organ doses measured by TLDs for the 5 year-old human phantoms, including the bias (mean difference) and the value of $\pm 1.96 \cdot SD$.

Table 2. The Bland–Altman statistics of relative difference (Δ) between doses of 19 and 12 radiosensitive organs estimated by software programs and measured by TLDs.

Calculated method	Parameter	19 organs			12 organs		
		1-y.o.	5-y.o.	Adult	1-y.o.	5-y.o.	Adult
CT-Expo	Bias	N/A	3%	3%	N/A	2%	6%
	$\pm 1.96 \cdot SD$	N/A	15%	21%	N/A	11%	15%
VirtualDose	Bias	0%	4%	-4%	1%	2%	-4%
	$\pm 1.96 \cdot SD$	16%	17%	26%	14%	14%	15%
NCICT	Bias	8%	9%	-7%	7%	7%	-7%
	$\pm 1.96 \cdot SD$	17%	19%	10%	12%	12%	12%

CONCLUSION

The relative difference in the organ dose estimation (by CT-Expo, VirtualDose, NCICT and direct measurements), for organs with similar location in computational models and physical phantoms (brain, adrenals, lung, urinary bladder, liver, esophagus, salivary glands, pancreas, kidneys, spleen, prostate, gall bladder), did not exceed 15% with the probability 95%.



Compliance to DRLs in Dutch hospitals: a survey by radiography students



Inholland University with the Ministry of Health Welfare and Sports

Harmen Bijwaard & Geert de Vries



2014 Holland+Utrecht
Pilot, 8 hospitals

2015 Netherlands
21 hospitals

2016 Netherlands
16 hospitals

2017 Netherlands
11 hospitals

In total nearly 6000 dose measurements

Outcomes

- Hospitals supported
- Part of radiography curriculum
- Publications:
 - Website of National Institute
 - Professional magazines (2x)
 - Radiography Journal

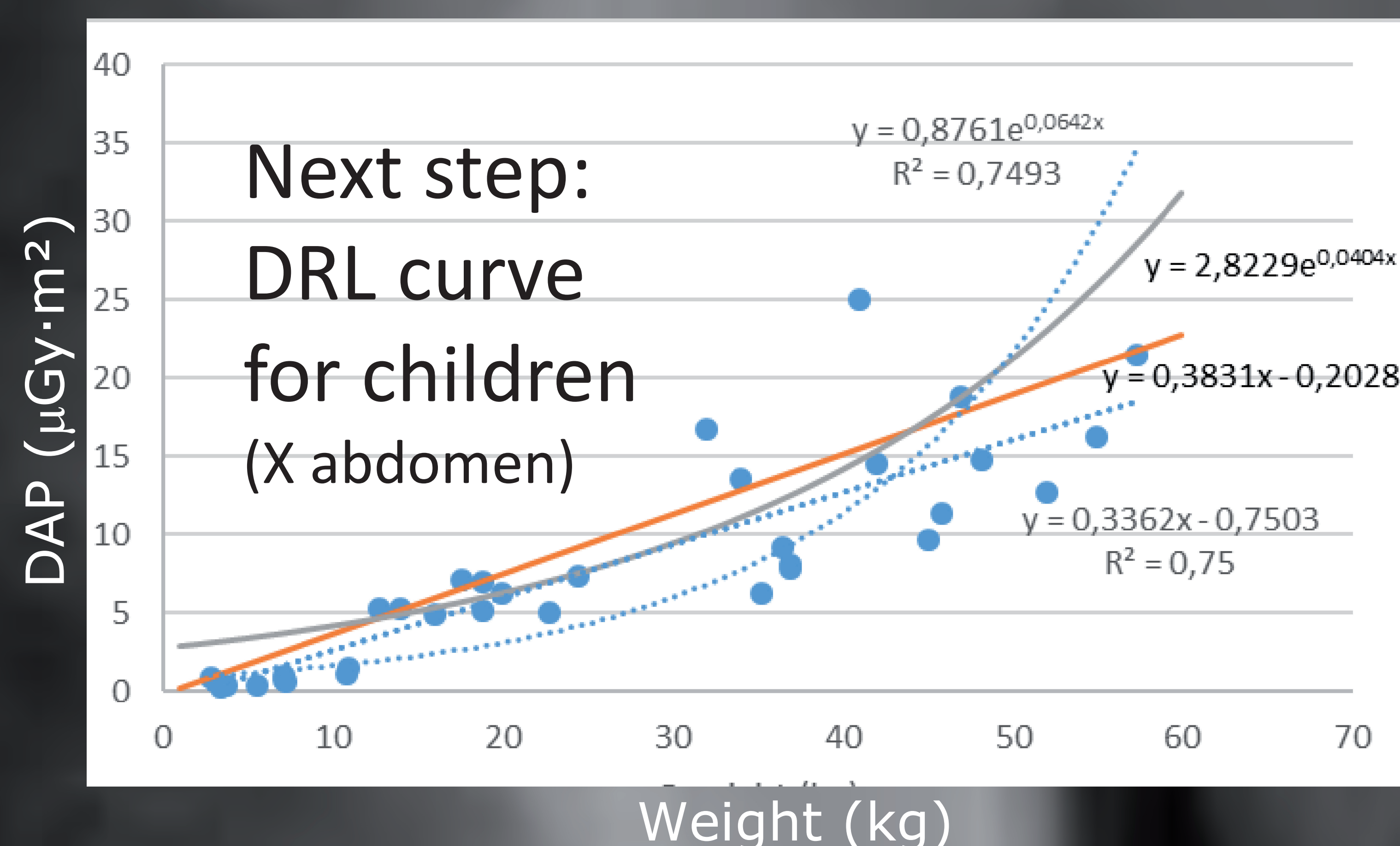
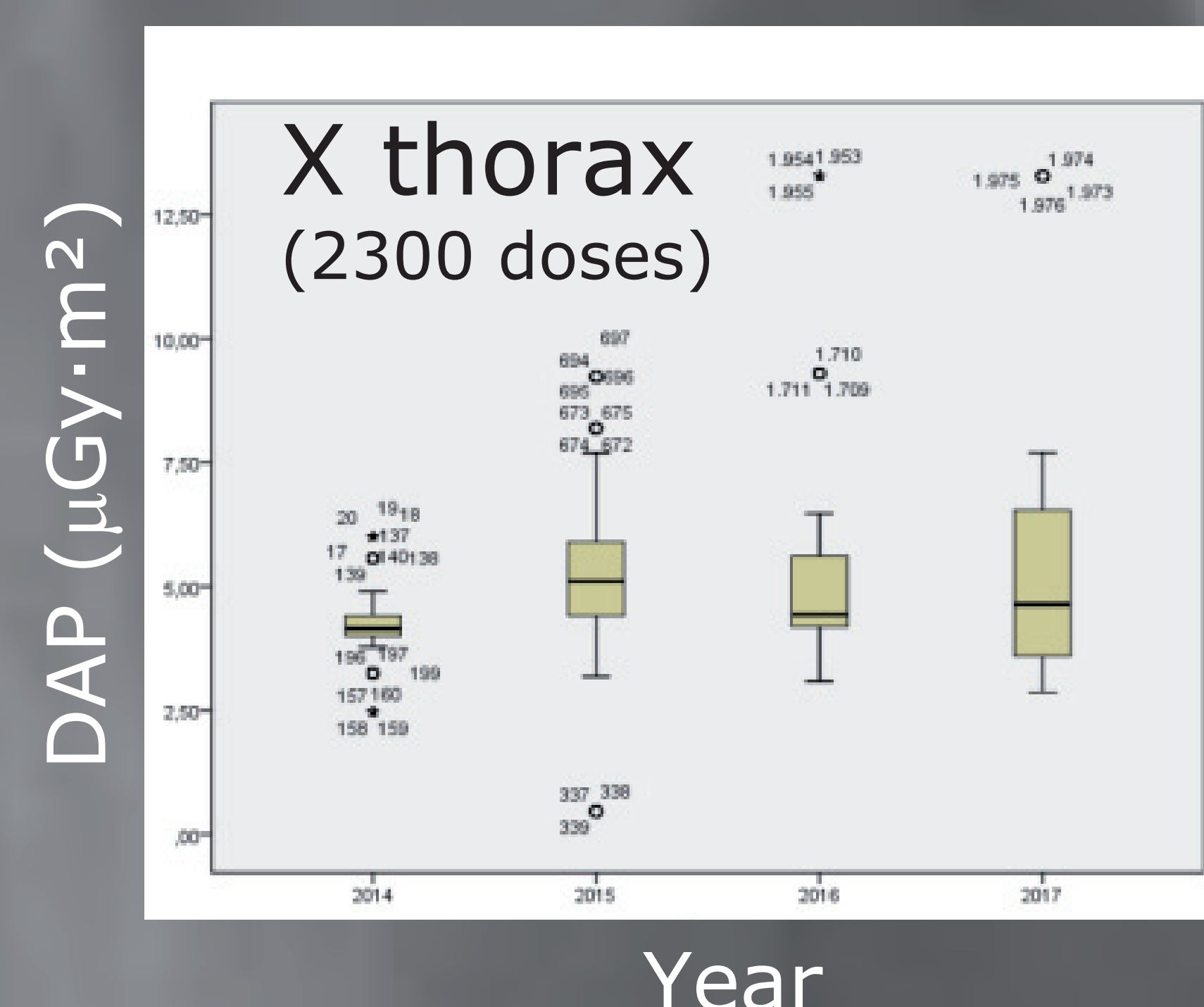
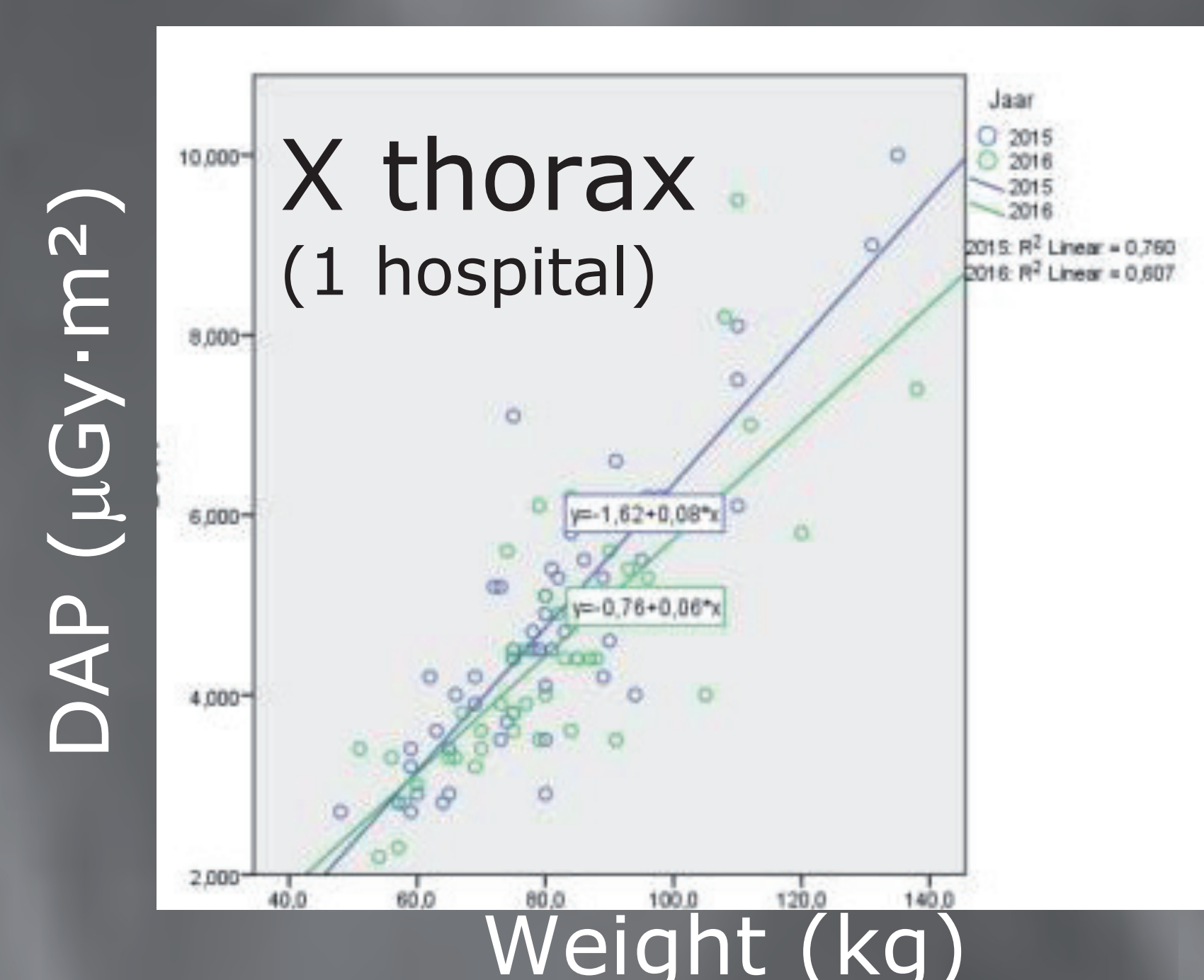
Radiography students

Registration of dose and weight for ≥ 20 patients
Interpolation for standard patient (77 kg)
Comparison with DRL



Results

Doses usually below DRLs
No apparent trend in time
DRLs can be reduced 50%





Consequences of Maternal Exposure: Stillbirth Rate and Infant Mortality in Offspring of Radiation-Dangerous Production Staff

Svetlana F Sosnina, Pavel V Okatenko, Mikhail E Sokolnikov
Southern Urals Biophysics Institute, Ozersk, Russia

A lot of studies were devoted to the biological effect of man-made radiation impact on the development of the embryo and fetus, most of which concern single exposure as a result of radiation-hazardous incidents, nuclear weapon tests and radiation accidents. The number of works about the effect of prolonged irradiation, to which women working at nuclear facilities are subjected in the context of their routine activities, is fewer. This data is relevant, since women make up at least 20% of the personnel of the nuclear industry and energy, whereas many of them are of reproductive age.

Mayak Production Association (PA "Mayak") is the first nuclear power plant in Russia which began operating in 1948.

- includes reactor, radiochemical and plutonium production and a number of auxiliary units;
- 25% of the staff are women;
- Significant doses of external gamma irradiation and internal alpha irradiation from incorporated 239Pu during the formation of technology

Objective: the analysis of stillbirth and infant mortality in the cohort of descendants of female Mayak workers who underwent preconceptive occupational long-term radiation exposure

Sources of information for the study:

- Mayak Workers Cohort: includes all who have ever worked at the enterprise;
 - The Ozersk Children's Health Register: a database of medical information on the children's population living near the PA "Mayak";
 - Children's Register: includes data on citizens born in Ozersk or who arrived in the city in childhood;
 - Dosimetric system "Dose-2008": includes information on the doses of external gamma and internal alpha (from the incorporation of Pu-239) of irradiation of personnel of PA "Mayak"
- N.B. 60-years observation period

Criteria for inclusion in the study group:

- descendants of female Mayak workers of reactor, radiochemical or plutonium production of PA "Mayak", hired in 1948-1972;
- mothers were subjected to preconceptive irradiation on the workplace;

Criteria for inclusion in the comparison group:

- children of mothers who never had professional radiation exposure;

Comparability of the groups was achieved due to:

- the same birth period (1951-1973);
- the same period of observation (1951-2009);
- the same place of residence mothers and children and therefore equal quality of medical care;
- analogical ratio by sex and calendar year and distribution by maternal age of child birth.

Characteristics of Groups

Indicators	Study group	Comparison group
Total number of children:	3234	11741
boys	1682 (52%)	5974 (51%)
girls	1552 (48%)	5767 (49%)
Median dose of external gamma irradiation of total body before conception (mGy)	284,0 (0,01-9509,0)*	0
Median dose of external gamma irradiation of ovaries (mGy)	179,0 (0,01-4066,0)*	0
Median dose of internal alpha-irradiation of ovaries (mGy)	0,06 (0,01-142,4)*	0

* - the range of doses is indicated in parentheses

Calculation of indicators:

- **Stillbirth rate** is the number of stillbirths per 1,000 live births and deaths;
- **Perinatal losses** include stillbirths and deaths in the first week, the perinatal loss rate is calculated per 1,000 live births and deaths;
- **Infant mortality** is the number of deaths from birth to 12 months per 1,000 children born alive;
- **Early neonatal mortality** is the ratio of the number of children who died before the age of 7 days, to the number of children born alive;
- **Late neonatal mortality** is the ratio of the number of children who died at the age of 8 to 28 days, to all live births except for children who died in the first week of life.
- **Postnatal mortality** is the ratio of the number of children who died at the age of 29 days to 1 year, to all children born alive, except for the deceased in the first month of life.

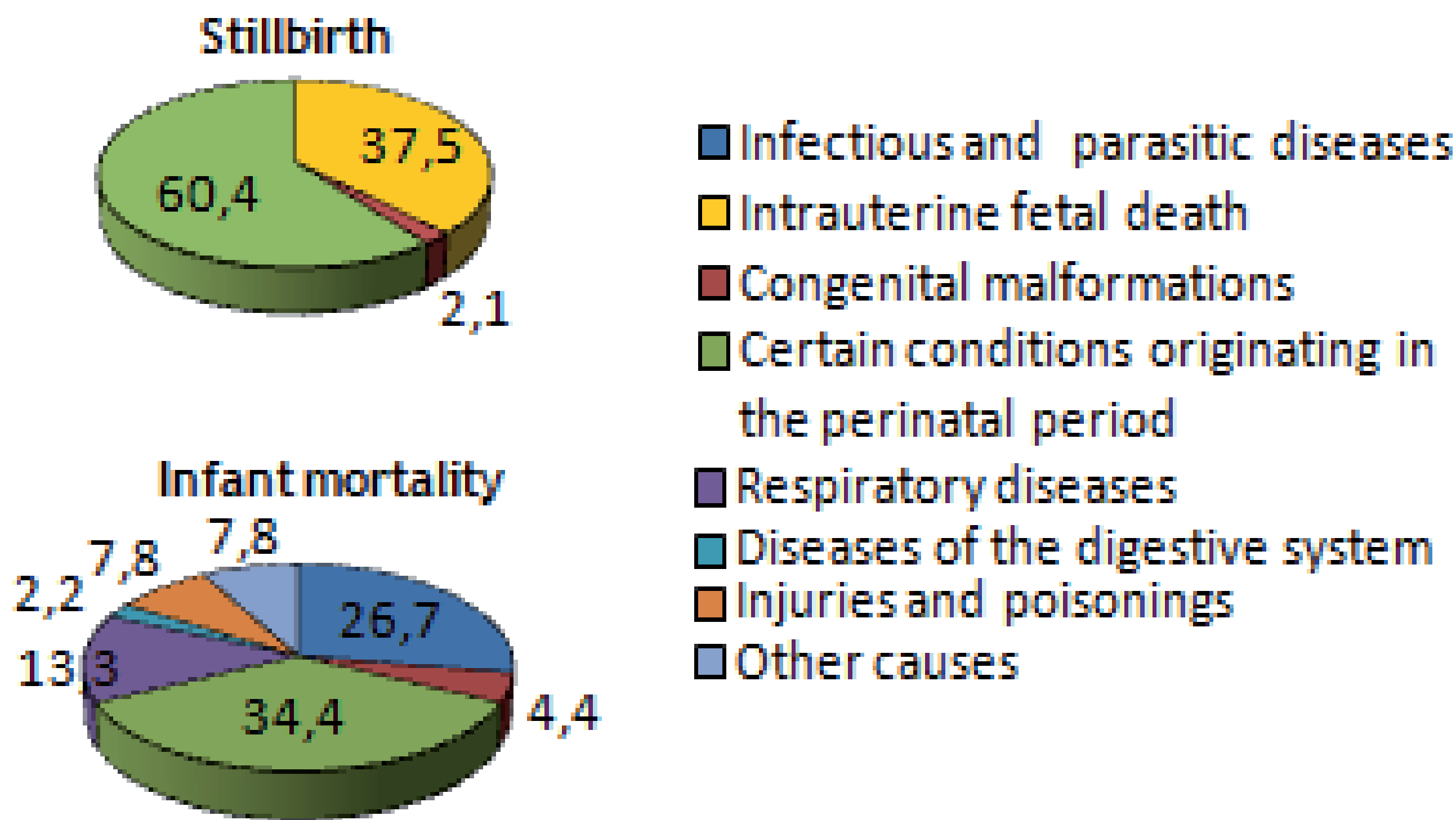
Stillbirth rate, perinatal losses and infant mortality

Indicators	Study group N*=3186		Comparison group N*=11646	
	Absolute number	per 1,000	Absolute number	per 1,000
Stillbirth rate	48	14,8**	95	8,1
Perinatal losses	78	24,1**	210	17,9
Infant mortality, including:	90	28,2	284	24,4
early neonatal mortality	30	9,4	115	9,9
late neonatal mortality	4	1,3	21	1,8
postneonatal mortality	56	17,8**	148	12,9

N * - number of live births

** - statistically significant differences with the comparison group

Structure of stillbirth and infant mortality, %



Conclusions

In the group of offspring of irradiated mothers:

- ❖ There was a significant excess of the stillbirth rate (14.8 cases per 1,000 in the study group versus 8.1 cases per 1,000 in the comparison group) and perinatal losses (24.1 cases per 1,000 in the study group versus 17.9 cases per 1,000 in the comparison group)
- ❖ Intrauterine fetal death and certain conditions originating in the perinatal period were registered often in the stillbirth rate structure
- ❖ Significant predominance of the number of stillbirths among the mothers with a dose of external γ -radiation before conception less than 1 Gy was noted.
- ❖ Postneonatal mortality (17.8 per 1,000) among descendants of Mayak workers significantly exceeded 12.9 per 1,000 in the comparison group.
- ❖ The level and structure of infant mortality in the groups as a whole did not differ. The main contribution to the structure of infant mortality in all groups was made by certain conditions originating in the perinatal period, infectious and parasitic diseases, respiratory diseases.
- ❖ Differences in the level of congenital malformations in groups were not found.

E-mail: sosnina@subi.su

Dissemination of Materials Regarding Exposure to Ionising Radiation in Diagnostic and Interventional Radiology by Using the Web Platform

Gabriel STANESCU

“Horia Hulubei” National Institute of Physics and Nuclear Engineering – IFIN HH, Nuclear Training Centre,
30 Reactorului, P.O.Box MG-6, RO-077125, Magurele, Romania,
e-mail: stanescu@nipne.ro, web: <http://cpsdn.nipne.ro>

INTRODUCTION

Nuclear Training Centre (CPSDN), department within the “Horia Hulubei” National Institute of Physics and Nuclear Engineering IFIN-HH, develops training programmes on radiation protection and radiation safety in medical, industrial and research practices. The CPSDN’s web platform is a module of a complex strategy that involves a coherent integration of classical methods and online information management systems.

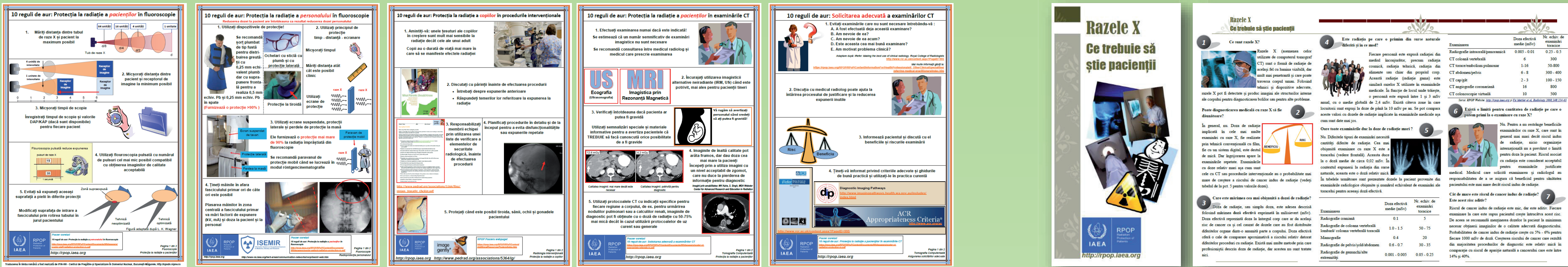
OBJECTIVES

The objective of this paper is to present the implementation of the Romanian version of some materials published by international bodies in the nuclear field within the dissemination module of the web platform. The aim is to increase the level of awareness of the visitors with regard to basic knowledge of radiation physics and radiation protection, maximizing the impact of information and dissemination actions carried out by CPSDN through training programmes. The results of our previous studies show a lack of knowledge about exposure levels in medical examinations with ionising radiation, even for a relatively knowledgeable audience in the field, like the visitors of the CPSDN’s web platform. Based on these results, it has been decided to achieve local versions of some materials published by international bodies (IAEA) in order to increase the attractiveness of the information and dissemination module.



RESULTS

The posters and leaflets developed by the International Atomic Energy Agency (IAEA) for dissemination of practical information on radiation protection in medical exposures were then translated in Romanian, with IAEA acceptance. All these informational materials were then published within the platform in order to be disseminated among workers and the general public.



Translated IAEA’s 10 Pearls Posters and the Leaflet

Because an analysis regarding the impact of publication of materials on the platform's audience has been considered useful, a tool to monitor downloads was implemented. The recorded results (2 years) indicate the clear interest of visitors for quality information on patient protection in widespread procedures with high level of radiation. To be noted the low interest on protection in pediatric interventional procedures, much rarer and less known.

Monitoring tool and the results on downloads

Published material	No. of downloads
Radiation protection of patients in fluoroscopy	648
Radiation protection of staff in fluoroscopy	1398
Radiation protection for children in interventional procedures	843
Radiation protection of patients in CT	1086
Appropriate referral for CT examinations	572
Leaflet “X rays - What patients need to know”	1164

Published material	No. of downloads
Radiation protection of patients in fluoroscopy	648
Radiation protection of staff in fluoroscopy	1398
Radiation protection for children in interventional procedures	843
Radiation protection of patients in CT	1086
Appropriate referral for CT examinations	572
Leaflet “X rays - What patients need to know”	1164

CONCLUSIONS

It can be considered that the web platform's dissemination component has been enriched with topical materials in the nuclear field. By adding new features, more capabilities have been acquired to monitor and analyse the impact of the published materials.



Effective dose estimation for barium swallow and barium meal fluoroscopic examinations performed in Russia: a hospital based study

A. V. Vodovatov*, V. Yu. Golikov: St-Petersburg Research Institute of Radiation Hygiene after Professor P.V.Ramzaev
I. G. Kamyshanskaya, V. M. Cheremysin, K. V. Zinkevich: FGBOU VO "Saint-Petersburg state University, Department of Oncology
C. Bernhardsson: Medical Radiation Physics, Department of Translational Medicine, Lund University, Skåne University Hospital Malmö
* e-mail: vodovatoff@gmail.com

CONCLUSIONS

- The following conversion coefficients ($\mu\text{Sv}\times\mu\text{Gy}^{-1}\times\text{m}^2$) were estimated: 2.3 and 1.7 for barium swallow (both departments); 2.4 and 2.0 for barium meal (surgical department); 2.5 and 3.8 for barium meal (therapy department) for the over-couch and under-couch exposure geometries, respectively;
- Main factors influencing effective doses and conversion coefficients: structure of fluoroscopic examination, patient irradiation geometry, energy characteristics of the X-ray beam
- Conversion coefficients should be established for typical clinical protocols considering the structure of examination an relative dose-area contribution for each projection of patient exposure

AIMS OF THE STUDY

- to estimate the effective doses and calculate conversion coefficients from dose-area product to effective dose for typical barium swallow and barium meal protocols based on a data collection in a general practice hospital in St-Petersburg, Russia;
- to evaluate the impact of different parameters of the examination on the resulting conversion coefficients.

RESULTS

Table 1. Patient DAP, effective doses and conversion coefficients for the whole examination

Parameter	Surgical department		Therapy department
	Barium swallow	Barium meal	Barium meal
Total DAP for the fluoroscopic examination, $\mu\text{Gy}\times\text{m}^2$	782±460 (260-2048)	3175±2155 (251-10309)	508±371 (228-2157)
Effective dose for the fluoroscopic examination, over couch tube position, mSv	1.8±1.1 (0.5-4.6)	7.9±5.7 (0.7-27.8)	1.9±1.4 (0.7-7.9)
Effective dose for the fluoroscopic examination, under couch tube position, mSv	1.4±0.9 (0.37-3.8)	6.7±5.3 (0.5-23.4)	1.3±0.9 (0.5-5.3)
Conversion coefficient, $\mu\text{Sv}\times\mu\text{Gy}^{-1}\times\text{m}^2$, over couch tube position	2.3±0.3	2.4±0.1	3.8±0.4
Conversion coefficient, $\mu\text{Sv}\times\mu\text{Gy}^{-1}\times\text{m}^2$, under couch tube position	1.7±0.2	2.0±0.2	2.5±0.3

Table 2. CCs ($\mu\text{Sv}\times\mu\text{Gy}^{-1}\times\text{m}^2$) for different irradiation projections

Projection	Surgical department		Therapy department
	Barium swallow	Barium meal	Barium meal
AP	2.8±0.3 (2.4-3.4)	3.1±0.3 (2.3-3.8)	3.9±1.2 (0.7-5.5)
PA	1.8±0.2 (1.5-2.4)	1.9±0.2 (1.4-2.6)	2.4±1.0 (0.2-6.2)
LATL	1.3±0.3 (1.1-1.9)	1.9±0.2 (1.3-2.4)	2.5±0.3 (2.0-3.0)
LATR	-	1.2±0.2 (0.9-1.8)	1.5±0.2 (1.3-1.8)
LPO	-	2.3±0.2 (1.4-2.8)	3.2±0.4 (2.1-5.0)
RPO	-	3.2±0.4 (2.3-3.8)	5.1±0.5 (2.2-7.4)
LAO	-	1.8±0.2 (1.4-2.3)	1.8±0.1 (1.8-2.0)
RAO	1.6±0.2 (1.3-1.9)	1.7±0.2 (1.0-2.3)	2.4±0.3 (1.7-3.8)

Table 3. Contribution of different projections into total DAP (%)

Projection	Surgical department				Therapy department	
	Barium swallow		Barium meal		Barium meal	
	Over couch tube	Under couch tube	Over couch tube	Under couch tube	Over couch tube	Under couch tube
AP	67%	-	45%	8%	26%	10%
PA	-	67%	8%	45%	10%	27%
LATL	6%	6%	14%	4%	1%	1%
LATR	-	-	4%	14%	1%	1%
LPO	-	-	7%	17%	35%	-
RPO	-	-	1%	5%	26%	1%
LAO	-	-	5%	1%	-	26%
RAO	27%	27%	17%	7%	1%	34%

MATERIALS AND METHODS

Data collection: surgical and therapy departments of St-Petersburg Urban Mariinsky Hospital. Samples of 20-40 patients for barium swallow (BS) and barium meal (BM) examinations for each department.

X-ray equipment: KRT-Electron (JSC "NIPK "Electron", Russia) digital remotely guided X-ray units, over couch X-ray tube, CCD-matrix detector.

Data collected for each patient: fluoroscopic study structure (number of fluoroscopic phases and X-ray images); for each phase and image: patient position (standing, supine, prone, recumbent), projection, total fluoroscopy time (s), fluoroscopy frame rate (frames·s⁻¹), field size (cm × cm), average tube voltage (kV), total DAP ($\mu\text{Gy} \times \text{m}^2$).

Effective dose calculation: PCXMC 2.0, over couch + under couch irradiation geometry, based on measured dose-area product, using tissue weighting coefficients form ICRP Pub. 60 (see Figure 1).

Typical projections of irradiation: anteroposterior (AP); posteroanterior (PA); left and right lateral (LATL, LATR); left and right anterior and posterior oblique (LAO, RAO, LPA, RPO).

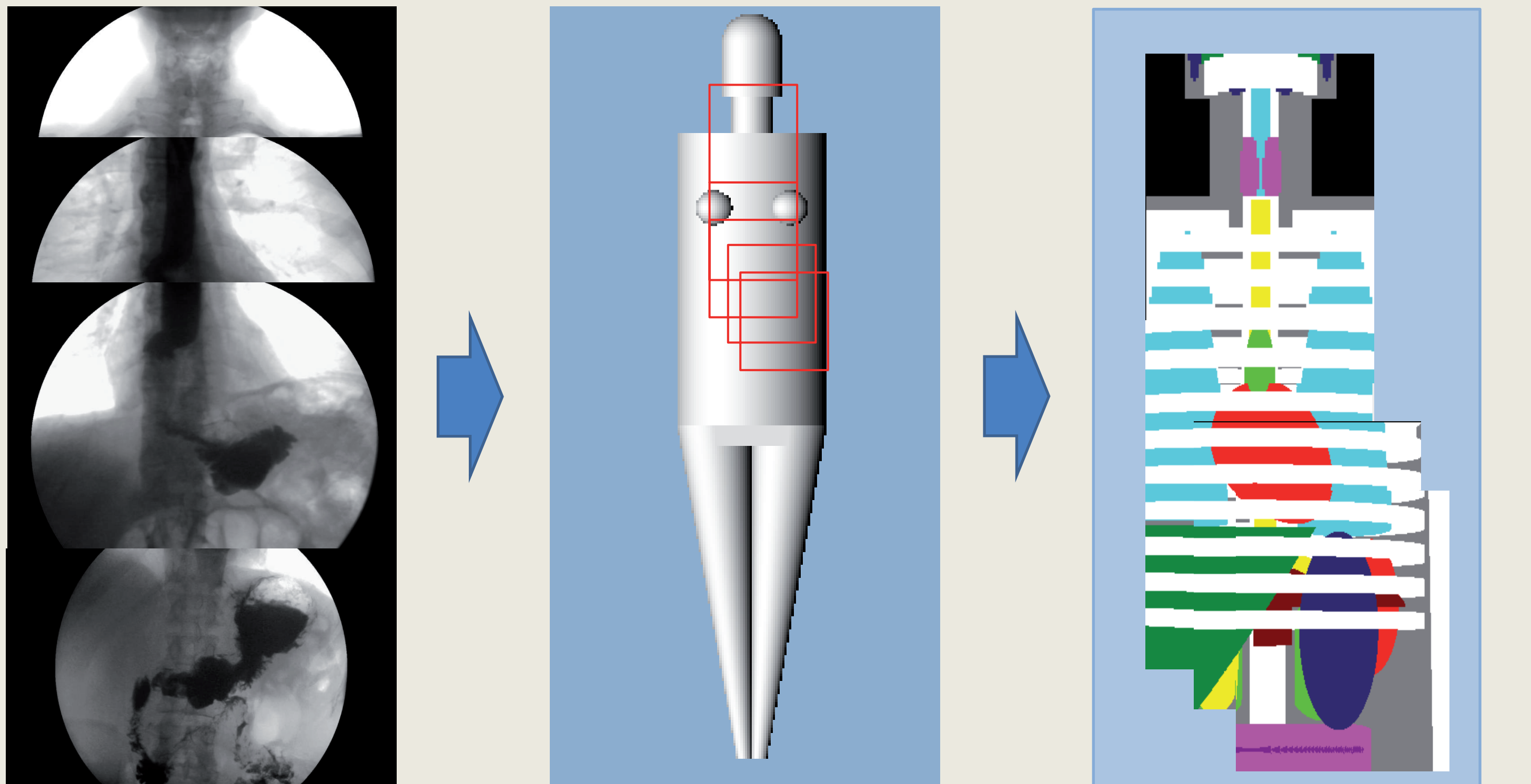


Figure 1. A model for the calculation of the effective dose

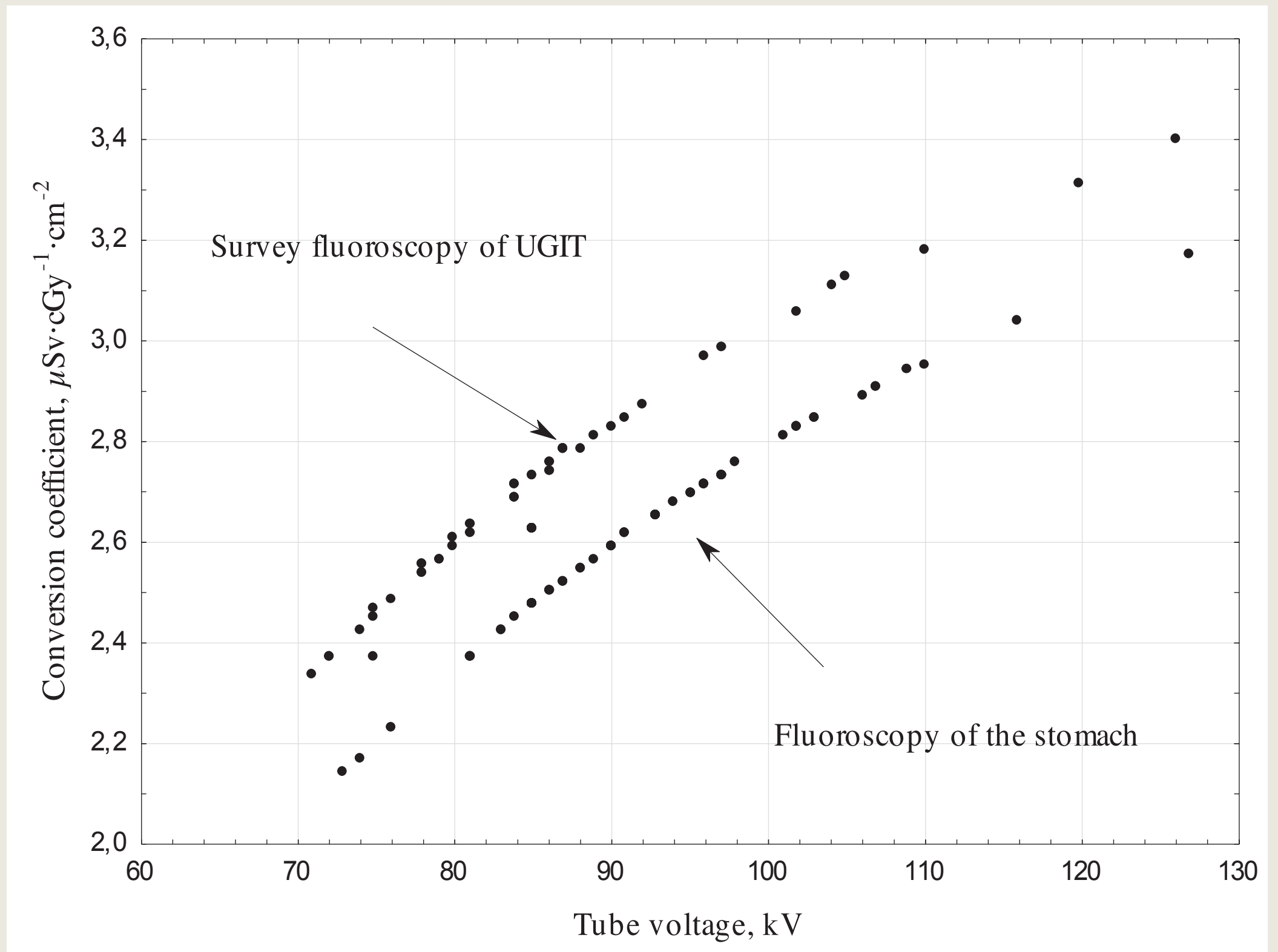
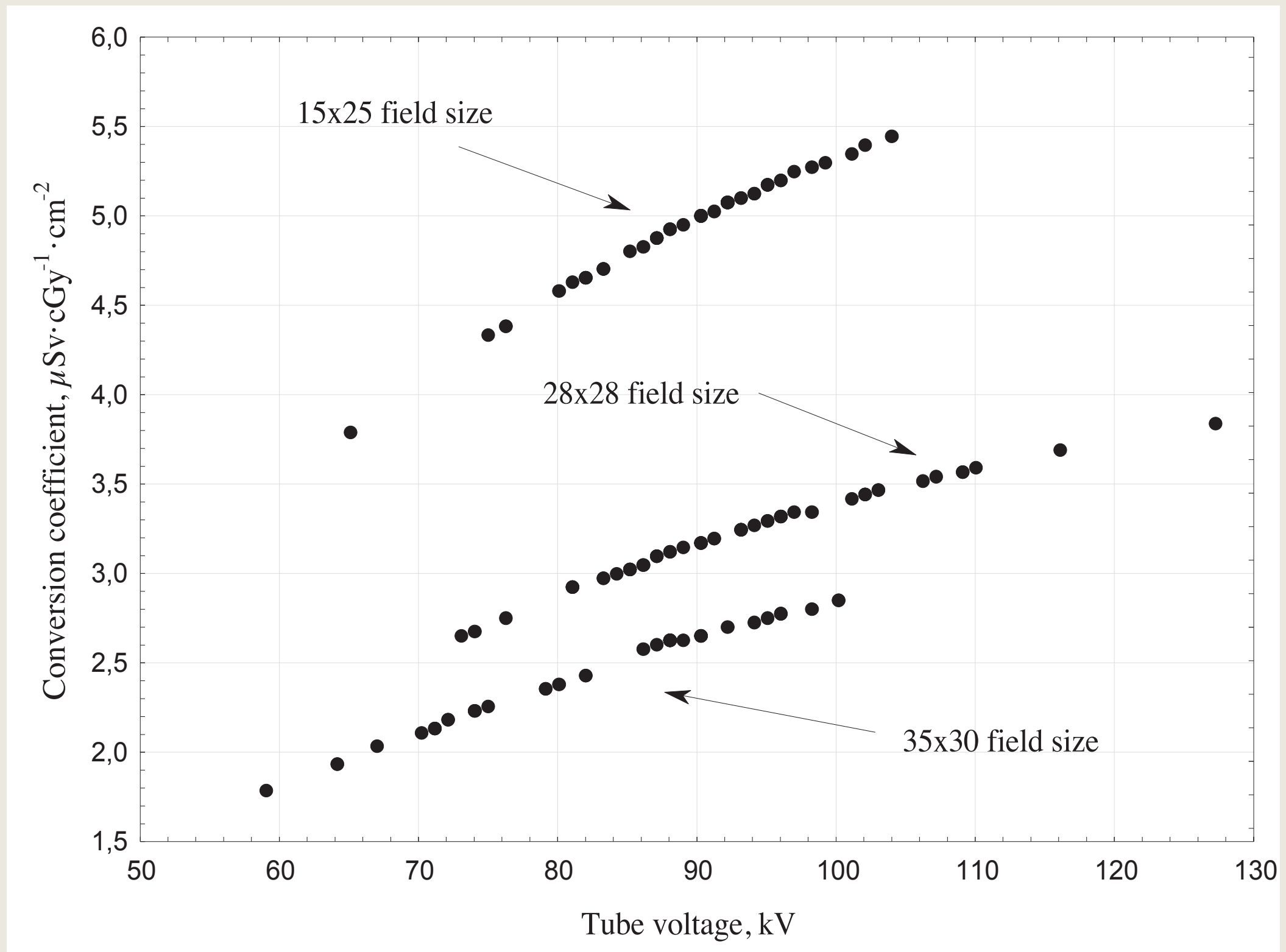


Figure 2. Relations between CCs, tube voltage, irradiation field size and exposed anatomic area



Estimation of radiation dose for hospital staff outside the department of nuclear medicine as a result of nuclear medicine examinations and treatments

Introduction

Patients undergoing a diagnostic examination or treatment at the department of nuclear medicine (NM) can cause a radiation dose to hospital staff outside this department. The procedure for combinations of random hospital appointments is to plan the administration of the radioactive compound after other hospital appointments. However, this is not always possible or known beforehand as most appointments are planned separately.

Aim

Over the recent years rough estimations have been made of number of combined appointments. Nonetheless, the number of NM appointments has grown substantially and there is a tendency to combine hospital visits on one day. Also more questions were asked by hospital staff about the risks from radioactive patients. The aim of this study was to get a better estimation of combined appointments and radiation doses this causes for hospital staff.

Methods

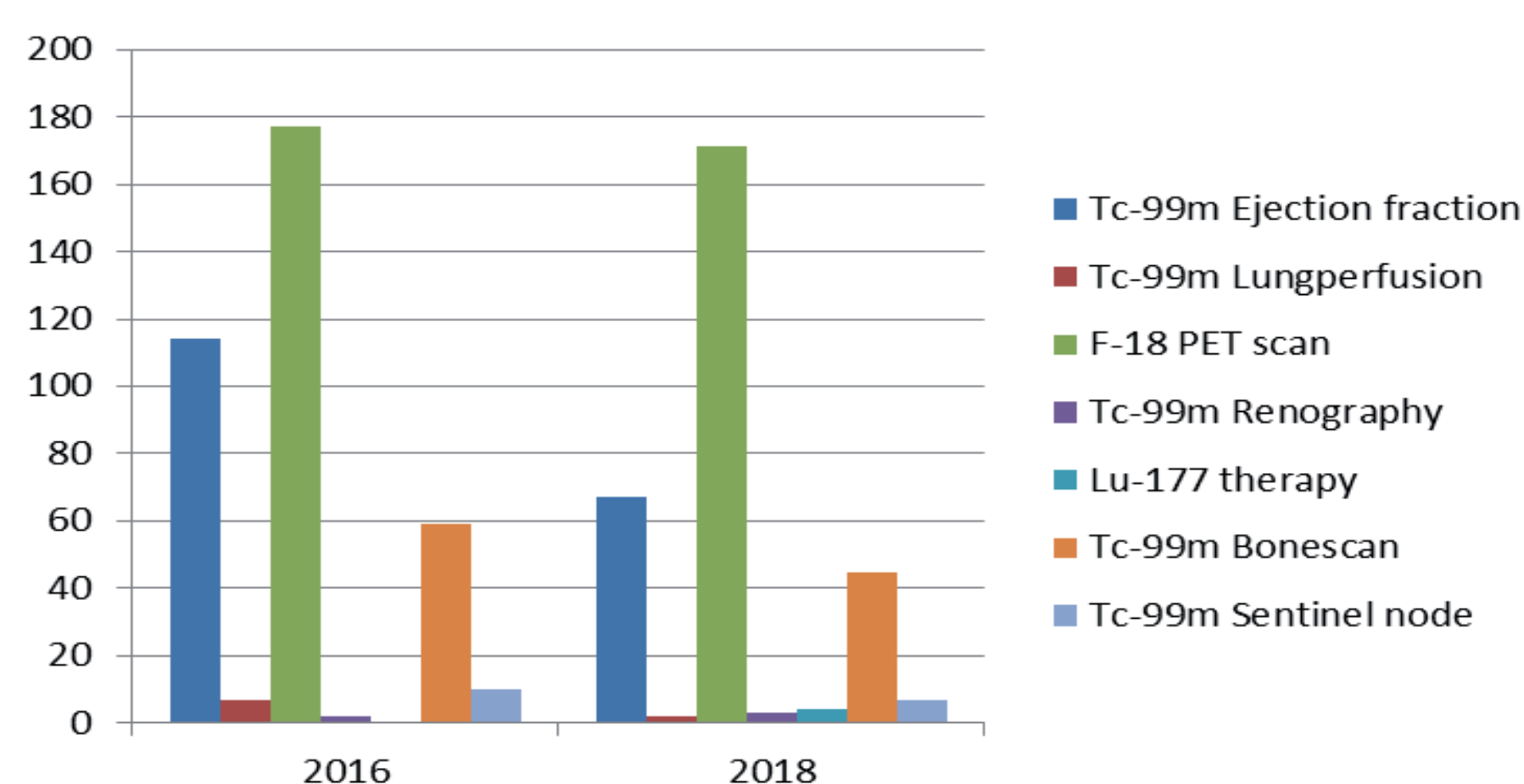
During the first three months in 2016 all so-called random combined appointments were registered. For diagnostic examinations this was defined as administration and all subsequent appointments on the same day, whereas for therapeutic visits this was defined as all appointments in the week after administration. Standard clinical combinations of appointments, already registered in risk analyses, were excluded. The following parameters were registered:

- NM appointment: date, time and standard activity of radioactive compound
- Subsequent appointments: date, time, duration and acts during the appointment

Based on this information a theoretical calculation of the received dose in one year was made for the staff in the subsequent appointment in worst-case scenario: no excretion of the radioactive compound and one worker by type of subsequent appointment. Decay of the radionuclide between and during appointments are taken into account as well the distance to the patient during the subsequent appointment. In the first three months of 2018 the study was repeated to analyse trends.

Results

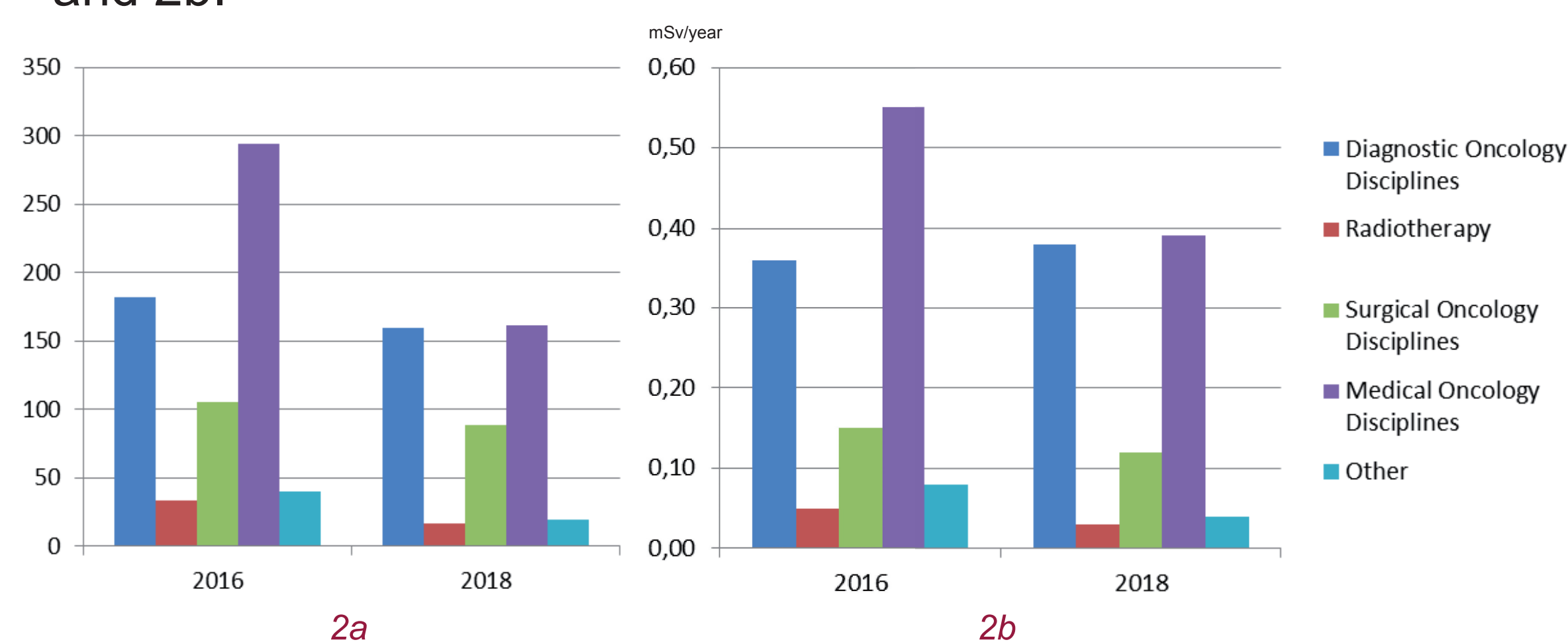
In 2016 18% of all nuclear medicine examinations had one or more subsequent hospital visits the same day. No NM treatment had a combination appointment. F-18 PET examinations were most combined (177 of the total 370 combinations) and Tc-99m ejection fraction (114 of the total 370 combinations). But these are also the most common NM examinations at NKI-AVL. In percentages 15% of all F-18 PET-scans were combined and 46% of all Tc-99m ejection fractions. In 2018 the percentage of combination appointments was dropped to 15%.



Graphic 1: Number of combination appointments

The distribution over the various examinations had remained the same. A new therapy using Lu-177 started in 2017. This therapy is sometimes combined (12%), which results in new data for 2018.

The total radiation dose caused by the combination appointments was 1,2 mSv/year in 2016 and 1,0 mSv/year in 2018, but must be distributed over various departments and workers. The distribution is divided over 5 groups of disciplines: Diagnostic oncology disciplines (DOD), Medical Oncology Disciplines (MOD), Surgical Oncology Disciplines (HOD), Radiotherapy and other. De distribution for numbers and doses over the disciplines in 2016 and 2018 is shown in graphic 2a and 2b.



Graphic 2: Distribution of numbers (2a) and doses (2b) over the disciplines

The highest numbers and doses are for MOD and DOD. In MOD the staff are non-radiological workers, with the highest dose 0,15 mSv/year in 2016 for workers making the ECG's. In 2018 this dose was much less due to the decrease in number of combined NM-ECG appointments. The highest dose in 2018 was for staff in short stay where patient receive their chemotherapy, with a dose of 0,2 mSv/year. In DOD the highest dose in both 2016 (0,1 mSv/year) and 2018 (0,3 mSv/year) is for radiological workers making the CT-scans. As radiological workers this dose is an extra radiation dose.

The calculated doses are conservative. In practice the doses will be lower because it will be received by several workers and excretion of the radioactive compound by the patient is not taken into account.

Discussion

The results of 2016 were presented to the departments and made staff more aware of combination appointments. This may have influenced the result in 2018.

This study was performed at NKI-AVL, but the growth of NM appointments and therefor the possible combination appointments is present in other hospitals as well. Not only the higher numbers of NM appointments but also the use of new radionuclides, can cause an extra effective dose to hospital staff. This must be monitored over the years. For the same reason the dose to the environment and the excretion of the radioactive compound by the patient in water must be monitored.

Conclusion

Calculated dose to non-radiological workers and extra dose to radiological workers is in worst case scenario low. After two years there is not a significant change in number of combination appointments and dose to hospital staff. Additional measurements are not necessary based on these results. The procedure to plan the administration of the radioactive compound after other hospital appointments must be pursued, but in case this is not possible it can be planned otherwise. The number of NM appointments and the combination appointments must be monitored over the next years in combination with the dose consequences.



Evaluation of Structural Radiation Protection in Radiotherapy by Monte Carlo Methods



Lena Landwehr*, Philipp Denger

*Presenting author; e-mail: llandwehr@tuev-nord.de

TÜV NORD EnSys GmbH & Co. KG
Am TÜV 1, 30519 Hannover
Germany
Tel.: +49 511 998 61810
www.tuev-nord.de

Introduction

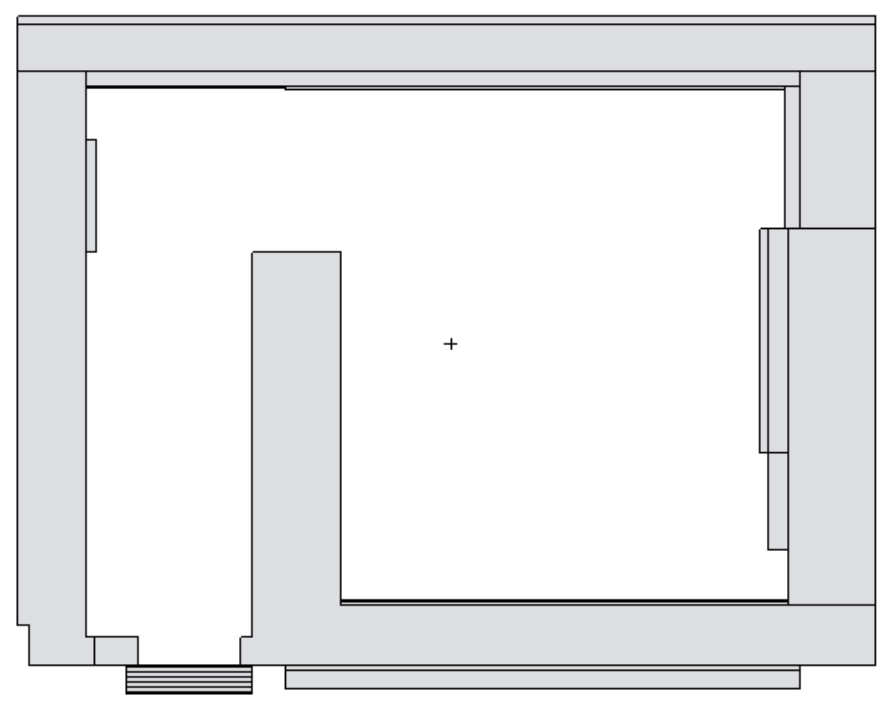


Figure 1 Modelled Radiation Therapy Facility

In radiotherapy adequate shielding for high energy gamma radiation and (above 8 MeV) also neutron radiation must be performed. Today, we have standards for many applications regarding radiation protection [2] and common regulations on national level [1]. In general, these regulations describe standard facilities. For more complex problems modelling with Monte Carlo methods [3] give reliable answers before building. But ducts, gaps or geometry overlaps may lead to weak spots, which are usually noticed in the late construction phase by real dose measurements and then are costly to correct. Hence, we evaluated complex structures for structural radiation protection in radiotherapy via Monte Carlo simulation by validated facility and accelerator models (fig. 1, 2).

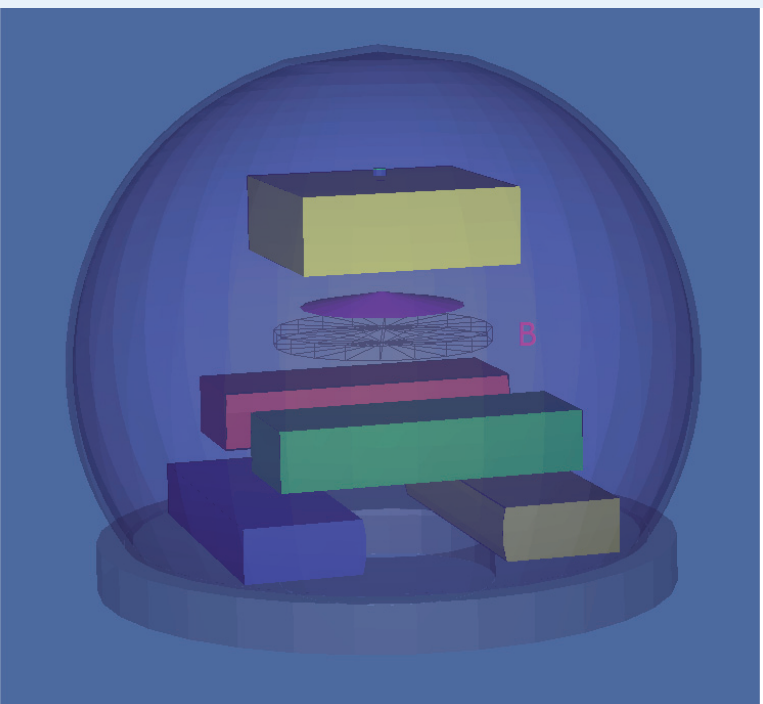


Figure 2 Modelled accelerator head

Modelling

1. Ducts

The supply of electrical power and fresh air should be guaranteed within a radiation therapy room and might cause problems for the structural shielding protection. We modelled different duct diameters for analysis of the impact of bent and straight ducts.

2. Gaps

In general, the radiation protection doors (fig. 3) have gaps between the floor and the door itself. These gaps are problematic for radiation protection because scattered radiation may leak trough the gap.

We evaluated the effectiveness of door lowerings.

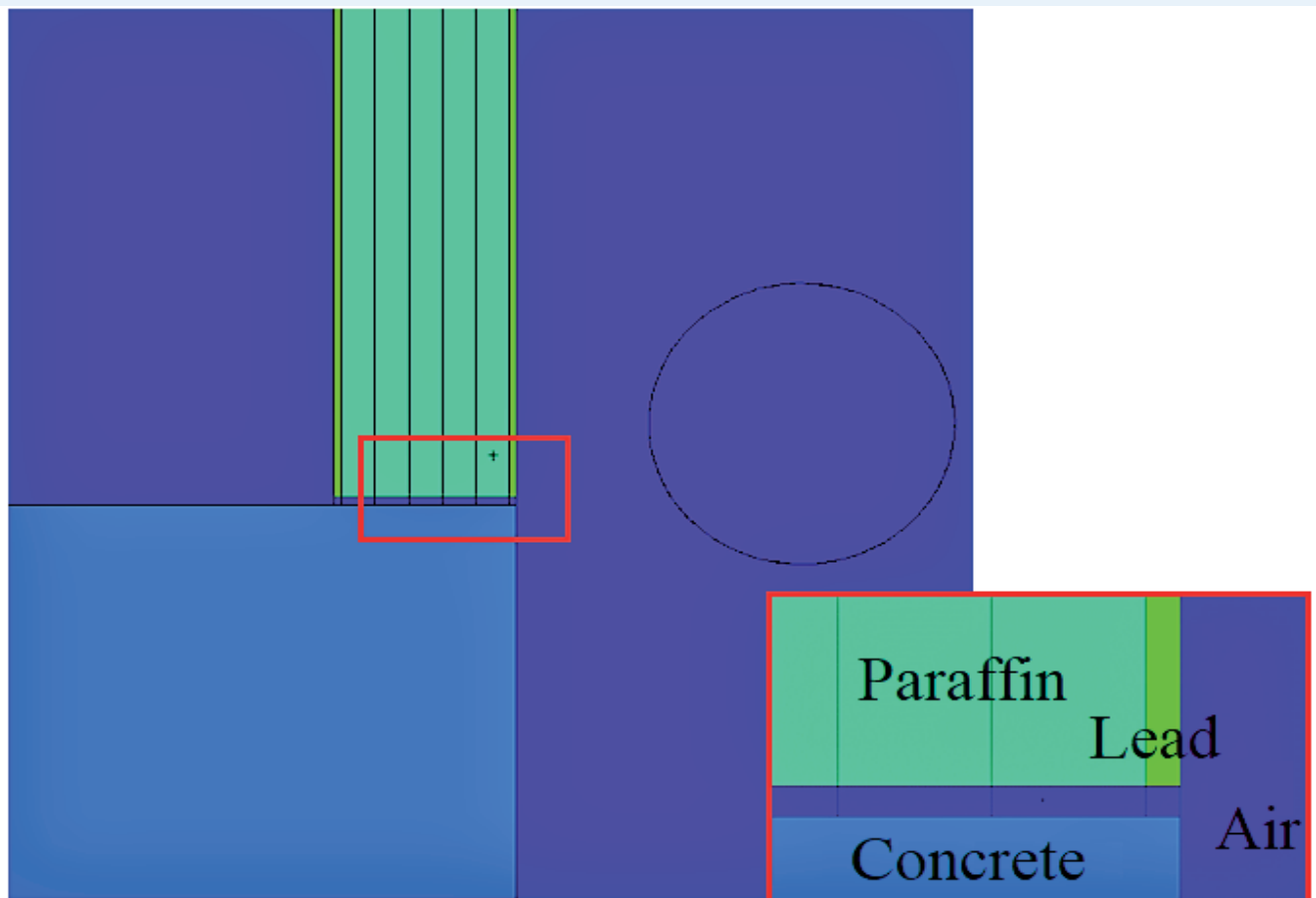


Figure 3 Simulated gap between door and floor

3. Overlap

Where different materials for shielding are used, there may occur leakage radiation due to a lack of shielding material. The efficiency of three different actions was evaluated (fig. 4) with 15 MeV. First the addition of concrete blocks (1), second the extension of the door (2) and third the closing of the gap between door and wall (3) was considered.

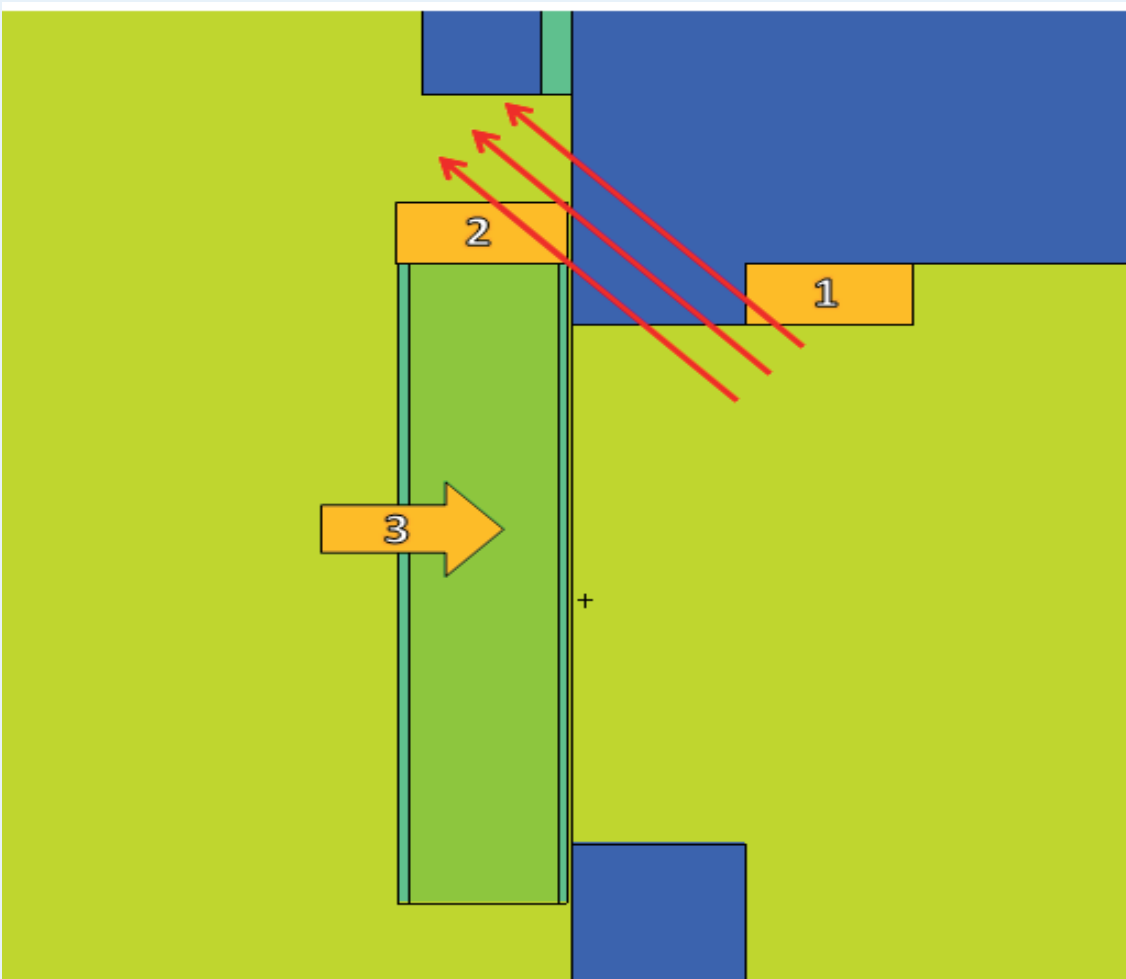


Figure 4 Three possible actions reducing the leakage radiation due to oblique radiation

Results

1. Ducts

In general, bent ducts have better shielding characteristics. To achieve adequate shielding for neutrons and high energy gamma rays, the duct diameter is not as important as a bent duct (fig. 5).

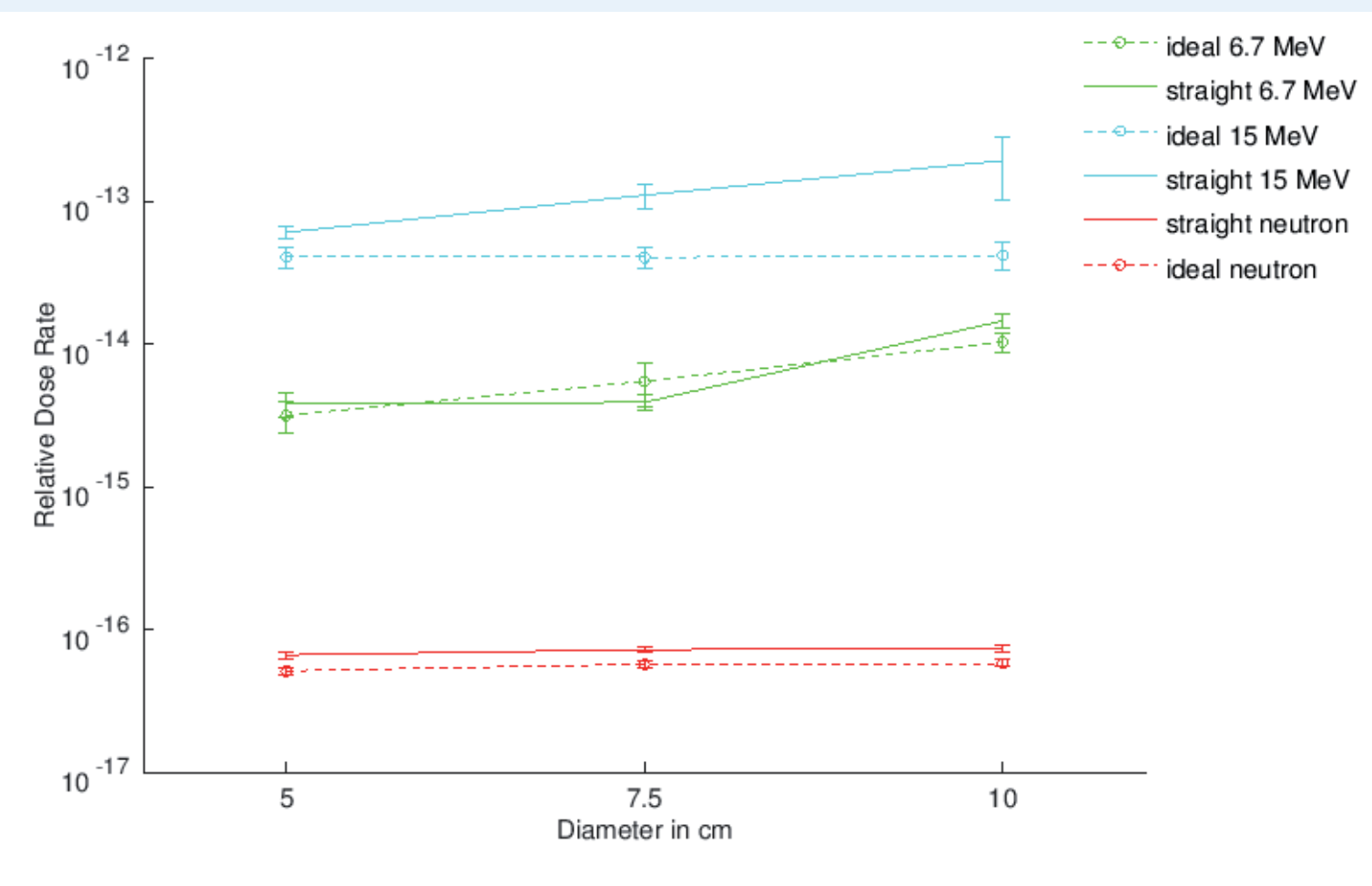


Figure 5 Comparison of dose rates for ducts

2. Gaps

The measured dose rate depends for low energies like 6.7 MeV highly on the gap size. For neutrons and higher energies the gap size is not as important (fig. 6).

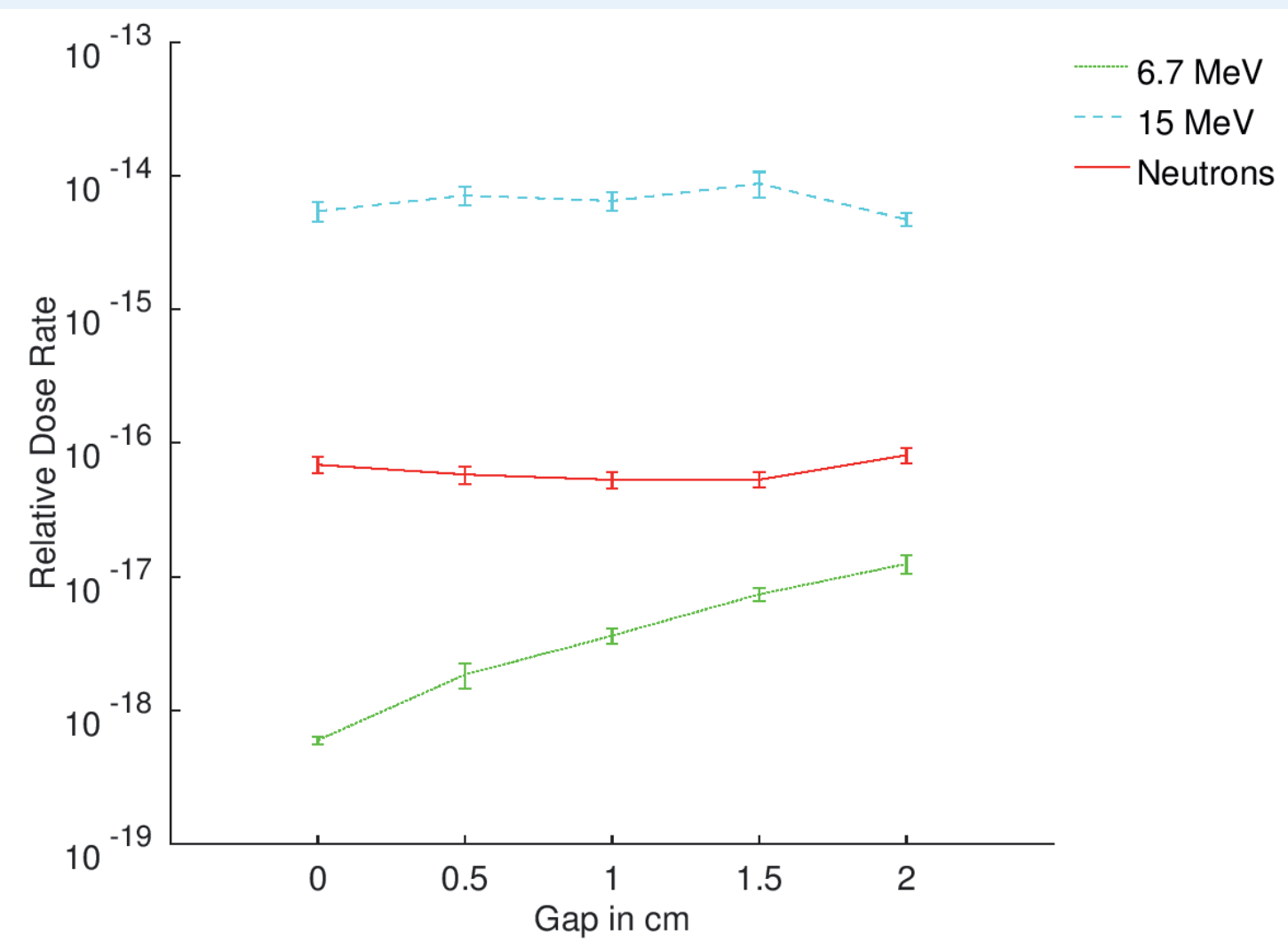


Figure 6 Relative Dose Rate behind the door in dependence to the gap size

3. Overlap

We can conclude that the avoidance of a gap between wall and door is not an efficient method (fig. 7). Extending the door reaches better attenuation. The usage of concrete blocks seems to be a practicable and cost-efficient method.

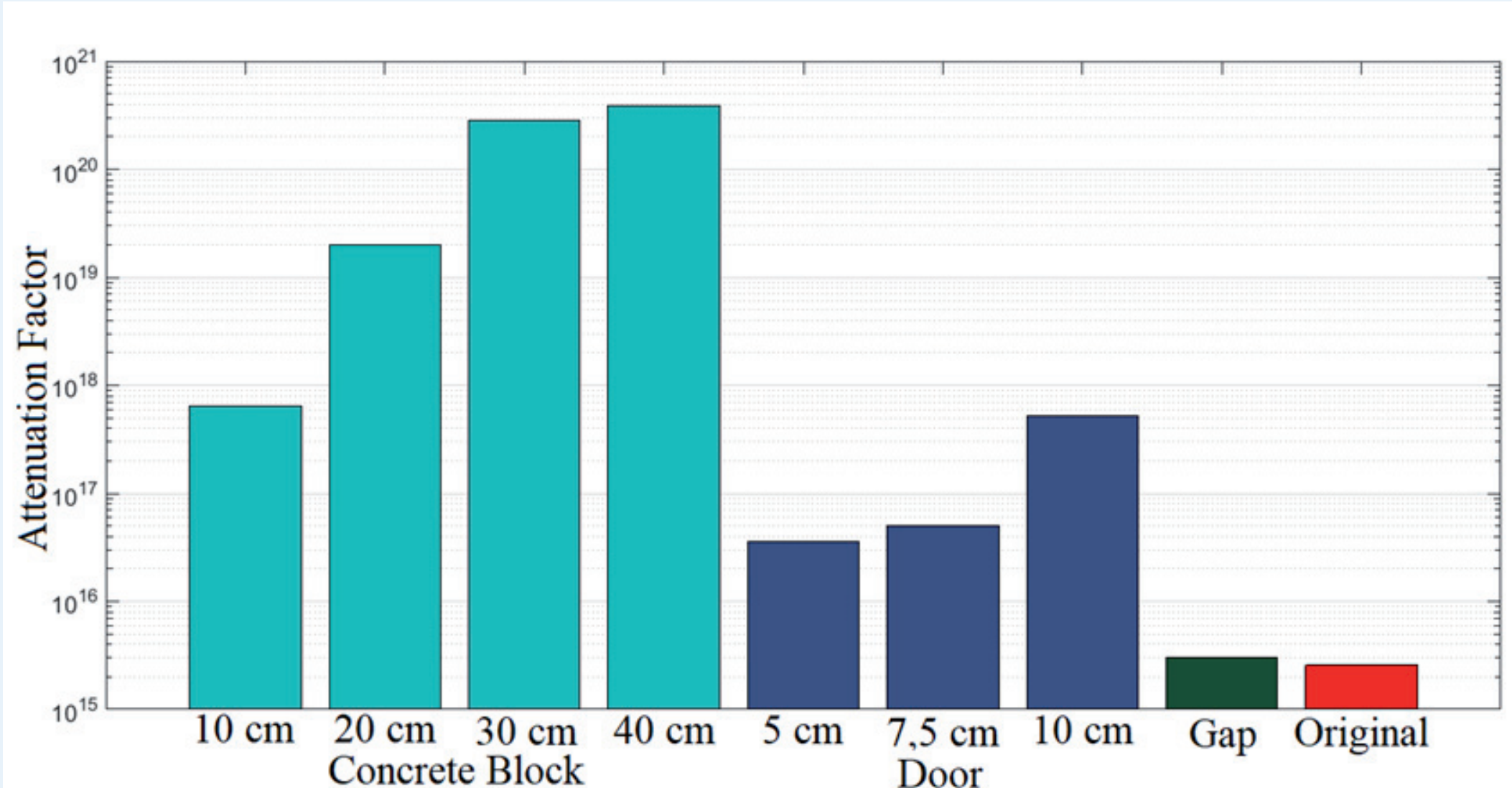


Figure 7 Attenuation for different shielding methods

Conclusion

In all cases, we see that reduction of gaps and ducts is important for lower energies. Especially for 6.7 MeV we notice that a decrease of diameter or gap also leads to a decrease of dose rate behind these structures. Decreasing door gaps and using small duct diameters decrease the dose rate perceptible for accelerators with lower energies.

For higher energies, where neutron creation has to be considered, we recommend bent ducts, because they decrease the dose rate considerably.

For problems with leakage radiation due to a lack of overlapping materials, we recommend the retrospective installation of concrete blocks. Also, the extension has a good impact on the reduction of leakage radiation.

References:

- [1] DIN 6847-2:2014-03, Medical electron accelerators - Part 2: Rules for construction of structural radiation protection
- [2] IAEA, 2006. Radiation Protection in the Design of Radiotherapy Facilities, Safety Report Series No. 47, Vienna
- [3] D.Pellowitz, 2008. MCNPX User's Manual, Version 2.6.0, Los Alamos National Laboratory



Eye lens doses of medical staff incurred in interventional procedures in Poland

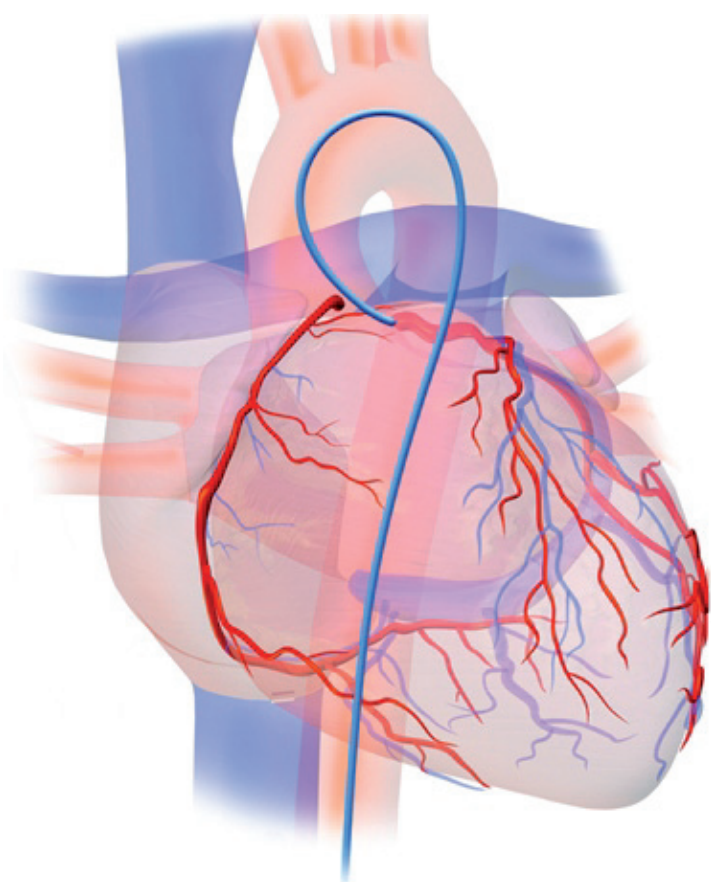
Agnieszka Szumska, Maciej Budzanowski, Izabela Milcewicz-Mika, Renata Kopeć
Institute of Nuclear Physics Polish Academy of Sciences (IFJ PAN), Krakow, Poland

INTRODUCTION

Radiation exposure in interventional cardiology procedures has recently been the subject of numerous studies. Because of the introduction of new techniques and equipment and the ever-increasing use of radiation in medicine, it is important to continue to assess the doses resulting from medical exposure to radiation.

Also the attention devoted in recent years to eye lens dose assessment was increased due to evidence that cataracts can be induced by ionizing radiation at dose levels lower than previously expected. Because of the potential for doses received by interventional cardiology personels to be high, it is important that they are monitored properly and the dose to the eye lens should be evaluated more carefully.

MATERIAL AND METHODS



PROCEDURES

The study included 75 cases of common diagnostic and therapeutic interventions.

DOSEMETERS

Used thermoluminescence detectors have been produced at the Institute of Nuclear Physics PAN in Krakow. Readouts were performed using the TLD RADOS Dosimetry System (Mirion Technology Oy).

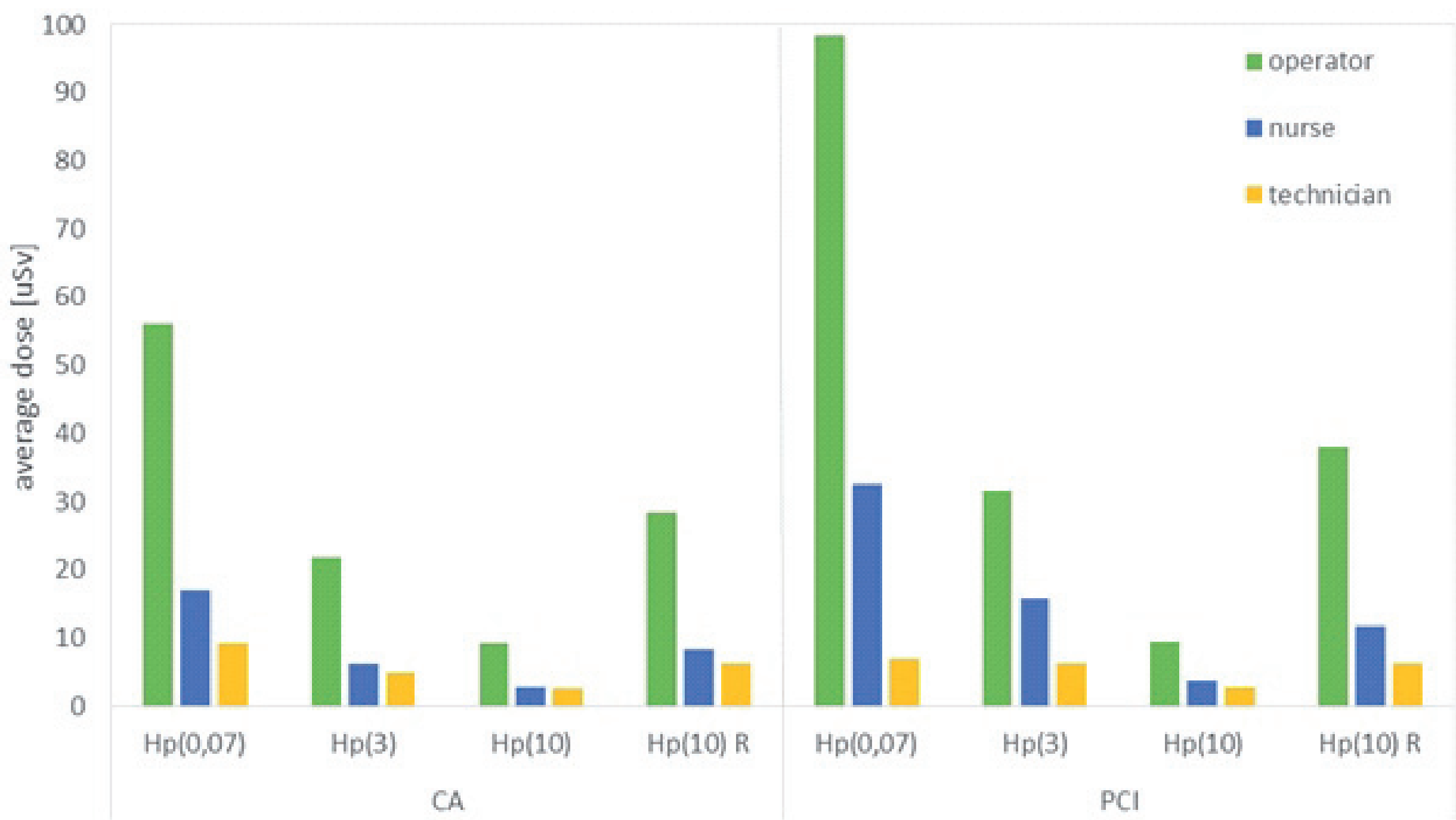
	Hp(10)	Hp(0.07)	Hp(3)
Dosimeter			
Detectors	4 x MCP-N 4.5x0.9 mm	1 x MCP-N 4.5x0.9 mm	1 x MCP-N 4.5x0.9 mm
Phantom	Slab – 30x30x15 cm; PMMA	Rod diameter: 1.9 cm, height: 30 cm; PMMA	Cylindrical 20x20 cm PMMA wall, Fill water
Pre-irradiation annealing	20 min/75°C		
Readout/Post-irradiation annealing	16 s/260°C		
Dedicated localization	chest	finger	head

Each person from medical staff wore 4 dosimeters with high sensitive MCP-N (LiF:Mg,Cu,P) detectors:

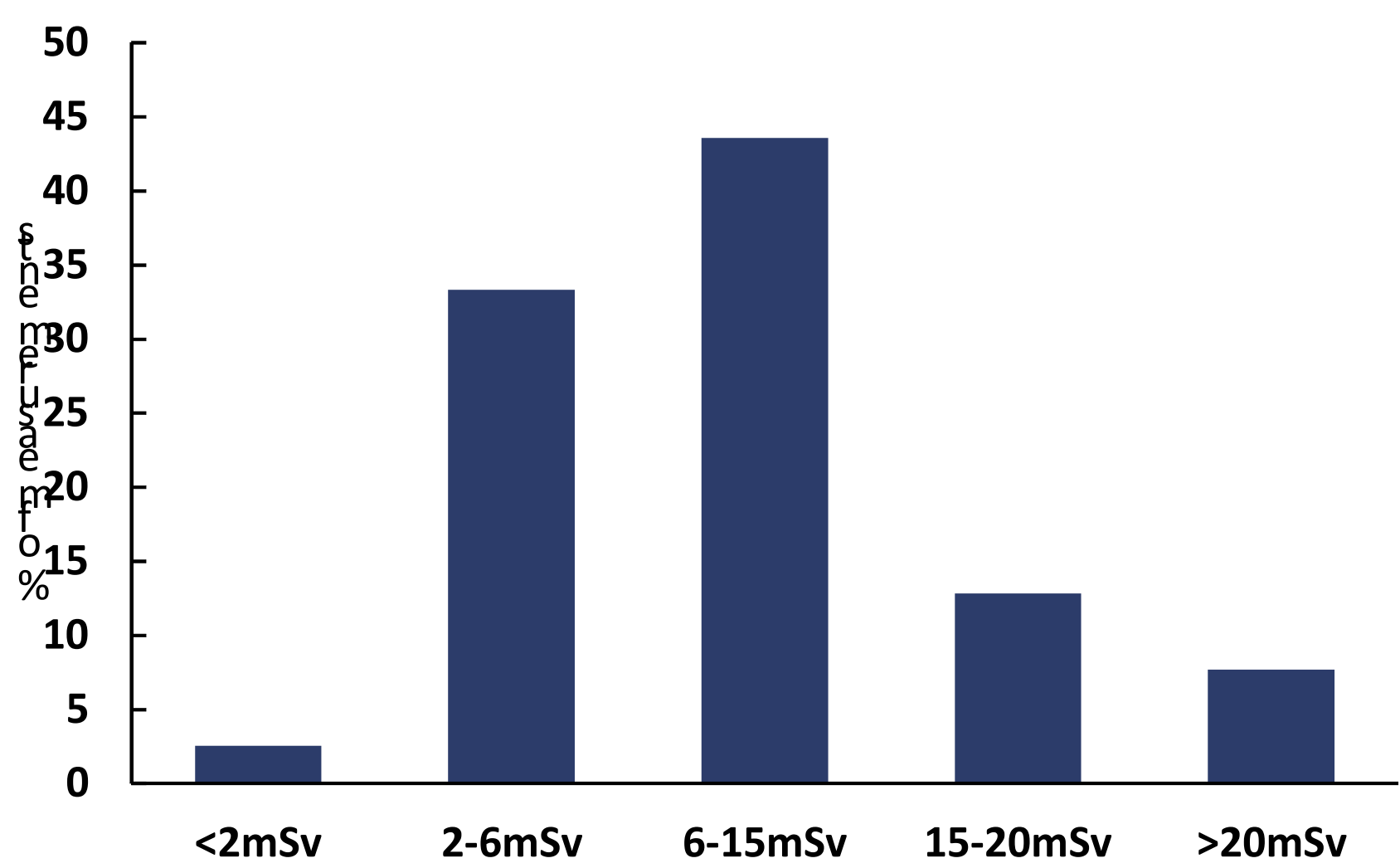
- whole body dosimeters for measuring Hp(10) worn under apron,
- whole body dosimeters for measuring Hp(10)R worn above apron,
- ring dosimeters worn on finger for measuring Hp(0.07)
- eye lens dosimeters for measuring Hp(3)



RESULTS



Average personal doses per procedure to CA and PCI procedure.



Frequency distribution of estimated annual doses to the lenses of the eyes.

	Eye dose [μSv]/procedure
	Mean eye lens dose ± variation (min - max)
This study	73 (1 ÷ 165)
[Antic et al., 2013]	121 ± 84 (4,5 ÷ 370)
[Donadile et al., 2011]	52 ± 77 (4 ÷ 644)
[Kim et al., 2008]	170 ÷ 439
[Vano et al., 1998]	170 (53 ÷ 460)
[Efsthopoulos et al., 2011]	13
[Bor et al., 2009]	72 (32÷107)
[Martin, 2011]	66 (5 ÷ 439)
[Pratt & Shaw, 1993]	15 ÷53
Lie et al., 2008	44

Comparison of published data on eye doses for interventional cardiology procedures

CONCLUSIONS

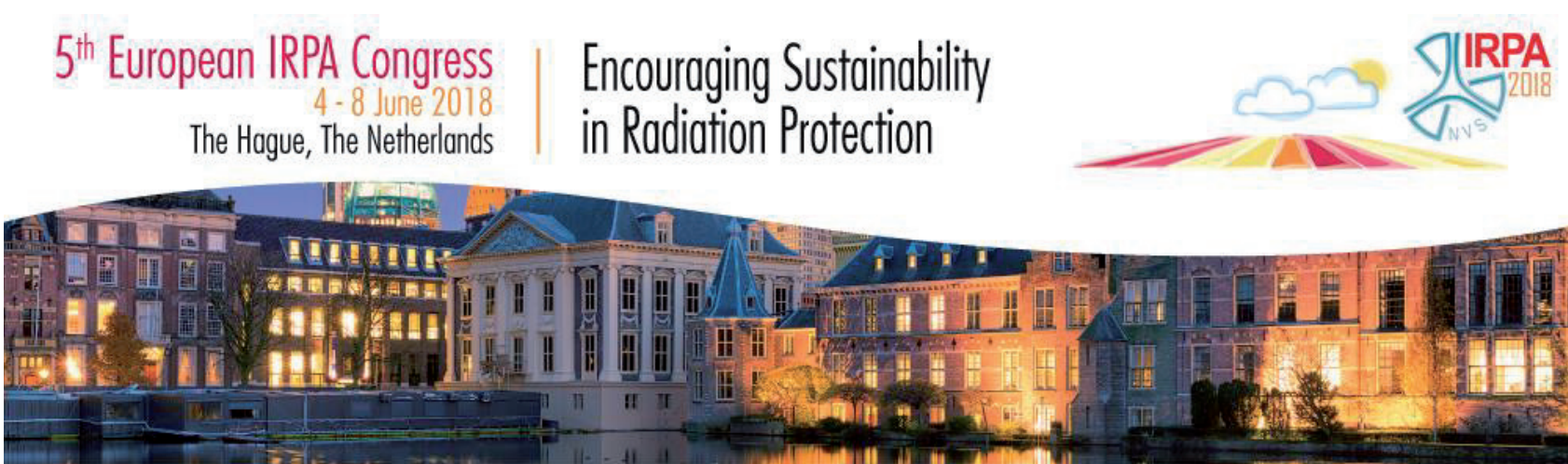
- Operators always received the highest doses, followed by nurses and technicians.
- Many workers exceed 20mSv/year for eye lens, and therefore radiation protection equipment like ceiling screen and eyeglasses, is highly recommended for medical staff to limit their risk of radiation-induced lens opacities and cataracts.
- The highest doses were monitored on the finger dosimeter, lower for the whole body dosimeter on apron then for eye lens dosimeter. The lowest doses were monitored for whole body dosimeter under apron.

Eye lens dosimetry for interventional procedures in cardiology

Grazyna Krajewska

Konwaliowa St.7, 03-194 Warsaw, POLAND; tel. 22 811 15 15

email: krajewska@clor.waw.pl



The eye lens is one of the most sensitive organs for radiation injury and exposure might lead to radiation induced cataract. Recently, the International Commission on Radiological Protection (ICRP) recommended a reduction in the annual dose limit for occupational exposure for the lens of the eye from 150 to 20 mSv, averaged over a period of 5 years, with the dose in a single year not exceeding 50 mSv. These recommendations are introduced in the European directive 2013/59 (EURATOM,2013).

Methods

This study investigated eye lens dosimetry in two medical institutions in Warsaw during a routine year of professional activity. The measurements were performed in the Hemodynamics Laboratory of Mazovia Brodnowski Hospital and the Heart and Angiography Laboratory of the Institute-Memorial Children's Health Center.



The radiation exposure measured in a normal working schedule of a intervention radiologists during 3 months and this cumulative eye lens dose was extrapolated to 1 year. Doses to the lens of the eye were estimated by measuring the operational quantity $H_p(3)$ with dedicated individual eye-lens dosimeter type EYE-DT™. This dosimeter uses MCP-N (LiF:Mg,Cu,P) thermoluminescent detectors, covered with a polyamide capsule and was optimized for X-ray exposures typical for intervention radiology.

Body and skin dose measurements were also performed, estimating $H_p(10)$ and $H_p(0.07)$ values.



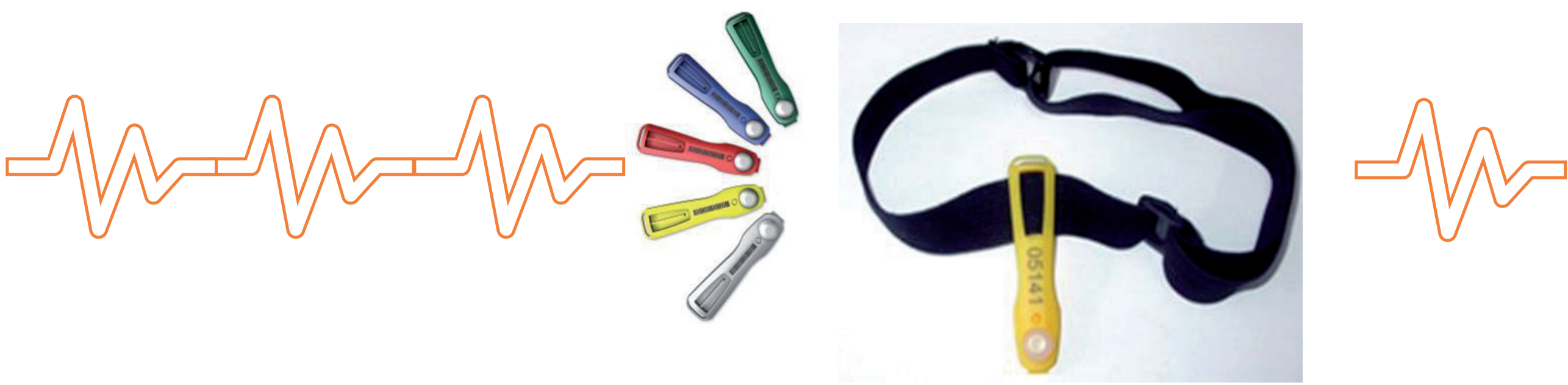
Results

The Hemodynamics Laboratory of the Mazovian Brodnowski Hospital is equipped with a modern digital angiograph Philips Allura type (70 kV, 480 mA). There are about 1200 coronary angiography and approx. 700 coronary angioplasty procedures annually. The laboratory performs: coronary angiography, coronary artery disease, coronary stent implantation and others.

The Center for Cardiac Catheterization and Angiography is located in the Memorial of the Children's Health Center (IPCZD), where under the control of X-rays are performed invasive cardiovascular diagnostic tests and therapeutic treatments in the field of cardiology and interventional radiology in children. The angiographies are intended to illustrate the vascular architecture of the pathological organs and, in the case of the heart, visualization of individual heart cavities and abnormalities.

Employee	Hp(3) [mSv]	Hp(10) [mSV]	Hp(0,07) [mSv]
1	0,21	X	X
2	X	X	X
3	0,02	X	0,44
4	0,21	X	0,14
5	X	X	X
6	X	X	X
7	0,64	X	X
8	X	X	X
9	X	X	X
10	2,26	X	6,2
11	X	X	X
12	0,46	0,31	1,24
13	0,28	X	X
14	X	X	X
15	0,08	X	X
16	0,73	x	0,59
17	X	X	0,29
18	X	X	X
19	X	X	X
20	0,41	0,20	X
21	0,39	X	X

X = limit of detection (0.1 mSv)



The estimated annual eye lens doses for investigated radiologists working in interventional cardiology, range from a minimum of 0.1 mSv to a maximum of 3.0 mSv, with an **average dose of 1.0 mSv**.

This study demonstrated that the estimated annual eye lens dose is well below the revised ICRP's limit of 20 mSv/year. However, we recorded increased doses during invasive cardiovascular diagnostic tests and therapeutic treatments in the field of interventional cardiology procedures. The interventional radiology causes the radiation risk exposure of eye lens both for persons who directly perform treatments a well as for the accompanying persons.

There is probably the correlation between doses on the skin (measured by the ring termoluminescent dosimeter) and doses on the eye lenses of the staff (numerical numbers not captured due to too few results), but further research is required.

Employee	Hp(3) [mSv]	Hp(10) [mSv]	Hp(0,07 [mSv])
1	X	X	X
2	X	X	X
3	X	X	X
4	X	X	X
5	0,33	X	X
6	X	X	X
7	X	X	X
8	X	X	X
9	X	X	X
10	X	X	X
11	X	X	X
12	X	X	X
13	0,19	X	X
14	X	X	X
15	X	X	X
16	X	X	X
17	X	X	X
18	X	X	X
19	X	X	X
20	0,03	X	X
21	X	X	X
22	0,13	X	X
23	X	X	X

With radiation induced cataract being explained as a possible stochastic effect, without a threshold dose, radiologists and anesthesiologists who regularly work in a radiological environment should stay awake and vigilant. These persons should also preserve radiation safety standards at all times, which includes adequately protective equipment, keeping distance, routine monitoring and periodic training in occupational safety.

Conclusions

- The interventional cardiology causes the radiation risk exposure of eye lens (doses have been registered both in persons directly performing treatments and the accompanying persons too).
- In the group of surveyed employees, no dose limit for the exposed workers was exceeded, the value did not exceed 3 mSv per year).
- There is probably the correlation between doses on the skin (measured by the ring dosimeter) and doses on the eye lenses of the staff (numerical numbers not captured due to too few results), but further research is required.

Acknowledgment

The work was funded by the Ministry of Science and Higher Education. Many thanks to the Radiological Protection Inspectors from the hospitals where the research was carried out - Mrs. Radoslaw Kulinski and Mariusz Masiuk.

Influence of low doses X-ray radiation exposure on human stem cells

Usupzhanova DYu ^{a*}, Astrelina TA ^{a*}, Nikitina VA ^{a*}, Suchkova YuB ^{a*}, Kobzeva IV ^{a*}, Brunchukov VA ^{a*}, Rastorgueva AA ^{a*},
Osipov AN ^{a*}, Barabash I.M. ^{a*}, Gordeev AV ^{a*}, Samoilov AS ^{a*}.

^{a*}State Research Center
Burnasyan Federal Medical Biophysical Center
FMBA of Russia



*sources of low-dose radiation

Relevance of the topic: along with background radiation a person is constantly exposed to low doses of radiation exposure, during medical diagnosis and treatment, air travel, and also due to professional activities. Effects of low radiation doses remain insufficiently studied, in particular, on stem cells

Research objective: to study the effect of low-dose X-ray irradiation on human stem cells to assess remote consequences *in vitro*.

MATERIALS AND METHODS

MATERIALS: In the study were used MSCs of the bone marrow, placenta, corneal limbus and mucosal gum tissue human

METHODS:

- Cultivation of cells
- Irradiation of cells
- Evaluation of viability
- Immunophenotyping
- Evaluation of proliferative activity
- Evaluation of focuses γ H2AX (estimation of double-strand breaks DNA)
- Cytogenetic methods

DESIGN OF THE EXPERIMENT

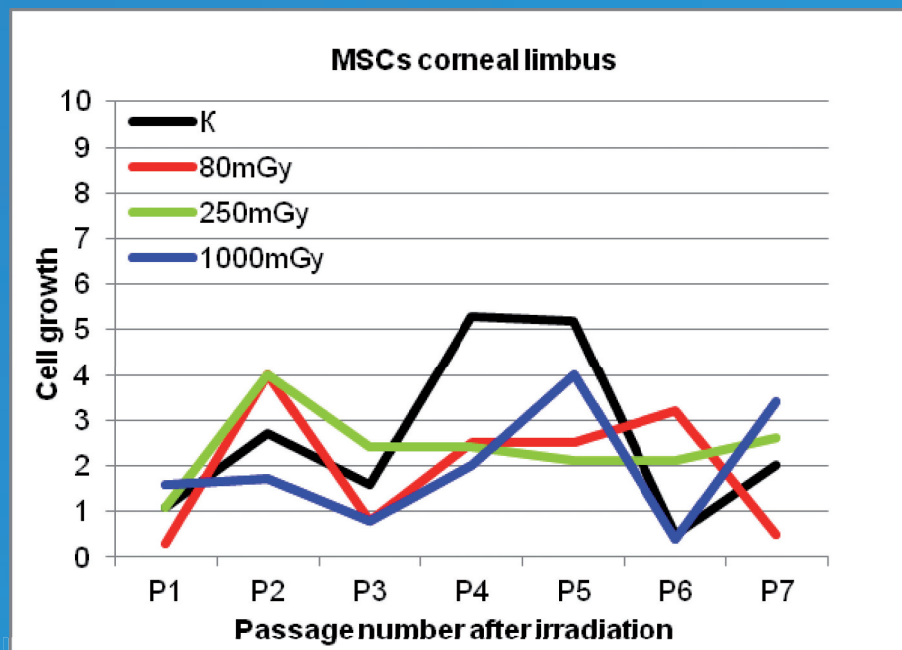
Irradiation MSCs was carried out at doses of 80 mGy, 250 mGy and 1000 mGy

Evaluation of :	MSCs of mucosal gum tissue	MSCs of placenta	MSCs of corneal limbus	MSCs of bone marrow
Focuses γ H2AX	+			
Chromosome aberrations		+		
Level of surface antigens		+	+	+
Proliferation		+	+	+

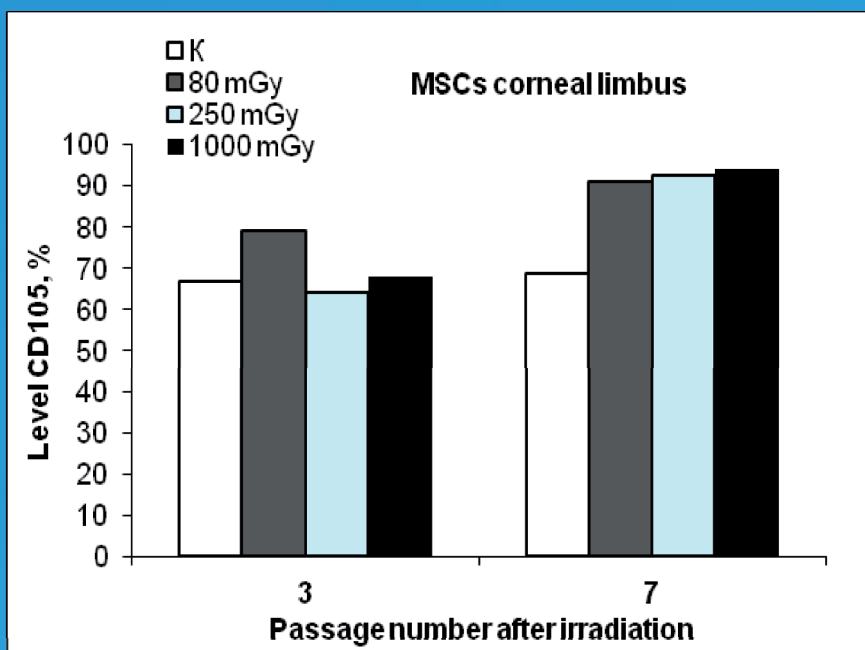
Irradiation
at the 6 passage

Cultivation continued until
the 13th passage

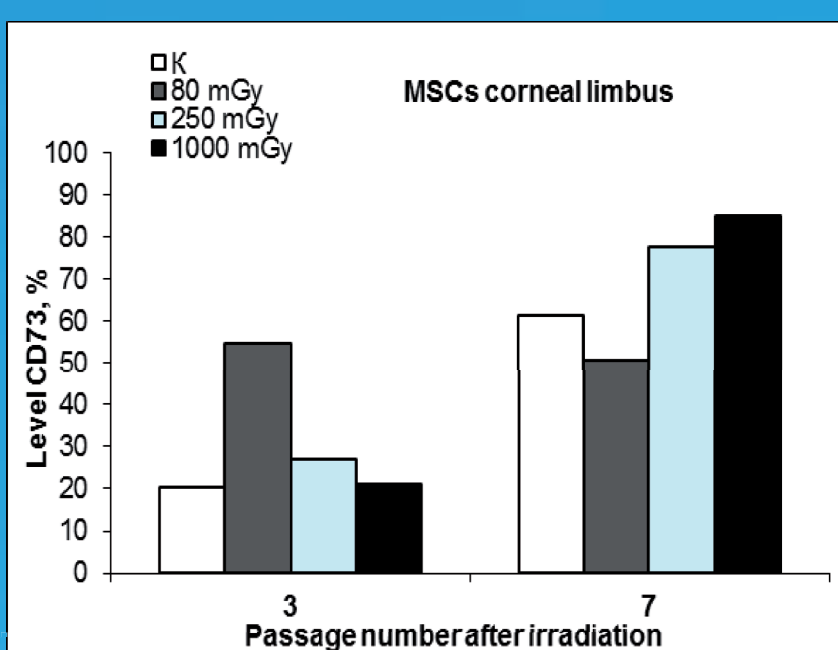
MSCs of the corneal limbus



proliferative activity



antigen CD105 level



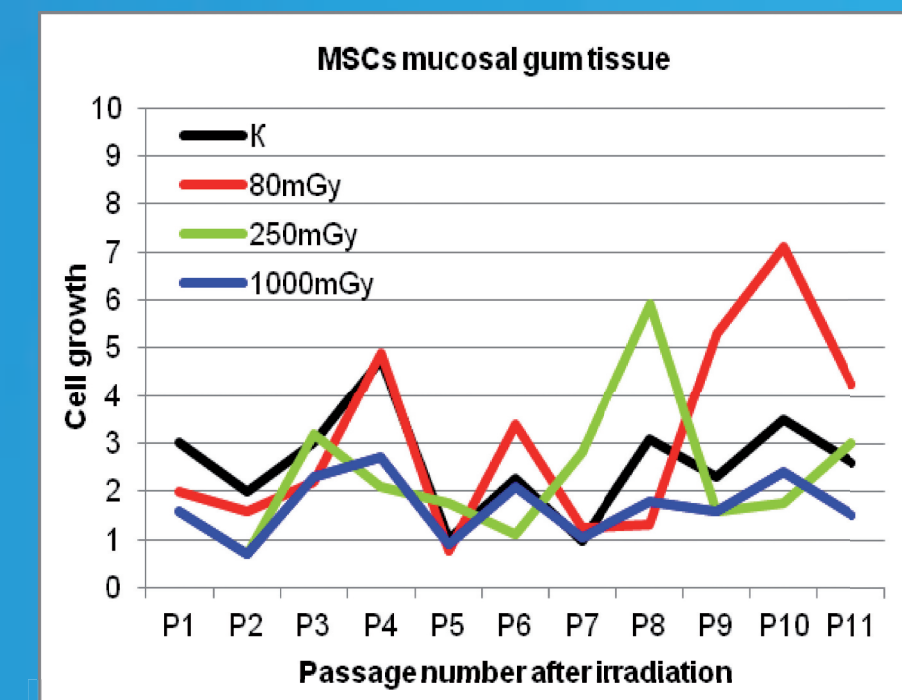
antigen CD73 level

An increase in the levels of antigens CD105 and CD73 MSCs of the corneal limbus irradiated at doses of 250 and 1000 mG was observed with prolonged cultivation, also in the remote passages in this group there was an increase in the level of proliferation in these doses.

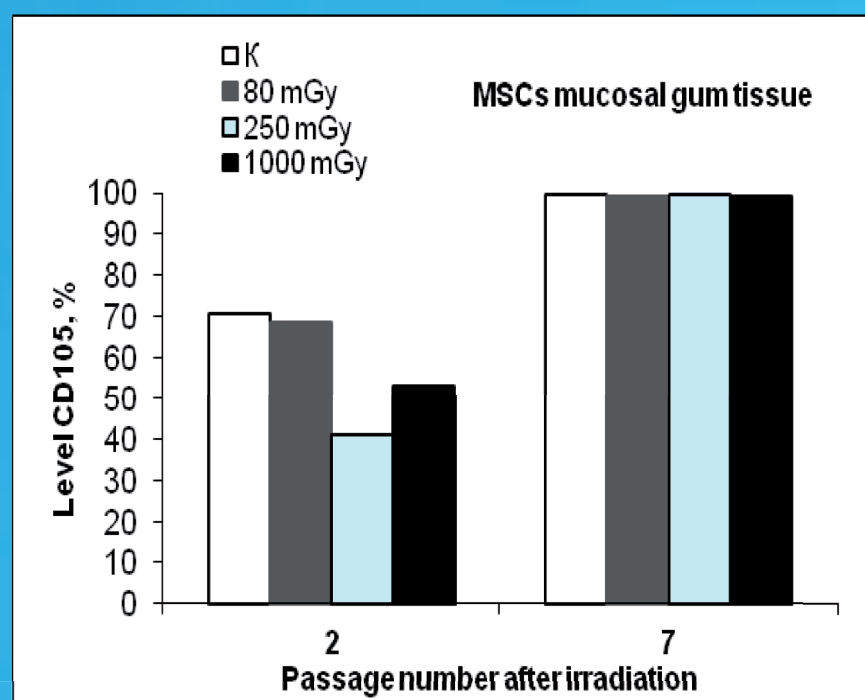
Irradiation
at the 3 passage

Cultivation continued until
the 14th passage

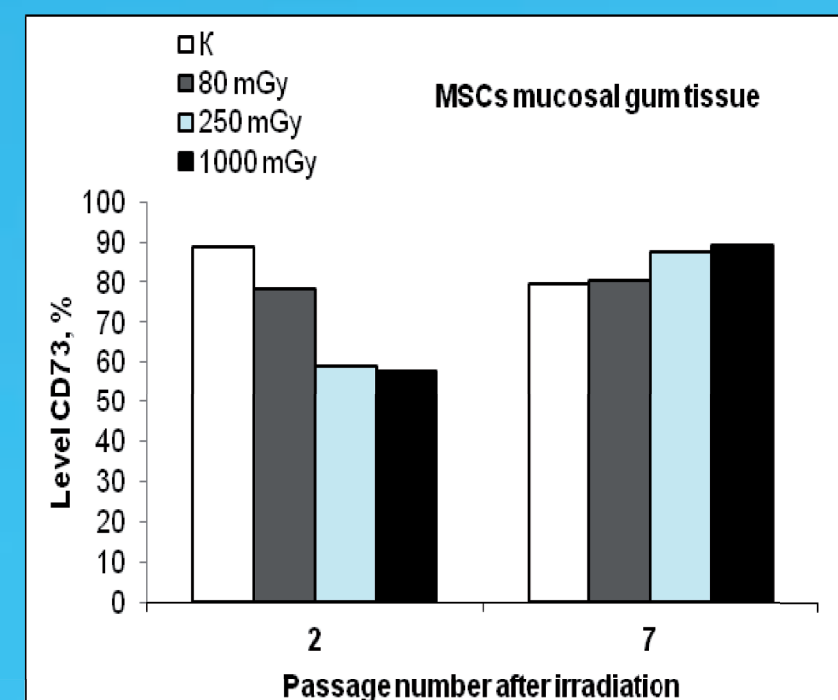
MSCs of the mucosal gum tissue



proliferative activity



antigen CD105 level



antigen CD73 level

There were significant changes in the level of antigens at doses of 250 and 1000 mGy, but with prolonged cultivation the level of antigens is equalized with the control group, and the proliferation in these doses is inhibited. In general, the stimulating effect of 80 mGy dose can be noted for this group:

increase in the level of proliferation, the number of chromosomal aberrations after irradiation increased most exactly in this dose.

Conclusion: The results of study showed that low doses of X-ray irradiation contribute to the formation and accumulation of lesions in stem cells, which can lead to disruption of normal vital activity of stem cells, in particular oncotransformation.

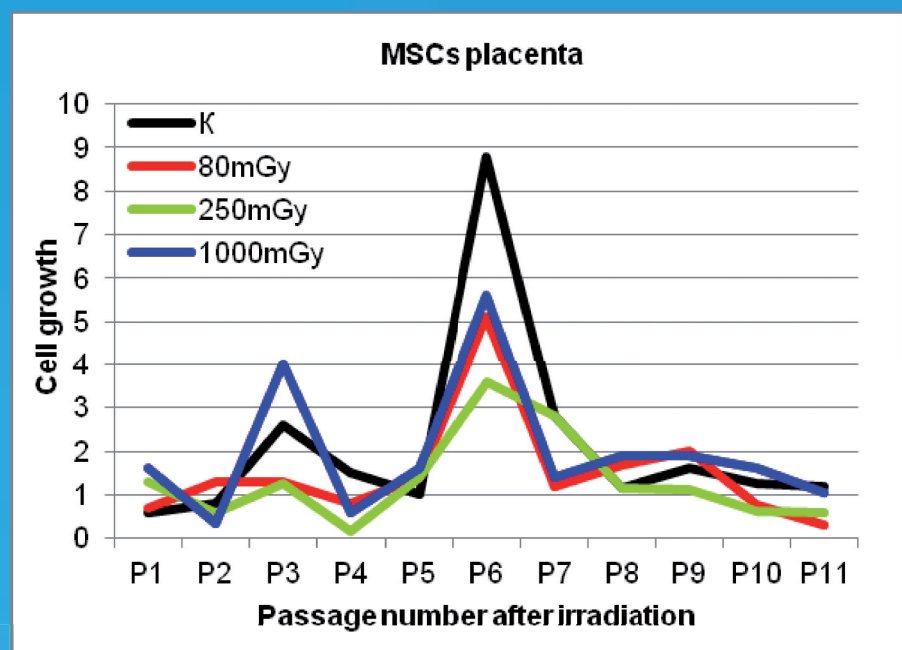
Groups	Passages	
	Passage 5	Passage 10
Control	7.5%	10%
80 mGy	20.75%	5%
250 mGy	11.4%	6%
1000 mGy	12.5%	8.8%

cytogenetic study of
chromosomal aberrations

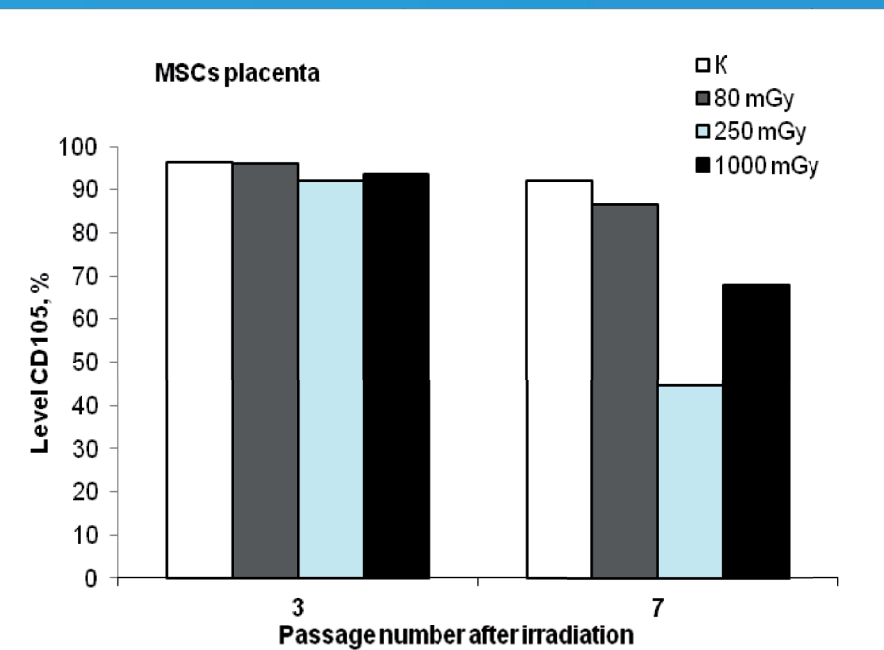
Irradiation
at the 3 passage

Cultivation continued until
the 14th passage

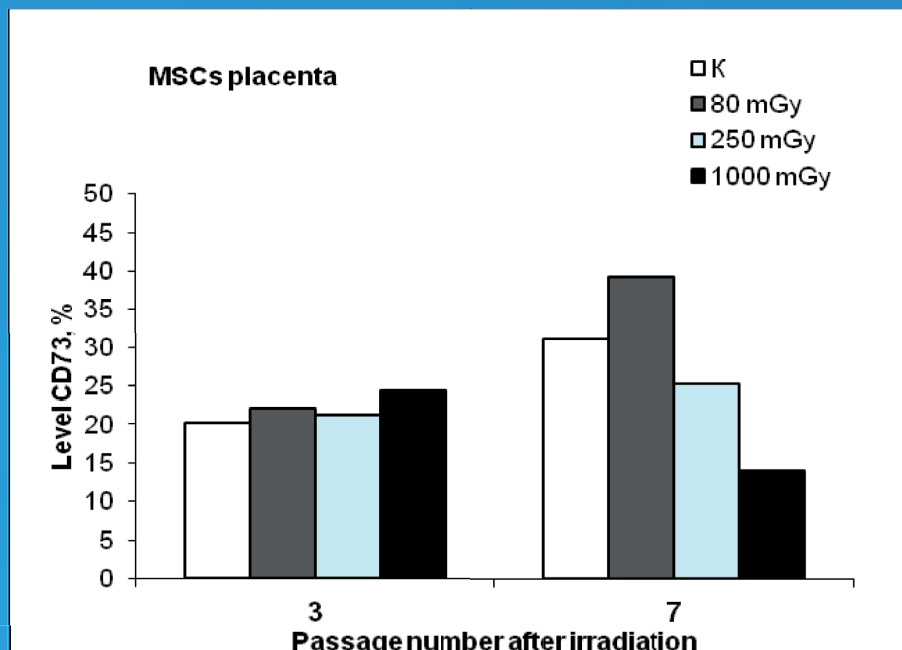
MSCs of the placenta



proliferative activity



antigen CD105 level



antigen CD73 level

For MSCs of the placenta was also characterized by an increase in the level of proliferation at a dose of 1000 mGy with prolonged cultivation.



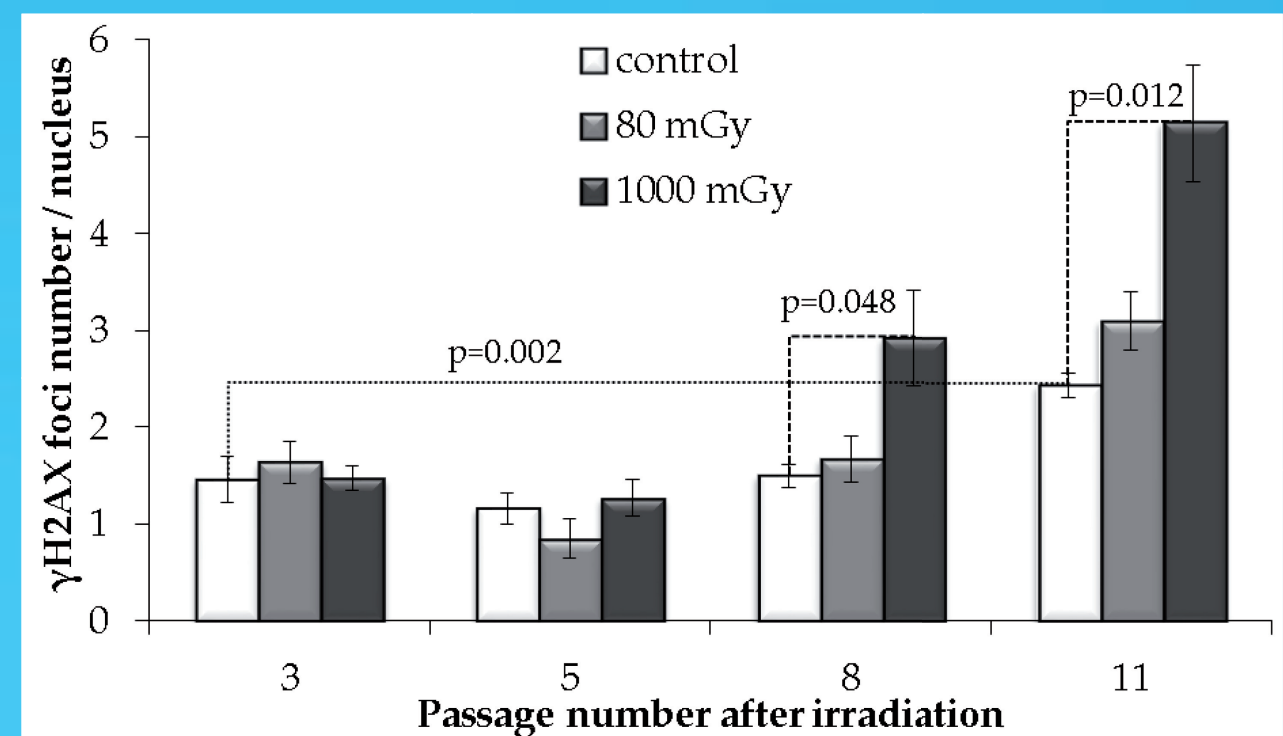
Control 80mGy 250mGy 1000mGy

Visual assessment of the growth of MSCs of the placenta at the 10th passage after irradiation

Irradiation
at the 3 passage

Cultivation continued until
the 11th passage

MSCs of the bone marrow



focuses γ H2AX

The number of histone focus γ H2A, indicative of double-strand breaks DNA in the MSCs of the bone marrow, as the number of chromosomal aberrations a dose-stimulating effect was 80 mGy at the first passage after irradiation.

With prolonged cultivation the number of chromosomal aberrations decreases in all doses in comparison with the control group, and double-strand breaks DNA increases. A negative effect of the dose of 1000 mGy is noted: the number of histone foci γ H2A significantly increases and the chromosome aberrations decrease not so much. We can conclude that the method for determining histone focus γ H2A unambiguously demonstrates the negative effect of a dose of 1000 mGy, while the negative effect of this dose on chromosome aberrations can be said about their decrease in comparison with other doses, but not with the control group. Thus, draw a conclusion about malignant transformation of bone marrow MSC after prolonged cultivation after irradiation with a dose of 1000mGy.



Physical aspects of angiographic procedures with CO₂: dosimetry and mechanics of a gaseous contrast medium

Pier Luca Rossi¹, Ivan Corazza², Alessandro Lombi¹, Jim Carid³, Romano Zannoli²

¹ U. Medical Physics, University of Bologna, Bologna, Italy

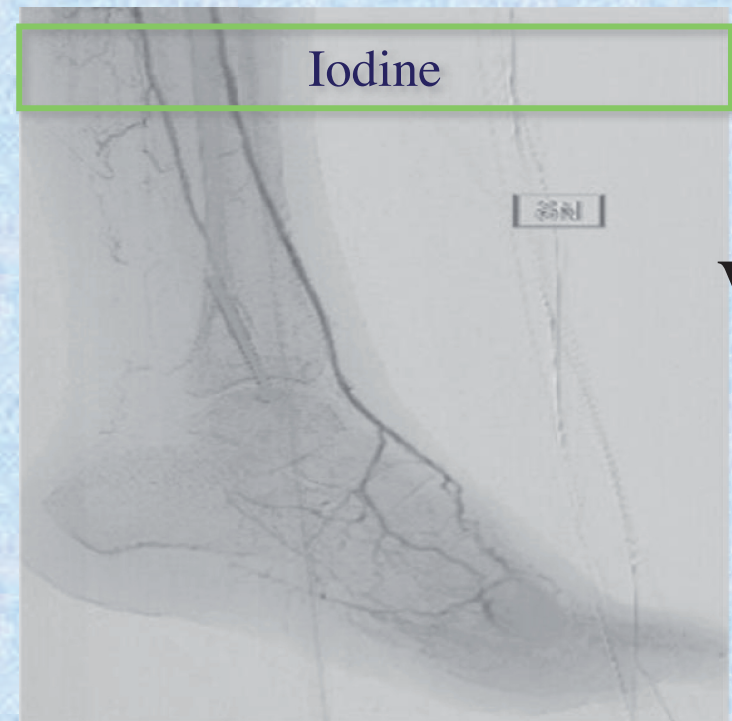
² Dept. DIMES, University of Bologna, Bologna, Italy

³ School of Medicine, Tulane University, New Orleans (LA), USA

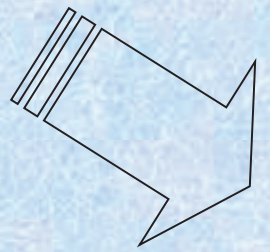
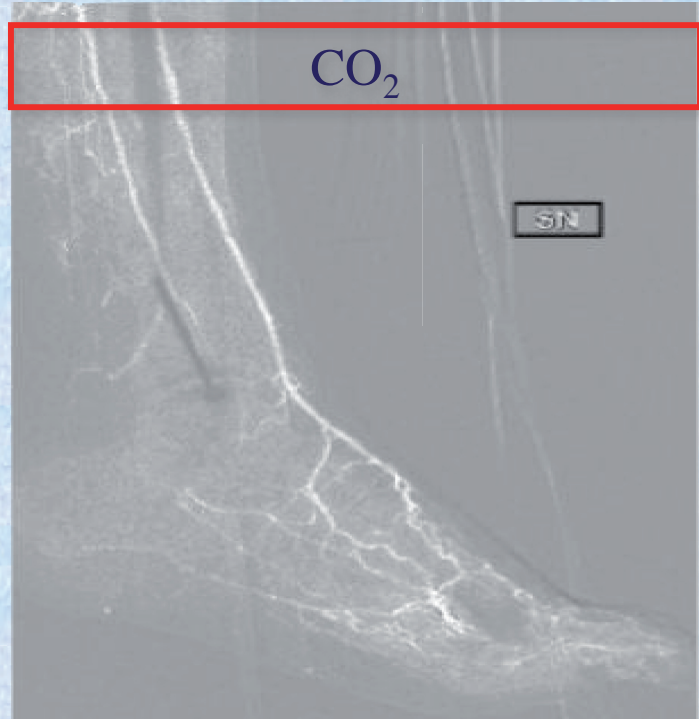
AIM - ABSTRACT

The number of CO₂ angiography procedures is rapidly increasing, due to changes in patients' population, availability of safe gas-injectors and dedicated protocols, mainly based on post-processing algorithms (such as "image stacking", "pixel motion", "mask subtraction"). Even if the physical and radiological properties of gaseous and liquid Contrast Media (CM) are completely different, nowadays the approach to angiographic procedures with CO₂ and iodine does not present significant differences: why? To optimize the CO₂ angiographic procedures, in terms of image quality to dose ratio, it is mandatory to consider the mechanical and radiological aspects of the gaseous CM, with respect the iodine one, such as the haemodynamic parameters of the patient.

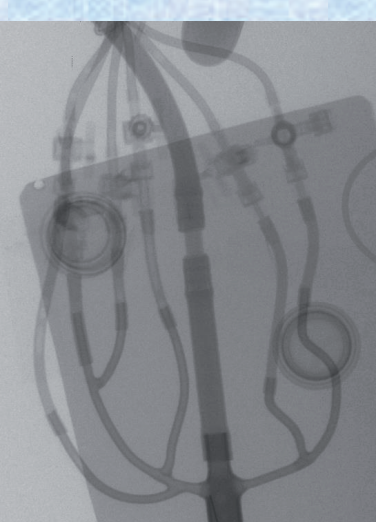
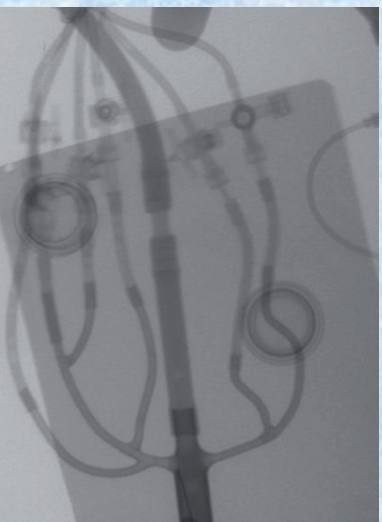
DSA imaging



VS



BACKGROUND: CO₂ vs. TRADITIONAL CONTRAST MEDIUM (IODINE) in DSA



Simulation of injection of CO₂ in vessels and radiological images of the phantom (phantom is made with vessels of different gages, inlaid in plexiglass of different thickness)

OPEN QUESTIONS:

- CO₂ is a bubble-gas....does CO₂ completely fill the vessel?
- Probably, it is mandatory the definition of new protocols for X-ray apparatus in terms of kV, frame rate and times per frames to obtain images with great quality

... to «optimize» images in CO₂ Angiography, all major vendors introduce DEDICATED PROTOCOLS

PHILIPS

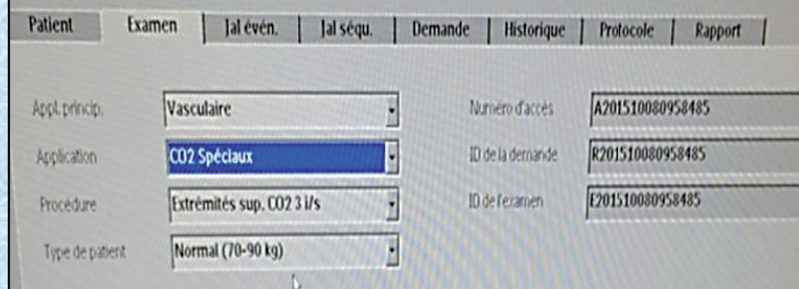
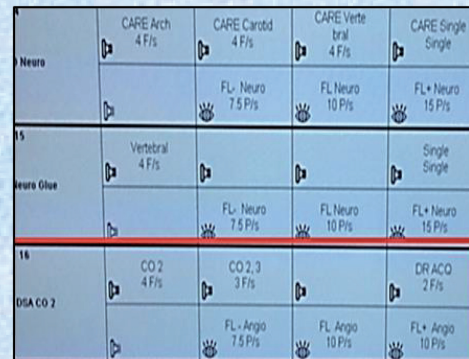
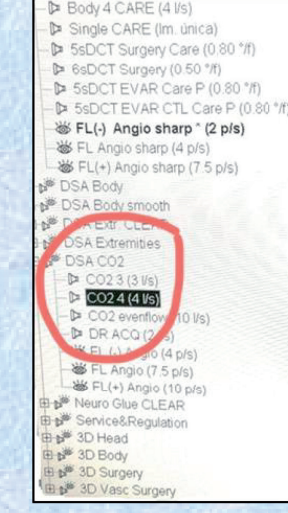
SIEMENS

TOSHIBA



ziehm imaging

SHIMADZU



How do these «dedicated protocols» work?

Which are the «modified» parameters?

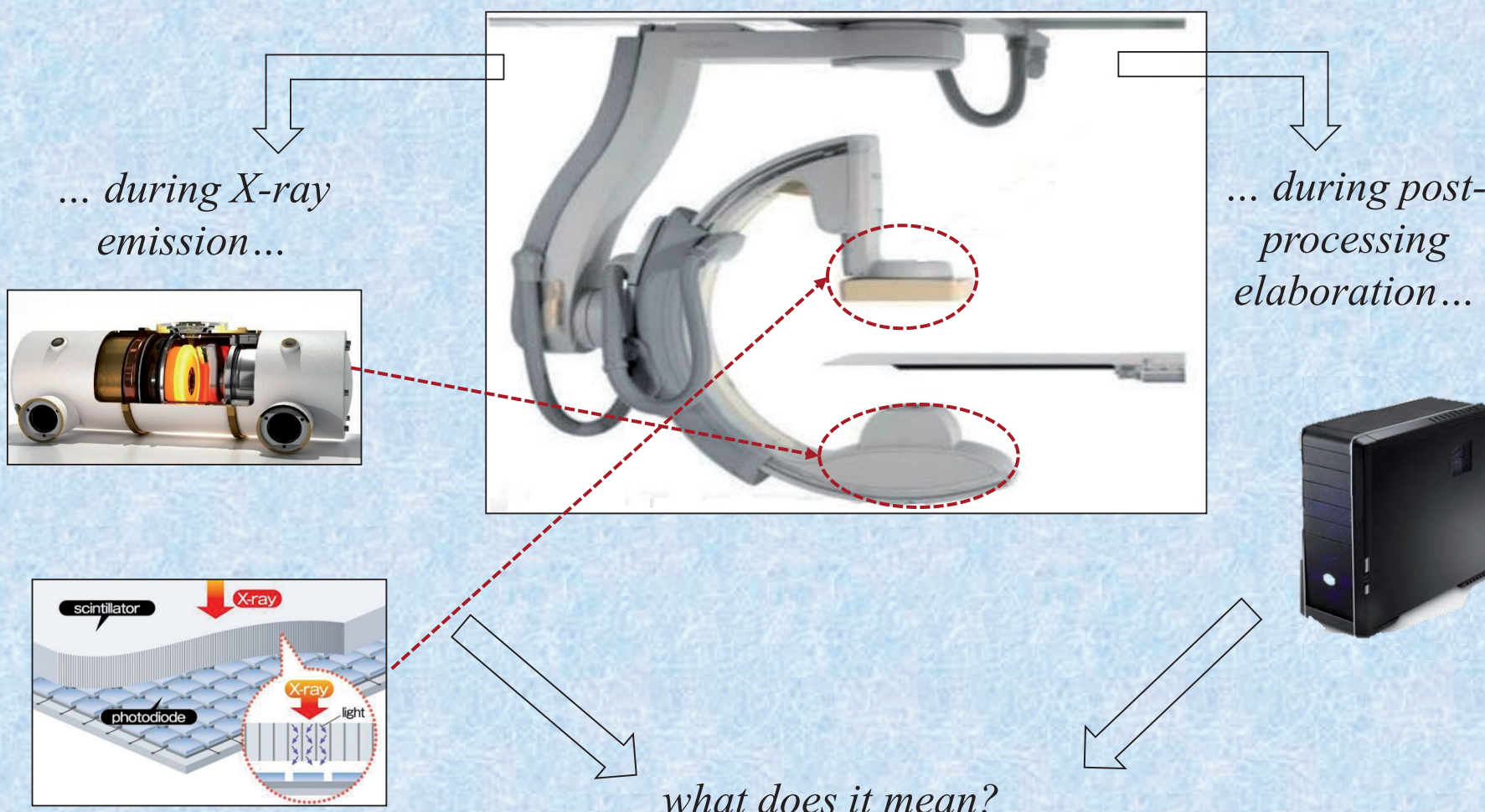
Do these parameters affect «perceived» image quality (and contrast) or even the «energetic shape» of the X-ray spectrum?

Despite typical liquid CM (i.e., iodine contrast medium), the visualization of a gas inside a vessel requires new considerations, related to the different dynamic behaviour and to the radiological characteristics. In fact, while the iodine CM is mixed with blood and has a sharp k-edge absorption peak at photon energy of 33.2 keV, CO₂ CM does not mix with blood but creates bubbles-train moving inside the vessel substituting blood.

Analysis of “dedicated protocols” for CO₂ DSA

- CO₂ doesn't mix with blood but substitutes it, so the radiological image quality is strictly related to the bubbles-trains moving inside the vessel with bubble dimensions that depend on injection parameters, blood flow and pressure. If a radiological system does not consider these aspects, a lot of data can be lost in the images.
- Since CO₂ is a gas and moves upwards, it is often necessary to change the patient position to fill the vessels of interest, avoiding pain during injections - so reducing involuntary movements between mask and images acquisition
- Iodine perfusion is very fast, but CO₂ requires time to fill and move along the vessel, depending on the blood flow. If the X-ray emission doesn't take care of it, the dose to the patient can be higher than other procedures, only due to longer emission-time.
- Since the linear absorption coefficients of CO₂ does not have any k-edge, the choice of the HV and current should be done with different LUT (look-up-table) if compared with Iodine procedures. At this moment, all X-ray apparatus uses the same AEC (Automatic Exposure Control) for all procedures, without any considerations about the type of contrast medium.

... CO₂ vs. I protocols could differ ...



what does it mean?

Possible situations

Using different kV - mA settings....

Using different filtration ... «automatic filtering»

Using different pulse rate (fps)...

Using different pulse width...

Using «image stacking» algorithms ...

Using «mask subtraction» algorithms ...

Using «reconstruction» algorithms ...

RESULTS

To test the protocols, we have studied patients, treated for the same interventional procedure with I and CO₂, to evaluate the dosimetric data related to the choice of the CM for a DSA procedure. In particular, we have analysed cases in 2 hospital equipped with 2 different CO₂ - injectors (Angiodroid and CO₂mmander)



System: PHILIPS ALLURA CLARITY
Place: S. Orsola Hospital - Bologna



System: PHILIPS ALLURA II
Place: Tulane University - New Orleans

- 10 patient cases analysed in each hospital
- All parameters collected during the exposures (kV, mA, times, frames number, F.O.V., positions)
- Due to the complexity of the procedures, the cases were grouped in 3 «body regions» (abdomen, legs, peripheric)
- Mean values presented in table

	TULANE UNIV. HOSPITAL		BOLOGNA UNIV. HOSPITAL	
Protocol	kV	mAs	kV	mAs
Abdomen	ICM: 83	ICM: 28	ICM: 86	ICM: 20
	CO ₂ : 80	CO ₂ : 33	CO ₂ : 82	CO ₂ : 16
Legs	ICM: 65	ICM: 3	ICM: 65	ICM: 3
	CO ₂ : 64	CO ₂ : 3	CO ₂ : 64	CO ₂ : 3
Peripheric Artery	ICM: 70	ICM: 10	ICM: 68	ICM: 10
	CO ₂ : 71	CO ₂ : 6	CO ₂ : 67	CO ₂ : 12

...only TIME OF THE PROCEDURES and GEOMETRIC PARAMETERS (such as irradiation geometry, field dimension, etc..) could be different affecting patient dosimetry

DOSIMETRY and RADIOPROTECTION for CO₂ DSA

- Same dosimetric system to evaluate the CO₂- and I- DSA
- Despite other authors, no significant dosimetric differences between procedures - with CO₂ or ICM - related to X-ray emission
- Time of exposure can be greater, due to the inhabit to have different visualization of vessels
- A proposal for an interesting work for a Medical Physicist: analysis of the protocols during the intervention

References

- Corazza, N. Taglieri, E. Pirazzini, et al., Carbon dioxide coronary angiography: A mechanical feasibility study with a cardiovascular simulator, AIP Adv. 8(1), 015225 (2018).
- J.G. Caridi and I.F. Hawkins, CO₂ digital subtraction angiography: potential complications and their prevention, J. Vasc. Interv. Radiol. JVIR 8(3), 383-391 (1997).
- P.B. Dimatakos, T. Stefanopoulos, A.G. Doufias, et al., The cerebral effects of carbon dioxide during digital subtraction angiography in the aortic arch and its branches in rabbits, AJNR Am. J. Neuroradiol. 19(2), 261-266 (1998).
- C.R. Lambert, E.J. de Marchena, M. Bikina, and B.K. Arcement, Effects of intracoronary carbon dioxide on left ventricular function in swine, Clin. Cardiol. 19(6), 461-463 (1996).
- E. Criado, L. Kabbani, and K. Cho, Catheter-less angiography for endovascular aortic aneurysm repair: A new application of carbon dioxide as a contrast agent, J. Vasc. Surg. 48(3), 527-534 (2008).
- M. Fujihara, D. Kawasaki, Y. Shintani, et al., Endovascular therapy by CO₂ angiography to prevent contrast-induced nephropathy in patients with chronic kidney disease: A prospective multicenter trial of CO₂ angiography registry: EVT by CO₂ Angiography in CKD Patients, Catheter Cardiovasc. Interv. 85(5), 870-877 (2015).
- I.F. Hawkins, K.J. Cho, and J.G. Caridi, Carbon dioxide in angiography to reduce the risk of contrast-induced nephropathy, Radiol. Clin. North Am. 47(5), 813-825, vii (2009).
- I. Corazza, P.L. Rossi, G. Feliciani, L. Pisani, S. Zannoli, and R. Zannoli, Mechanical aspects of CO₂ angiography, Phys. Medica-Eur. J. Med. Phys. 29(1), 33-38 (2013).

... no great differences IN ACQUISITION for CO₂ dedicated protocols if compared with Iodine ones..

...that means:

- No different LUT for the dedicated protocols
- No differences in filters
- Small differences in fps or pulse width



Practical radiation protection during intervention radiology at animals

Siebre van Tuinen (RIKILT Wageningen), Astrid de Greeff (WBVR Lelystad)

Background

Under the general license for radiological activities of Wageningen University & Research a lot of very different radiological applications are operational, varying from quite simple diagnostic X-ray equipment to the operation of radiological laboratories handling open radioactive sources, and from age-determination of geological earth layers to research studies with radioactive substances and X-ray equipment on food, feed and animals.

Objective

In 2017 a new research program at Wageningen Bioveterinary Research (WBVR) has started with aiming to perform heart catheterisations on pigs under examination with an X-ray device. Since this application was relatively new to Wageningen University and Research, a proper risk analysis was performed, with the special request to confirm the calculations with measurements.

Risk analysis

The risk analysis is performed according to the regularly defined steps of the Dutch radiation protection legislation:

- 1) Risk identification of the experiments and regular maintenance
- 2) Risk calculation for all personell involved
- 3) Risk evaluation, and conclusions concerning the classification of exposed workers, controlled areas and ALARA measures

To check the calculated doses a measuring campaign was performed with two measurement systems: the Dose Aware system from Philips and MGP personal dosimeters. With this combination the varying dose rates could be registered during the treatment.

Regular exposure of workers

Based on the risk analyses the maximal total personal dose (without lead apron) calculated amounts almost 5 mSv based on 40 treatments a year. Calculated regular doses for assisting personnel were below 1 mSv a year



Figure 1. Impression of an experiment, and the staff involved.

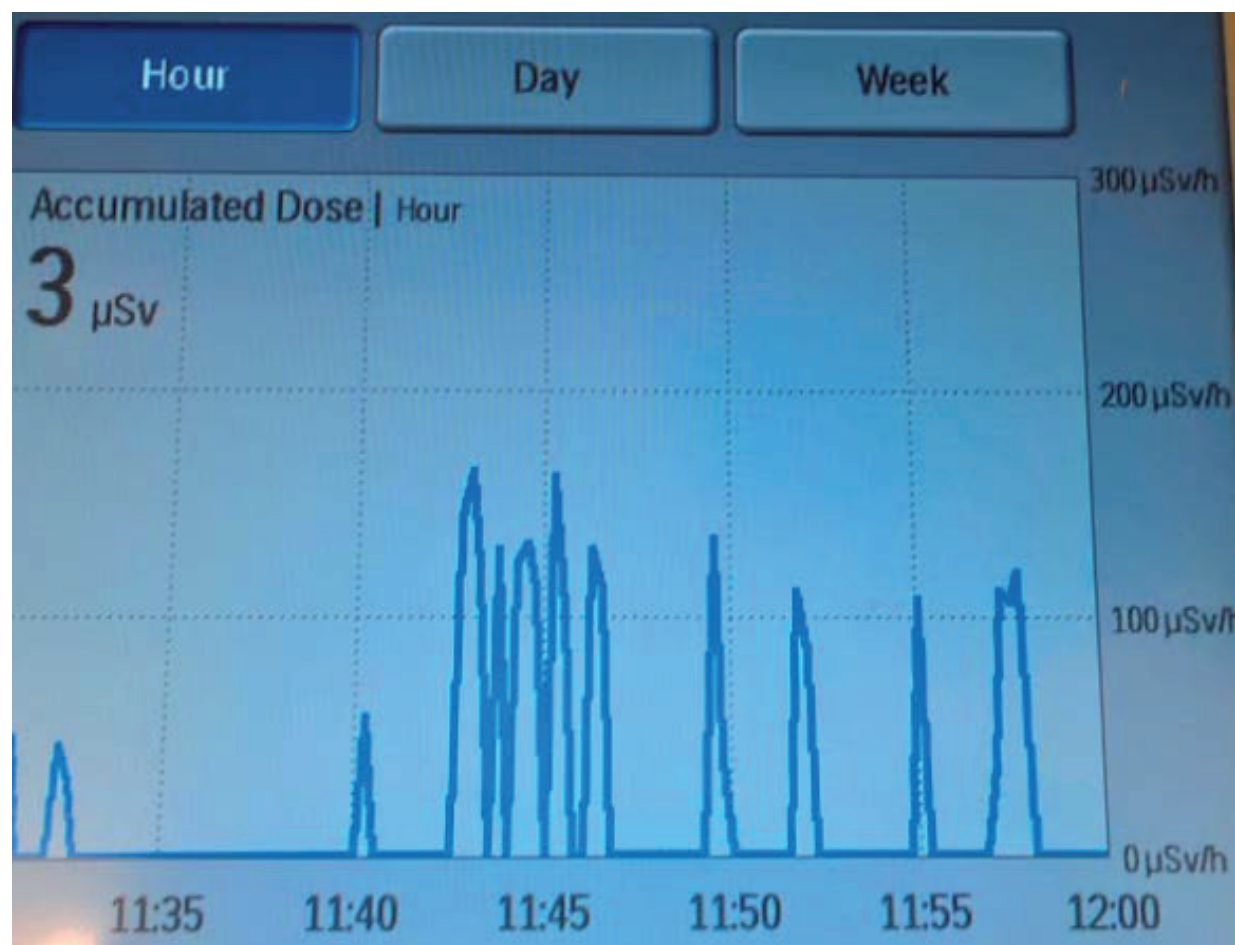


Figure 2. Varying dose rate level of the veterinary doctor, registered by the Dose Aware system.

Calculated dose results

Activity	Role	Regular dose	Potential dose	Total dose
		(mSv/a)	(mSv/a)	(mSv/a)
catheterisation	medical doctor	4.84	0.19	5.03
catheterisation	medical assistant	0.89	0.16	1.05
catheterisation	anesthetist	0.09	0.19	0.28
catheterisation	assistants	0.08	0.003	0.08
maintenance	technician Siemens	0.02	0	0.02
maintenance	technician WBVR	0.01	0	0.01
visitor			0.003	0.003

- The maximal regular extremity dose (34 mSv a year) was found for the medical doctors. The potential extremity dose for the other workers is much lower (about 1 mSv a year).
- The eye lense dose is estimated to be the same as the regular dose (about 5 mSv a year).

Comparison calculated and measured values

Role/location	Dose per procedure (mSv)		
	Calculated	Measured	
		MGP	Dose Aware
medical doctor	0.12	0.035	0.018
medical assistant	0.022	0.018	0.013
anesthetist	0.002	0.001	0.003
assistants	0.002	0.002	0.004
outside area	0.001	0.001	N/A

Conclusions & main ALARA recommendations

- Good agreement between the calculated and experimental dose values was observed for most workers.
- Logically, the highest deviations were found at the lowest doses.
- The medical doctor showed a factor 4 lower personal dose than calculated. This could be quite easily explained by the variation in the distance of the medical doctor to the (porcine) patient.
- The area monitoring dose results showed a good agreement between the calculated and experimental values
- It was advised to operate the X-ray apparatus in the horizontal direction. This can decrease the regular exposure with a factor 5.
- To reduce the potential exposure two persons monitor the possible irradiation of the hands on the screens during the operation all the time.

Acknowledgements

The WUR is thanking the Rijnstate Ziekenhuis for using their Dose Aware equipment and software, and Siemens and HES Kampen for providing data considering the technical and maintenance data of the Siemens CIOS alpha radiological equipment



Radiation Protection Challenges

Building a new Academic Medical Centre on an Operational Site

2005

Challenge 1: Optimization with limited information

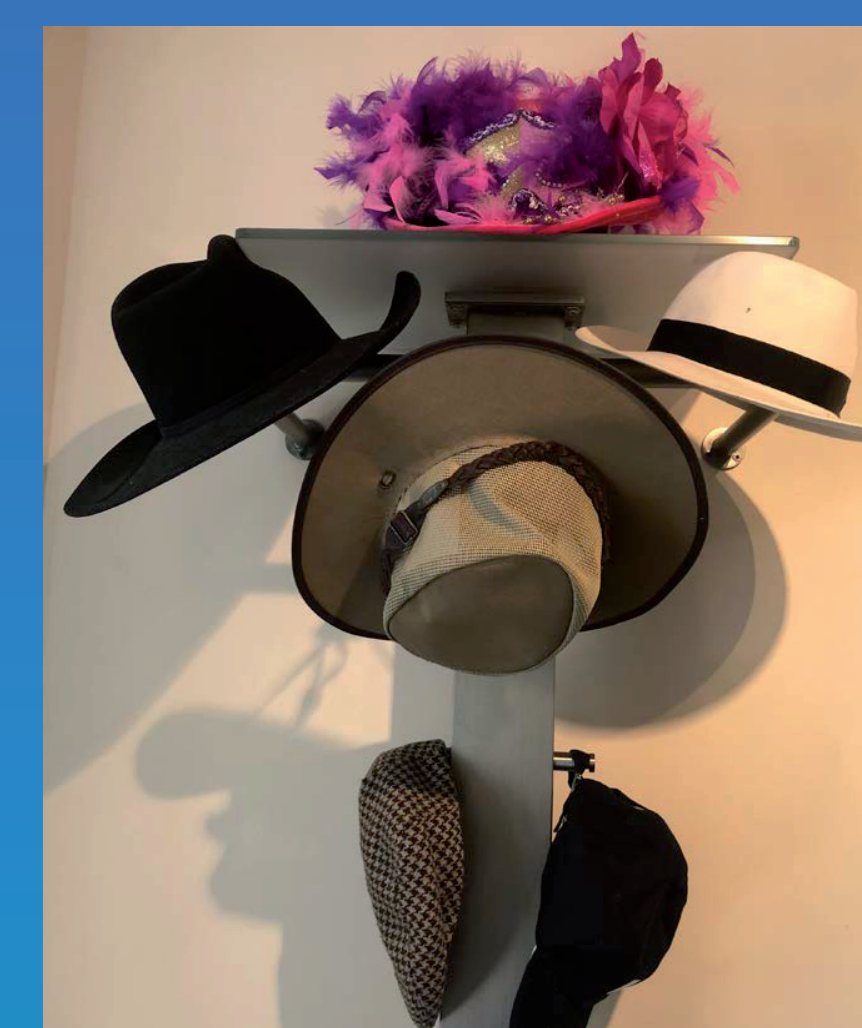
Optimization of radiological protection wasn't easy because there was barely information about selected radiation sources at the time the design decisions were made. Despite lack of information, the radiation protection expert had a role at that stage. For instance, he informed the architect about the mass of concrete and lead needed for shielding. After that, a number of plans, such as vaults situated on higher floor levels, ended up in the trash.



...

Challenge 2: Playing multiple roles

In the process the Radiation Protection Unit played multiple roles. On one hand we had to give advice with respect to the design, and on the other hand we had to accept the radiological areas and granted internal permissions, both based on our own given advise. In addition, the project management of demolition and construction was split up, which required additional communication skills from the RPU.



...

2014

Challenge 3: Building on an operational site

Because of the impossibility to stop treatment of patients, departments had to be temporary relocated in another part of the city resulting in having to create the design for the Radionuclide Therapy department twice. The decommissioning of this department therefore also had to take place twice. This said and on a positive note, learning's from the first design and decommissioning could be included in the redesign and in the optimization process of the final decommissioning. An advantage that is not available to every RPU.



2015

Challenge 4: Apply for comprehensive licence

We had to explain to the government that radiation sources were needed at two different locations because of the need of ongoing treatment of patients. So there was a need for permits at both locations for the various radiation sources, while the sources would only be present, and be used, at one location at the time. Because HDR-brachytherapy had never been applied to the main location the authorization procedure took 3 months longer then previously estimated.



2016

2017

Challenge 5: Dealing with external nuisance factors

In the final stage we were dealing with a number of external nuisance factors, such as changing legislation and damage to our radioactive facilities caused by building activities in the neighbourhood. These external factors required a lot of additional effort from the RPU.



2018

Authors: C.J.J. Eggels-Hofman (RPE); R.J.H.L. van Gorp (RPE)
SBE@erasmusmc.nl

RISK MANAGEMENT OF THE RADIATION-INDUCED CATARACT

Ana Dolcet Llerena¹, Luis Corpas Rivera¹, M^a Victoria Marfil Robles²

¹GESTISA Radiation Protection Service

²GESTISA Prevention of Occupational Risks Service

INTRODUCTION

The Council Directive 2013/59/EURATOM of 5 December 2013 [1], following the new ICRP guidance [2], established a considerable reduction on the limit for equivalent dose for the lens of the eye in occupational exposure, from 150mSv to 20mSv in a single year. That requires from the Radiation Protection and Prevention Units of the hospitals a new method to evaluate the risk of cataract in exposed professionals and a new guideline to assign PPEs (Personal Protective Equipment) such as lead glasses. The purpose of this work is to propose a method for this task.

MATERIALS AND METHODS

Our Company, GESTISA, leads the “Crystalline Project” [3], manufacturing a new eye lens dosimeter and starting a pilot program with 15 hospitals in Spain, in order to collect data about the accumulated doses in 12 selected medical specialties.

Each of the hospitals has participated in the project with a different number of professionals (including doctors, nurses, medical imaging technologists and nursing assistants) during a minimum period of 3 months in a total of 15 months that the project has been running so far.

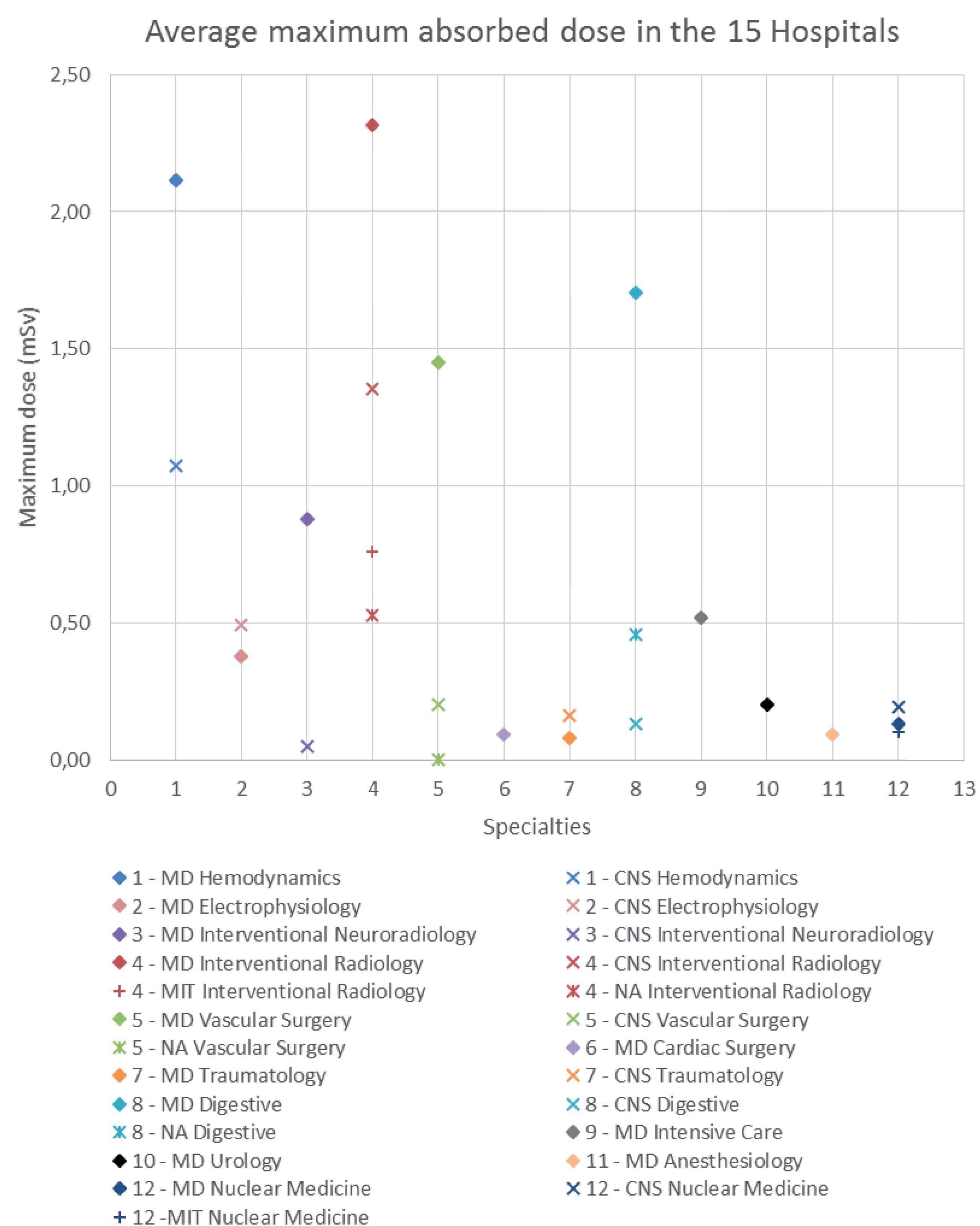
The dosimeters used for the study were those designed by GESTISA for that purpose, based on the DOSES™ model created and patented by this entity for patient dosimetry, but properly calibrated in the magnitude Hp (3). They consist on a lightweight device that is included in a protective case that attaches to the front of the surgery hat of the user, in order to reproduce the distance and orientation of the eye-lens without interfering with his/her work. If the user works in more than one installation, he/she must carry a different dosimeter in each of them.

The eye lens dosimeter should only be used during the interventional processes. The rest of the time must be kept by each professional in the box that accompanies it. Nevertheless, a recommendation was given, that the operating room assistants should keep track of the dosimeters that enter and leave the room.

The dosimeters were sent to each hospital to be used during one month. After this period, they were collected by GESTISA for reading and recording of the doses, after replacement by blank dosimeters, for the following month. Also, each hospital received a dosimetry report with the results from the previous month.

RESULTS

The results for the average acquired dose per specialty are shown in the following graphic.



CONCLUSIONS

Our recommendations[4], on whether a certain medical specialty should wear led glasses or dosimeter, were based on the Spanish Royal Decree 783/2001[5] that imposes the obligation of wearing a dosimeter in Controlled Zones, that is, the areas where there exists the possibility of reaching doses of more than 3/10 of the annual occupational limit for the lens of the eye.

According to this, every professional that can reach the limit of 6mSv/year, that is, 0.5mSv/month, should wear an eye lens dosimeter. If we have a look at the results, we find that those specialties are: Hemodynamics, Interventional Neuroradiology, Interventional Radiology, Vascular Surgery, Gastroenterology and Intensive Care.

To make a recommendation on the use of lead glasses, we considered the limit of 1.67mSv/month (that would make 20mSv/year), so the resulting specialties were Hemodynamics, Interventional Radiology and Gastroenterology.

REFERENCES

- [1] COUNCIL DIRECTIVE 2013/59/EURATOM of 5 December 2013 laying down basic safety standards for protection against the dangers arising from exposure to ionising radiation.
- [2] ICRP Publication 103 Ann. ICRP 37 (2-4), 2007
- [3] <http://www.crystallineproject.eu/en/>
- [4] *Gestión Preventiva de la catarata radioinducida en radiología médica*, L. Corpas Rivera, M.V. Marfil Robles, XI Congreso Nacional de Prevención de Riesgos Laborales en el Ámbito Sanitario, H.U. 12 de Octubre, Madrid
- [5] Spanish Royal Decree 783/2001, of the 6th of July, which approves the Regulation on Sanitary Protection against Ionizing Radiations.



Some Practical Aspects on Implementation Council Directive 2013/59/Euratom in the medical field in Romania

Constantin Milu, PhD, constantinmilu@upcmail.ro
Expert Pro-Rad srl, Bucharest, Romania



ABSTRACT

The Council Directive 2013/59/Euratom of 5 December 2013 laying down basic safety standards for protection against the dangers arising from exposure to ionizing radiation, and repealing Directives 89/618/Euratom, 90/641/Euratom, 96/43/Euratom and 2003/122/Euratom was published on 17th of January 2014 in the Official Journal of the European Union [Ref. 1]. As it is well known, the Directive, as well as IAEA/International BSS [Ref. 2] are based on the Recommendations of the International Commission on Radiological Protection (ICRP), published in 2007 as ICRP Report No.103 [Ref. 3]. According to Article 106 in CHAPTER X – Final provisions, Member States shall bring into force the laws, regulations and administrative provisions necessary to comply with Directive by 6 February 2018. This transposition process is now in a final phase in Romania too. Many activities shall be performed during the next few years, for effective and practical implementation of this Directive, particularly in the medical field. This paper provides some important practical aspects on implementation of this Directive in the medical field in Romania.

GENERAL REVIEW ON THE PROBLEM

This work included a general review of the medical exposure situation in Romania and particularly regarding:

- the identification of the real new provisions in the revised Euratom Directive, in relation with the identification of responsibilities for the different Romanian competent authorities and stakeholders involved and of the potential technical regulatory problems;
- the detection of issues and the identification of good practices;
- the identification of topical issues which require further attention, action and activities, within a national approach for a proper implementation process of the Directive

PRINCIPAL GAPS IN CURRENT RADIATION SAFETY REGULATION IN MEDICINE IN ROMANIA

All new definitions from Directive shall be used further uniform, in all future documents, during implementation, special attention regarding to the following definitions:

NEW DEFINITIONS	CURRENT USE IN ROMANIAN REGULATION
- “Planned exposure situation”	- “Practice”
- “Emergency exposure situation”	- “Radiological accident”
- “Exposed worker”	- “Occupational exposed worker”, “Radiation worker”
- “Referrer”, which replaced “prescriber”	- “Ordering”, “Ordonateur”
- “Practitioner”	- “Medical practitioner”
- “Medical radiological installation”	- “Radiological laboratory”
- “Carers and comforters”	- “Helper”
- “Medical Physics Expert”	- “Medical physicist”, “Expert in physics radiation”
- “Sealed source”	- “Closed source”
- “Licence”	- “Authorization”
- “Undertaking”	- “Authorization holder”, “legal person”
- “Unintended exposure”	- “Incident”
- “Non-medical imaging exposure”	- A NEW DEFINITION
- “Occupational health service”	- A NEW DEFINITION

LICENCE

The licence in medicine still is now a complicated procedure. A new guidelines on authorization procedures need to be elaborated soon, applying the graded approach to regulatory control (notification, registration, licence) and deciding some exception from authorization (ex., for possession or for renting a radiological equipment, the present Authorization Safety Authorization – ASR, for European products, a.s.o.).

ACCEPTABILITY OF MEDICAL RADIOLOGICAL EQUIPMENT

The Directive 2013/59/Euratom prescribes a number of measures to ensure that medical exposures are delivered under appropriate conditions. It required, among other things:

- * acceptance testing of new equipment,
- * identification of criteria of acceptability for equipment safety and performance throughout its life, and
- * establishment of quality assurance programmes.

In Radiation Protection No. 162 (2012), the European Commission established new “Criteria for acceptability of medical radiological equipment used in diagnostic radiology, nuclear medicine and radiotherapy” [Ref. 5], which addresses the second of these (criteria of acceptability). New definitions and concepts are included. The criteria for acceptability (for clinical use!) are applied and they are divided into two categories “qualitative criteria” and “quantitative” criteria, also known as “suspension levels” (for clinical use!).

DIAGNOSTIC REFERENCE LEVELS

As it is well known, Diagnostic Reference Levels (DRLs) means dose levels in medical radiodiagnostic or interventional radiology practice, or, in the case of radio-pharmaceuticals, level of activity, for typical examination for group of standard-sized patients or standard phantoms for broadly defined types of equipment.

In the future “Norms” (GSR-11 and GSR-12) the new definition mentioned above has to be used, plus:

- some more and clear technical recommendations for the implementation of the DRLs concept;
- new values, particularly for interventional radiology and for different age groups for children.

ACCIDENTAL AND UNINTENDED MEDICAL EXPOSURE

The accidental and unintended medical exposures are a source of continuing concern. Apart the need to use the new definitions (instead of “accidents and incidents”!), the new Romanian regulation on radiological safety in medicine has to increase the role of the competent authority in radiation protection (CNCAN) to address the prevention of accidental and unintended medical exposure and the follow-up in case of their occurrence. The role of quality assurance management, as part of a Radiation Protection Programme (RPP), including a study of risks in radiotherapy, to avoid such incidents should be emphasized, and recording, reporting, analysis and corrective action be required in such cases. The 2015 EC- Guidelines on risk management in external beam radiotherapy [Ref. 8] is very useful for this purpose and elaboration of appropriate guidance, during the implementation of Directive 2013/59/Euratom.

NEW DOSE LIMIT FOR LENS OF EYE

A real new task for radiation protection, due to a new equivalent dose limit for lens of eye for occupational exposure in planned exposure situation, e.g. 20 mSv/year, instead of 150 mSv/year, keeping 15 mSv/year as a dose limit for the public. Many categories of problems arise, particularly for practitioners from interventional radiology. According to the new Directive, in planned exposure situations an occupation exposure more than 20 mSv/year equivalent dose in lens of the eye is NOT ACCEPTABLE (as it is above the dose limit!) and less than 15 mSv/year is ACCEPTABLE, because it is less than dose limit for the public!

Consequently, the practical measurable dose interval for occupational exposure is now very narrow, between 15 and 20 mSv/year.

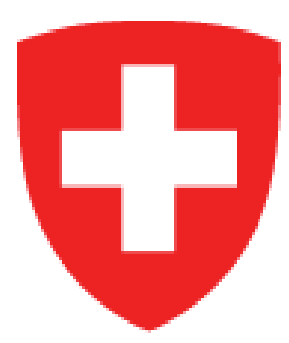


CONCLUSION

For a successful implementation of the Directive 2013/59/Euratom there is a real need to be developed several technical guidelines, using available EC guidelines and to improve the whole system for Education and Training of Medical Professionals in Romania on Radiation Protection, according to European Commission Guidelines, published in 2014 in Radiation Protection No.175 [Ref. 7]. The recognized training centres in radiation protection and the available professional associations have an important role in this field.

REFERENCES

- [1] The Council Directive 2013/59/Euratom of 5 December 2013 laying down basic safety standards for protection against the dangers arising from exposure to ionizing radiation, and repealing Directives 89/618/Euratom, 90/641/Euratom, 96/43/Euratom and 2003/122/Euratom, The Official Journal of the European Union, 17 January 2014.
- [2] Radiation protection and safety of radiation sources: International basic safety standards, General Safety Requirements Part 3, No. GSR Part 3, STI/PUB/1578, Vienna – International Atomic Energy Agency, 2014
- [3] The International Commission on Radiological Protection (ICRP), International Recommendations of the ICRP, ICRP Report No.103, 2007.
- [4] European Guidelines on Medical Physics Expert, European Commission, Radiation Protection No.174, 2014.
- [5] Criteria for acceptability of medical radiological equipment used in diagnostic radiology, nuclear medicine and radiotherapy, European Commission, Radiation Protection No.162, 2012.
- [6] Referral Guidelines for Medical Imaging Availability and Use in the European Union, European Commission, Radiation Protection No.178, 2014.
- [7] Guidelines on Radiation Protection Education and Training of Medical Professionals in the European Union, European Commission, Radiation Protection No.175, 2014.
- [8] General guidelines on risk management in external beam radiotherapy, European Commission, Radiation Protection No.181, 2015.
- [9] Diagnostic Reference Levels in Medical Imaging, ICRP publication 135, Ann. ICRP 46(1), 2017.



Stakeholder involvement throughout the revision process of the Swiss radiation protection legislation and the implementation of clinical audits: experience and lessons learned

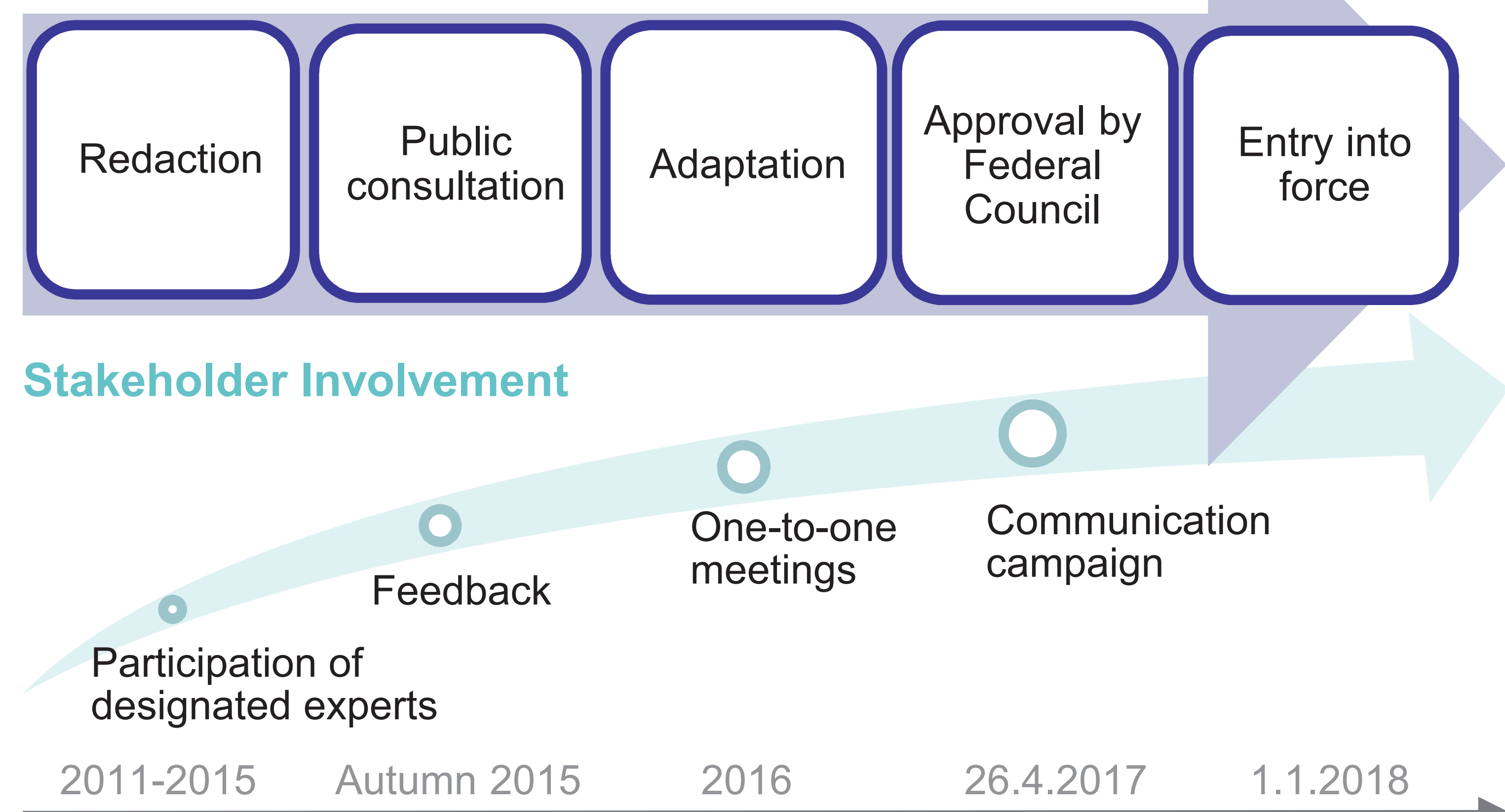
Barbara Ott; Carine Galli Marxer; Philipp R. Trueb; Sébastien Baechler

Overview

- The aim of the revision was to introduce a risk-based approach covering all exposure situations and reflecting the current state of science and technology.
- The integrated legislation (ten ordinances) was adapted according to the new international standards - namely the ICRP103 recommendation as well as the IAEA and Euratom BSS.
- Stakeholder involvement was crucial for the acceptance of the revised legislation, especially in medicine with respect to new provisions regarding justification and the introduction of clinical audits.
- Communication platforms were created during the revision process:

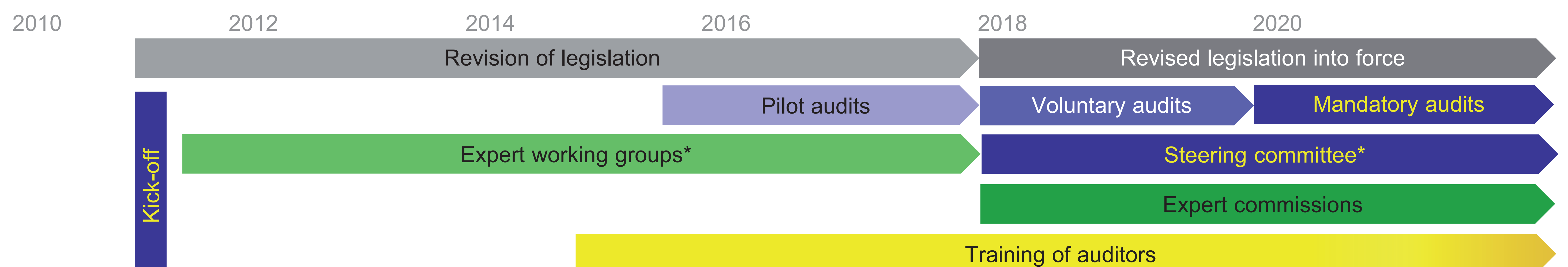
Revision of Legislation: www.strahlenschutzrecht.ch (de)
www.legislationradioprotection.ch (fr)
www.dirittoradioprotezione.ch (it)
Swiss Clinical Audits Initiative: www.clinicalaudits.ch (de, fr, it)

Revision Process

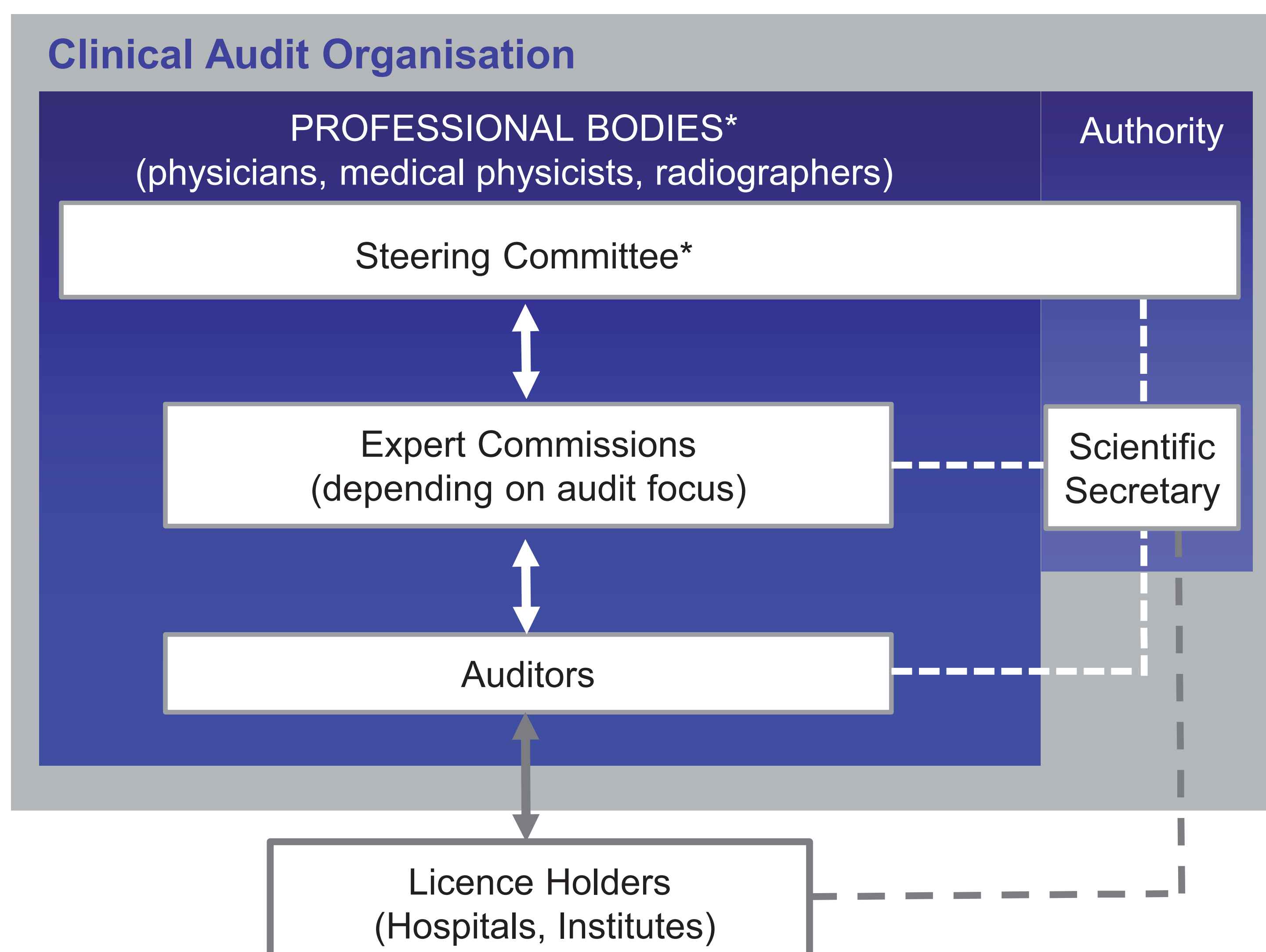


Clinical Audits in Switzerland

- Mandatory from 2020 in **high dose procedures**: CT, interventional radiology (cardiology, angiology, urology etc.), nuclear medicine and radiation therapy.
- Can be imposed by the authority at most **every 5 years**.
- Authority can assign **third parties** (→ **auditors**) to coordinate and carry out audits (**peer-review**).
- A yearly **self-evaluation** must be carried out by license holder based on the **quality manual**.



Clinical Audit Organisation



Lessons Learned

Involving all relevant stakeholders in early stages and throughout all processes of the revised radiation protection legislation promoted their acceptance and enabled an efficient implementation of clinical audits.

Keys to successful stakeholder involvement:

- elaborate a vision that is supported by the strategic decision makers
- involve the stakeholder from the beginning and specify their roles
- define and communicate the decision making competence of each stakeholder
- define and start the communication campaign at an early project phase
- be aware of the different roles of the authority: forerunner, rule maker, advisor, communicator, supervisor, network creator, trainer^[1]

^[1] HERCA: Stakeholder Involvement in Medical Practices, Report of Working Group 5



State of Digital Radiography Reject Analysis in Dutch Hospitals – Preliminary Results

Ischa de Waard – Schalkx¹ [Ischa.de.waard@rivm.nl], Sandra Noij², Harmen Bijwaard^{1,2}

¹ National Institute for Public Health and the Environment (RIVM)

² Inholland University of Applied Sciences (InhU)

Introduction

In the past decades Dutch radiology departments have shifted from conventional to digital radiography. In digital imaging, it is easier to remake an image and delete the previous ones. From a radiation protection perspective every additional image carries a radiation risk for the patient and should be avoided when possible.

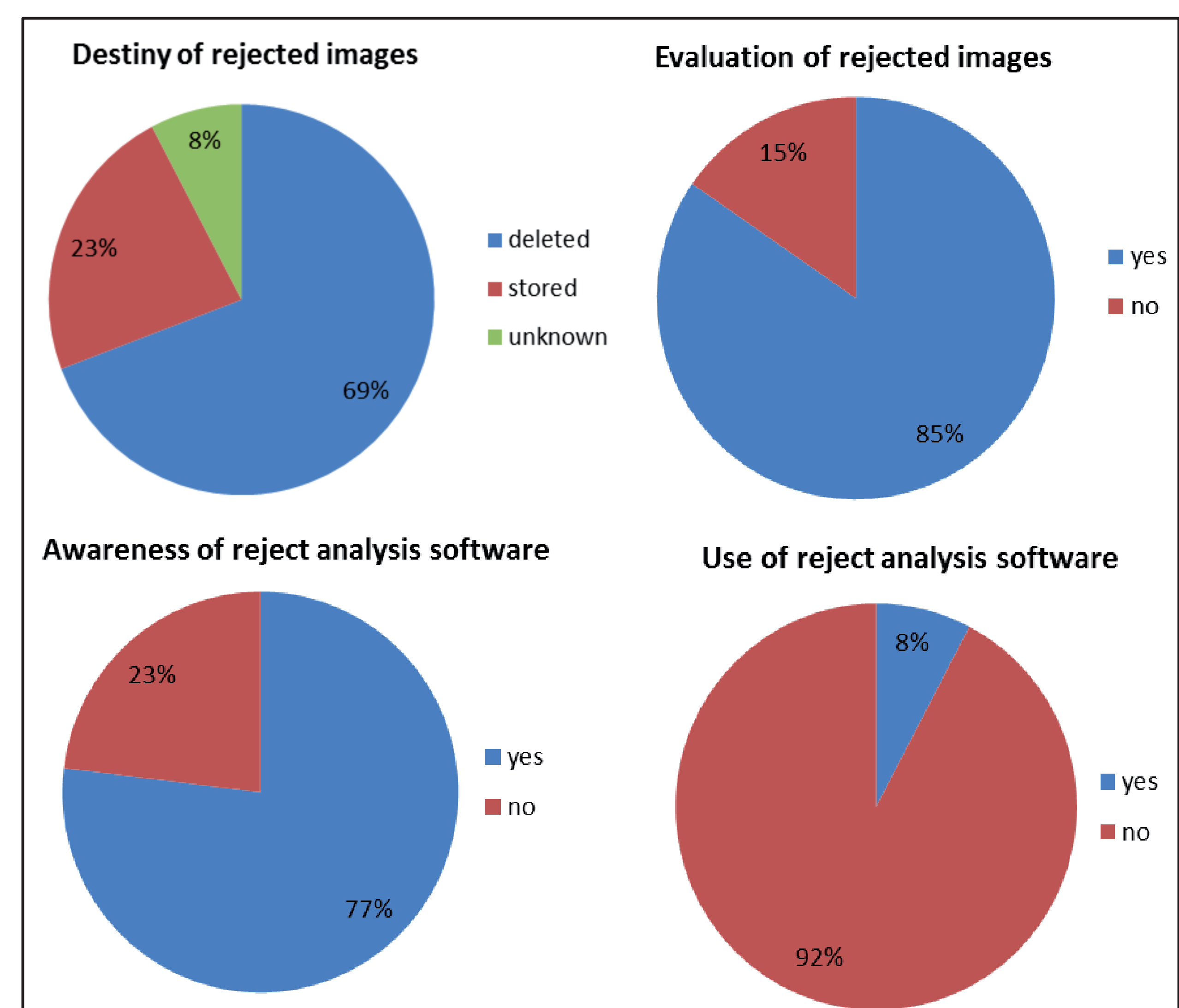
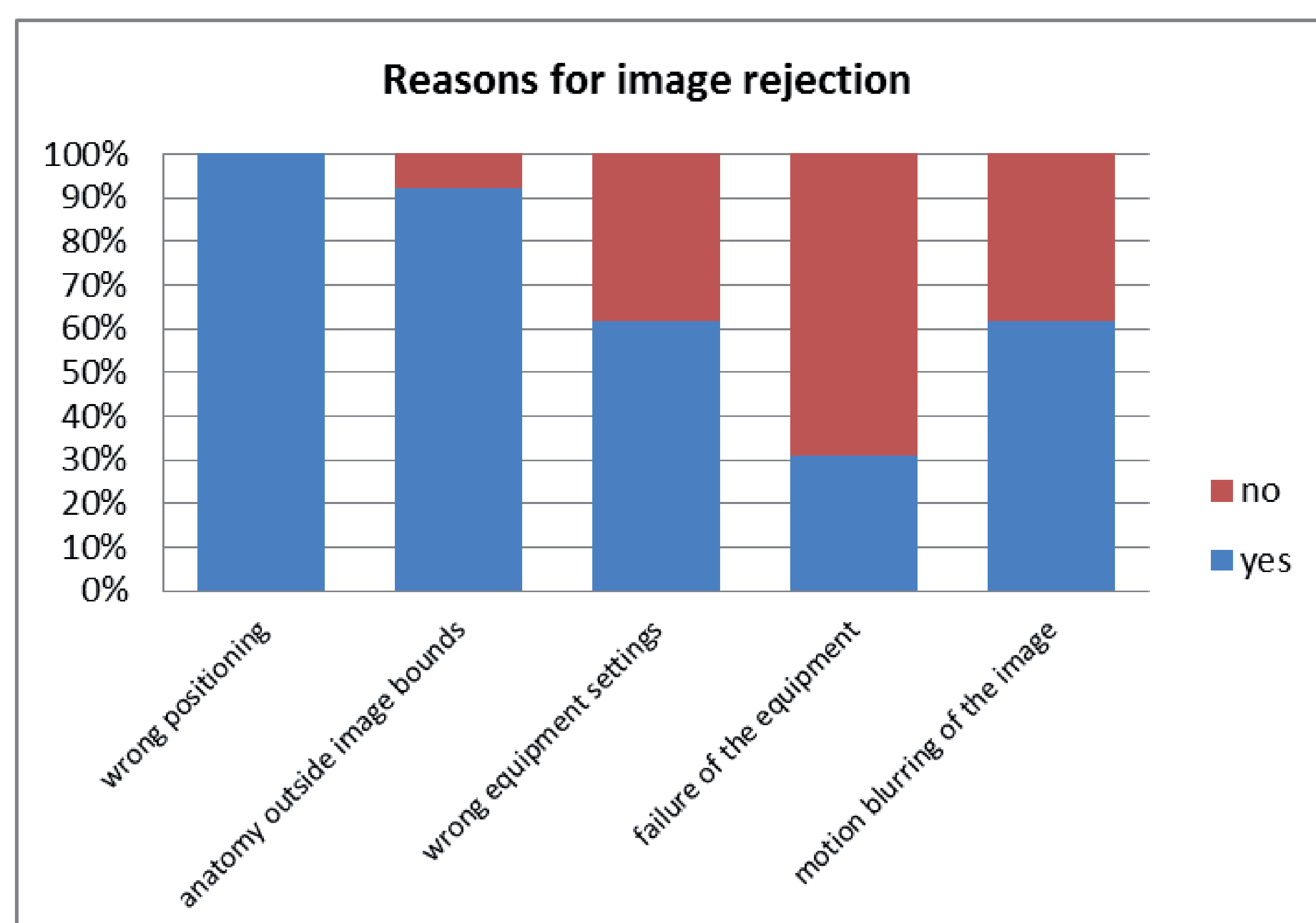
In the time of conventional imaging films that could not be used for diagnostic purposes (and were rejected) were collected. The rejected films were analyzed and recommendations for improvements in imaging were made to avoid the same mistakes in the future. A similar analysis of digital images is more complex but several software tools have become available for this purpose. The Dutch Healthcare Inspectorate asked the National Institute for Public Health and the Environment (RIVM) to investigate the current state of reject analyses in digital imaging. RIVM conducted this study in collaboration with Inholland University of Applied Sciences.

Methods

To investigate the current state of the art a literature study was conducted and a questionnaire was set up. Questions included the frequency of reject analyses, the procedures and the software tools used, the amount of rejected images and the registration of these. The questionnaire was used for guidance during interviews with quality managers at radiology departments in 13 Dutch hospitals.

Results

Participating hospitals report that on average 0.7 % of all images is rejected. In most cases this concerns bucky imaging for which poor positioning is often the reason for rejection. In 70% of the hospitals the rejected images are not stored. In 85% of the hospitals a sample of the rejected images is analyzed, but only four hospitals (30%) perform an analysis of all rejected images. Most hospitals (77%) are aware of sophisticated software for reject analysis, but for financial reasons only 8% use it.



Discussion

The reported reject rate of 0.7% is low compared to other studies. For example, Foos et al. (2009) report 4-5%, Hoffman et al. (2015) 11%, Jones et al. (2011) 8-10 %, Lau et al. (2004) 1-2%, and Lin et al. (2016) 5%. However, in this study the reject rate is self-reported and participation of hospitals was voluntarily.

Images that were often rejected were bucky images of knees and back of elderly patients for which the positioning is more difficult. Fortunately, this imaging incurs low radiation doses to the patient and radiation risks decrease with age.

Even though many rejected images are deleted and reject analysis software is seldom used, most hospitals do analyze a sample of the rejected images. Furthermore, all hospitals indicate that actions are undertaken to reduce the number of rejected images.

For CT, angiography and fluoroscopy, registration and analysis of rejected images is less common than for standard radiography. For these modalities images are rejected less, but the doses incurred are relatively high.

Take home message

The 13 interviews with radiology departments throughout the Netherlands constitute a small sample from the approximately 80 hospital conglomerates in the country. These preliminary results indicate that few radiology departments still carry out reject analyses. Software tools that are available for such an analysis of digital images seem to be only used sporadically. For radiation protection purposes it is recommended that radiology departments put more effort in collecting rejected images for educational purposes and to avoid similar mistakes in the future.



university of
 groningen



National Institute for Public Health
and the Environment
Ministry of Health, Welfare and Sport

Strategies for the sustainable production of medical radio isotopes

■ Dr LP (Lars) Roobol

National Institute for Public Health and the Environment, Bilthoven, the Netherlands.

■ Prof Dr S (Sytze) Brandenburg

KVI – Center for Advanced Radiation Technology, University of Groningen, the Netherlands

Presenting author: lars.roobol@rivm.nl www.rivm.nl

Highlights:

- A few ageing nuclear reactors are making the bulk of the medical radio-isotopes in the world, they are used for therapy and diagnosis.
- It is difficult to develop the next generation of sustainable production of medical isotopes in Europe.
- In our paper, we give advice on the sustainability of: health care, environment, economy, knowledge and innovation.

1. Sustainable health care



Robust supply chain: significant number of suppliers of primary product (irradiated targets/purified radioisotopes) linked by agreements on production planning and shortages due to unplanned non-availability. Most logic solution: publicly financed supply chain: the final bill is paid from public money anyway. Additional benefit: solves legal issues on state support and cartel.

2. Environmental sustainability



Environmental impact of accelerator and reactors difficult to compare:

- High power accelerator: large electric power, much more than research reactor.
- Reactor: large amount of long-lived radioactive waste, including minor actinides. Waste research reactor small compared to that nuclear power generation, so is this a relevant issue?

Development of infrastructure for isotope supply requires care: building a new reactor should not block the development of new options, and vice versa.

3. Economic sustainability

Availability broad range of isotopes for diagnostics, therapy and R&D essential. Risk of leaving it to the market:



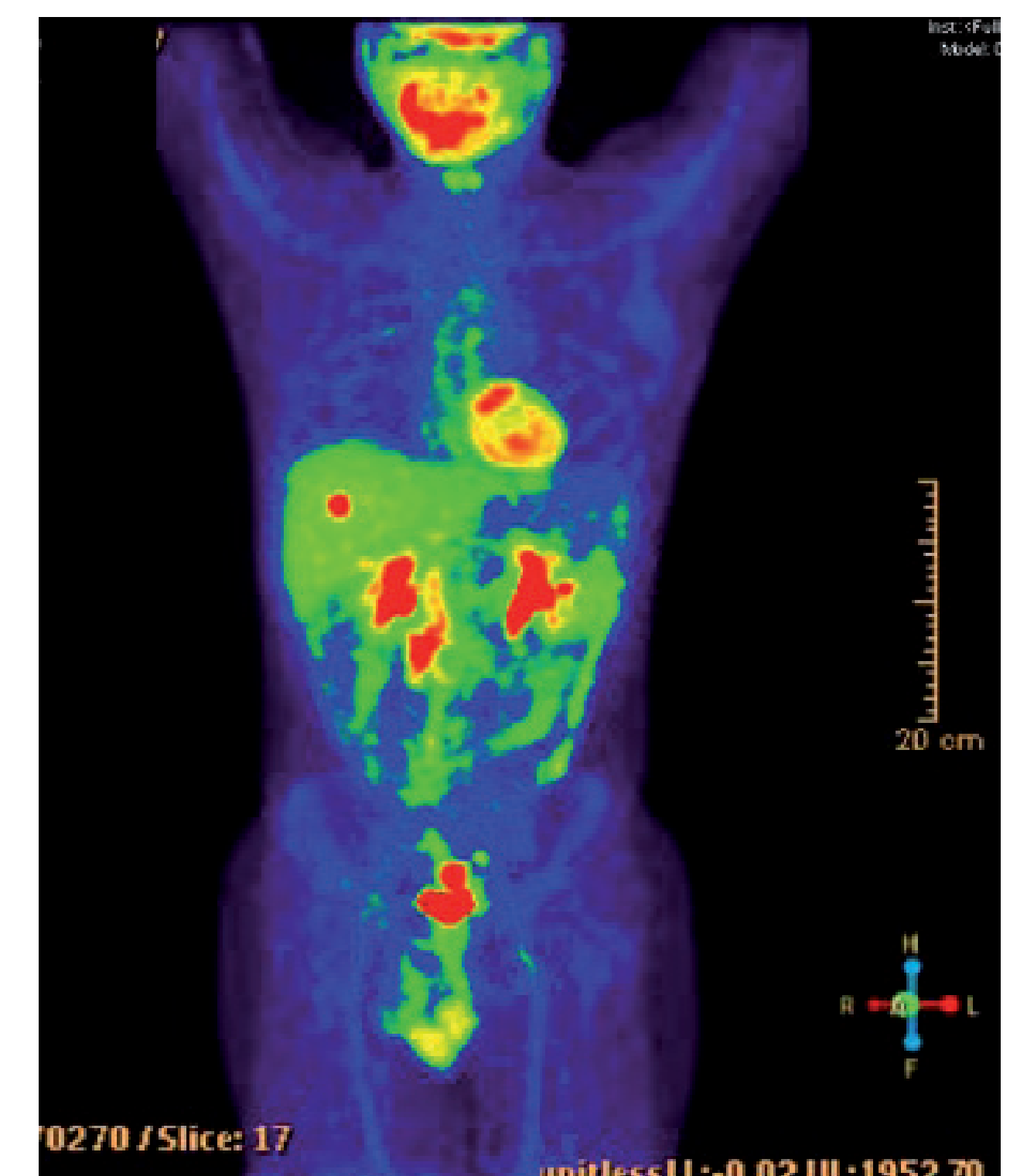
- only most frequently used and easy to produce isotopes will be available
- development of new isotopes stalled because of low margins and high risks.

4. Sustainability of knowledge and innovation

Dwindling research capacity in nuclear-related science compromises high level education, long term availability expertise and innovation capacity. Action on a European scale needed to counter this tendency. Build innovation capacity: Europe-wide coordinated action for development new isotopes (primary production; purification; QA) similar to US National Isotope Development Center.

Options:

- EU-operated accelerators and reactors, similar to EU JRC
- distributed facility consisting of facilities in the participating states completed with EU-operated facilities to fill the holes.



The Influence of Magnetic Fields on the Response of Thermoluminescent Dosimeters

Atallah Coptý¹, Günter Rabineg¹, Andreas Berg²



¹ Radiation Protection Laboratory, Magistrate Division 39, Vienna, AUSTRIA

² Medical University Vienna, Center for Medical Physics and Biomedical Engineering, High-field MR Centre of Excellence, Vienna, AUSTRIA

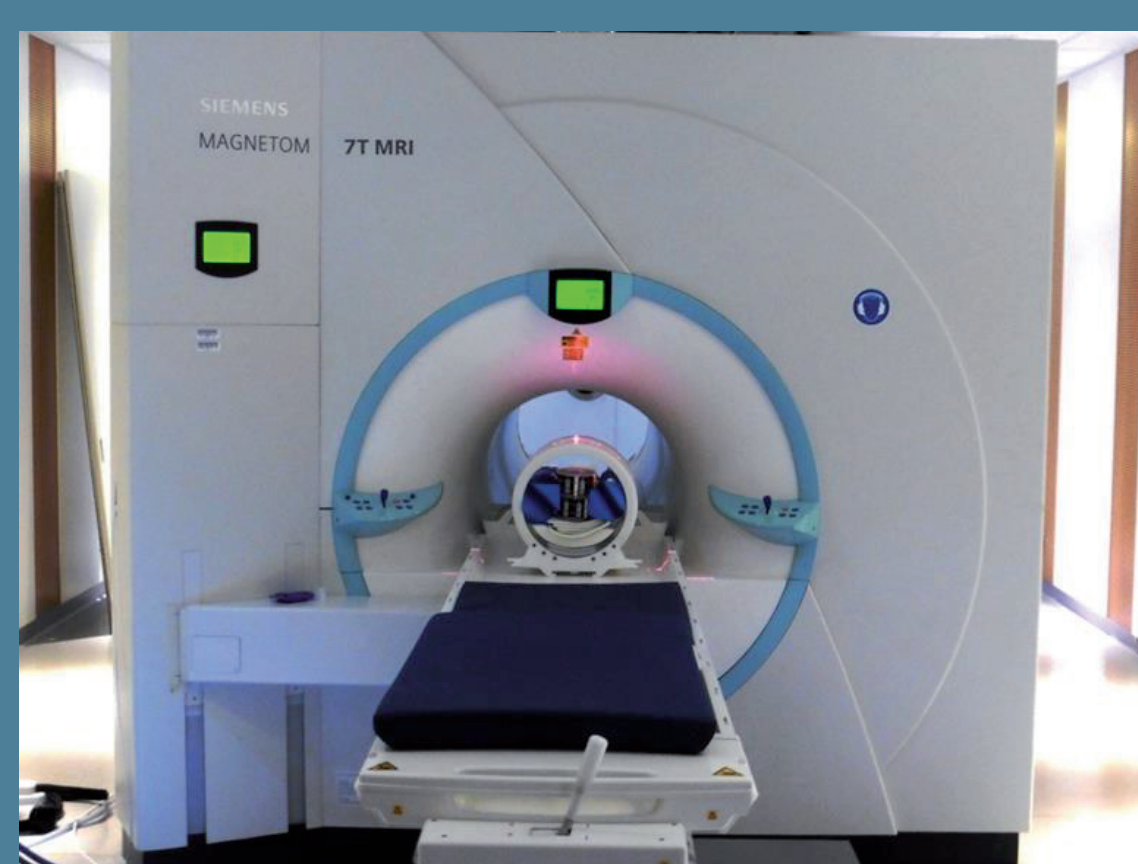


Fig. 1a MRI-scanner 7 T with TLDs positioned inside a RF-coil to investigate a potential RF-impact

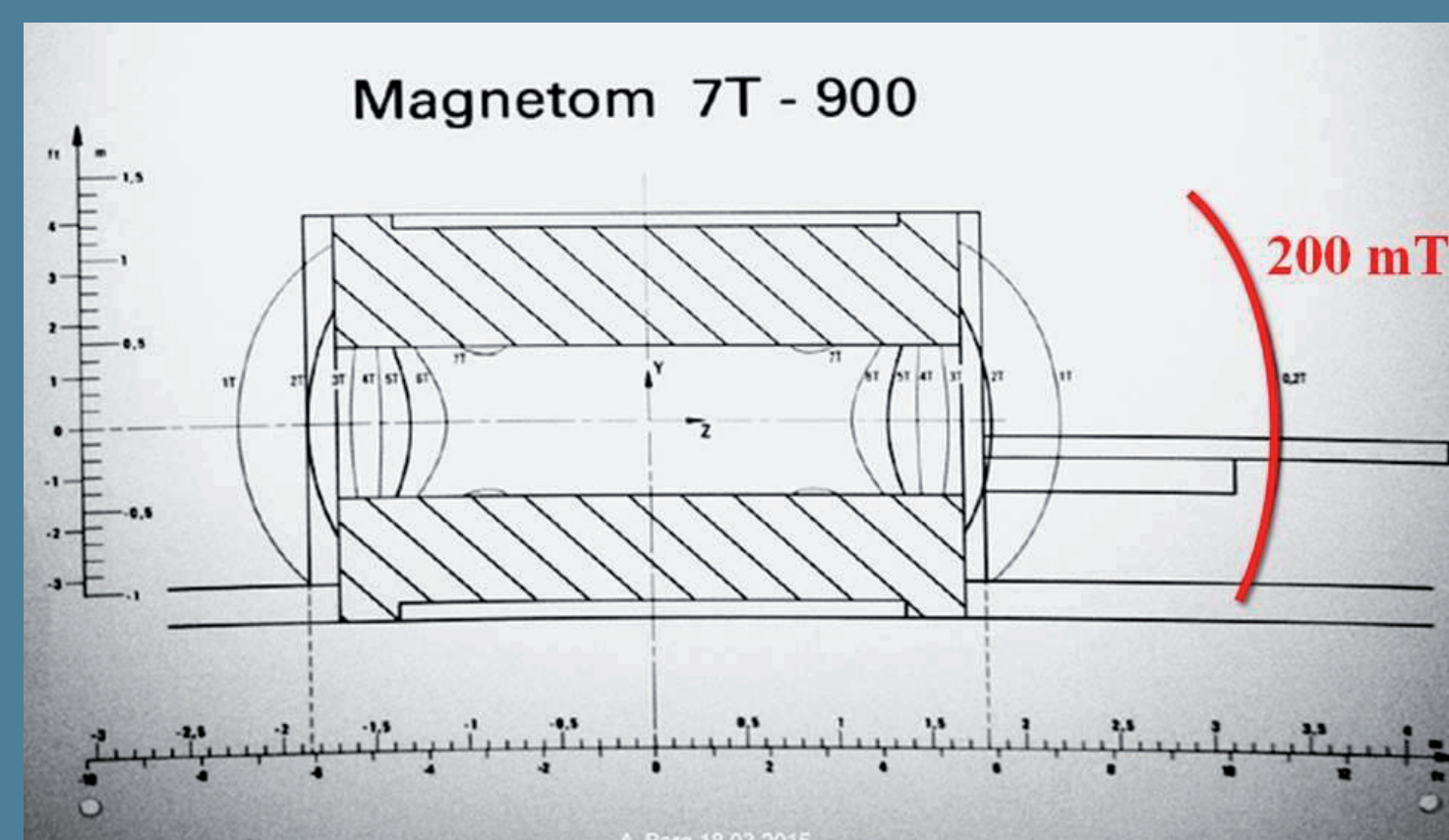


Fig. 1b Fringe field of the high field human 7 T MRI-scanner (sagittal section)



Fig. 2a MRI-scanner 3 T

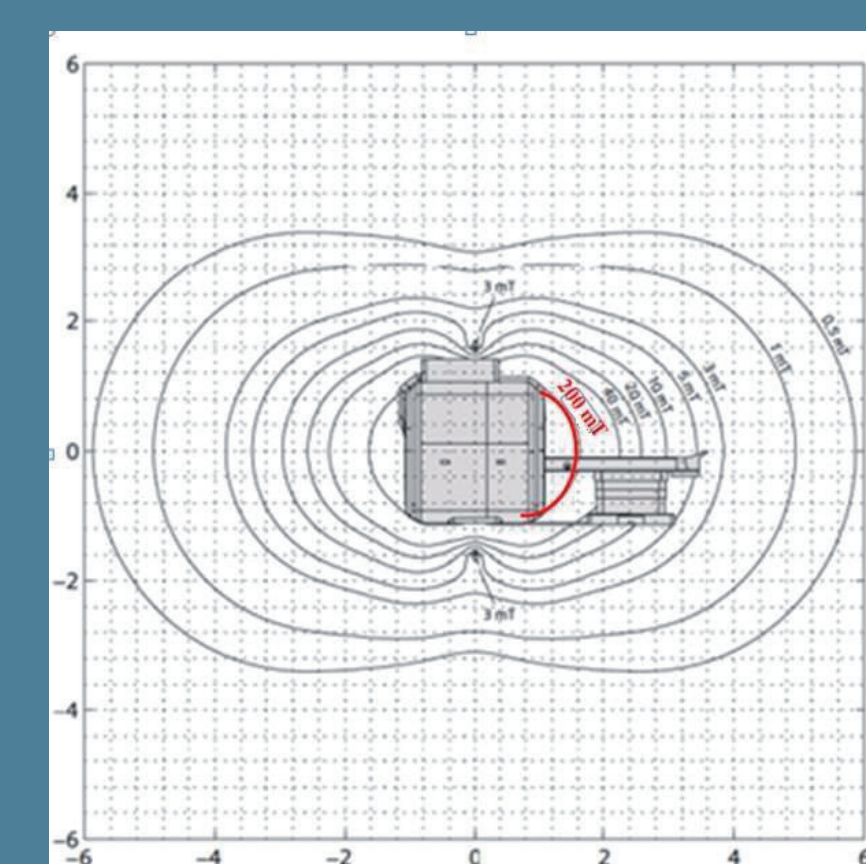


Fig. 2b Fringe field of the human 3 T MRI-scanner

Introduction

Medical personnel working in radiology, oncology or nuclear medicine are being regularly monitored with TL-dosimeters. They might also enter the magnetic field of a MRI-scanner while supervising patients. PET-MRI and MRI-LINAC integrated systems are increasingly using morphological data originating from MRI due to the improved soft tissue and cancer contrast of this imaging modality, compared to CT and CBCT. Monitored personnel will therefore be exposed to the magnetic fields of MRI-scanners and the low stray fields of several mT outside of the MRI-scanner, not only before and after [1] but also during irradiation [2].

Objectives

Do thermoluminescent personal dosimeters (TLDs) indicate the correct dose when being exposed to magnetic fields from low stray fields up to high MRI-fields inside of human MRI-scanners ($0.05 \text{ T} < B < 7 \text{ T}$) during and after irradiation?

Materials and Methods

Panasonic TLD-badges and ring dosimeters for personal monitoring (Fig. 4, 5) were exposed to magnetic fields originating from a 7 T and a 3 T human MRI-scanner as well as neodymium permanent magnets (Fig. 1a, 2a, 3). Three different sealed Cs-137 sources (Fig. 3, 7) were used in two sets of experiments:

- 1.) magnetic induced fading:** TLDs were exposed to a strong magnetic field of a human 7 T MRI-Scanner after irradiation ($D \leq 100 \text{ mSv}$)
- 2.) magnetic induced attenuation:** TLDs were placed during irradiation in a magnetic field, for about 60 hours. Three experimental geometric setups were chosen: double decker (Fig. 6, 7), sandwich (Fig. 3) and honeycomb geometry (Fig. 7, 8).

Results

- 1.) Magnetic induced fading (B after irradiation):** No magnetic induced fading or eventual increase (magneto-luminescence) for LiBO:Cu or CaSO:Tm was observed (Fig. 9).
- 2.) Magnetic induced attenuation (B during irradiation):** A significant reduced dose response up to about 50 % was observed for LiBO:Cu, not at maximum $B \approx 7 \text{ T}$ but at $B \approx 0.2 \text{ T}$ (Fig. 10).

Discussion

Our results indicate no significant impact of the magnetic field on the investigated TLDs after irradiation (no magnetic induced fading). These impact-negative results were also reported for TLD-100 for higher dose levels ($D = 2.6 \text{ Gy}$) and lower magnetic fields ($B = 2.5 \text{ T}$) by Mathis et al. [1]. The same group reported also no relevant differences in dose response for TLDs (ratio: 1.003) with a magnetic field of $B = 1.5 \text{ T}$ vs. $B = 0 \text{ T}$, if higher dose levels typical for radiation therapy are applied [2]. With difference to these results we observe a significant impact at lower dose levels around 0.6 mSv , typical for radiation protection dosimetry, being strongest at $B \approx 0.2 \text{ T}$ (lower than used in ref. [2]). The differences in results might be related to different types of TLDs used (no type was reported in [2]), fixed high magnetic field strength or higher radio-therapeutically relevant dose levels. A field strength of $B \approx 0.2 \text{ T}$ with up to 50 % dose response deviation on personal TL-dosimeters is relevant especially for medical and technical personnel caring for patients in nuclear medicine before and during an MRI-scanning procedure (Fig. 1b, 2b). The observed differences in the measured dose response may have medical as well as legal consequences. However, the physical reasons have not been cleared up yet.

Summary and Conclusion

The influence of magnetic field strengths ($0.05 \text{ T} < B < 7 \text{ T}$) during irradiation on the response of thermoluminescent dosimeters (LiBO:Cu) was measured and a significant attenuation of dose response up to 50 % with a maximum at about $B = 0.2 \text{ T}$ was observed. The physical mechanisms establishing this reduction could not be cleared up within the experimental design and available physio-analytical instruments. The results are reported as a possible and likely impact of magnetic fields, being of possible medical and legal relevance.

References

- [1] M. Mathis, Z. Wen, R. Taylor, G. Sawakuchi, D. Flint, S. Beddar, G. Ibbott, Effect of a Strong Magnetic Field on Selected Radiation Dosimeters. Med. Phys. 41, 309 (2014)
- [2] Z. Wen, J. Wang, W. Jiang, D. O'Brien, G. Sawakuchi, G. Ibbott, Investigation on the Magnetic Field Effect on TLDs, OSLDs and Gafchromic Films using an MR-Linac. Med. Phys. 43, 3632 (2016)

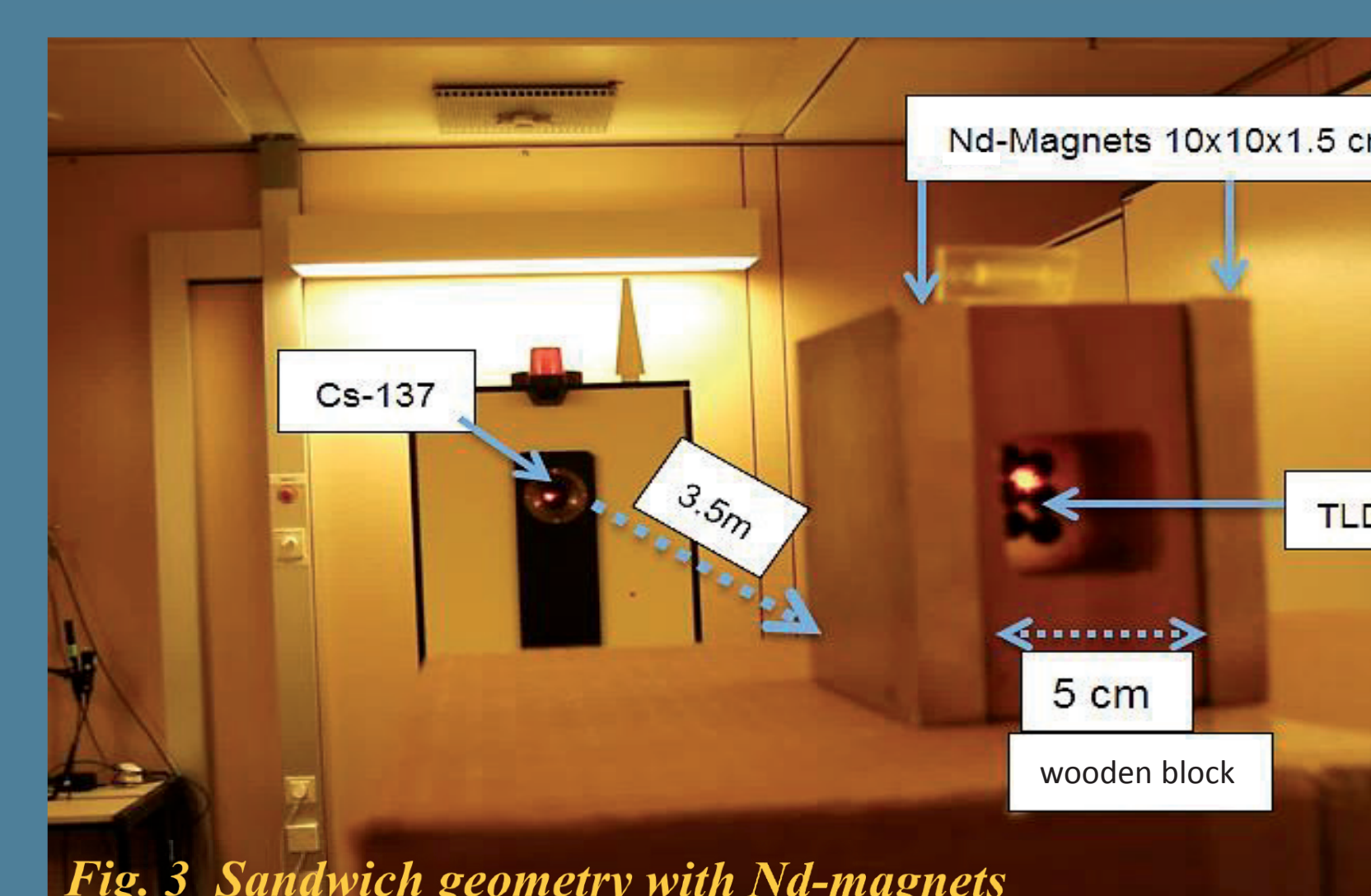


Fig. 3 Sandwich geometry with Nd-magnets

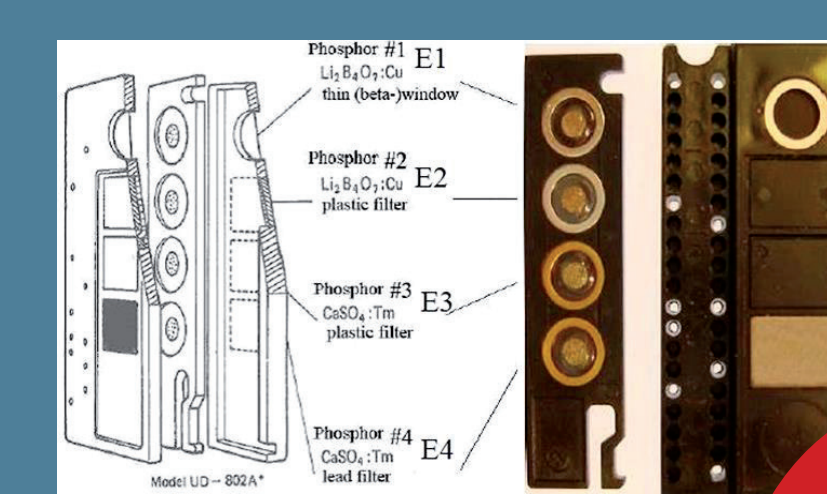


Fig. 4 TLD UD-807 LiBO diam. 3mm

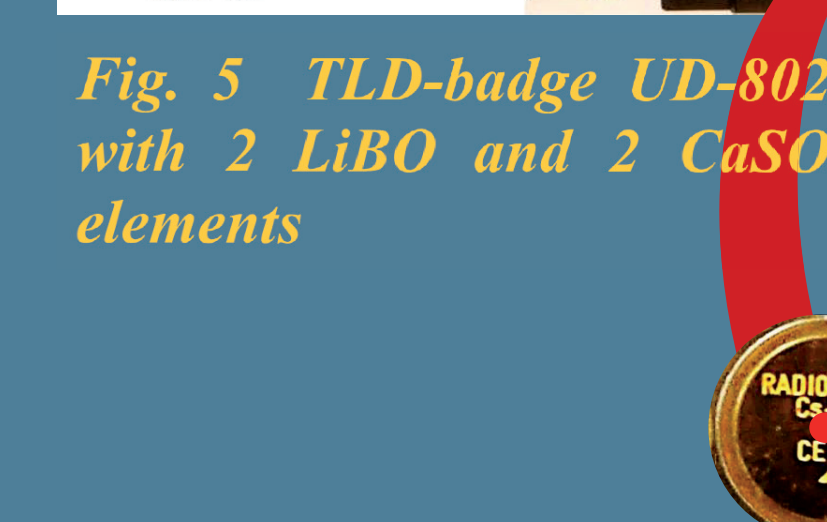


Fig. 5 TLD-badge UD-802 with 2 LiBO and 2 CaSO elements



Fig. 6 Double decker geometry



Fig. 7 Cs-137 Point-source



Fig. 8 Honeycomb geometry

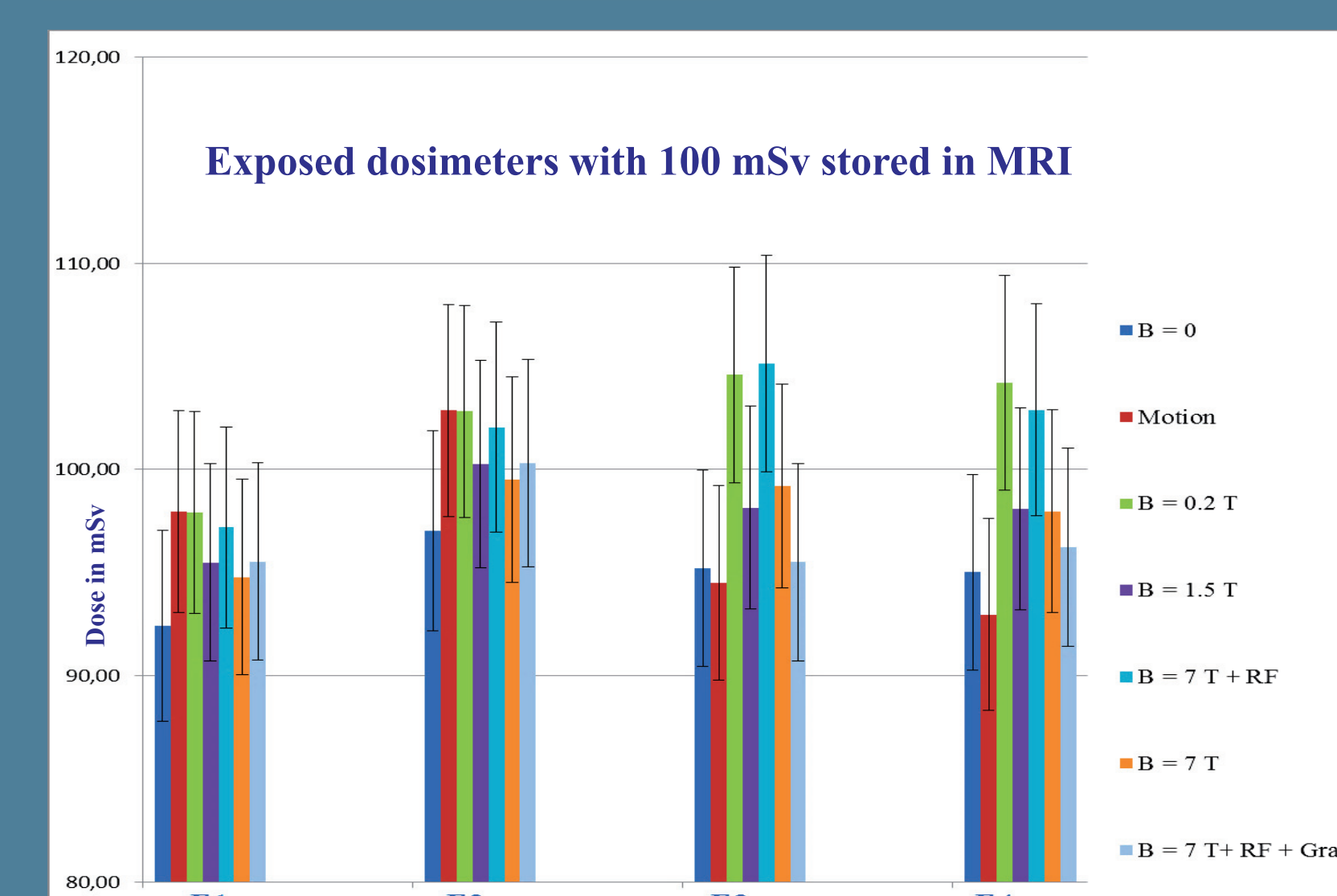


Fig. 9 Dose response for applying a magnetic field of 7 T after irradiation. No change is observed within experimental error

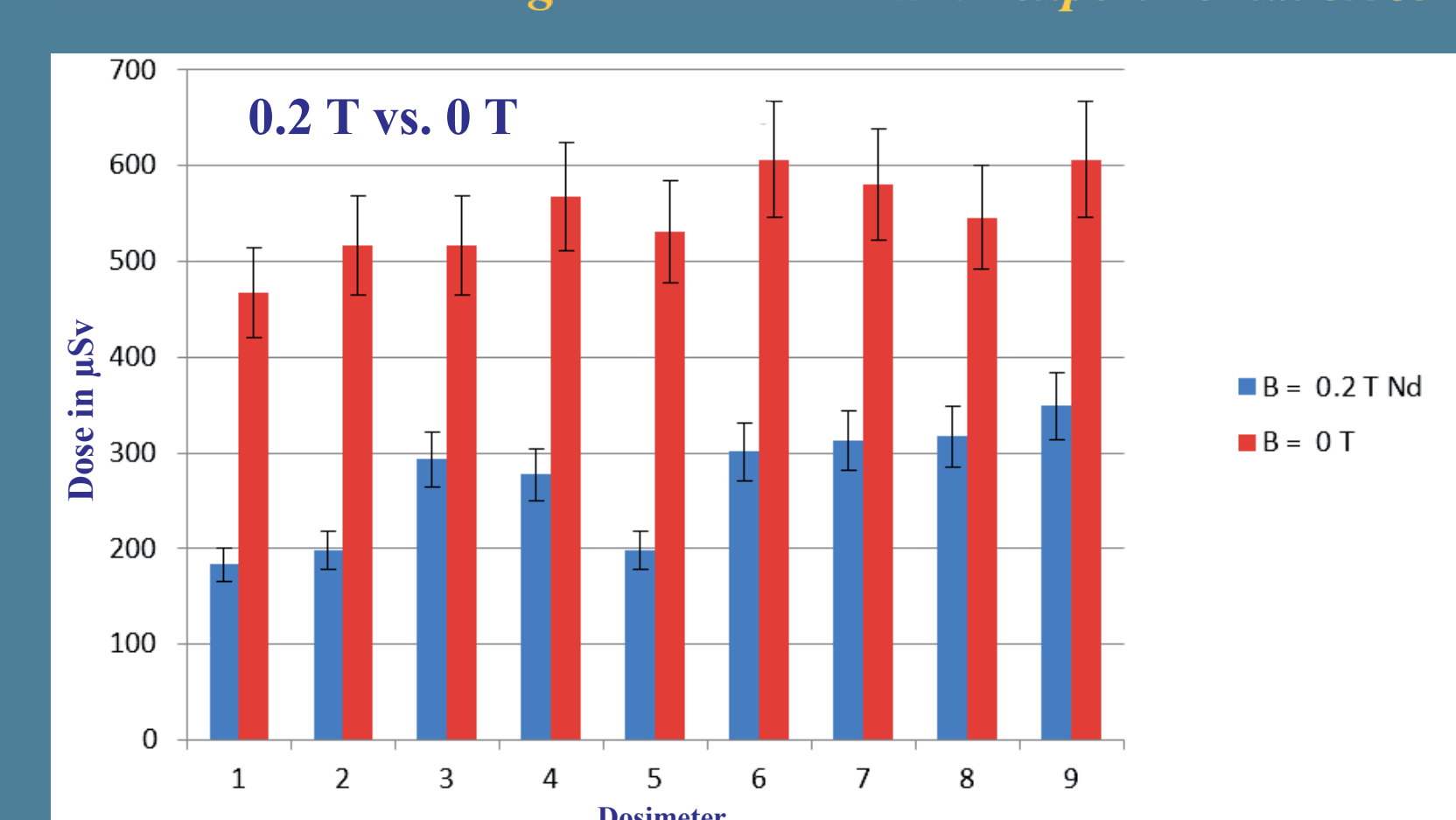


Fig. 10 Dose response during irradiation. Note the high changes in dose response (40 % - 50 %) for the LiBO TLDs at $B = 0.2 \text{ T}$

THE “OCCUPATIONAL HEALTH SERVICE” FOR MEDICAL SURVEILLANCE IN RADIATION PROTECTION

Raffaele Pennarola¹, Elena Pennarola², Pietro G. Iacoviello³, Angelo Lauro³, Roberto Formicola³

¹Università di Napoli “Federico II”, ²ASL NA2 Nord, ³INAIL Direzione Regionale Campania

Introduction

The medical surveillance of workers exposed to ionising radiation is now extended to natural radiation (radon, etc.) and furthermore, due to ever so frequent nuclear or radiological emergencies, it could and should be extended to the exposed population, and to the environment.

In this context the occupational health service as defined by EURATOM Directive 2013/59 (G.U.E. 17 January 2014) plays an important role, also addressing environmental issues.

In fact, the Commission's Recommendations demand an adequate level of protection for people and the environment against the detrimental effects of radiation exposure "without unduly limiting the desirable human actions that may be associated with such exposure." Moreover, "The Commission's system of radiological protection aims primarily to protect human health. Its health objectives are relatively straightforward: to manage and control exposures to ionising radiation so that deterministic effects are prevented, and the risks of stochastic effects are reduced to achievable effect."

Objectives and Methodology

In terms of procedures, it is necessary to complete the medical record (Personal Health Document) for every worker exposed to the ionizing radiation risk. That medical record includes information regarding preventive measures, routine and specialized health screening.

On this subject two types of harmful effect are recognized by ICRP 103. High doses will cause deterministic effects (harmful tissue reactions), often of an acute nature, which only appear if the dose exceeds a threshold value. Both high and low doses may cause stochastic effects (cancer or heritable effects), which may be observed as a statistically detectable increase in the frequencies of these effects occurring.

Results

The occupational health service is of great importance in the prevention of deterministic effects using monitoring techniques (for instance, microcirculation capillaroscopy, thermography, etc., of the tissues exposed) and stochastic effects (Fig.1-2 3) using epidemiology and monitoring of biological data (genetic, etc). The objective is always the workers' occupational health.

Fig. 1 - Occupational health service for Emergency exposure (University of Naples Federico II) **Fig. 2 - Videocapillaroscopy with optical probe**

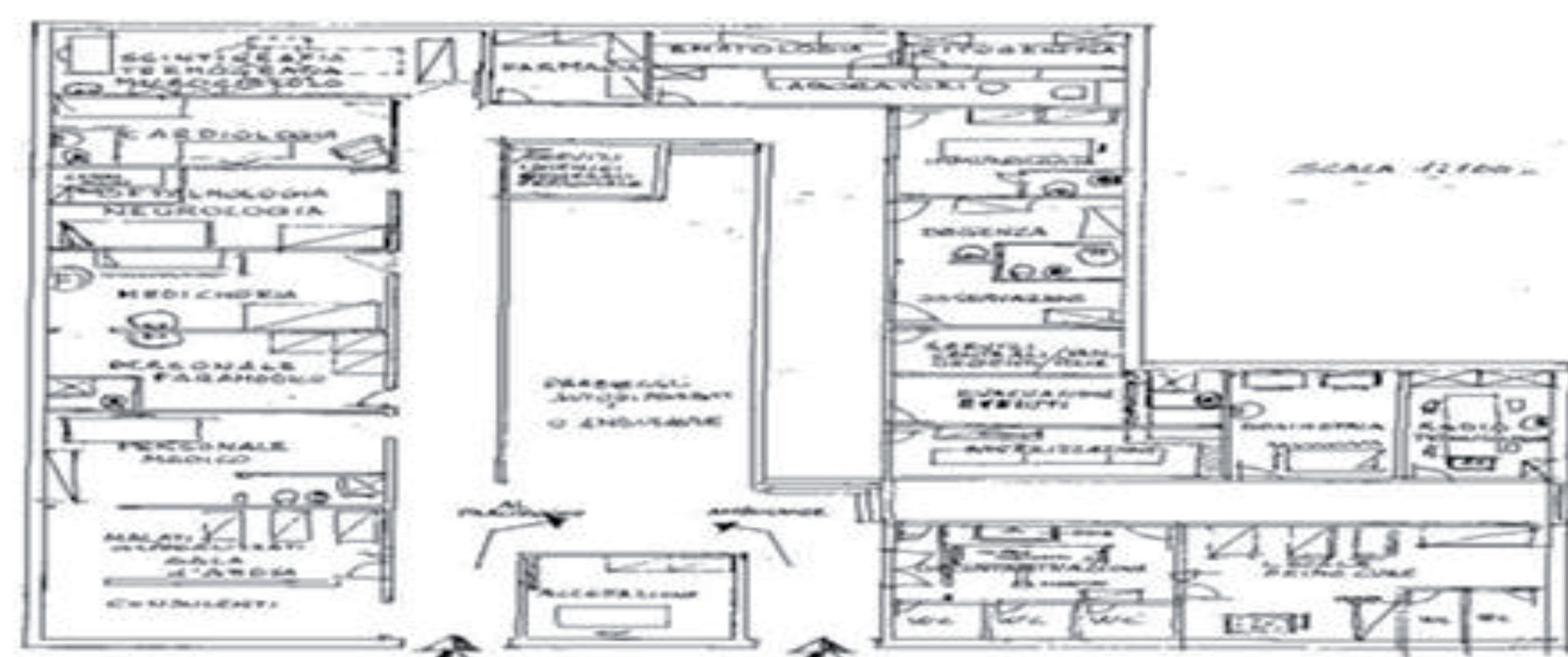
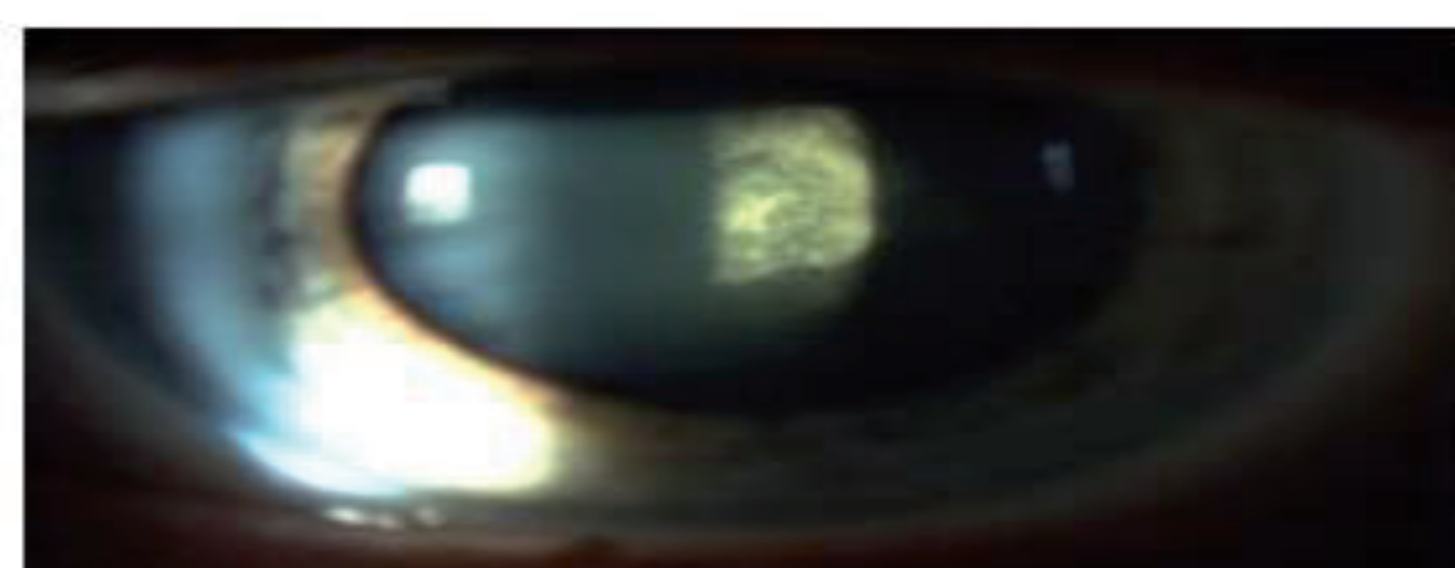
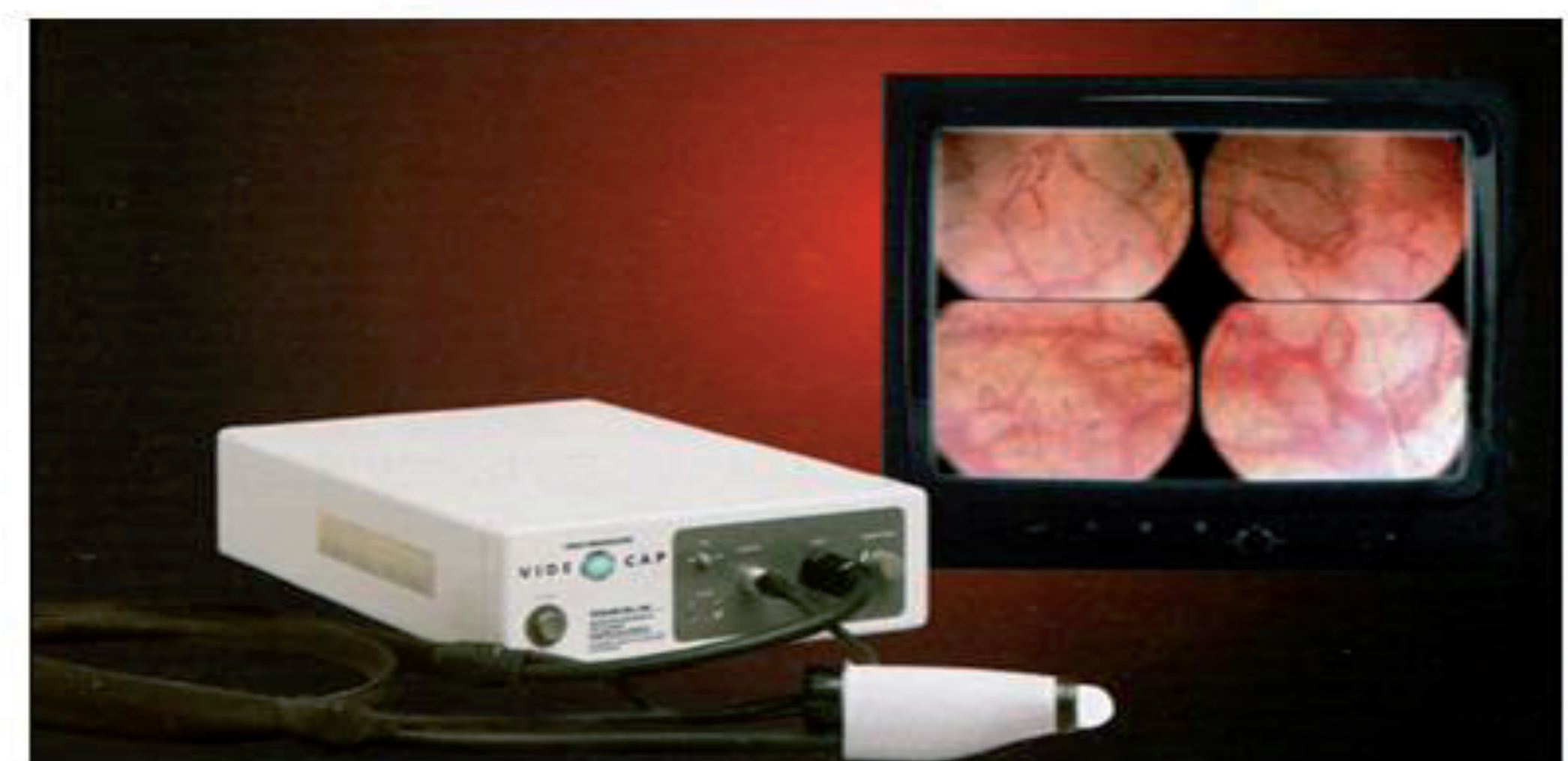


Fig. 3- Medical Surveillance: skin, ocular, microvascular examination (Videocapillaroscopy)



Conclusions

In accordance with the European Directive n.59 / 2013, art.59, concerning the identification of the "Occupational Health Services", they become highly innovative and effective in the management of the radio-exposed worker, also in relation to the personalization of the risk. Determining an easier and more efficient management of all personal, clinical, dosimetric, working and medical data relating to the radio-exposed workers, in order to protect their health and safety.

BIBLIOGRAPHY

1. AIRM. Linee Guida.Sorveglianza medica dei lavoratori esposti a radiazioni ionizzanti.IPSOA.I NDICITALIA, 2013.
2. COUNCIL DIRECTIVE 2013/59 / EURATOM of 5 December 2013 laying down basic safety standards concerning the protection against dangers arising exposure to ionizing radiation, and repealing Directives 89/618 / Euratom, 90/641 / Euratom, 96/29 / Euratom, 97/43 / Euratom and 2003/122 / Euratom
3. Vacca R.J.-Biometric Technologies and verification Systems : A Performance Evaluation of Biometric. Ed.Elsevier, USA, 19-56, Oxford (2007).

Occupational

5th European IRPA Congress
4 - 8 June 2018
The Hague, The Netherlands

Encouraging Sustainability
in Radiation Protection



Application of traditional type test standards to non-traditional dosimetry

Using IEC 62387-2012 to type test the Mirion instadose products

Michelle A. Baca
2652 McGaw Aven, Irvine, CA USA

Introduction



The instadose product line contains a semi-passive dosimeter; it communicates dose information via USB or low-energy Bluetooth at

scheduled intervals or when activated by the user. The DIS operates similarly to an ion chamber and has been commercially available since the mid-1990s, but only recently has been designed for use as a service dosimeter rather than a wholesale dosimetry system.

The instadose 2 has two direct-ion storage (DIS) detectors, providing independent Hp(10) and Hp(0.07) measurements. Each detector has two elements contained in a chamber, a high sensitivity element and a low sensitivity element.

Materials and methods

Testing was performed using the IEC standard. Relative responses were compared to reference exposures. For photon response, the reference conditions were Cs-137 at 1.5m with the dosimeter oriented with normal incidence at 20°C. For beta response, the reference exposure was Sr-90/Y-90 at 30cm with the dosimeter oriented at normal incidence at 20°C.



Figure 1. Photon reference set-up using a collimated Cs-137 irradiator.

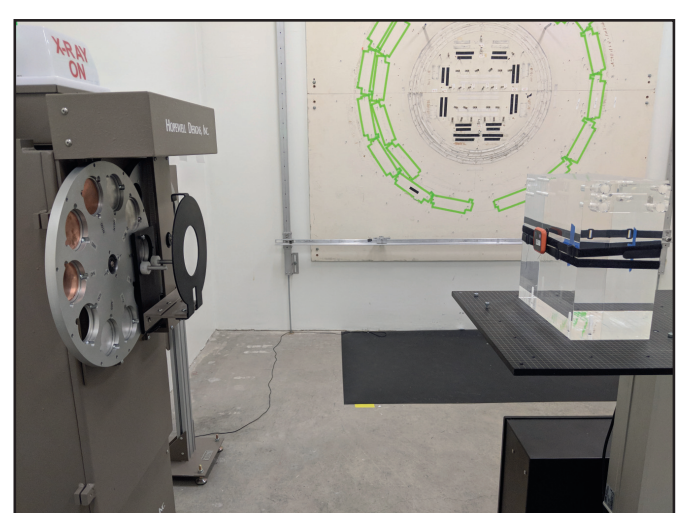


Figure 2. X-ray exposure set-up using a Hopewell X80-225kV irradiator (N-series exposures).

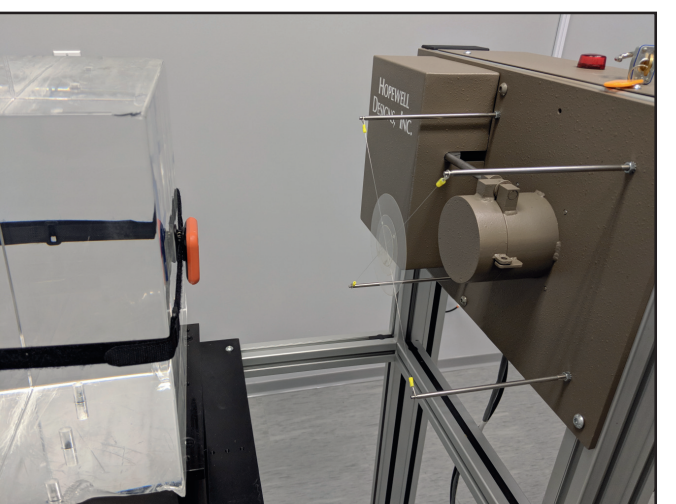


Figure 3. Beta reference set-up using a Sr-90/Y-90 irradiator with flattening filter.

Results

The type tests were conducted per the standard, or, when necessary, with the intent of the standard in mind while adjusting for the unique service model of the instadose 2. All tests were performed in 2016 and 2017, at the Mirion Technologies (DSD), Inc. Irvine facility, SCK·CEN in Mol, Belgium, and PNNL in Richland, Washington. The instadose 2 meets the requirements of IEC 62387-2012.

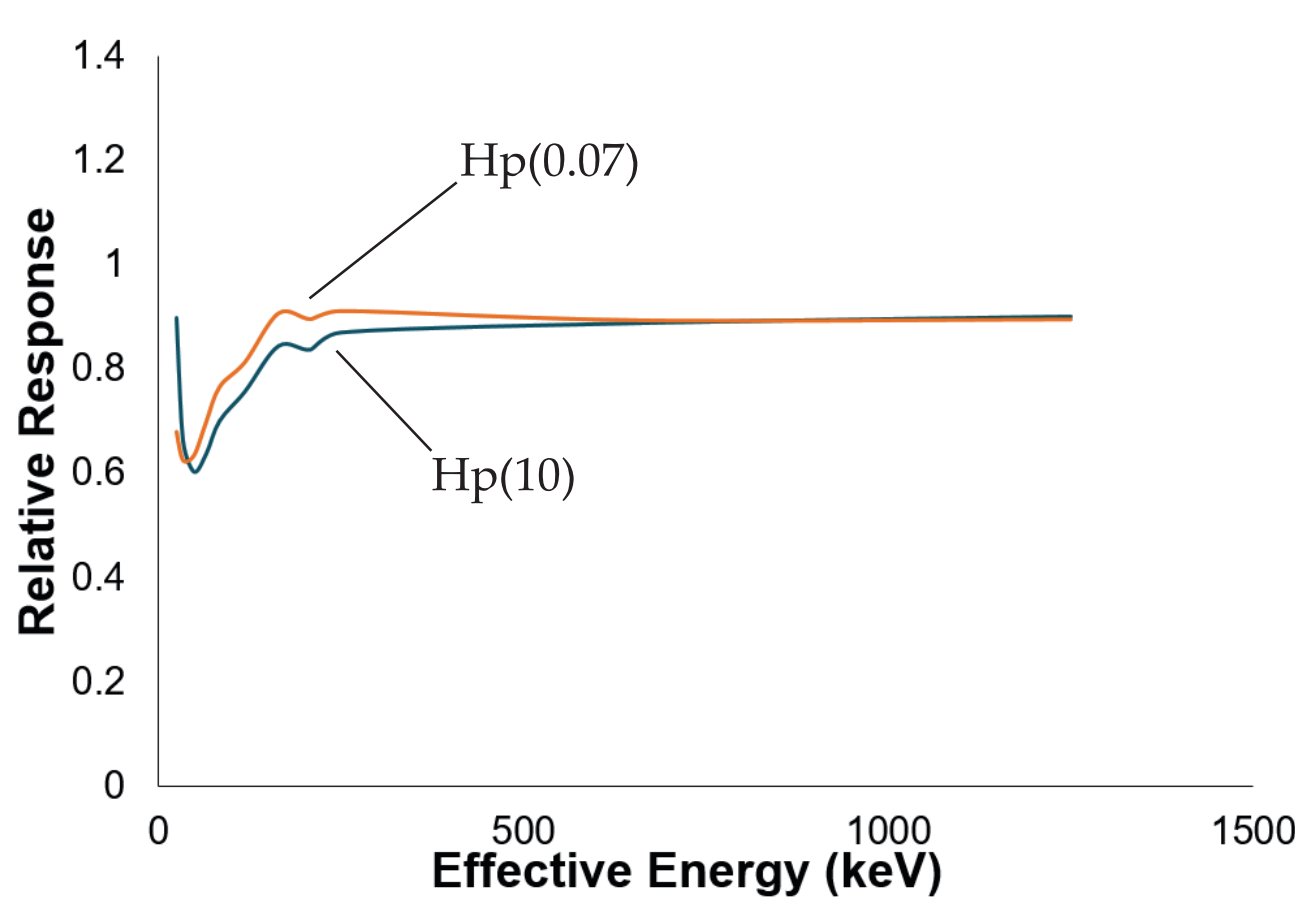


Figure 4. Relative response for Hp(10) and Hp(0.07) for section 11.5 and 11.7 photon testing. The energy and angular response test was able to be performed using the same devices in a short period of time. Fewer dosimeters were required to complete the test, and validate individual device performance over a range of energies and angles.

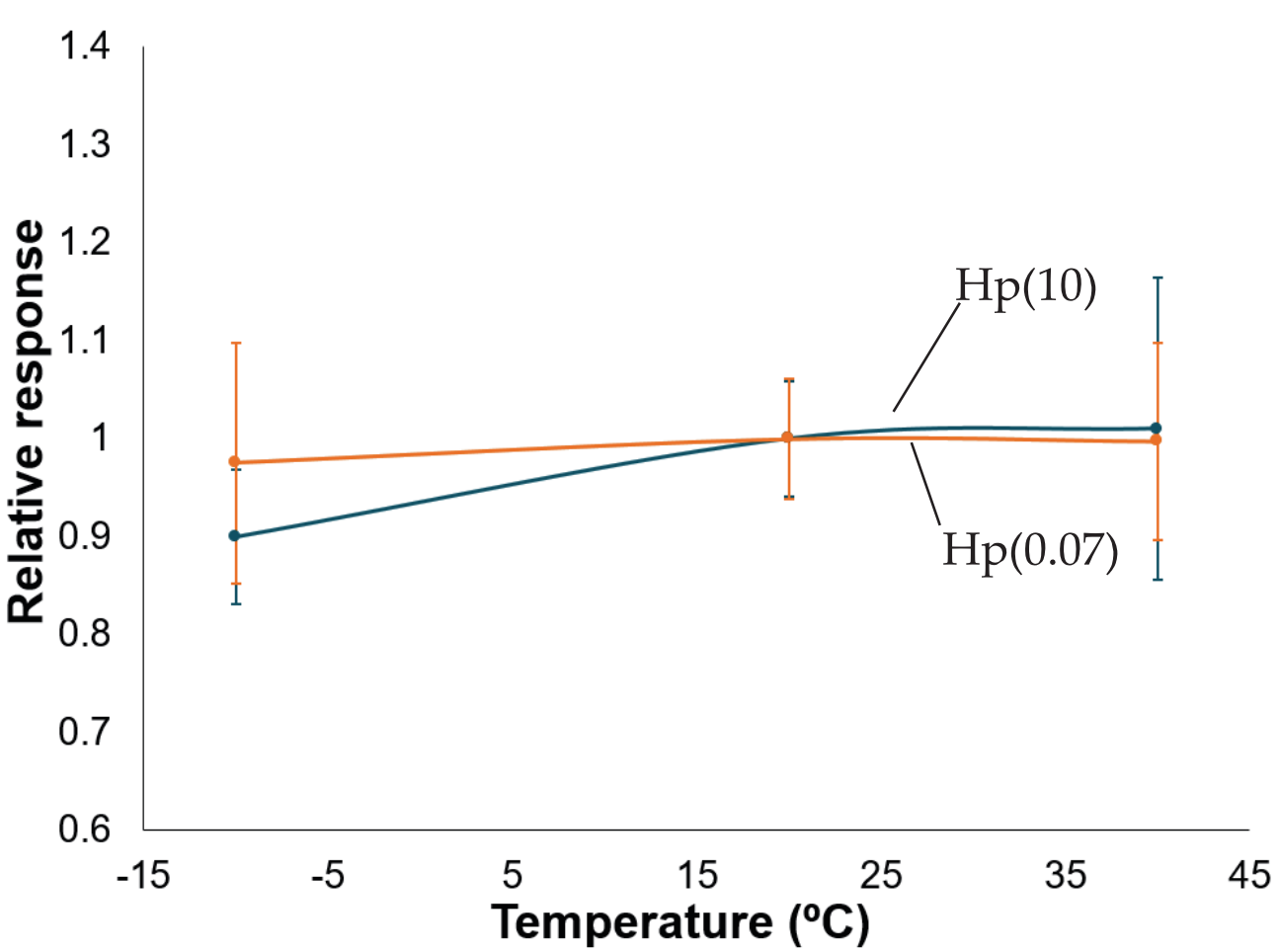


Figure 5. Relative response for Hp(10) and Hp(0.07) for section 13.2 testing. The temperature and humidity test was modified to use the same devices for all three rounds of temperatures. Doing so validated device performance in a wide range of temperatures.

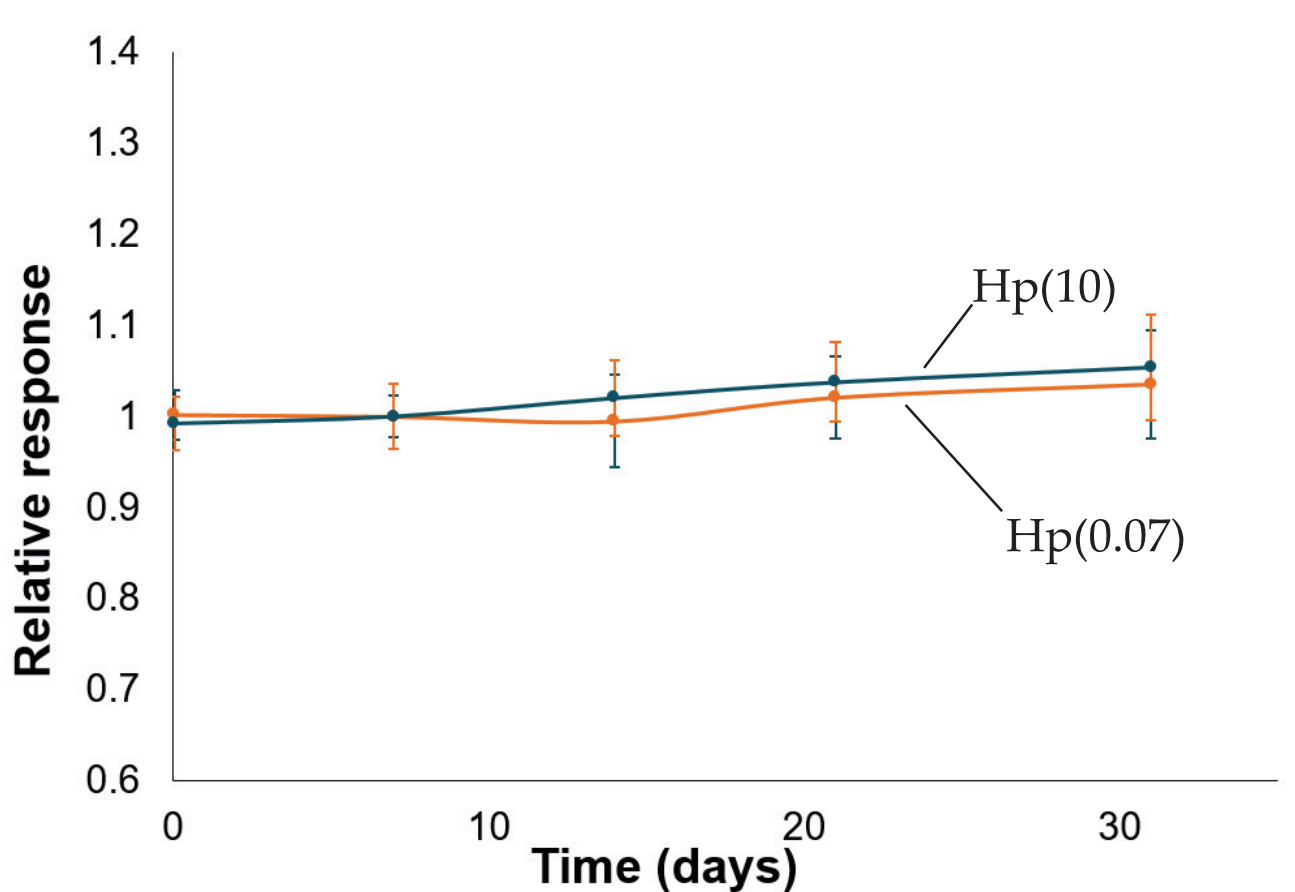


Figure 6. Relative response for Hp(10) and Hp(0.07) for section 13.4 testing (31 days). The background test was able to be amended to take advantage of the cumulative dose behavior of the instadose2. Fewer dosimeters were required to complete the test, yet still achieve expected results.

All instadose products act as both the dosimeter and reader. This configuration enabled the reader-specific tests to be eliminated (taking credit for the dosimeter specific tests as both). This reduced the resources needed for type testing and simplified analysis.

Conclusions

The IEC type test standard was written for traditional dosimetry services; one that consists of separate readers and dosimeters; a service that expects the routine return of devices for processing; and a service that can periodically perform physical inspections of the dosimeters after return and prior to re-issue.

As the instadose2 is both a reader and a dosimeter, interpretation and application of the standard quickly becomes challenging; it is imperative to test the devices adequately, ideally while minimizing overlap of dosimeter and reader tests and capitalizing on the unique capabilities of the dosimeter.

As dosimetry technology advances, the methods to test the performance of dosimetry needs to advance alongside. Any deviations from those standards should be evaluated and justified. As these standards are revised, service providers and manufacturers should be part of the discussion. Tests should be representative of field conditions but also give room for innovation.

Literature cited

1. International Electrotechnical Commission (IEC). IEC 62387 Edition 1.0, Radiation protections instrumentation - Passive integrating dosimetry systems for personal and environmental monitoring of photon and beta radiation. Geneva : IEC Central Office, 2012. ISBN 978-2-83220-518-1.
2. International Organization for Standardization (ISO). ISO 4037-3:1999E, X and gamma reference radiation for calibrating dosimeters and doserate meters and for determining their response as a function of photon energy - Part 3: Calibration of area and personal dosimeters and the measurement of their response . Geneva : ISO, 1999. ISO 4037-3:1999(E).
3. —. ISO 6980-3, Nuclear Energy - Reference beta-particle radiation - Part 3: Calibration of area and personal dosimeters and the determination of their response as a function of beta radiation energy and angle of incidence. Geneva : ISO, 2006. ISO 6980-3:2006.

Further information

Michelle Baca, CHP
Email: mbaca@mirion.com
Phone: +1.949.296.2205

Mirion Technologies (DSD), Inc.
2652 McGaw Ave, Irvine, CA USA
website: www.mirion.com

Acknowledgements

The writer would like to thank PNNL and SCK·CEN for performing the irradiations and the following individuals for providing technical input: Kip Bennett, Eric Wieand, and Kevin Hindra



MIRION
TECHNOLOGIES
Dosimetry Services
Division

Characterization of scattered radiation field in interventional radiology theatres



M. Nowak^{1,2}, L. Ilustos¹, M. Campbell¹, P. Carbonez^{1,3}, F.R. Verdun², J. Damet^{1,2,3}

¹ CERN, European Organization for Nuclear Research, CH-1211, Geneva 23, Switzerland
² Institute of Radiation Physics, Lausanne University Hospital, Lausanne 1007, Switzerland
³ Dept. of Radiology, University of Otago, Christchurch, New Zealand



1. Introduction

The use of an energy resolving hybrid pixel detector in theatres, provides a **new tool for radiation protection and dosimetry**.

The Timepix3 chip is able to give spatial, temporal and energetic information for each incoming photon[1]. This allows to **measure the energy spectrum** in real time.

2. The Timepix3 chip

The Timepix3 chip is a hybrid pixel detector developed in the framework of the Medipix3 collaboration at CERN [2], and is a successor to the Timepix [3] readout ASIC. This readout chip has a pixel matrix of 256 x 256 square pixels with 55 μm side, and can process up to 40 Mhits/cm²/s. The Timepix3 chip can operate in three data acquisition modes. In the data driven mode, after each photon hit the readout chip sends a data set that includes pixel coordinates, time over threshold (TOT) and time of arrival (TOA).

We chose to use the Timepix3 chip (figure 1) with a 500 μm thick silicon sensor produced and bump bonded by ADVACAM [4]. During the measurement, a 300 V bias was applied. The Timepix3 chip was operated in single photon mode, and data driven mode. Collected data were then corrected for the detector efficiency.



Figure 1. Timepix3 chip

3. Measurement setup

Measurements were carried out :

- in an interventional radiology theatre at Christchurch hospital – NZ.
- within a 3m radius half-sphere centred on the patient (figure 2).

The protocol used was the standard pelvis/iliac set-up for patient of 70 kg:

- 3 fps
- 74 kVp
- 12.0 mA

Measurements were carried out at four different heights corresponding to the eye lens, chest, belt and knee of an average 1.76 m medical staff member (figure 3).

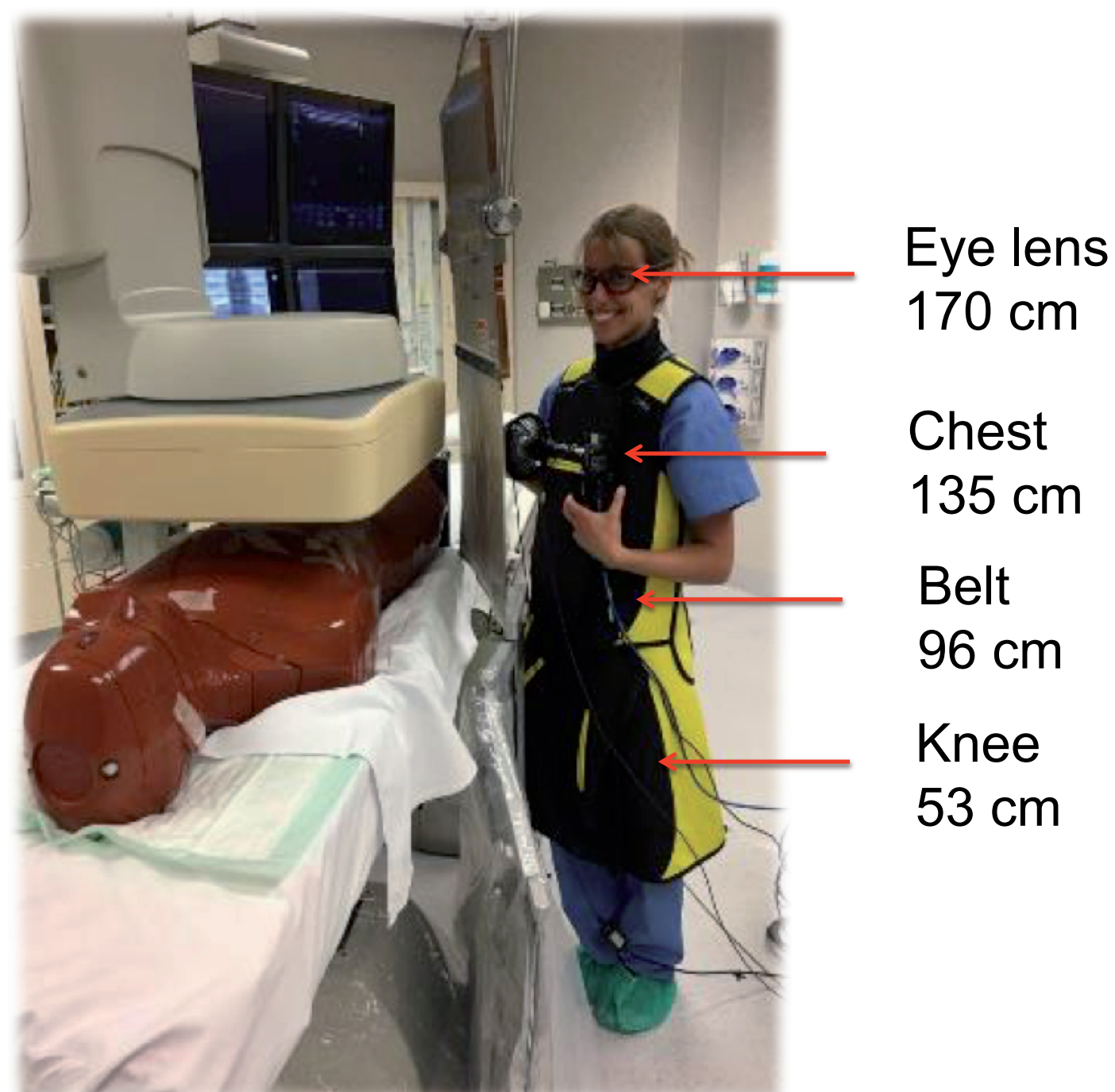


Figure 3. Measurement carried out at 4 different heights

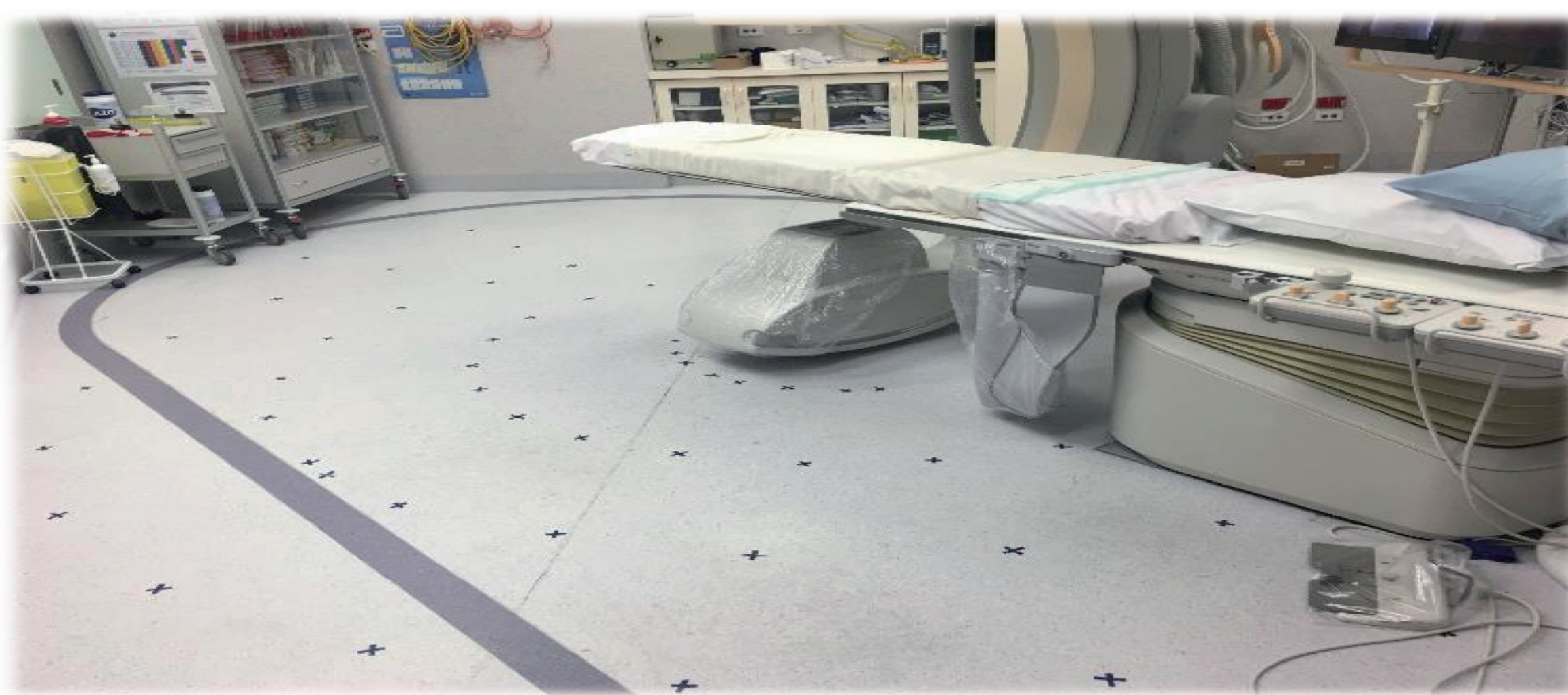


Figure 2. Reference grid for the measurements in the theatre

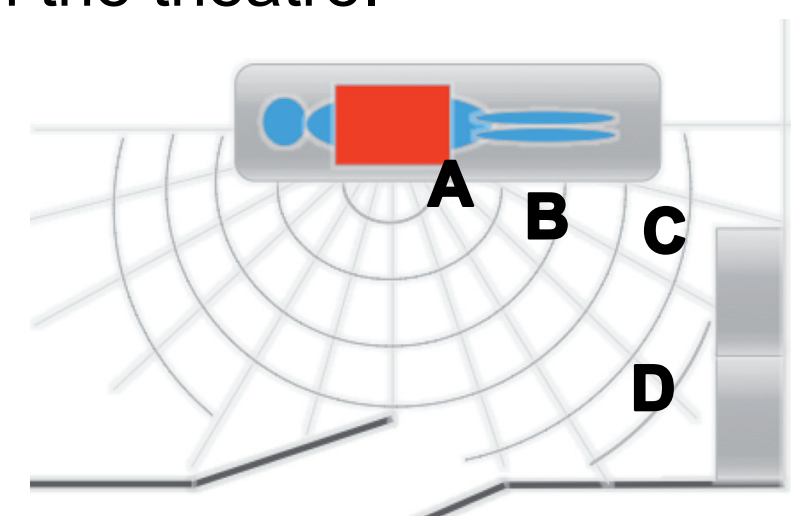


Figures 4. Position of the staff members in the theatre during a standard procedure

The person in position A (figure 4) is the closest to X-ray tube and right behind protective shields (such as ceiling panels and lead table drape).

People in position B and C are positioned close to the patient's legs and are therefore further away from the primary beam and the isocenter that generates the scattered radiation field, and further away from the lead protections

The person in position D stands the furthest away from the X-ray tube, and only partially stays in the theatre.



4. Calibration

The detector calibration was performed using the time over threshold mode for each of the 65'536 pixels.

Calibration was done with :

- radioactive sources : Am 241 or Fe 55 (figure 5a),
- X-Ray fluorescence from metallic foils (figure 5b)

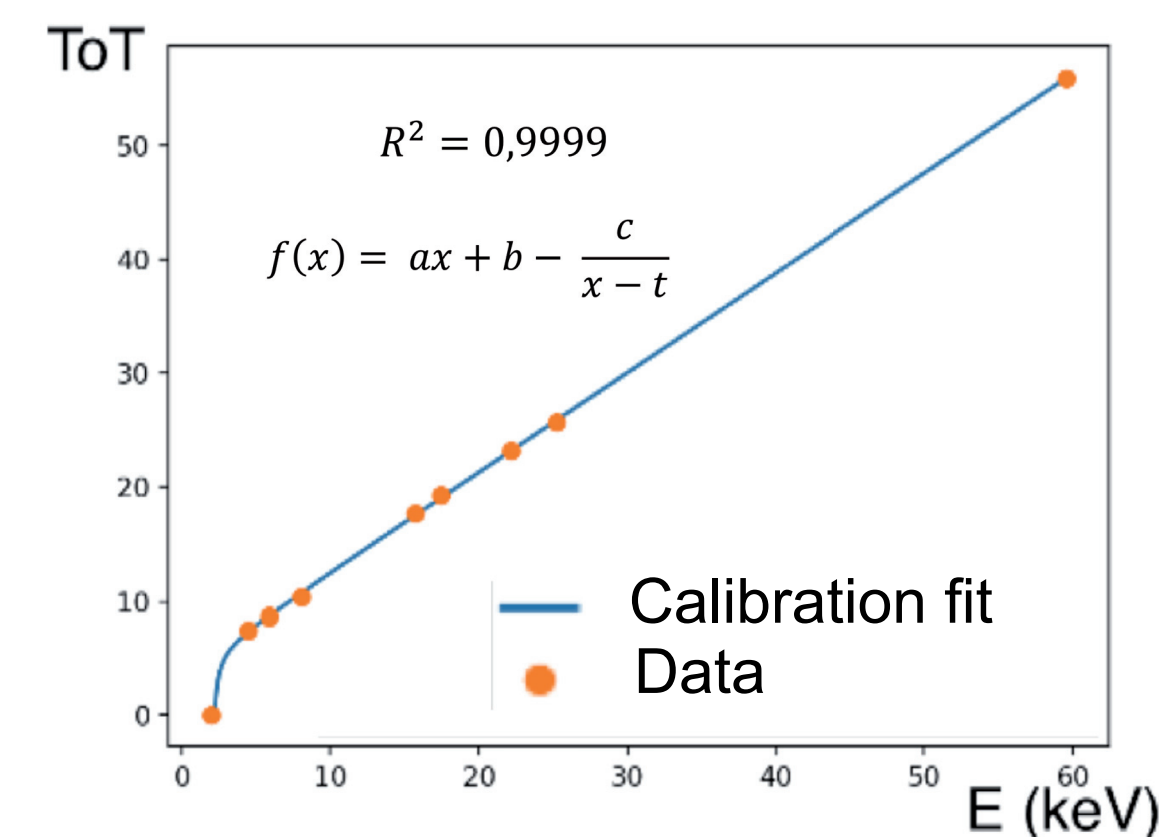


Figure 6. Calibration curve

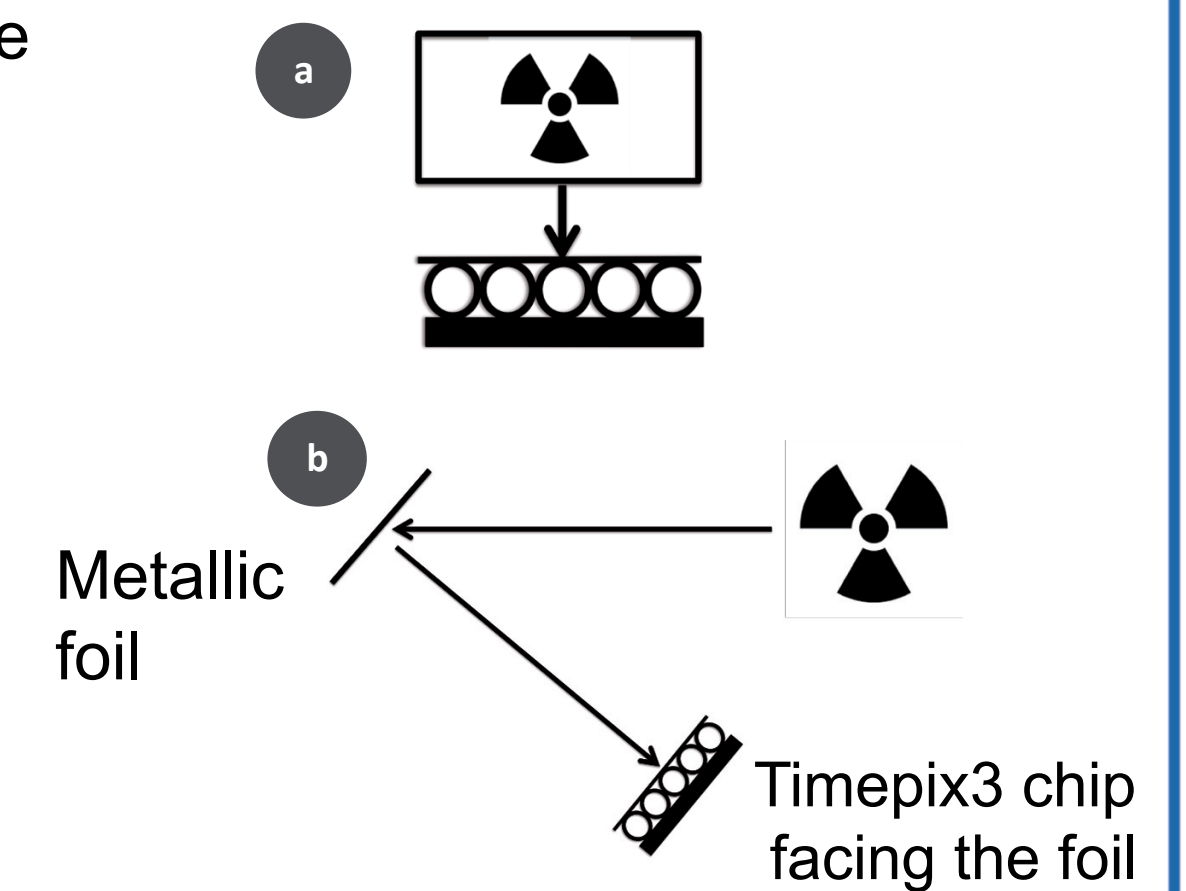


Figure 5. a. Calibration with source above the chip sensor
b. Calibration with x-Ray fluorescence from metallic foils

5. Results

All results are normalised to 1 min.

Figure 7 presents the spectrum obtained at four different heights for each staff member. The curves in figure 7 are normalized to the maximum photon counts.

Figure 8 shows the energy spectrum at four heights for a given staff member. Curves are normalized with respect to the maximum photon counts of each position.

A clear difference in fluence is observed, as expected, for each staff member. A shift in energy is observed from head to toes on position A, indicating a non homogenous exposure of the surgeon. Other positions show more homogeneous exposure.

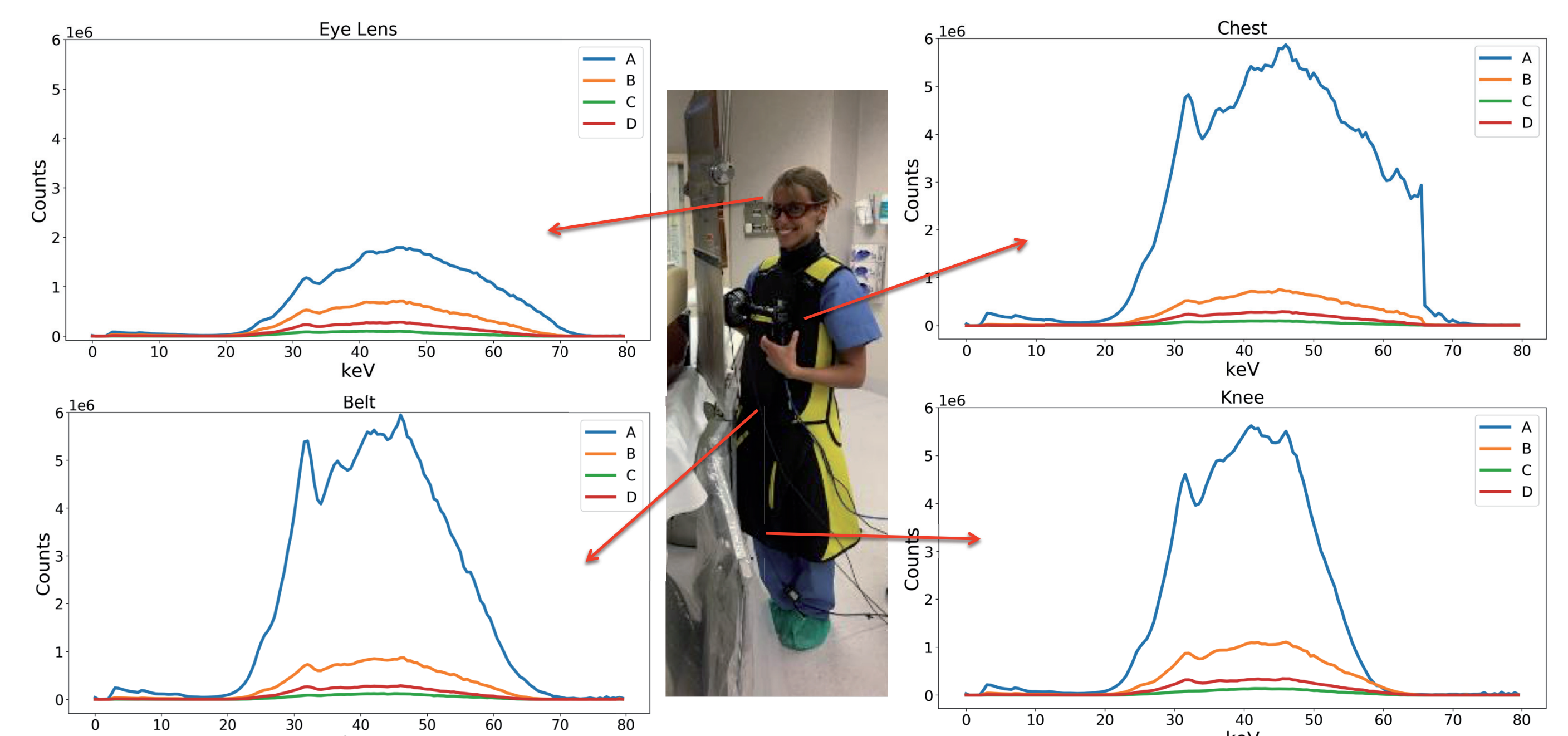


Figure 7. Energy spectra for each medical staff at a given height

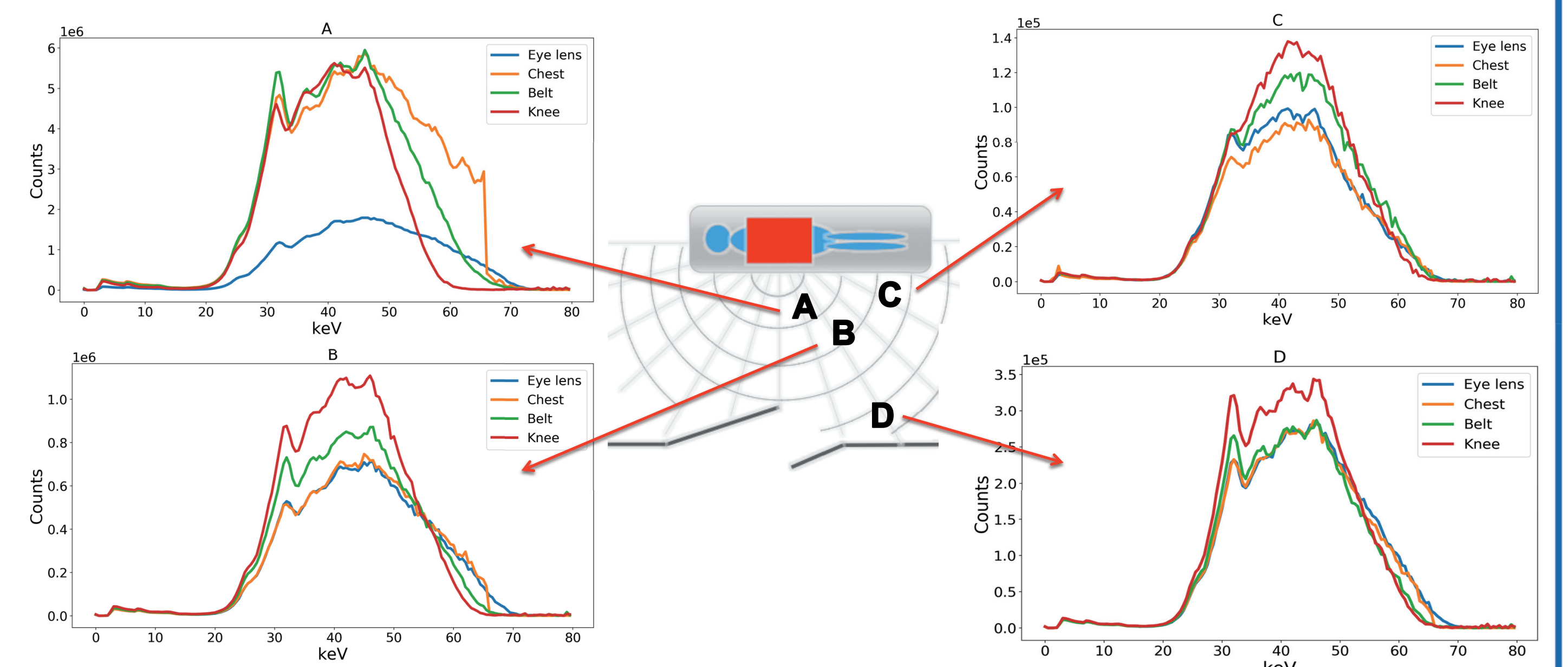


Figure 8. Energy spectra for each height for a given person

7. Conclusions and future outlook

The scattered radiation field has been characterised in an operating theatre .

This new approach allows to characterise and to compare the different energy spectra to which staff members are exposed to and thus guide practitioners in choosing the appropriate radiation protection gears.

This tool provides on-line information on the homogeneity of the radiation field to which each staff is exposed.

These data do not account for attenuation at depth in the body and are not dose-related yet at this stage, but spectra show that annual eye lens dose compliance can not only rely on a chest dosimeter. A dedicated dosimeter would also be needed.

Works cited

- [1] Poikela, T., et al. "Timepix3: a 65K channel hybrid pixel readout chip with simultaneous ToA/ToT and sparse readout." *Journal of instrumentation* 9.05 (2014): C05013.
- [2] Medipix3 collaboration. <https://medipix.web.cern.ch/collaboration/medipix3-collaboration>
- [3] Llopert, Xavier, et al. "Timepix, a 65k programmable pixel readout chip for arrival time, energy and/or photon counting measurements." *Nuclear Instruments and Methods in Physics Research Section A: Accelerators, Spectrometers, Detectors and Associated Equipment* 581.1-2 (2007): 485-494.
- [4] ADVACAM s.r.o. U Pergamenky 12, 17000 Praha 7, Czech Republic. <http://advacam.com/>

Acknowledgements

The authors would like to thank the Medipix3 Collaborations and Laurent Desorgher for the use of its simulation code. Authors are grateful to Dr Martin Krauss and the interventional radiology team in Christchurch for their kindness, technical support and help during measurements.

Dosimeters for monitoring of eye lens irradiation at nuclear power plants

Marko Fülöp¹, Dušan Solivajs², Denisa Nikodémová¹, Pavol Ragan¹, Ľubica Foltínová³

¹Slovak Medical University, Bratislava, SLOVAKIA

²Slovak Legal Metrology, NGO, Bratislava, SLOVAKIA

³UEBA, University of Economics in Bratislava, SLOVAKIA

Introduction

Recent change in dose limit

- The importance of the accuracy of eye lens monitoring was significantly increased by reducing its annual dose limit from 150 to 20 mSv.

Motivation

- For increasing of eye lens monitoring, instead of $H_p(3)$ monitor position on chest, it is proposed to measure of eye lens exposure closer to an eye area. Recently there have been proposed several models of eye lens exposure.
- There are only a few publications dealing with monitoring eye lens exposures in neutron and photon radiation fields occurring, for example, at accelerators of charged particles, or at nuclear reactors where workers should control technologies during operation of NPP.
- Workers in NPP are usually irradiated multilaterally and this give specific requirements on directional independence of monitoring system.

Aim

- This work is focused on proposal, verification and practical using of personal monitor for eye lens exposure at NPP.

Methods

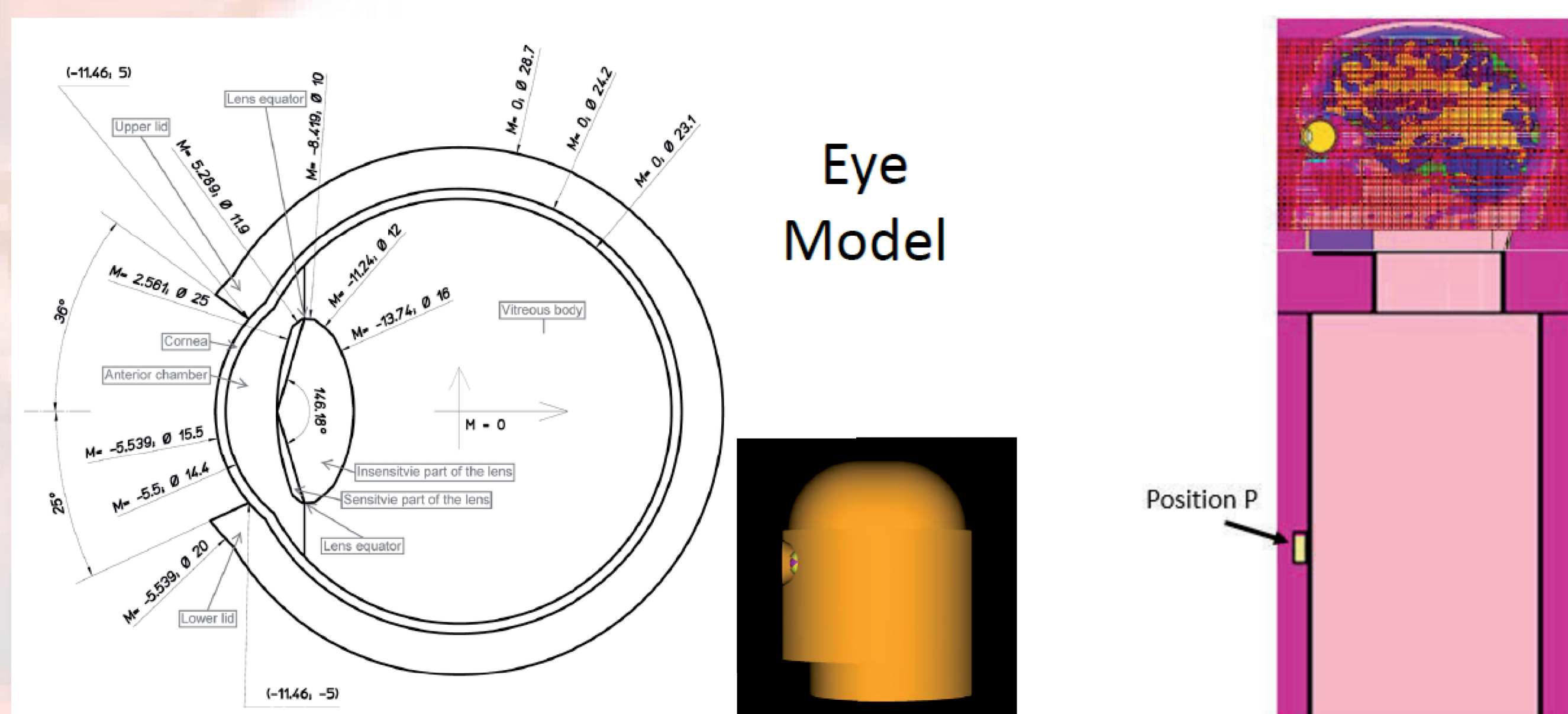
Monitoring of neutron doses is performed by albedo detectors with TLD 600 & 700

Energy and angular dependencies of the monitoring system were determined by the MCNP simulation of hybrid voxel and mathematical head and trunk phantoms.

Verifications of the eye lens exposure monitoring systems simulations were performed by calibration with AmBe neutron source and by ^{137}Cs gamma source.

Neutron spectra in NPP were determined using a Bonner spectrometer with SAND II deconvolution method.

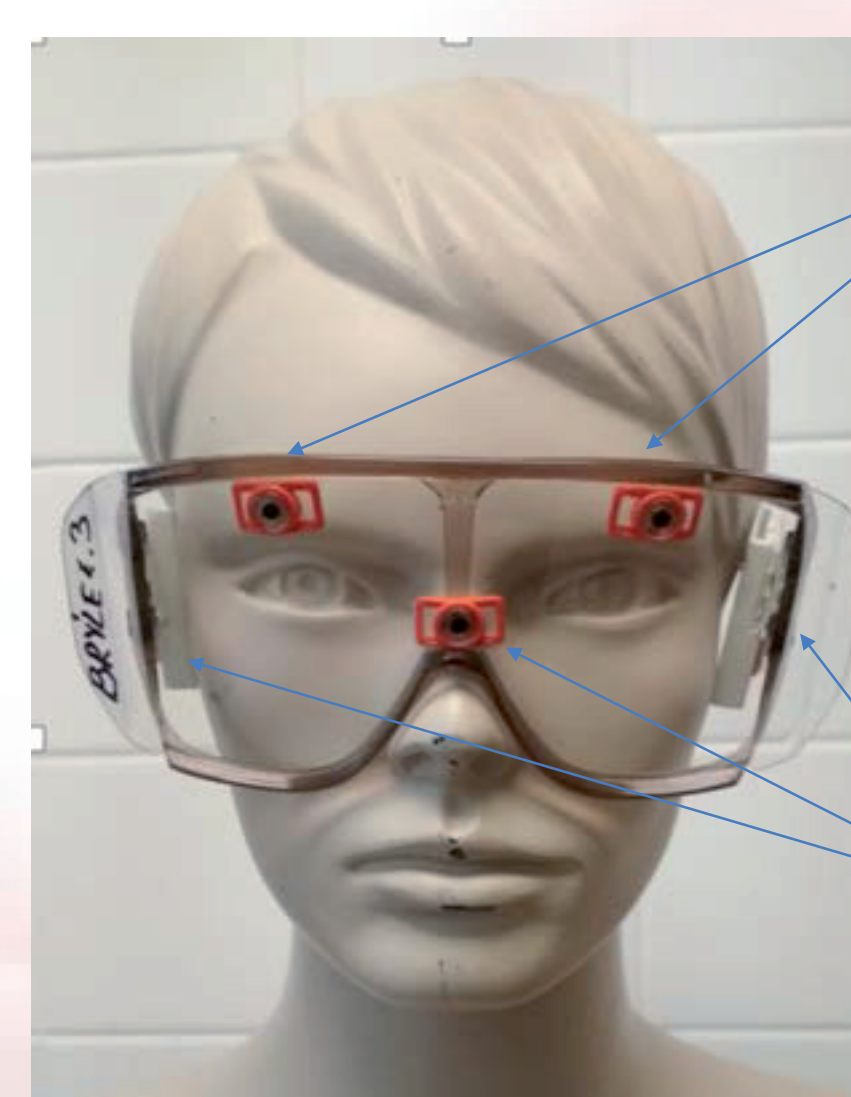
Monitor systems were positioned at both sides of the head at temporal bones and at a root of nose. Correction factors for these systems and measured neutron spectra present in NPP were calculated.



Eye Model

Voxel phantom of the head is not describing detailed eye structures and therefore the mathematical models of eyes were inserted into the Zubal head phantom.

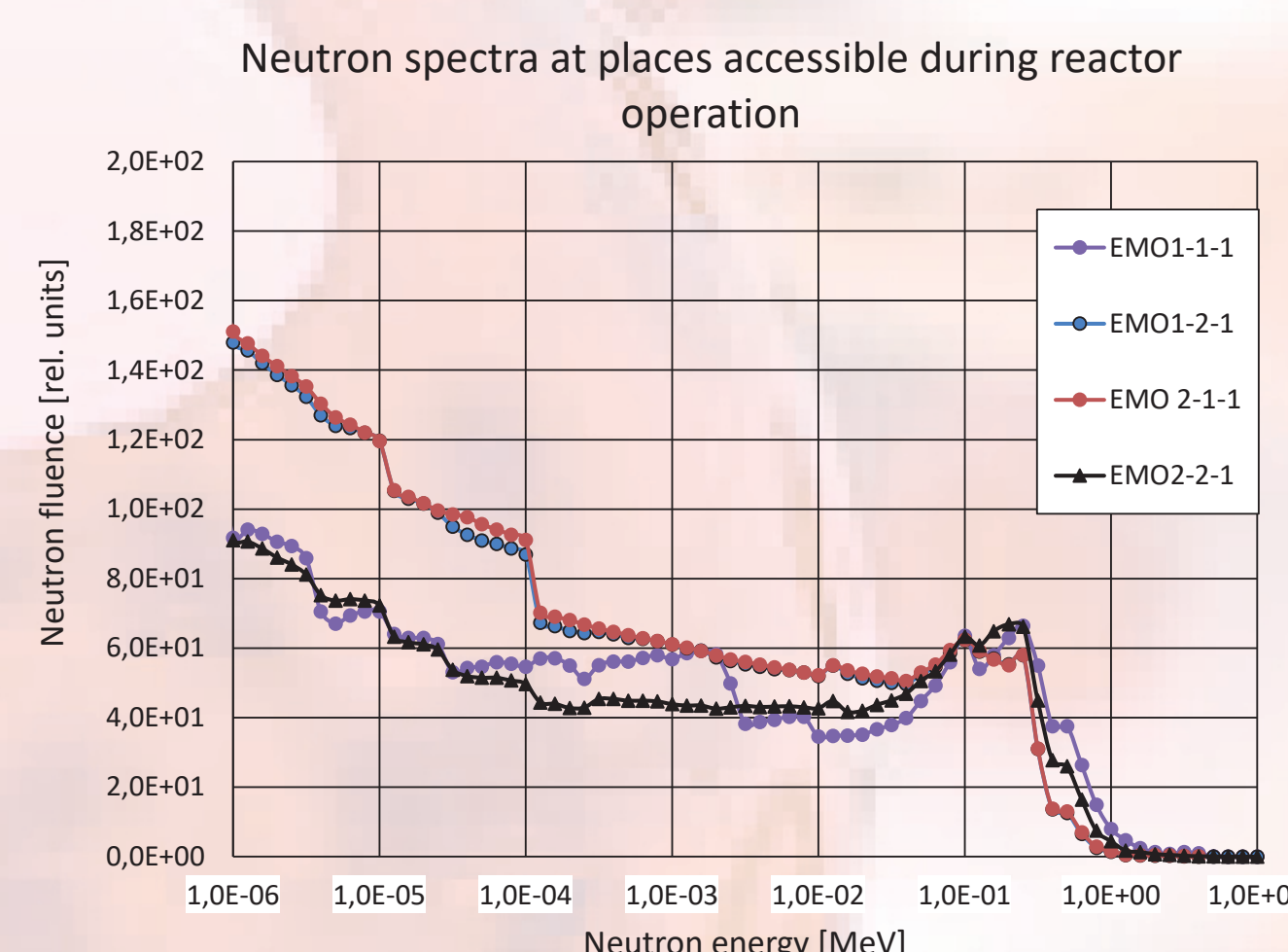
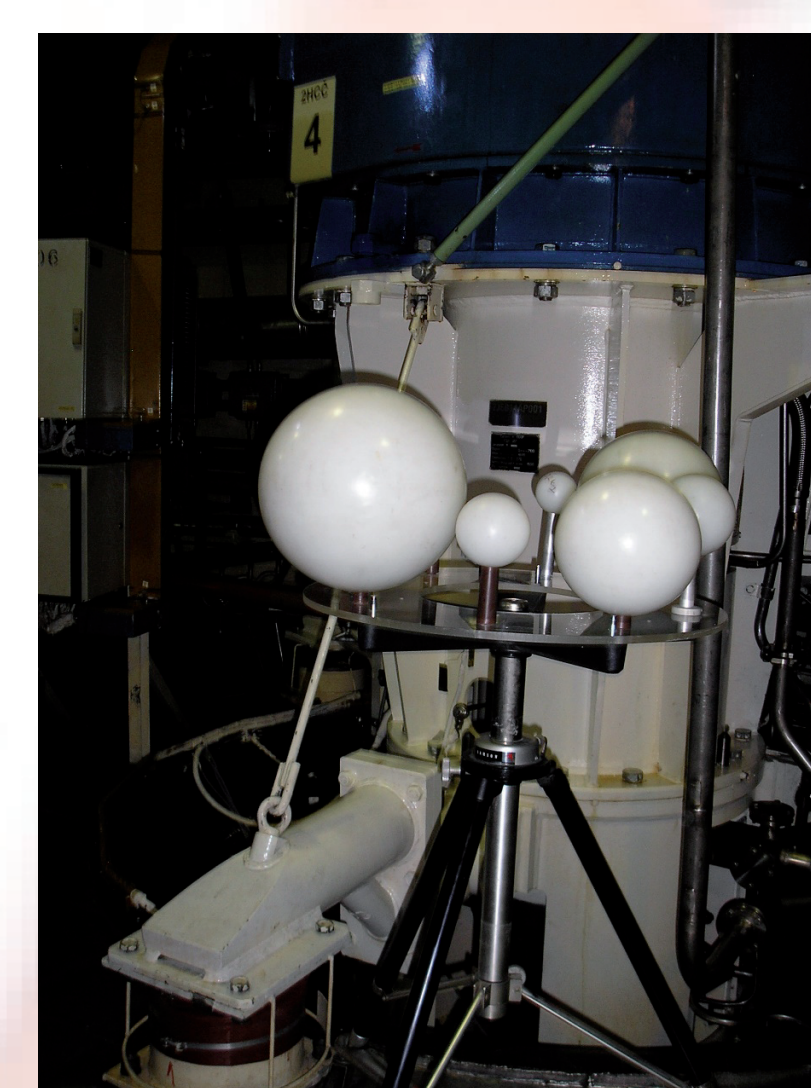
Results



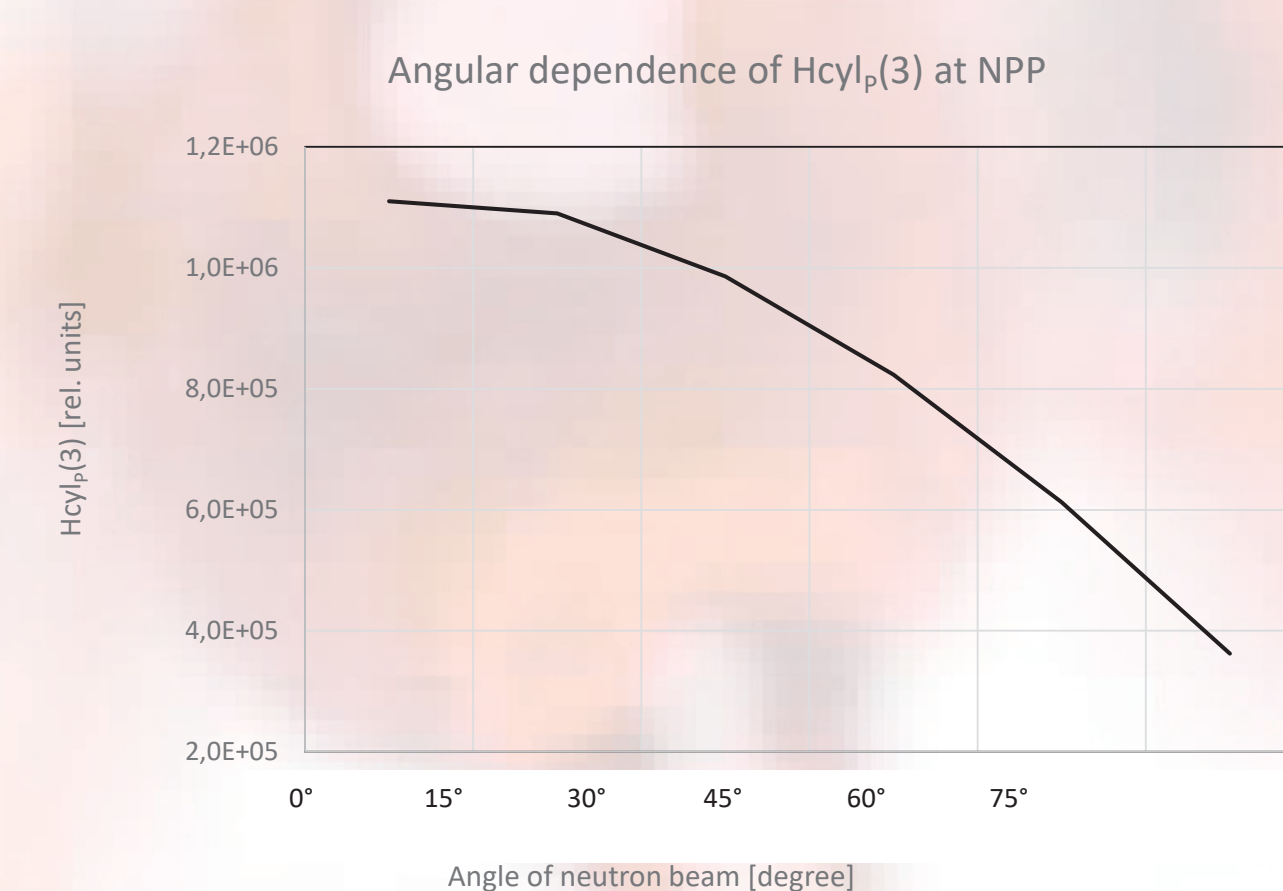
Photon monitors

Bonner spectrometer (2,3,4,2,5,8,10,12 ") with pairs of TLD 600 & TLD 700

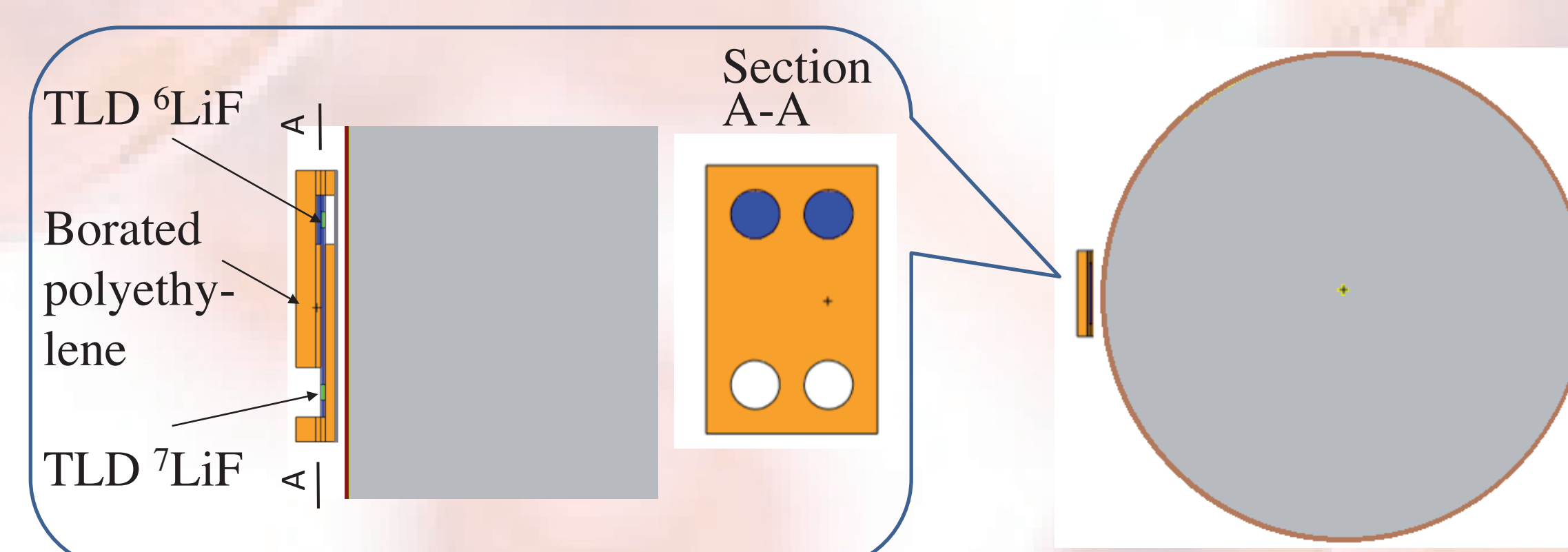
Albedo neutron monitors



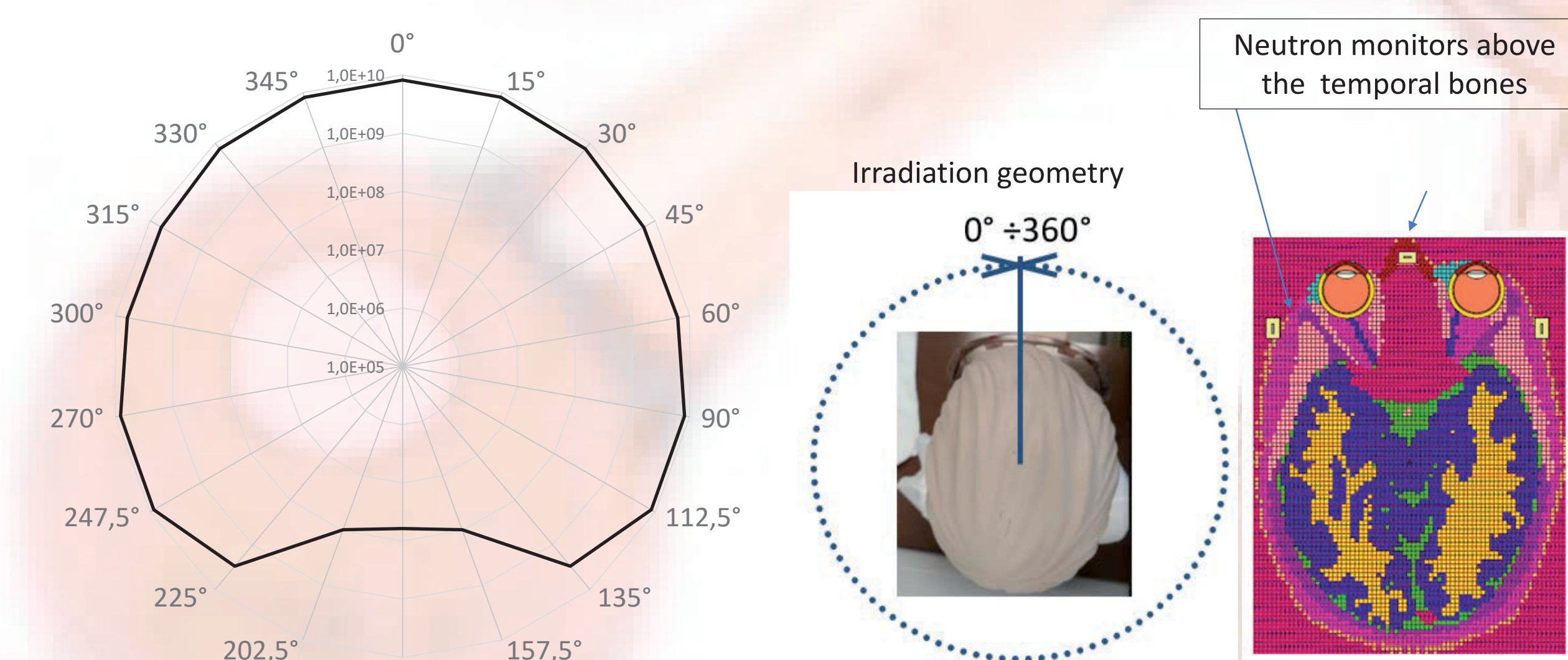
Neutron spectra were measured at workplace near the reactor - at the main circulation pump



Angular dependence $H_{e^l p}(3)$ for the real NPP neutron energy spectrum from 0 to 75 ° incidence angle based on conversion coefficients from (1).



Geometry for MCNP simulation of albedo dosimeter response, monitor is placed on water head phantom – cylinder with diameter of 20 cm, NPP spectra were used as input for calculation



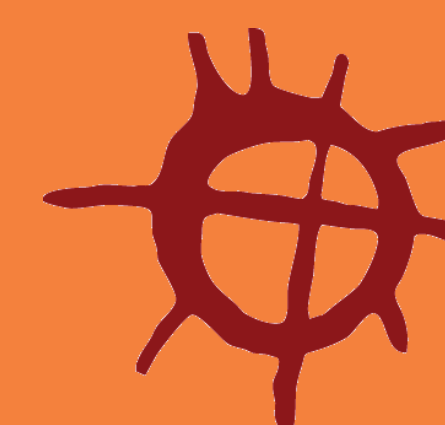
Monitoring system using superposition of the responses of three albedo monitors is sufficiently directionally independent (at frontal angle 270 °) for use in real conditions at NPP. Lower response for rear irradiation is not so important as the eyes are shielded by the whole head.

Acknowledgement

This work was supported by EURADOS.

References

- Gualdrini et al., Fluence to $H_p(3)$ Conversion Coefficients for Neutrons from Thermal to 15 MeV, Rad. Prot. Dosim. 157(2), 278-290 (2013)



Effective Doses from the Norwegian Diet

Mari Komperød and Lavrans Skuterud

Main points

Ingestion doses to the Norwegian public were calculated using national dietary statistics and radionuclide concentration data for each of approximately 50 food groups. The age-weighted mean effective dose was estimated at 0.42 mSv/y from naturally occurring radionuclides and 0.010 mSv/y from anthropogenic radionuclides.

Seafood was found to be the single food group that provides the largest dose contribution from the average diet in Norway. Although the mean dose from anthropogenic radionuclides today is low, this exposure may still be significant for certain critical groups.



Approach

- Food consumption data were primarily derived from national diet survey reports.
- Radionuclide levels in each food product were primarily obtained from monitoring data and from scientific literature. If no Norwegian or other Nordic/Northern European data were available, UNSCEAR reference levels and literature reviews were used.
- Effective ingestion dose coefficients from the ICRP were used to calculate effective doses from each radionuclide for three separate age groups: infants (1 y), children (10 y) and adults. Norwegian population statistics were used to calculate the corresponding national age fractions.
- Ingestion doses from ^{222}Rn in drinking water were calculated using dose coefficients described by the U.S. National Research Council.

Fig. 1. Estimated mean effective dose (mSv/y) from each radionuclide. "Other" represents the sum of ^{234}U , ^{235}U , ^{238}U , ^{228}Th , ^{230}Th , ^{232}Th , ^{90}Sr , and ^{99}Tc . The higher dose from ^{210}Po to infants is due to the high ICRP dose coefficient.

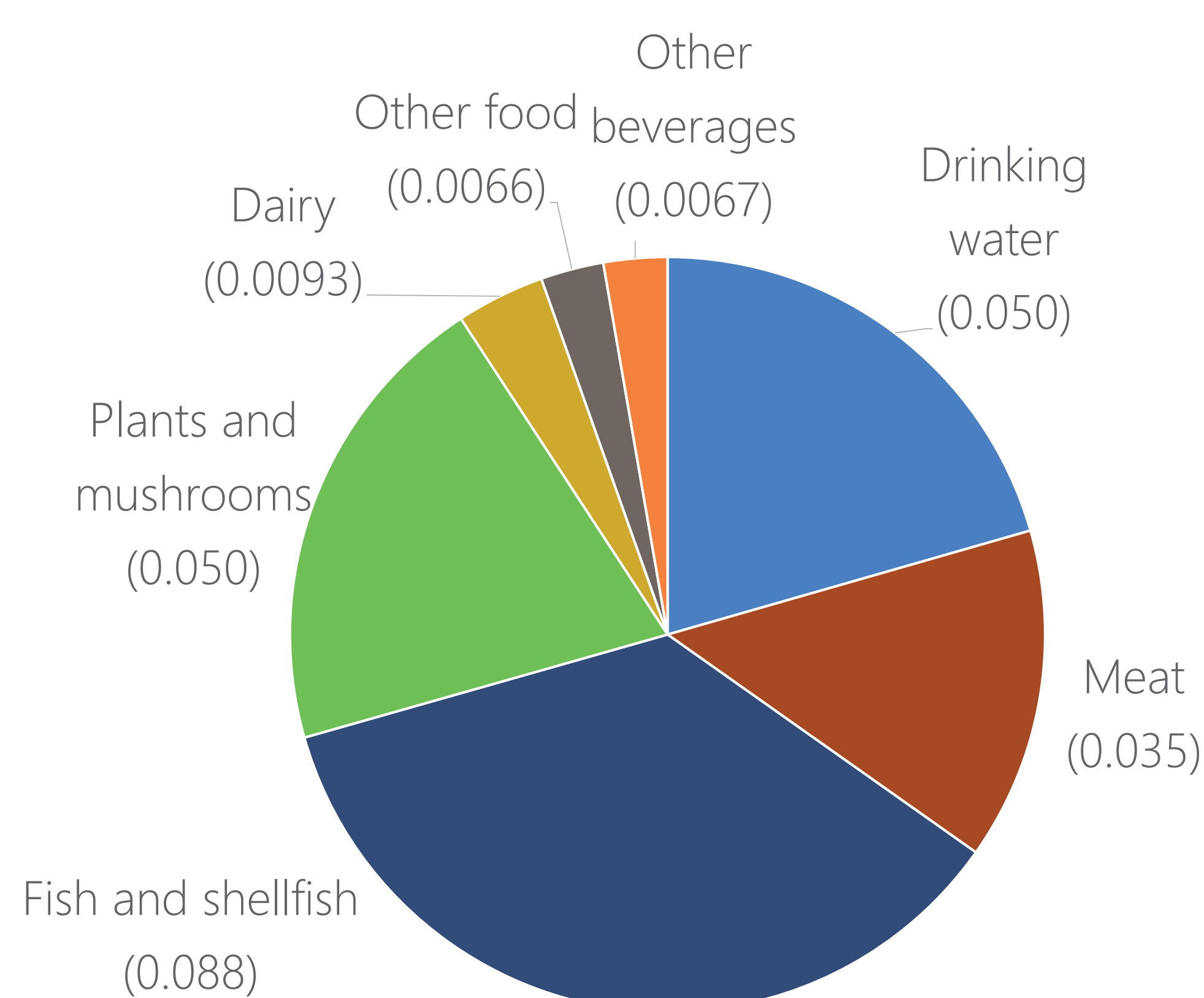
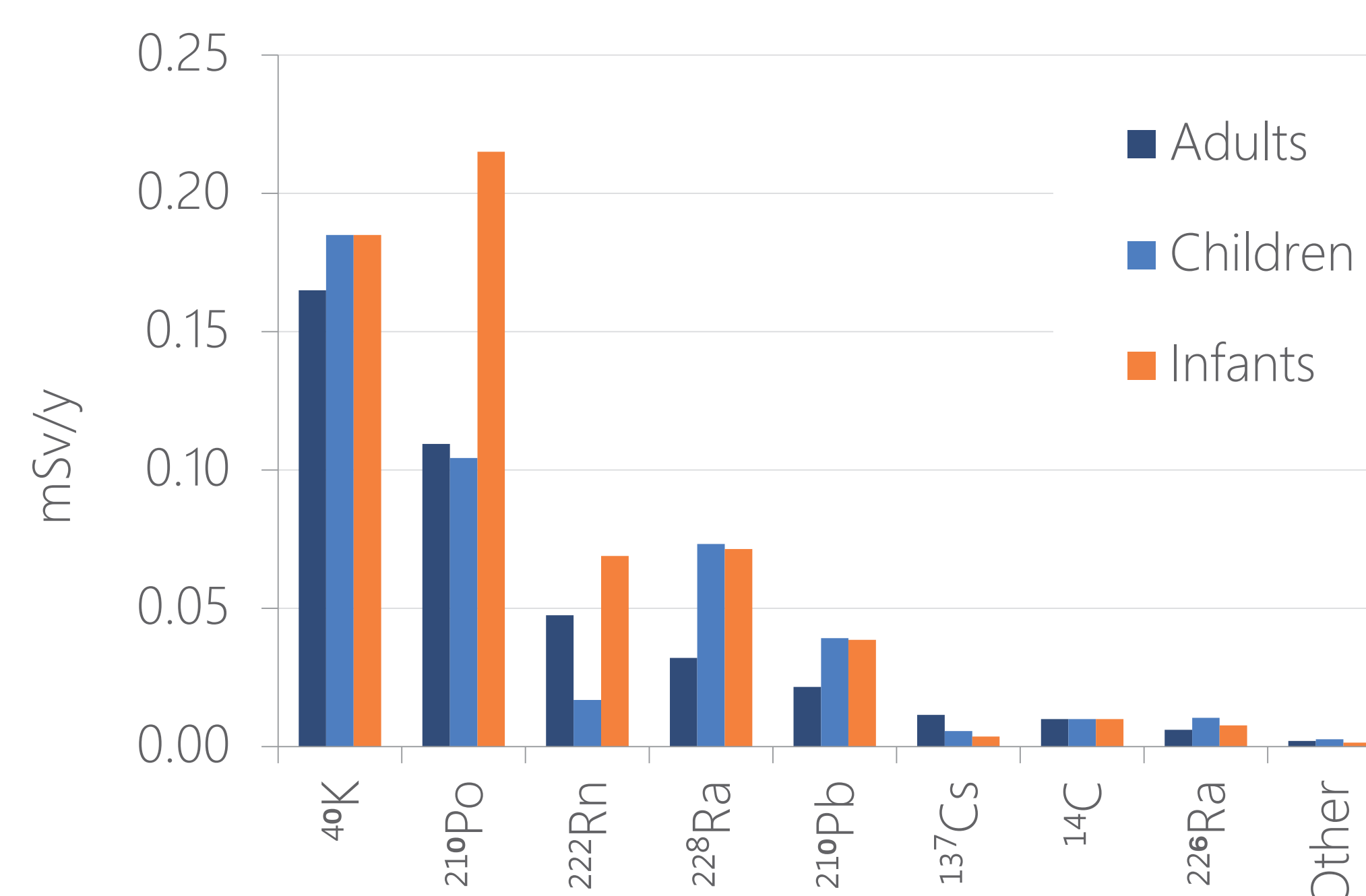


Fig 2. Age-weighted mean doses (mSv/y) from artificial and U- and Th-series radionuclides. Doses from ^{40}K and ^{14}C were considered separately from calculations based on dietary intake.

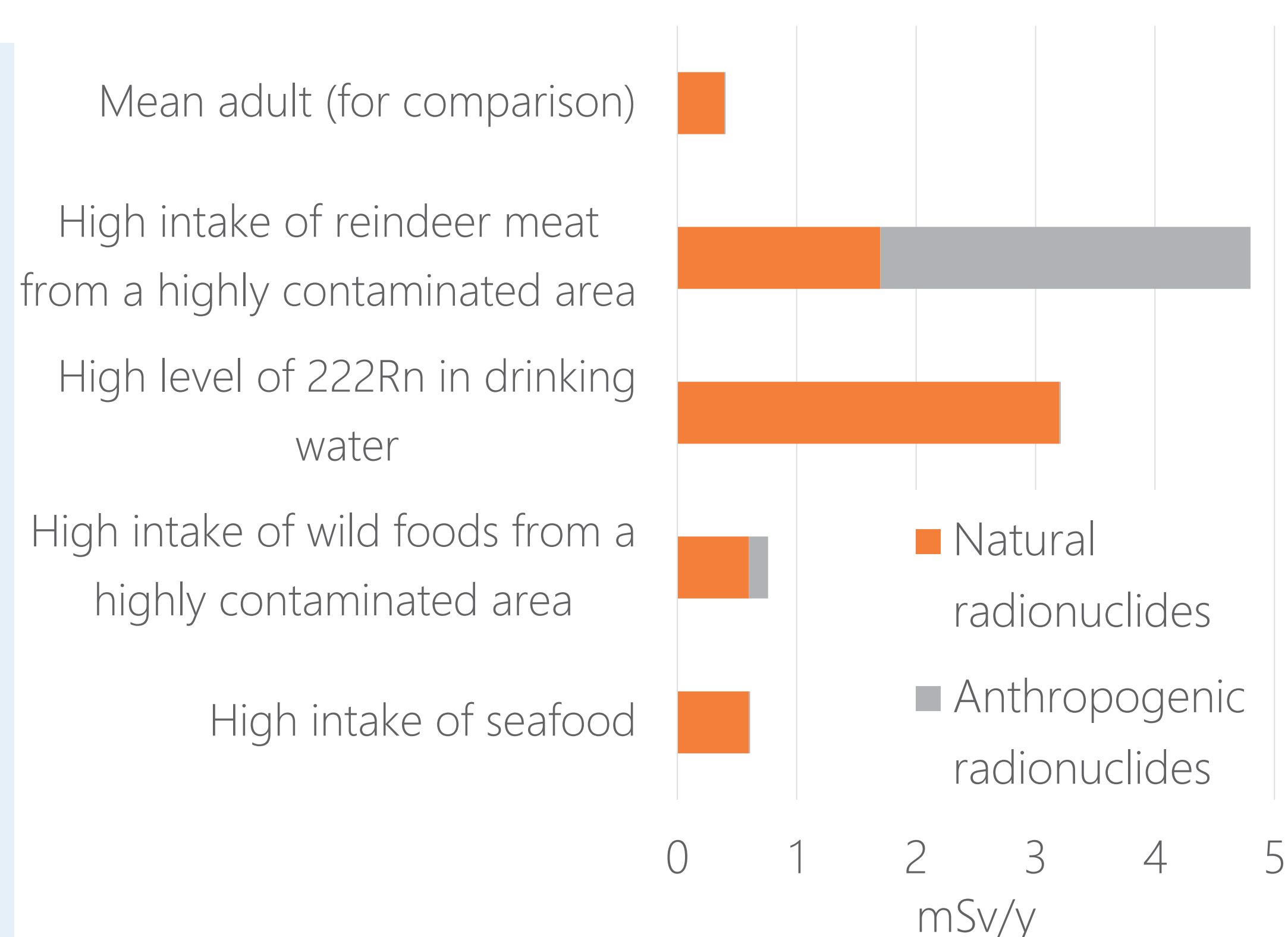
Average population

- The mean ingestion doses were estimated at 0.60, 0.45, and 0.41, mSv/y for infants, children and adults, respectively. ^{40}K and ^{210}Po provide by far largest dose contributions (Fig. 1).
- Marine animals generally contain relatively high levels of naturally occurring radionuclides. Aside from the constant dose from ^{40}K , naturally occurring radioactivity in seafood is the largest single contributor to the total ingestion dose (Fig. 2).
- In the terrestrial environment, we generally find higher concentrations of both anthropogenic and naturally occurring radionuclides in wild food products compared with agricultural products. Although radionuclide levels in agricultural products usually are low, their contribution is significant due to high consumption.
- The mean dose from ^{222}Rn ingestion is caused by high levels in ground water sources – especially wells drilled in bedrock, which in turn are assumed to supply less than 10% of the population.

Individuals with elevated exposure

- Some individuals receive higher radiation doses from their diet, depending on what they eat and local elevations in radionuclide levels (Fig. 3).
- Individuals with a high intake of contaminated wild foods may receive a significant dose contribution from anthropogenic radionuclides. In Norway, this is particularly the case for Sami reindeer herders, who consume a lot of reindeer meat.
- Calculated doses indicate that persons with a high intake of reindeer meat from a contaminated area (1900 Bq/kg ^{137}Cs and 120 kg/y) potentially can receive ingestion doses as high as at 4.8 mSv/y. However, whole body monitoring has not indicated ingestion doses above 1 mSv/y in any individual during the last 10–15 years.
- ^{222}Rn levels in drinking water at the 95th percentile for wells drilled in bedrock (2200 Bq/L) will result in a total ingestion dose of 3.2 mSv/y. ^{222}Rn levels in water as high as 31,900 Bq/L have been recorded in Norway. ^{222}Rn in water also contributes significantly to the levels in air.

Fig 3. Total ingestion dose estimates (mSv/y) calculated as examples of adult individuals with elevated exposure.





EURADOS INTERCOMPARISONS FOR PHOTON AND BETA PERSONAL DOSEMETERS: A REVIEW OF RESULTS AND CONCLUSIONS

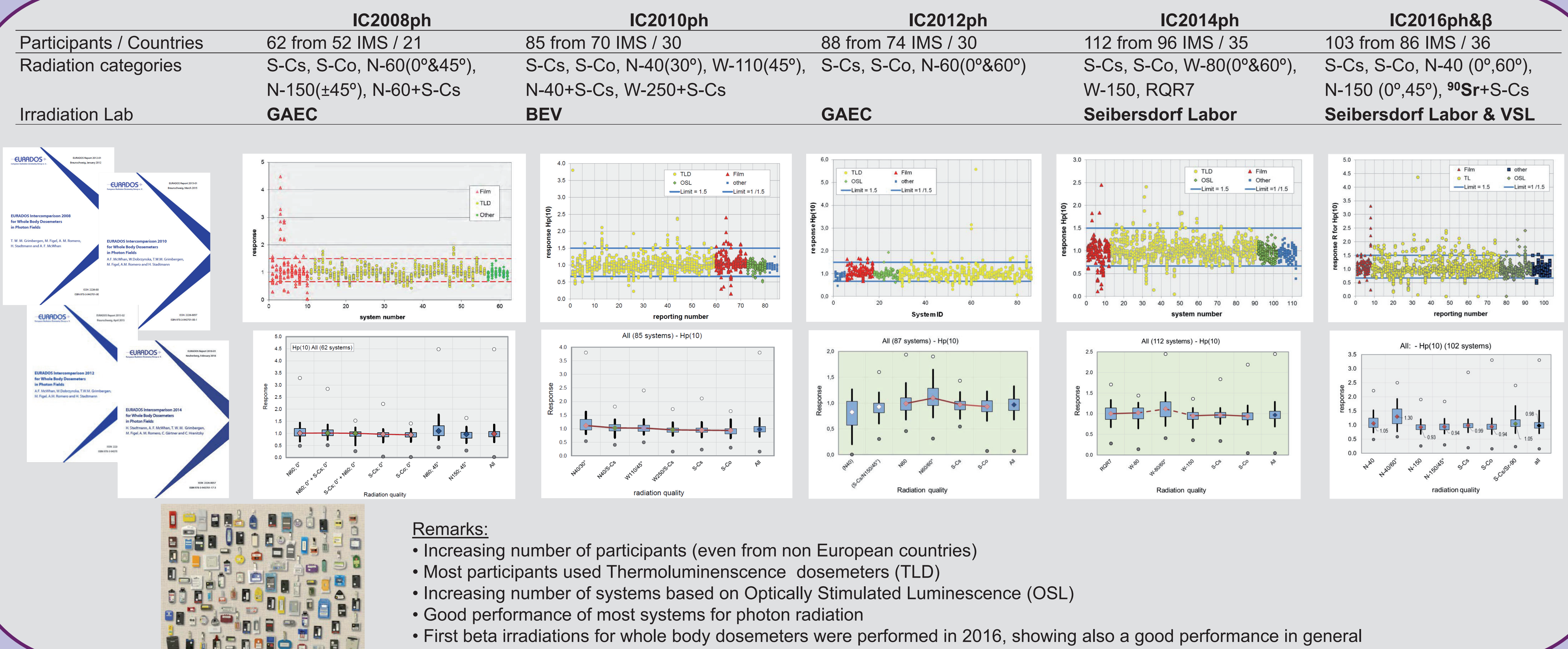
A. M. Romero¹, T. Grimbergen², A. McWhan³, H. Stadtmann⁴, M. Figel⁵, C. Gärtner⁴, W. Dobrzynska³

- 1 CIEMAT, Radiation Dosimetry, Avda Complutense 40, 28040-Madrid, Spain
- 2 NRG, Individual Monitoring, PO Box 9034, 6800 ES Arnhem, The Netherlands
- 3 Cavendish Nuclear Limited, Berkeley Approved Dosimetry Service, A11 Berkeley Centre, Berkeley, Gloucestershire, GL139FB, United Kingdom
- 4 Seibersdorf Labor GmbH, A-2444 Seibersdorf, Austria
- 5 Helmholtz Zentrum München, Auswertungsstelle, Otto-Hahn-Ring 6, D-81739 München, Germany

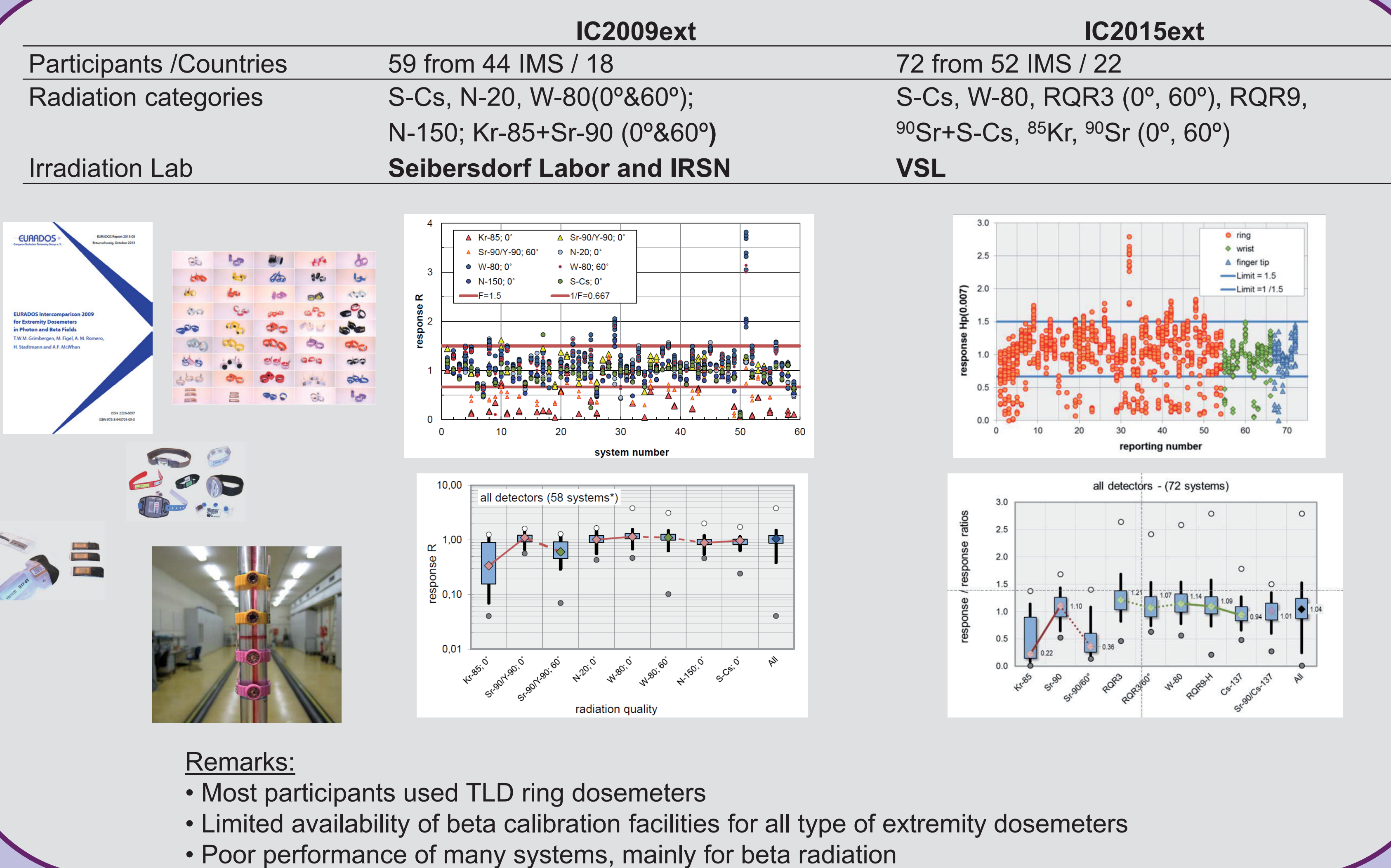
INTRODUCTION

In response to growing demand from Individual Monitoring Services (IMS) for independent performance tests for dosimetry systems, the European Radiation Dosimetry Group (EURADOS) has been organizing dosimetry intercomparisons (IC) for many years. These ICs are being coordinated by EURADOS working group 2 (WG2) and started in 2008. Up to now, five intercomparisons for whole-body dosimeters and two for extremity dosimeters in photon and beta fields, and two intercomparisons for whole body dosimeters in neutron fields, have been successfully performed. The ICs for whole body dosimeters have been carried out regularly every two years (IC2008, IC2010, IC2012, IC2014 and IC2016) and those for extremity dosimeter were performed in 2009 and 2015 (IC2009ext and IC2015ext). They were open to all participants and the costs were totally covered by the participation fee. For each intercomparison, the irradiation plan is defined so that participants can obtain information of their dosimetry systems on characteristics such as linearity, reproducibility, energy and angular dependence, and response to mixed irradiations. Irradiation laboratories are selected on the basis of their accreditation, previous experience in similar tasks and price. Irradiations are performed in terms of personal dose equivalent, $H_p(10)$ and $H_p(0.07)$. From IC2014 on, an on-line platform for supporting the entire registration process, communication and data exchange was implemented. The platform is easy to use and secure; it allows the participants to monitor the status of their dosimetry systems in real-time and to download all relevant information and documents. The results were in all cases analysed according to the performance criteria established in the standard ISO 14146 (2000): “Criteria and performance limits for the periodic evaluation of processors of personal dosimeters for X and gamma radiation”, commonly known as the ‘trumpet curve’.

WHOLE BODY PHOTON and BETA DOSEMETERS (IC2008, IC2010, IC2012, IC2014, IC2016)

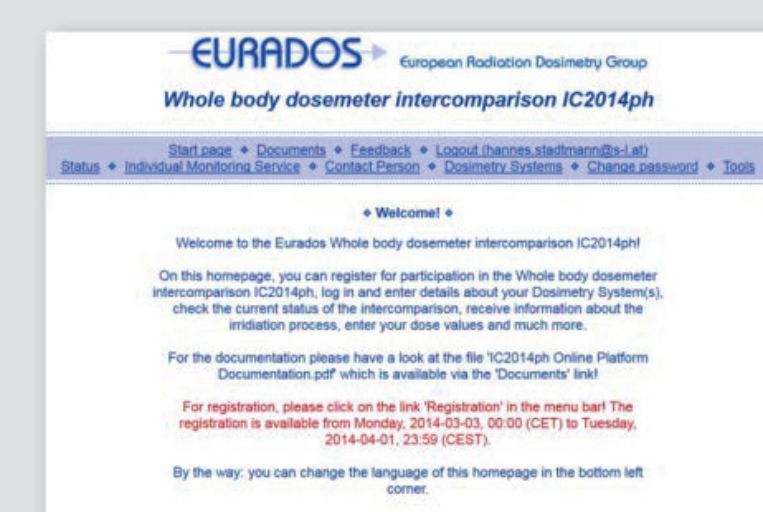


EXTREMITY DOSEMETERS (IC2009ext, IC2015ext)



GENERAL ORGANIZATION

- ✓ Intercomparisons were open to all participants
- ✓ A fee was charged to cover the costs
- ✓ Irradiations performed in accredited laboratories in terms of $H_p(10)$ and $H_p(0.07)$
- ✓ Participants received a “Certificate of Participation”
- ✓ A participant’s meeting was held at the end of each exercise
- ✓ An online platform was set up from 2014 to improve the management
- ✓ The results were analysed anonymously and published in EURADOS reports and in scientific journals
- ✓ Eurados IC2018ph for whole body dosimeters is currently in progress



ON-LINE Platform



Certificate of Participation

Free download of reports:
http://www.eurados.org/en/Documents_Publications

CONCLUSIONS

The participation in intercomparisons gives IMSs the opportunity to show compliance with their own quality management system, compare results with other participants and develop plans for improving their dosimetry systems. The increasing number of participants confirms its need and usefulness for European dosimetry services. The analysis of results shows that most of participants in whole body dosimeters intercomparisons comply with the criteria of the standard ISO 14146 (2000): “Criteria and performance limits for the periodic evaluation of processors of personal dosimeters”. However, for the extremity dosimeters there is still room for improving measurement techniques and methods. In general, some participants could improve the quality of their systems by reviewing their calibration procedures.



Evaluation of FNTD and PADC Neutron Dosimeters in Yearly Intercomparisons

A. Stabilini^{1,5}, E.G. Yukihiro^{1,2}, M.S. Akselrod^{2,3}, V. Fomenko³, J. Harrison³, M. Million⁴, F. Assenmacher¹, K. Meier¹ and S. Mayer¹

¹Department of Radiation Safety and Security, Paul Scherrer Institute, 5232 PSI Villigen, Switzerland

²Physics Department, Oklahoma State University, Stillwater, OK 74078, USA

³Landauer Inc., Crystal Growth Division, 7231/2 Eastgate St., Stillwater, OK 74074, USA

⁴Landauer Europe, 9 rue Paul Dautier CS 60731, 78457 Vélizy-Villacoublay, France

⁵Department of Physics, Basel Universität, Klingelbergstrasse 82, 4056 Basel, Switzerland

eduardo.yukihiro@psi.ch

Objective of the work

Since 2016 PSI has been collaborating with Landauer Inc. to compare the innovative fluorescence nuclear track detector (FNTD) [1] with the PADC detector system [2]. In 2016 [3] and 2017 we participated in the neutron dosimeter intercomparisons organized by the Physikalisch-Technische Bundesanstalt (PTB, Germany) with both of these systems. This work provides an overview of these intercomparison results.

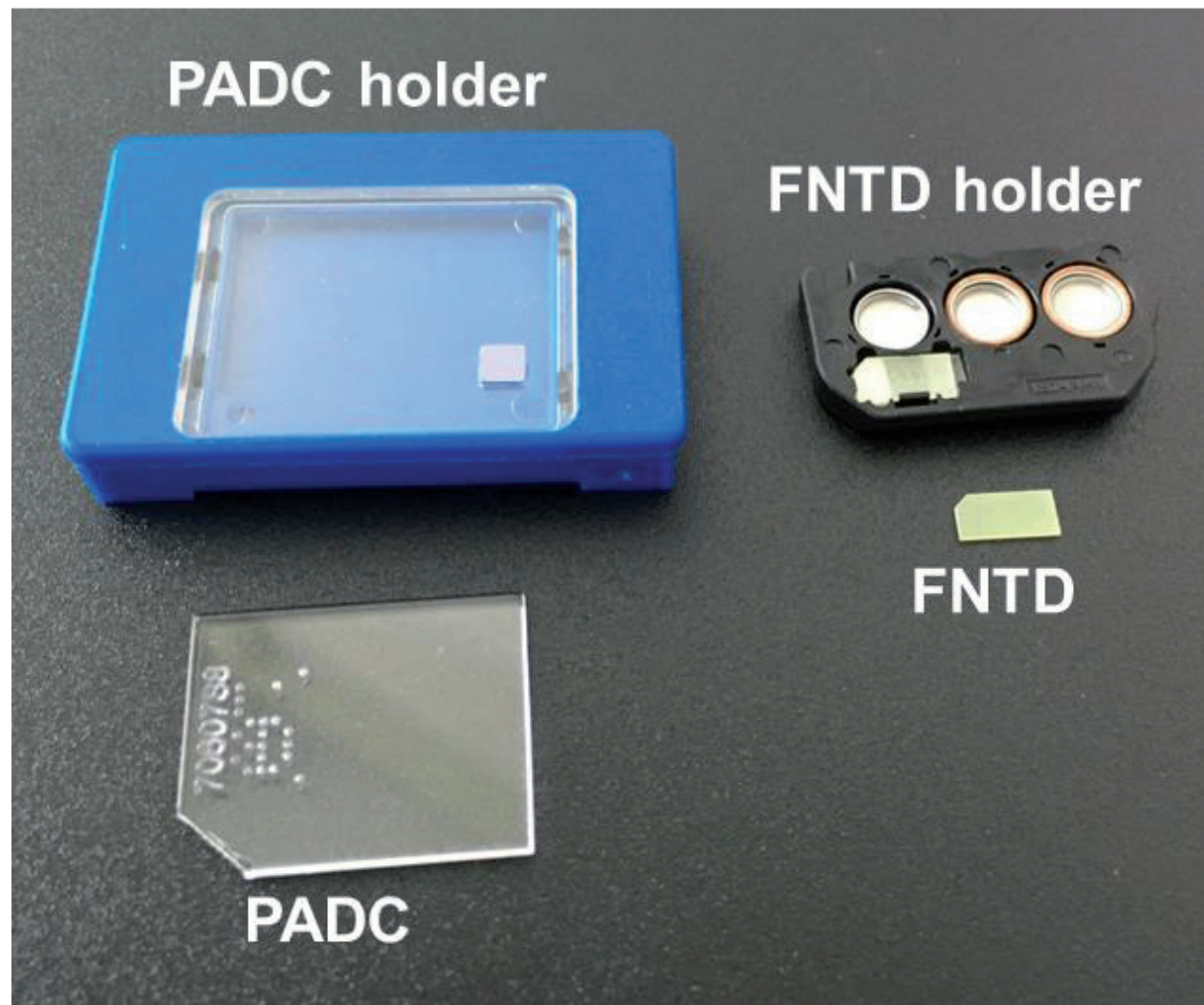


Figure 1: PADC and FNTD detectors and holders

Irradiation conditions (2017)

Irradiation Setup	Source	Angle (deg.)	Distance (cm)	H _p (10) (mSv)
1	²⁵² Cf (+ ¹³⁷ Cs)	0	58	0.500 ± 0.024 (+ 1.5 mSv γ)
2	²⁵² Cf	0	58	8.0 ± 0.4
3	²⁵² Cf	15	100	3.00 ± 0.09
4	²⁵² Cf	0	170	1.000 ± 0.029
5	²⁴¹ Am-Be	0	58	2.50 ± 0.16
6	²⁴¹ Am-Be	30	100	0.80 ± 0.04

Materials & Methods

	FNTD	PADC
Detectors	Al ₂ O ₃ :C,Mg crystals (Landauer Inc.)	TASTRAK® (Track Analysis Systems Ltd.)
Dimensions	(4.0 × 8.0 × 0.5) mm ³	(20.0 × 25.0 × 1.5) mm ³
Converters	Fast n: Polyethylene Thermal n: ⁶ Li-glass γ: Teflon®	Fast n: 2 mm polyamide Thermal n: LiF chip (TLD 600)
Etching	—	PSI ⁽⁴⁾ : NaOH 6.25 M - 85 °C - 2h 50min
Readout	Landauer US: FXR 700-N Landauer Europe: —	PSI: TASLIMAGE™ (Track Analysis Systems Ltd.)
Calibration Standard	²⁴¹ Am-Be; ²⁵² Cf	²⁴¹ Am-Be

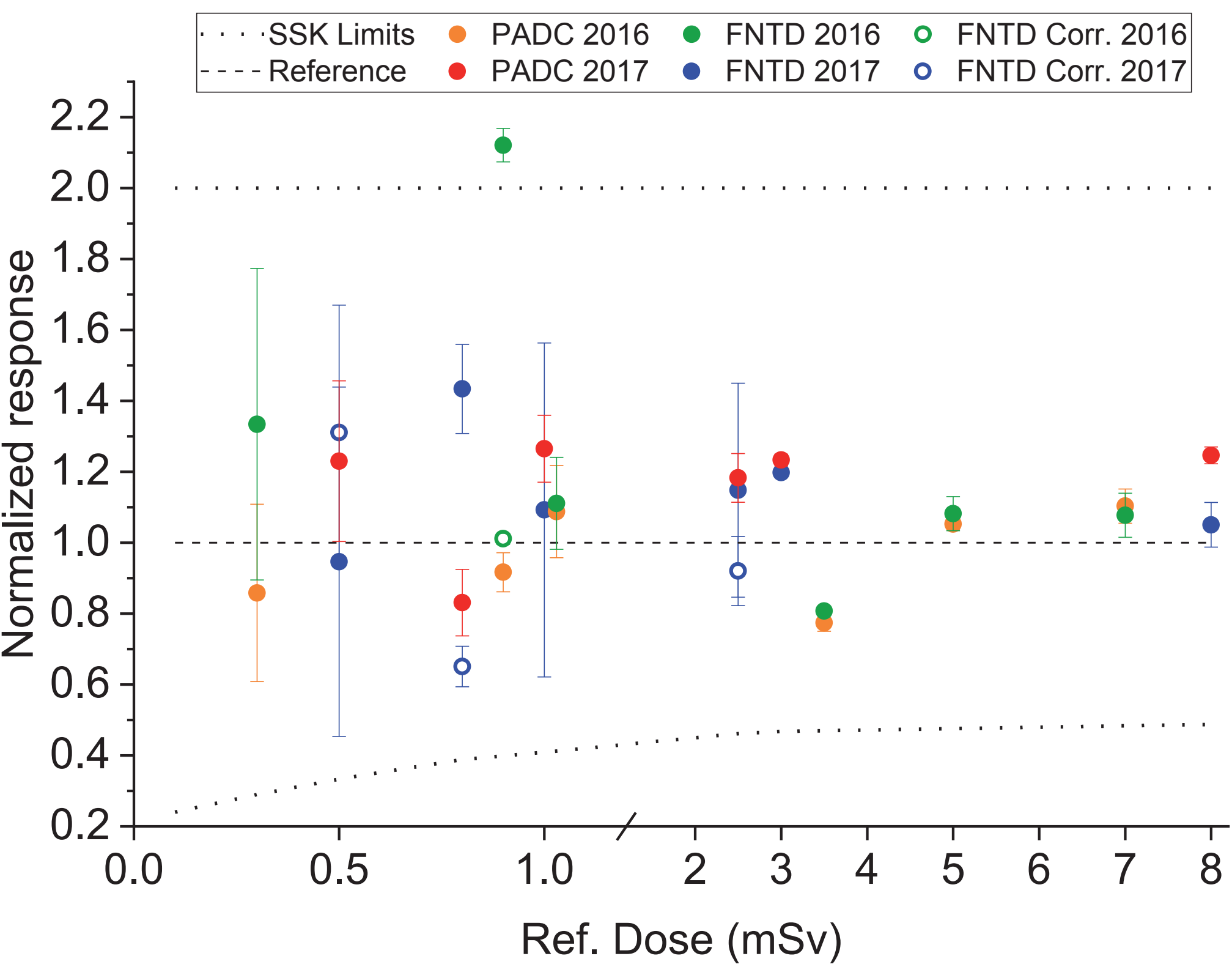


Figure 2: Measured dose normalized to reference for PADC and FNTD. Open points show the FNTD reassessment assuming a correct calibration factor.

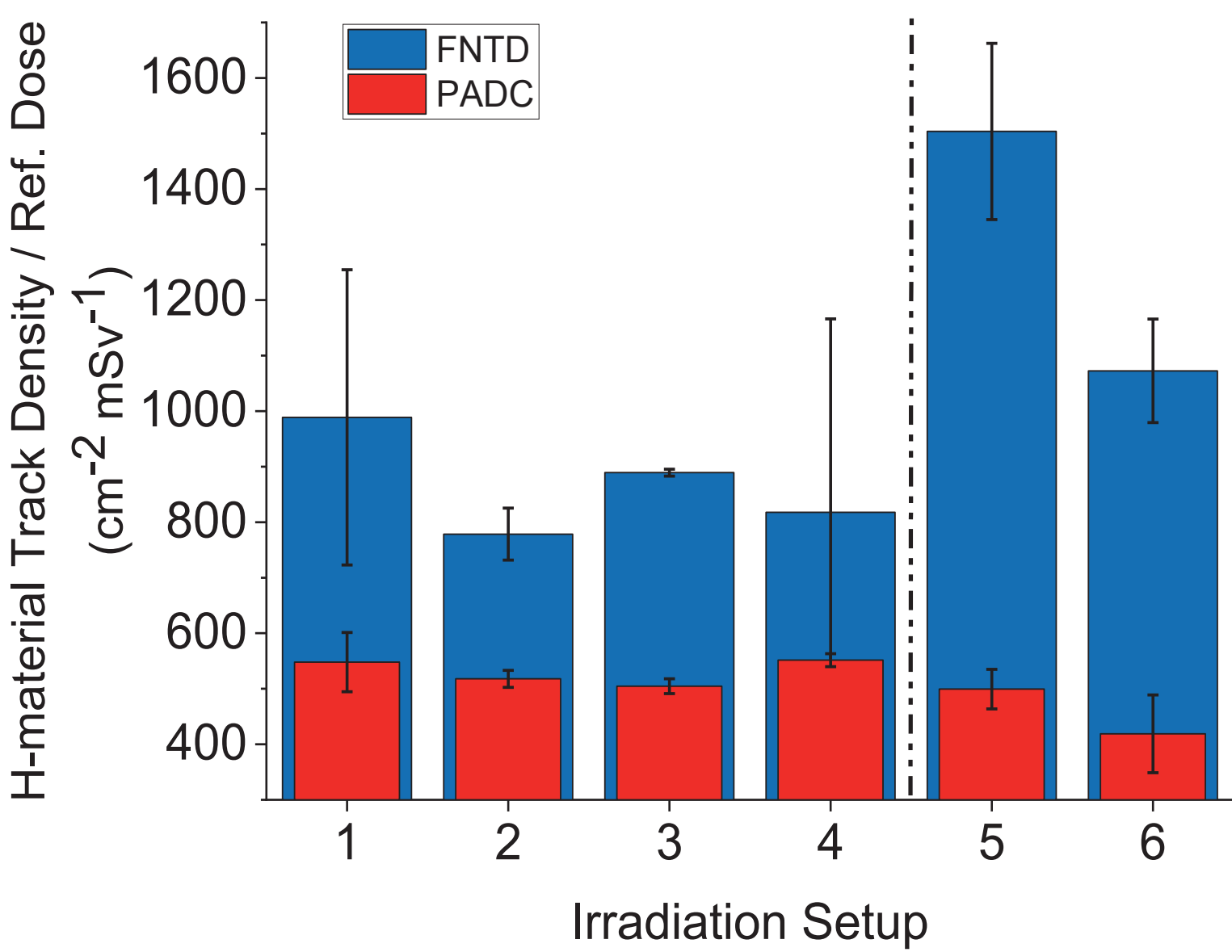


Figure 3: Dose normalized track densities behind fast converter (PADC and FNTD) for each irradiation setup.

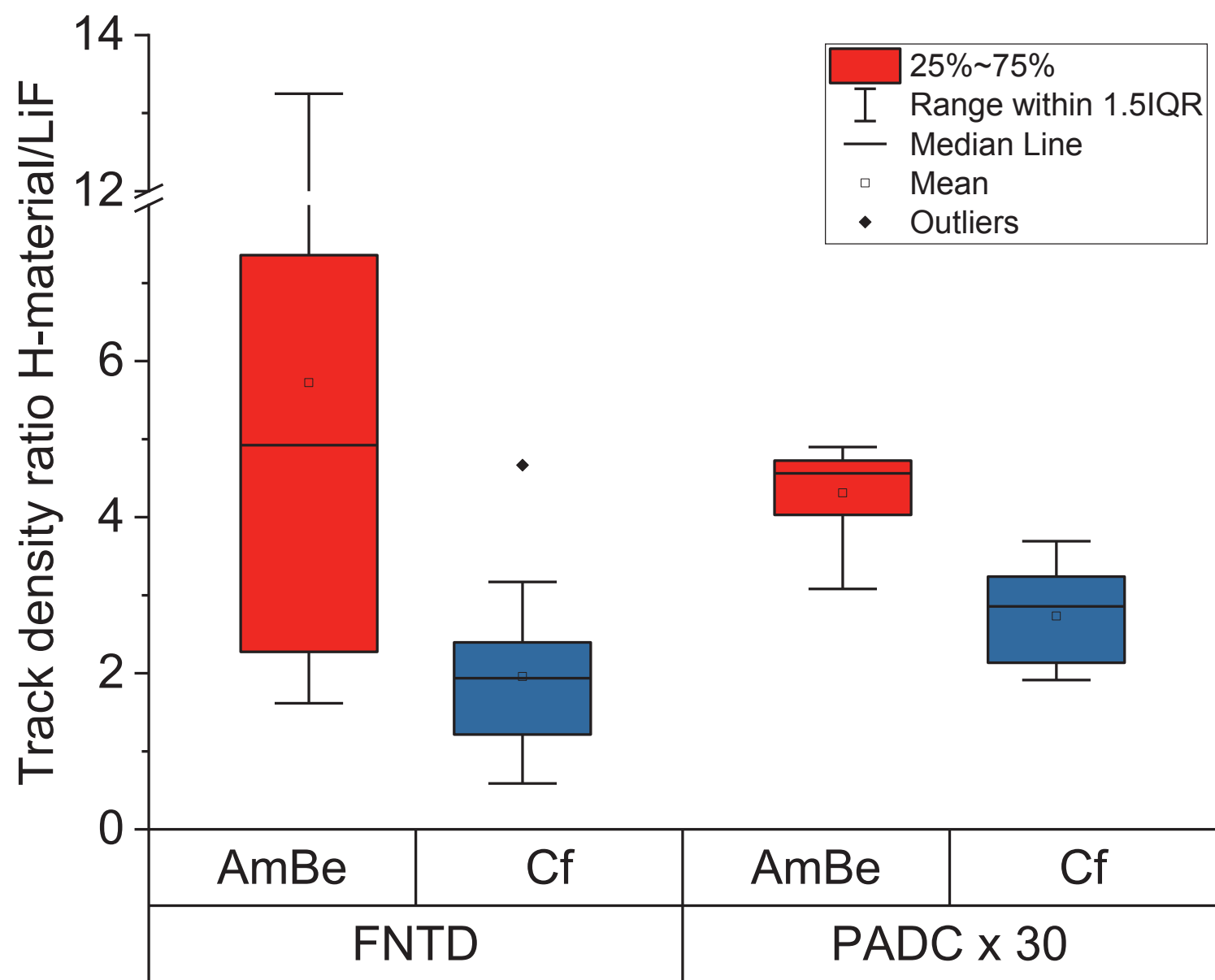


Figure 4: Ratio of the track densities behind fast and slow neutron converters in PADC and FNTD.

Conclusions

Results show general agreement between the two detector types and the reference values. In the intercomparison of 2017, the maximum deviation from the reference dose was a factor 1.6 for PADCs and a factor 1.8 for FNTDs. Both PADC and FNTD dosimeters can distinguish between sources used for irradiation, relying on the track density ratio behind converters for fast and slow neutrons. Further developments of the dosimeters may focus on enhancing the sampling statistics for FNTD and improving the sensitivity of fast neutrons for PADC.

References

- (1) Akselrod, M. S., et al. (2014). "FNTD radiation dosimetry system enhanced with dual-color wide-field imaging." *Radiation Measurements* **71**: 166-173.
- (2) Fiechtner-Scharrer, A., et al. (2011). "Influence of Variation of Etching Conditions on the Sensitivity of PADC Detectors with a New Evaluation Method." *Radiation Protection Dosimetry* **144**(1-4): 150-154.
- (3) Yukihiro, E. G., et al. (2017). "Comparison between PADC and FNTD Neutron Detector Systems in Blind Tests." *Radiation Protection Dosimetry*: 1-5.
- (4) Assenmacher, F., et al. (2016). "Comparison of Different PADC Materials and Etching Conditions for Fast Neutron Dosimetry." *Radiation Protection Dosimetry* **170**(1-4): 162-167.

Acknowledgements

The authors thank Helga Schröter for the chemical etching of the detectors, the Swiss Nuclear Safety Inspectorate (contract no. H-101196) for the support, and PTB for the opportunity to participate in the intercomparisons.



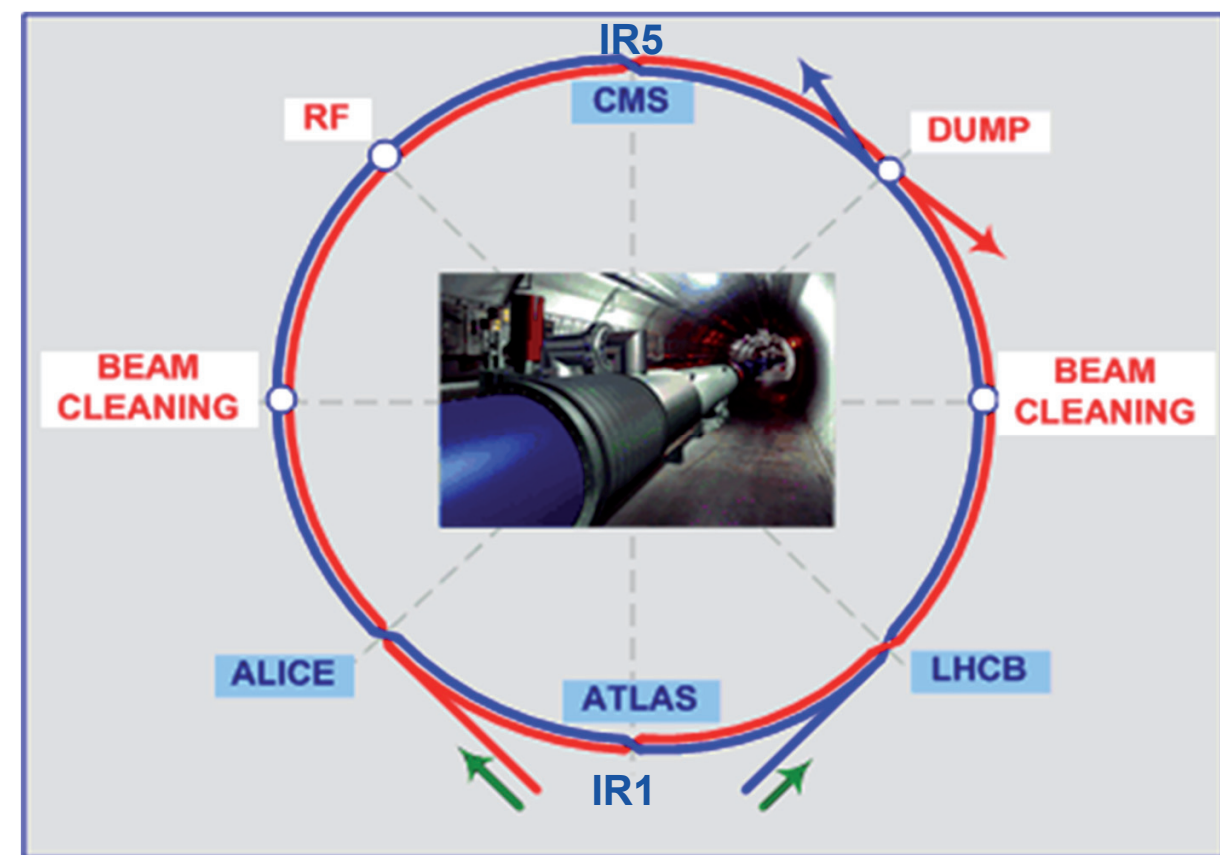
Induced activation studies for the LHC upgrade to High Luminosity LHC

C. Adorisio, S. Roesler
CERN, HSE-RP, Geneva, Switzerland

CERN

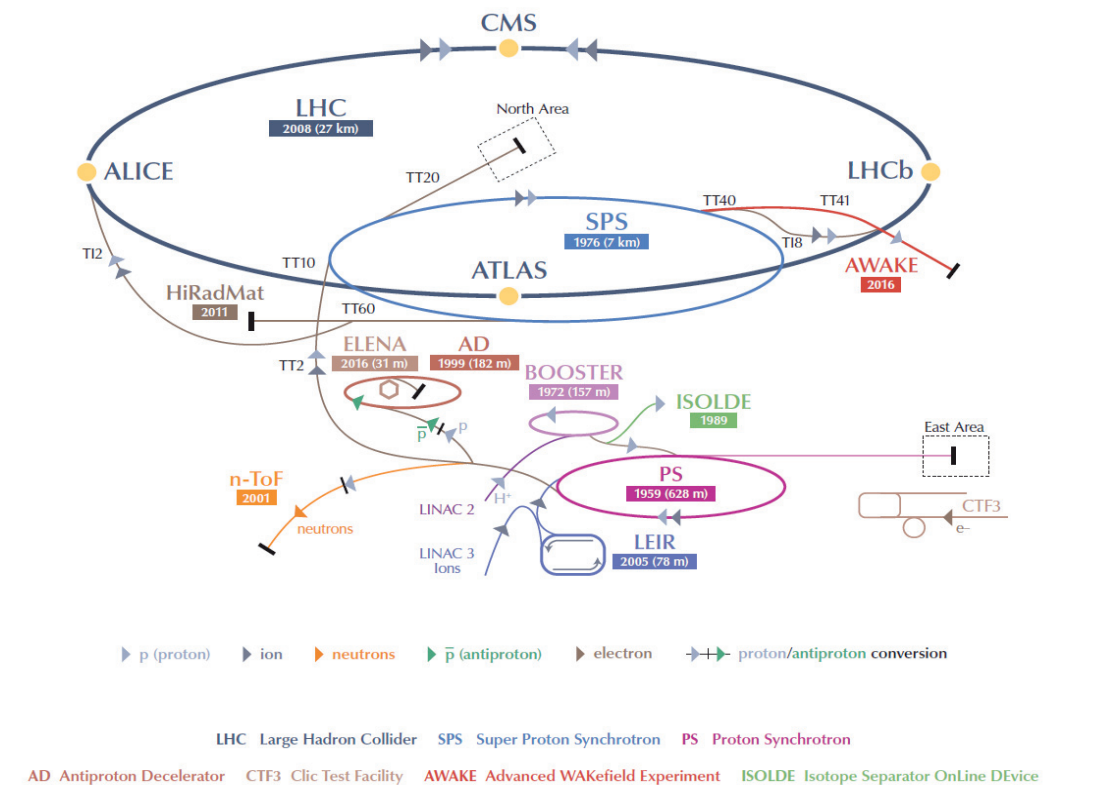
At CERN, the European Organization for Nuclear Research, physicists and engineers are probing the fundamental structure of the universe. They use the world's largest and most complex scientific instruments to study the basic constituents of matter – the fundamental particles. Founded in 1954, the CERN laboratory sits astride the Franco-Swiss border near Geneva. It was one of Europe's first joint ventures and now has 21 member states.

LHC and its upgrade to HL-LHC



The Large Hadron Collider (LHC) is the biggest accelerator constructed at CERN. The LHC accelerates and collides proton beams, but also heavier ions. It is installed in a **27 km** circumference tunnel, about 100 m underground.

The High-Luminosity Large Hadron Collider (HL-LHC) project aims to crank up the performance of the LHC in order to increase the potential for discoveries. The objective is to increase integrated luminosity by a factor of 10 beyond the LHC's design value. To this aim, HL-LHC is exploring new beam configurations and new advanced technologies in the domain of superconductivity, cryogenics, rad-hard materials, electronics and remote handling.



LHC/HL-LHC Operational scenario

Year of (HL-)LHC Operation	Peak / levelled luminosity [$\text{cm}^{-2}\text{s}^{-1}$]	Integrated luminosity [fb^{-1}]
LS1		
2015	6.30×10^{33}	4
2016	1.40×10^{34}	40
2017	1.60×10^{34}	50
2018	1.60×10^{34}	50
LS2 (2 years)		
2021	2.0×10^{34}	60
2022	2.0×10^{34}	60
2023	2.0×10^{34}	60
LS3 (3 years)		
2027	5.0×10^{34}	250
2028	5.0×10^{34}	250
2029	5.0×10^{34}	250
LS4 (1 year)		
2031	5.0×10^{34}	250
2032	5.0×10^{34}	250
2033	5.0×10^{34}	250
LS5 (1 year)		
2035	5.0×10^{34}	250
2036	5.0×10^{34}	250
2037	5.0×10^{34}	250
LS6		
TOT		$\sim 2600 \text{ fb}^{-1}$
TOT		$\sim 3050 \text{ fb}^{-1}$

Luminosity gives a measure of how many collisions are happening in a particle accelerator

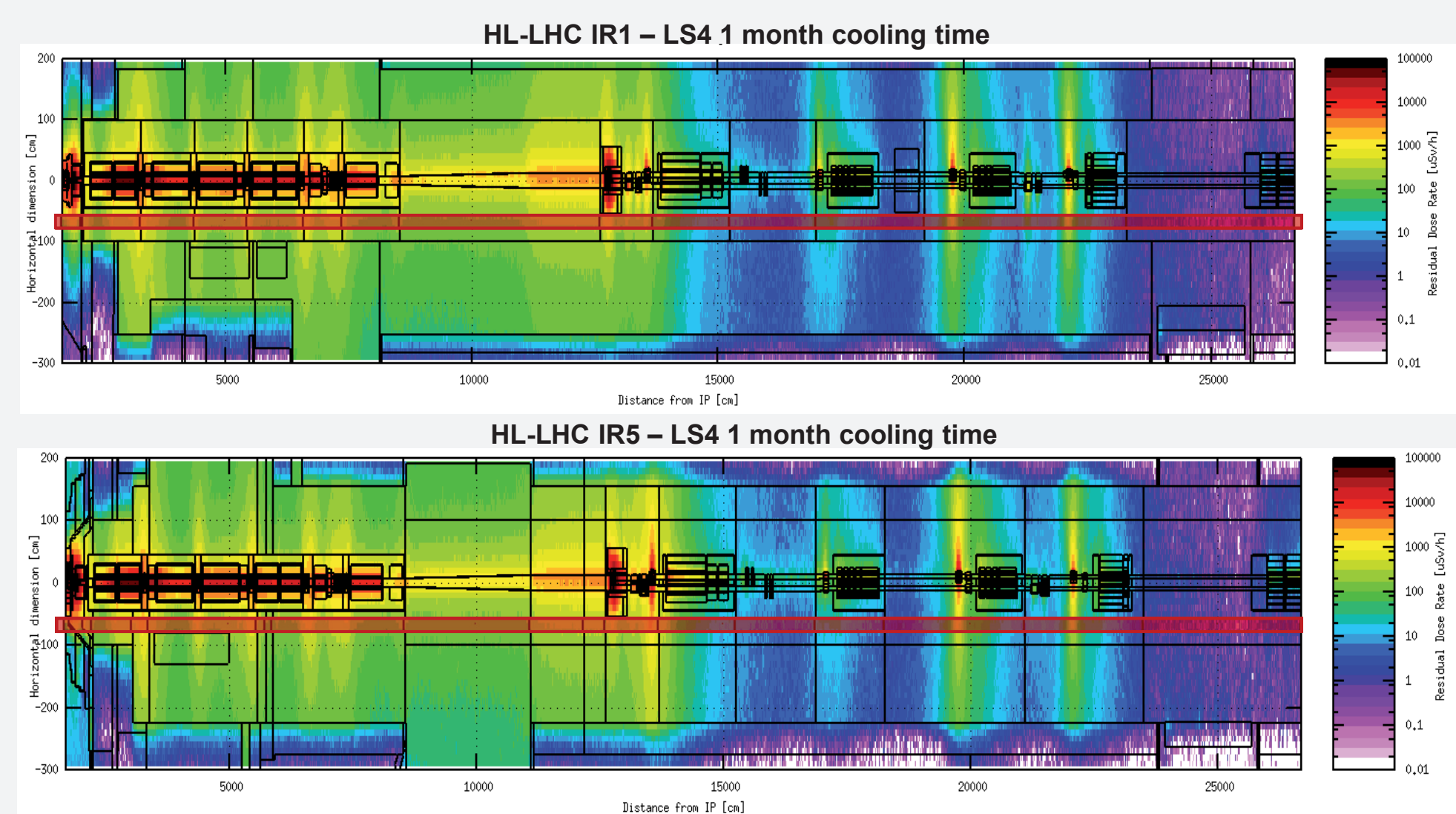
Simulation is done considering the luminosity targets announced by the LHC Operation team

~TOT 350 fb⁻¹

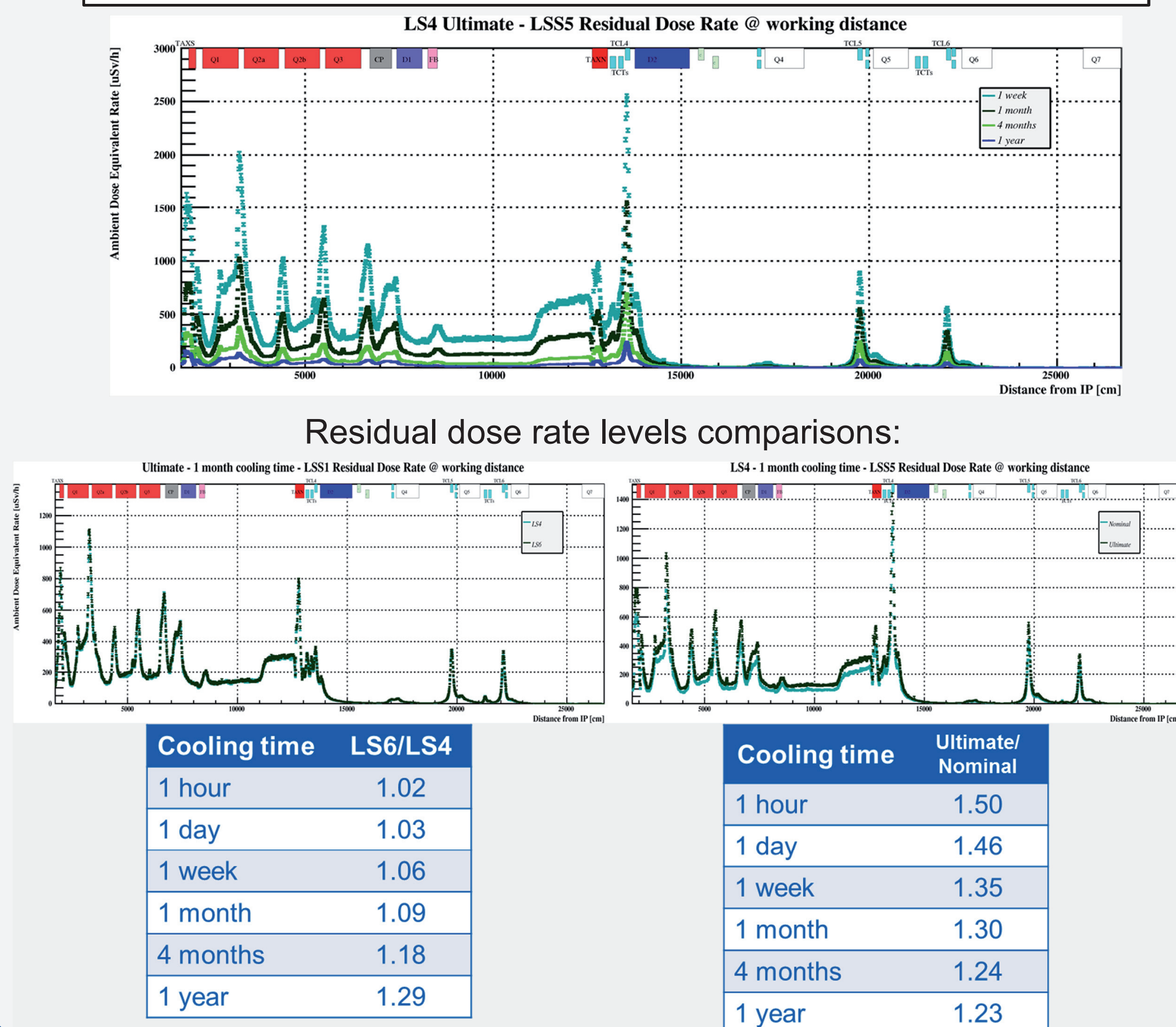
- 3 blocks of 3 consecutive years of operation + 1 year Long Shutdown each
- Nominal: $5.0 \times 10^{34} - 250 \text{ fb}^{-1}/\text{y}$
 - Ultimate: $7.5 \times 10^{34} - 300 \text{ fb}^{-1}/\text{y}$

FLUKA Monte Carlo code [1], [2], [3] has been used to evaluate the induced activation.

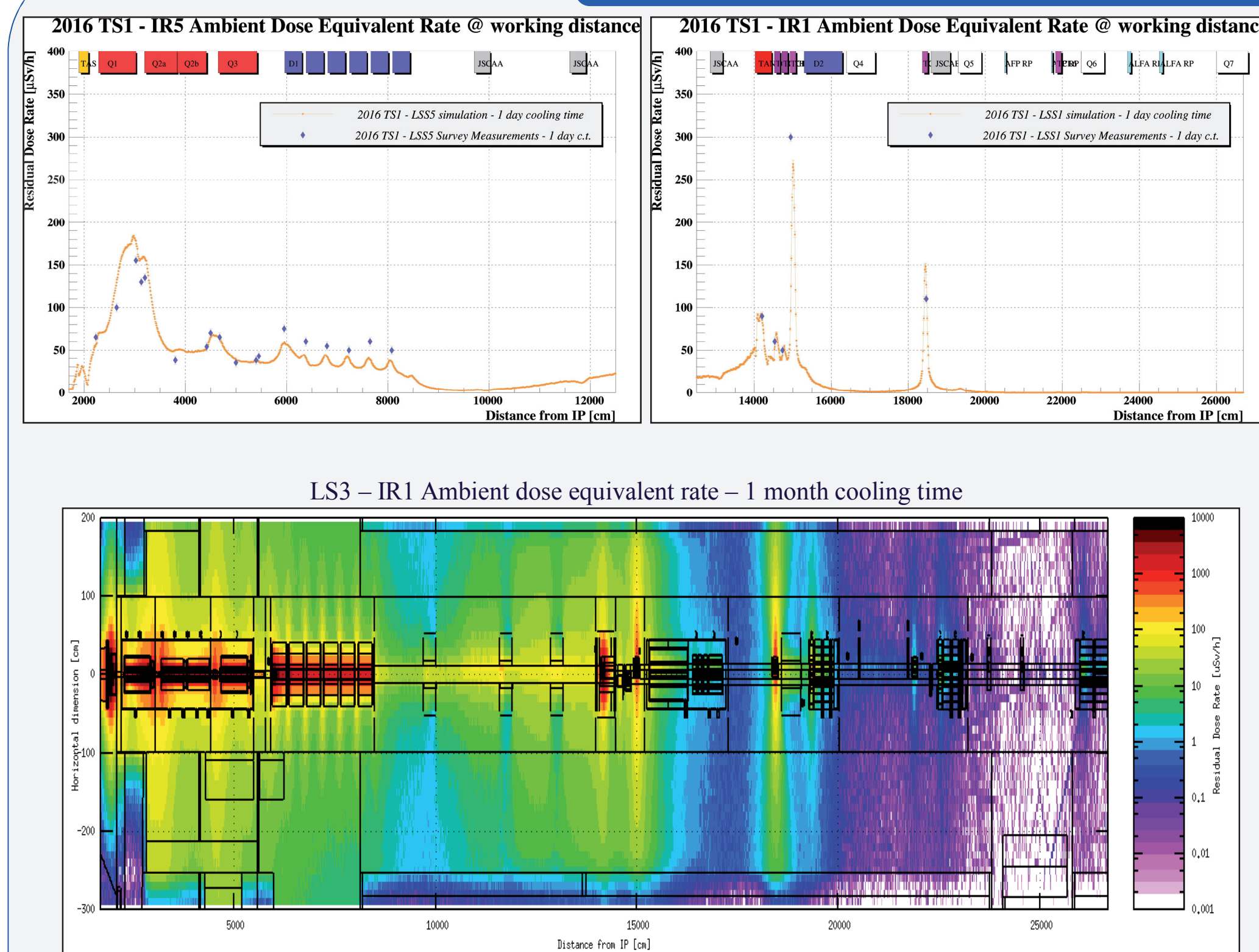
HL-LHC Monte Carlo simulation



The accelerator optics and the collimator settings are the same for IR1 and IR5. Only difference is crossing angle plane.

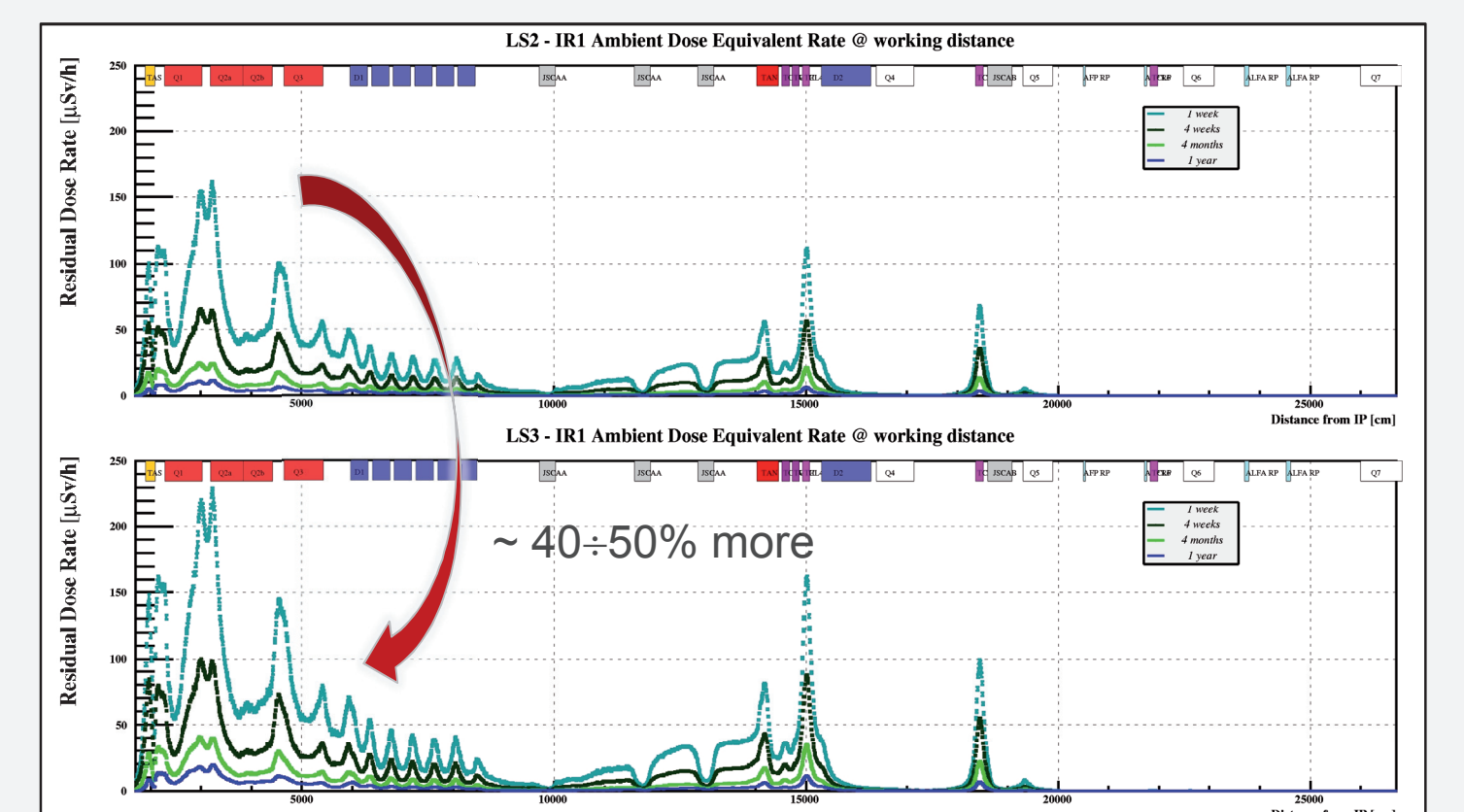


LHC Monte Carlo simulation



Radiation measurement performed during the technical stops of the machine, are used to benchmark the simulation.

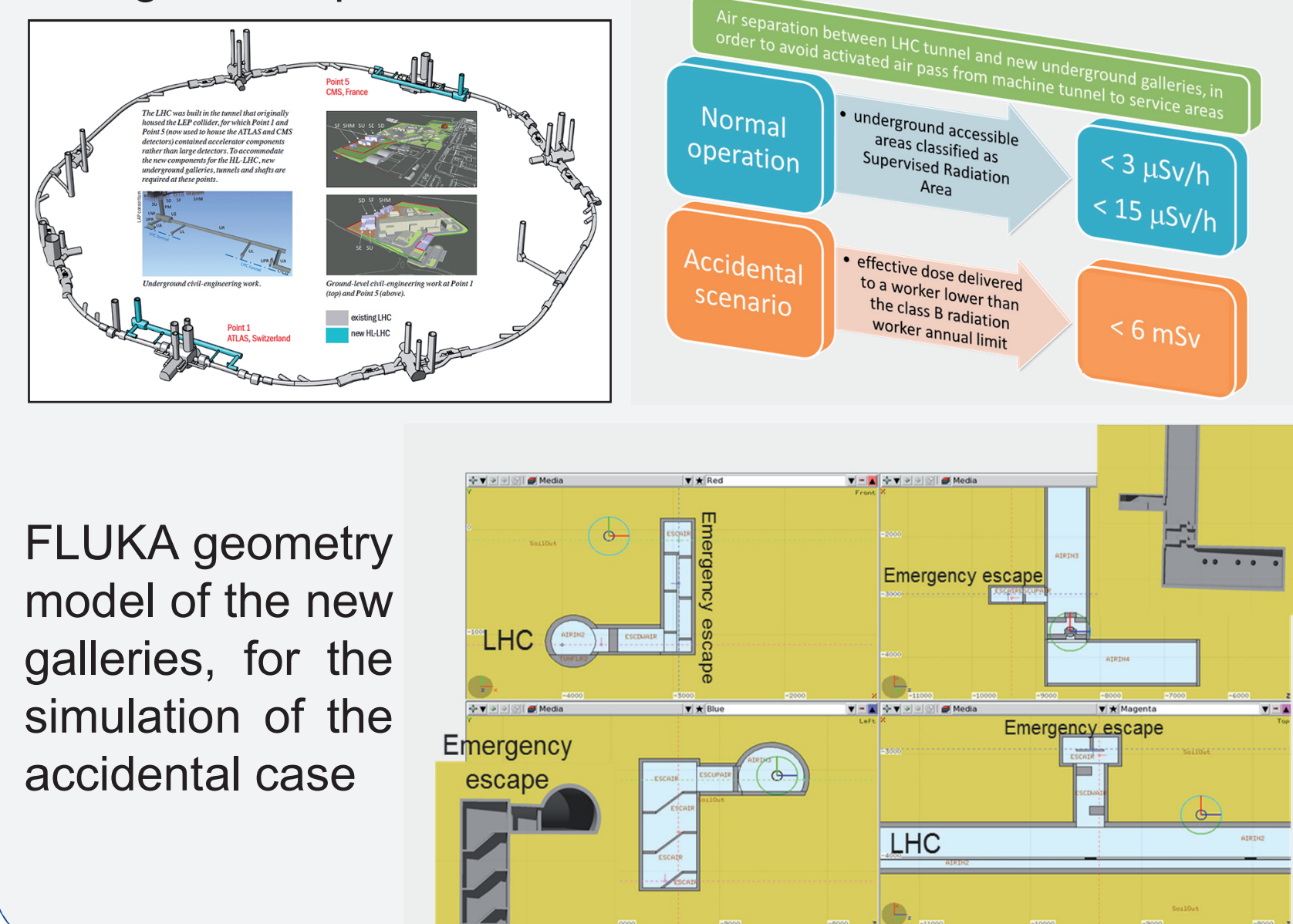
The residual dose rates in the accelerator area next to the high luminosity experiment (IR1 and IR5), are expected to be 40-50% higher in the LS3 compared to the expected value in LS2.



During LS3 the full Long Straight Section in IR1 and IR5 will be dismantled and new equipment will be installed in order to reach the target luminosity.

HL-LHC new underground galleries

The new underground service galleries will be accessible during beam operation.



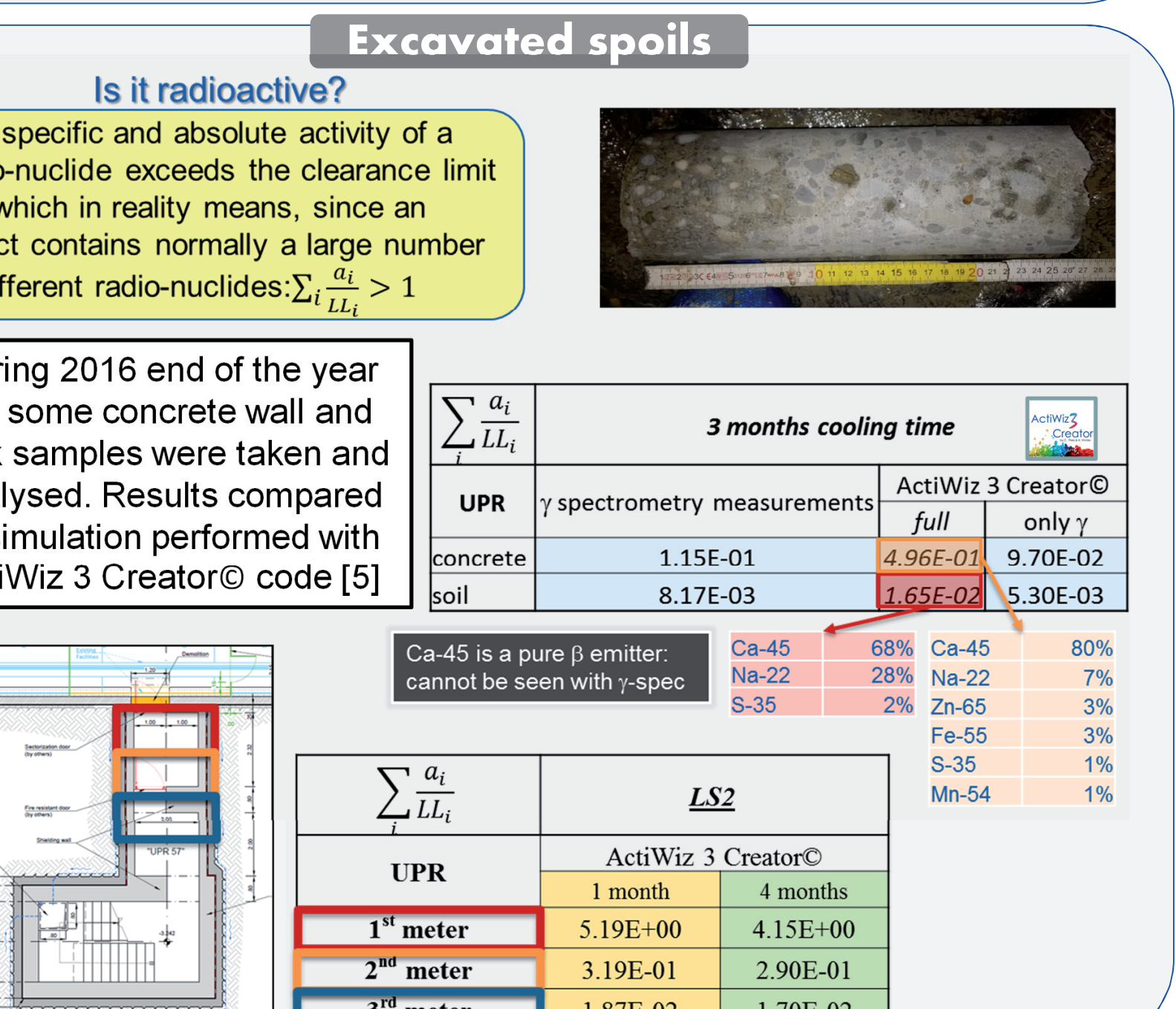
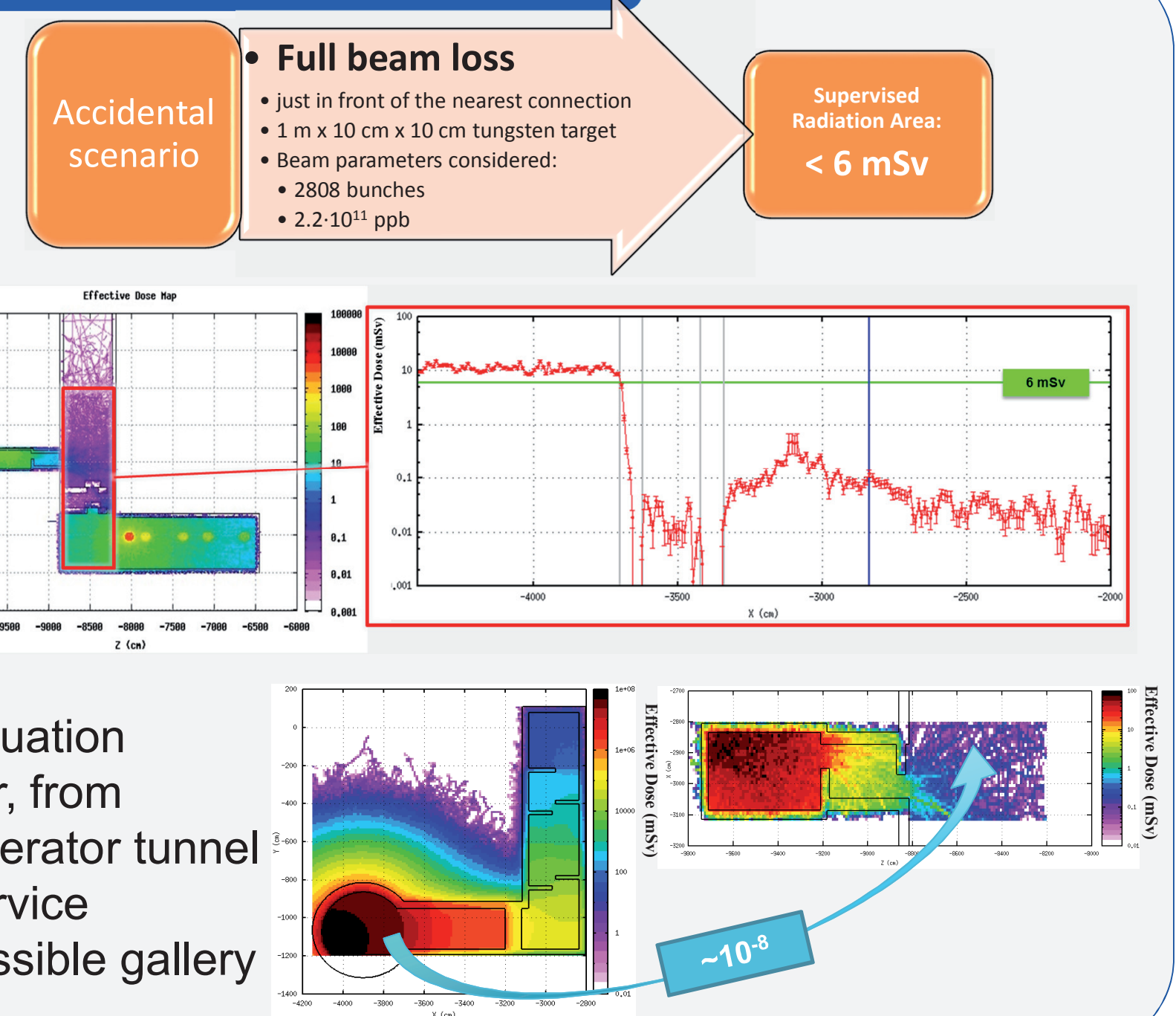
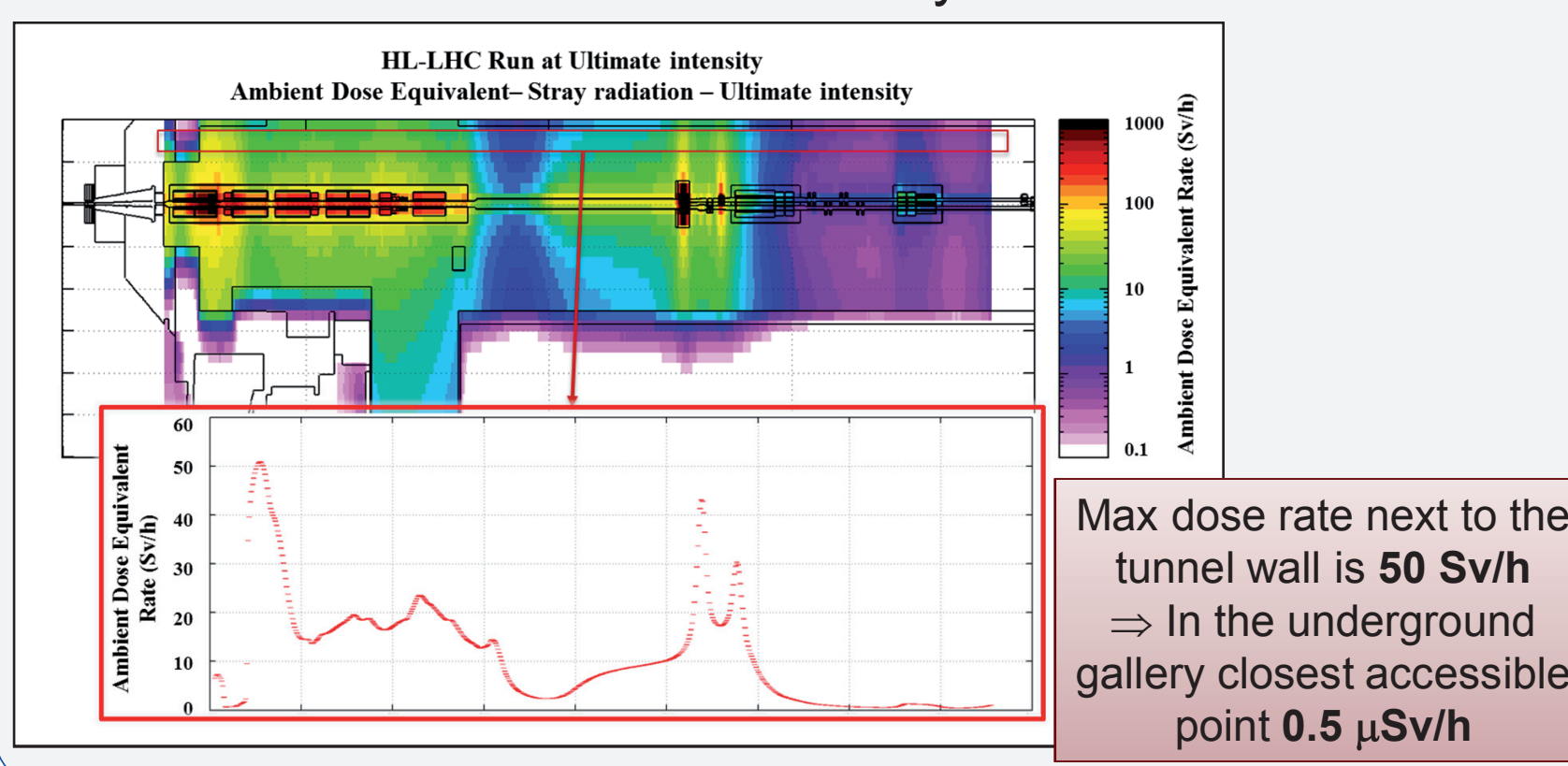
Normal proton operation

- Ultimate scenario
- Levelled luminosity $7.5 \times 10^{34} \text{ cm}^{-2}\text{s}^{-1}$

Supervised Radiation Area:

- $< 3 \mu\text{Sv/h}$
- $< 15 \mu\text{Sv/h}$
- $< 6 \text{ mSv}$

→ The attenuation provided by the shielding walls and the concrete stairs is evaluated by the accidental case



Conclusion

Fluka Monte Carlo code has been extensively used to perform induced activation studies for the LHC accelerator machine and its High Luminosity upgrade. The simulation have been performed using a very detailed geometry which reproduce the real accelerator environment.

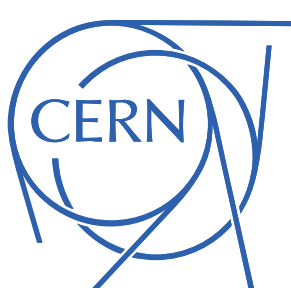
Ambient dose equivalent and activity estimation have been done using Fluka Monte Carlo code and the Activiz 3 Creator code .

The simulation results have been benchmarked with the radiation measurements performed in the LHC machine (residual dose rates) and with the γ -spectrometry measurement (activity).

References

- [1] T.T. Böhlen, F. Cerutti, M.P.W. Chin, A. Fassò, A. Ferrari, P.G. Ortega, A. Mairani, P.R. Sala, G. Smirnov and V. Vlachoudis, "The FLUKA Code: Developments and Challenges for High Energy and Medical Applications," Nuclear Data Sheets 120, 211-214 (2014).
- [2] A. Ferrari, P.R. Sala, A. Fassò, and J. Ranft, "FLUKA: a multi-particle transport code", CERN-2005-10 (2005), INFN/TC_05/11, SLAC-R-773.

- [3] S. Roesler, E. Enge and J. Ranft, The Monte Carlo Event Generator DPMJET-III. Vols. in Proceedings of the Monte Carlo 2000 Conference Lisbon, October 23-26. A. Kling, F. Barao, M. Nakagawa, L. Tavora and P. Vaz, Eds., Springer-Verlag Berlin, 1033-1038 (2001), 2000.
- [4] Ordonnance sur la radioprotection (ORaP) du 28 avril 2017 (état le 24 avril 2018).
- [5] C. Theis, H. Vincke, "Activiz 3 – an overview of the concepts, architecture & new features," in CERN Technical Note CERN-RP-2016-117-REPORTS-TN, EDMS 1706010, 2016.



HSE
Occupational Health & Safety
and Environmental Protection Unit

IRPA 2018 – The Hague, The Netherlands 4-8 June 2018

New software to integrate uncertainty in the optimization of monitoring for internal contamination



Estelle DAVESNE^{1,*}, Pierre LAROCHE², Eric BLANCHARDON¹

¹ Institut de Radioprotection et de Sûreté Nucléaire (IRSN), Fontenay-aux-Roses, France

² ORANO, Courbevoie, France

Context

In case of risk of **occupational intakes** of radionuclides:

1. Monitoring of potential internal contamination by measuring activity excreted or retained in the body
2. Interpretation in terms of committed effective dose using biokinetic and dosimetric models

BUT **uncertainty** in the dose assessment introduced by **measurement variability** and **incomplete knowledge** of exposure conditions

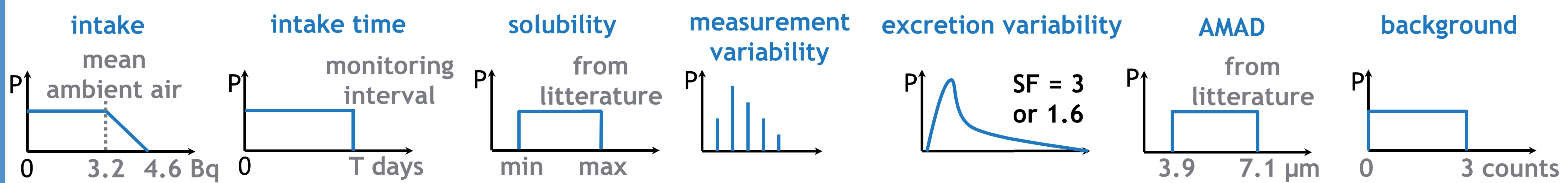
Objective

to **optimize** routine and special individual **monitoring** programs through **uncertainty evaluation**

Means

OPSCI software integrating statistical methods to **guarantee compliance with dose limits or dose constraints** with a **defined level of confidence** and using reasonable operational means

1. Uncertainty modelling by probability P

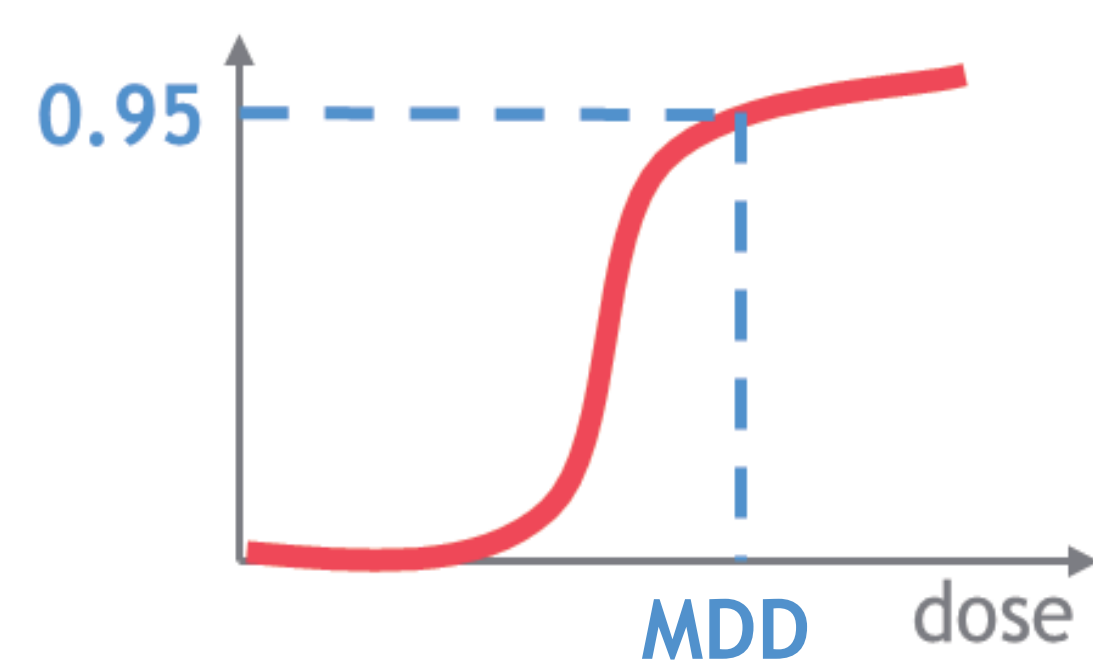


2. OPSCI

Routine monitoring

Statistical methods:

Minimum Detectable Dose (MDD) estimated from cumulative probability of dose given measurement results below detection limit (DL)



If measurement results < DL, then, considering all sources of uncertainty, the corresponding dose < MDD with a 95% level of confidence.

3. Minimum Detectable Dose (MDD) calculation

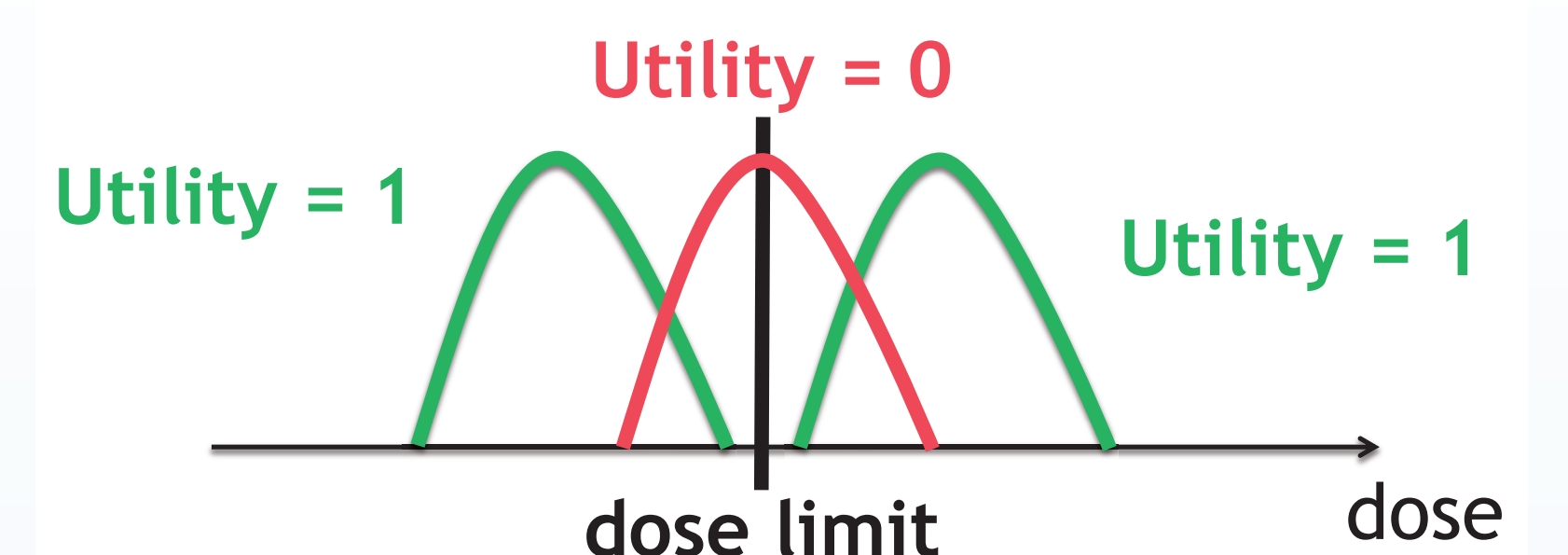


Special monitoring

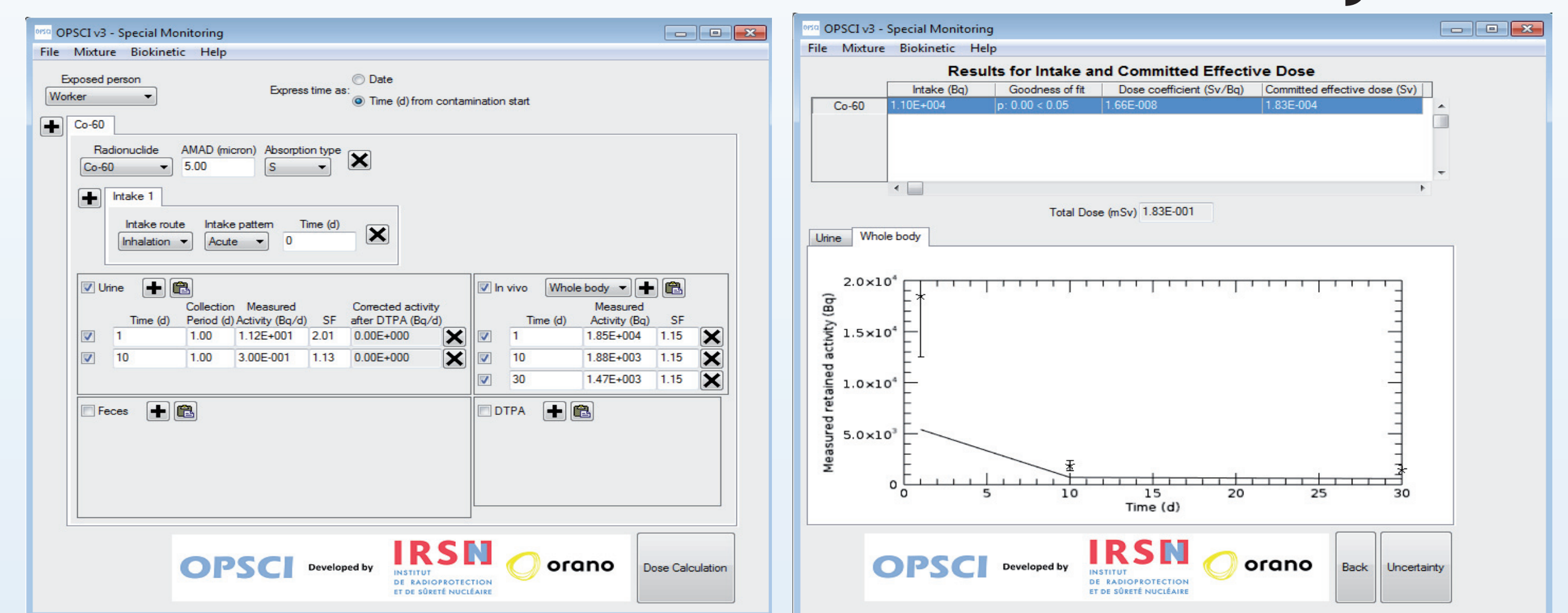
Statistical methods:

Utility function based on probability distribution of the dose given measurement results (Λ)

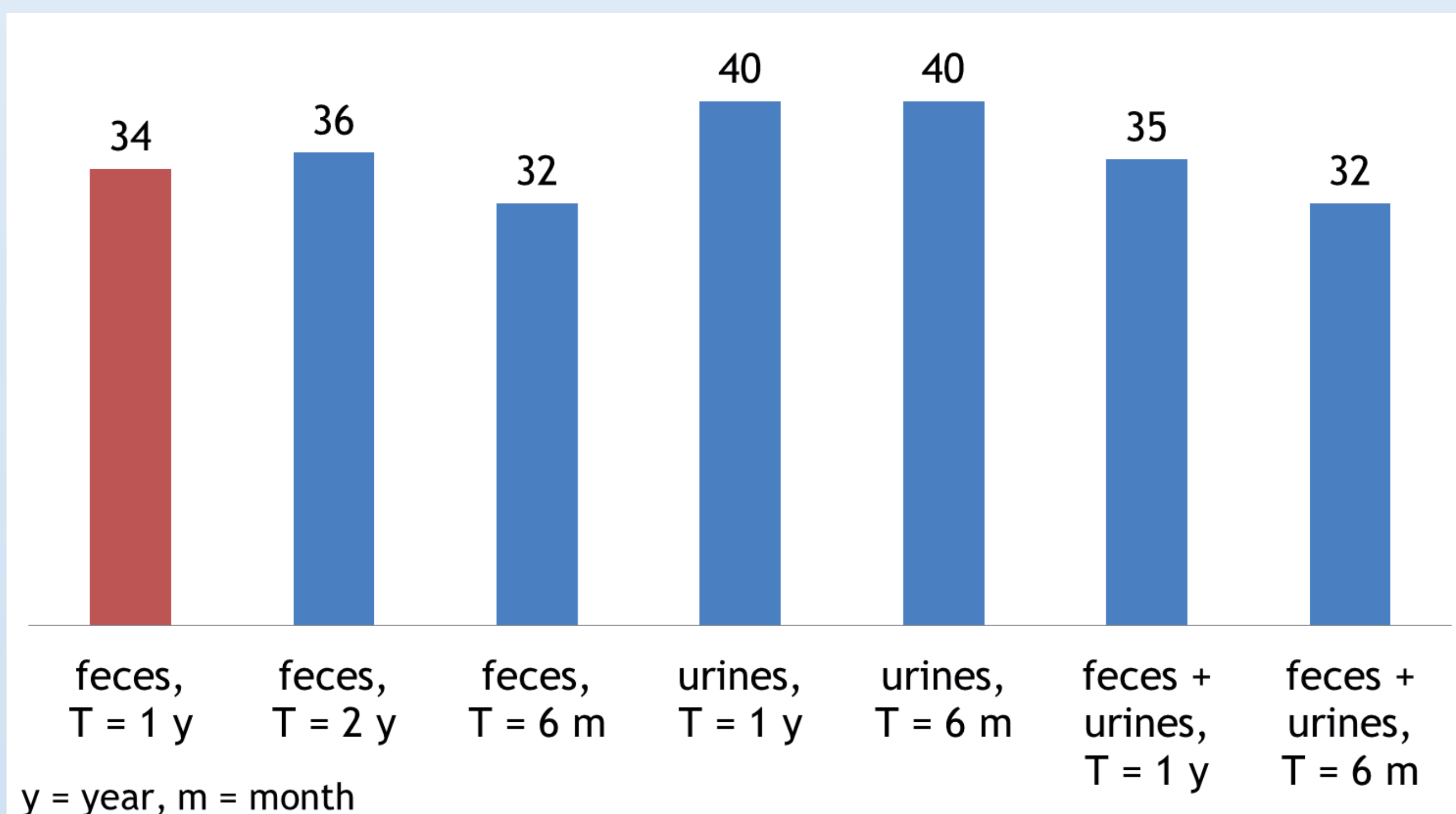
If planned bioassay may allow concluding that dose is certainly higher/lower than dose limit then Utility = 1, else Utility = 0.



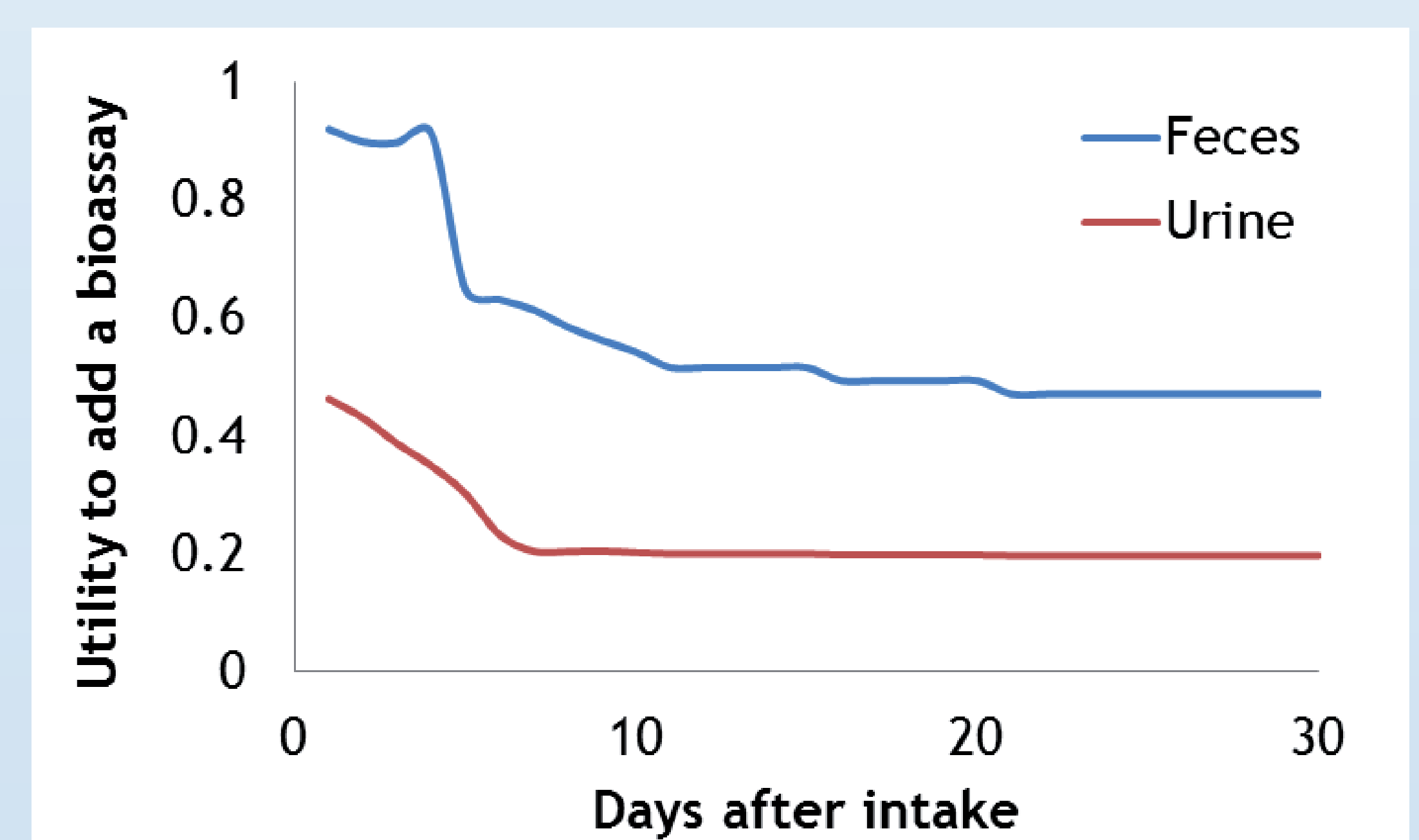
3. Calculation of dose and uncertainty



4. Optimization: comparison of MDDs (μSv)



4. Optimization: comparison of utility to perform a given bioassay at a given date



Conclusion

OPSCI software provides operational tools allowing, by integrating uncertainty:

- optimizing routine monitoring program by comparing MDDs determined for possible programs;
- assessing the committed effective dose following a contamination incident, along with its associated uncertainty;
- optimizing special monitoring by comparing the utility of performing bioassay at different time after intakes.



OCCUPATIONAL DOSES OF AIRCRAFT MAINTENANCE WORKERS DUE TO THORIATED MAGNESIUM ALLOYS

A. SCHIRMER, M. KERSTING, U. WARNECKE
GS I 3 Strahlenmessstelle der Bundeswehr
Humboldtstraße 1, D 29633 Munster, Germany

Motivation:

Magnesium vs. Aluminum alloys [1,2] :

- + lower density
- + higher creep resistance
- + high thermal conductivity
- higher cost
- high tendency for corrosion

Th replaces other usual alloying constituents

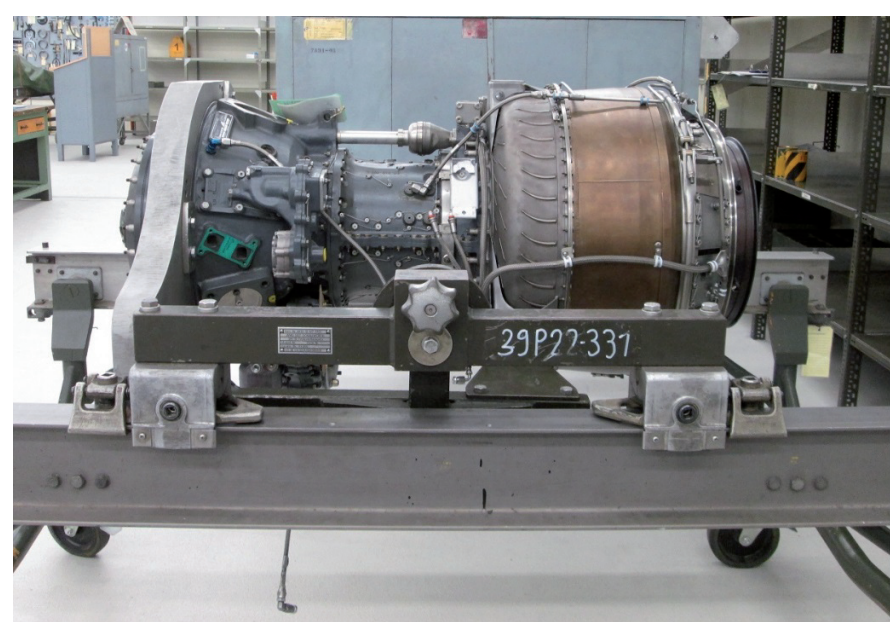
- ➔ **weak radioactivity**
- predominantly used for aircraft engine parts
- up to 4% weight Th added, (average 1.7%)

Examples:

Jet/turbine-engine components (of military aircraft)

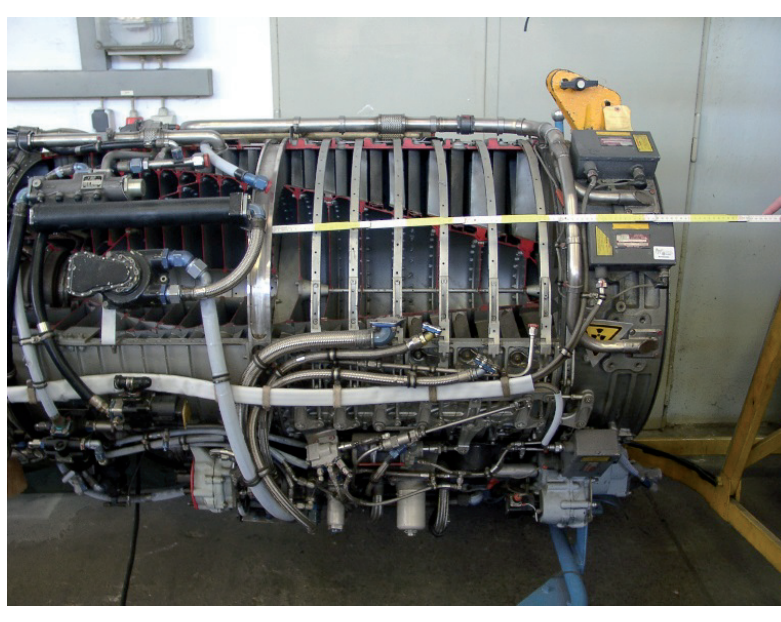
Helicopter BELL UH-1D

Shaft turbine **T-53**



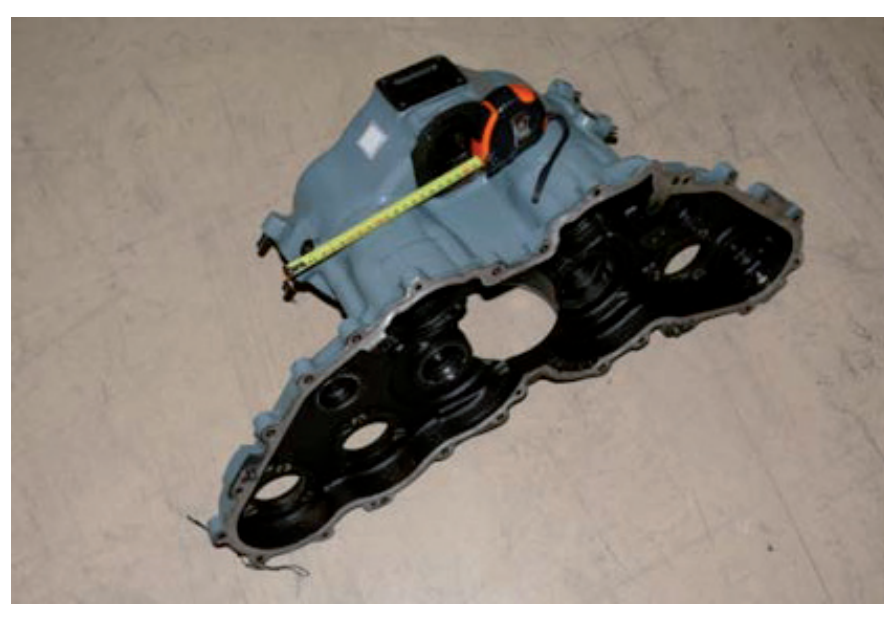
Fighter aircraft: F-104 G Starfighter

Jet engine **J-79** *)



F-4 Phantom

J-79 (twice) *)



*) different versions

Fighter aircraft T-33

Turbo-jet engine **J-33**



Combat aircraft Tornado

Auxiliary power unit (APU)



Reconnaissance aircraft BR 1151 Breguet Atlantic



Turbo engine:
propeller control unit
(marked)



Flap control mechanism
below cockpit

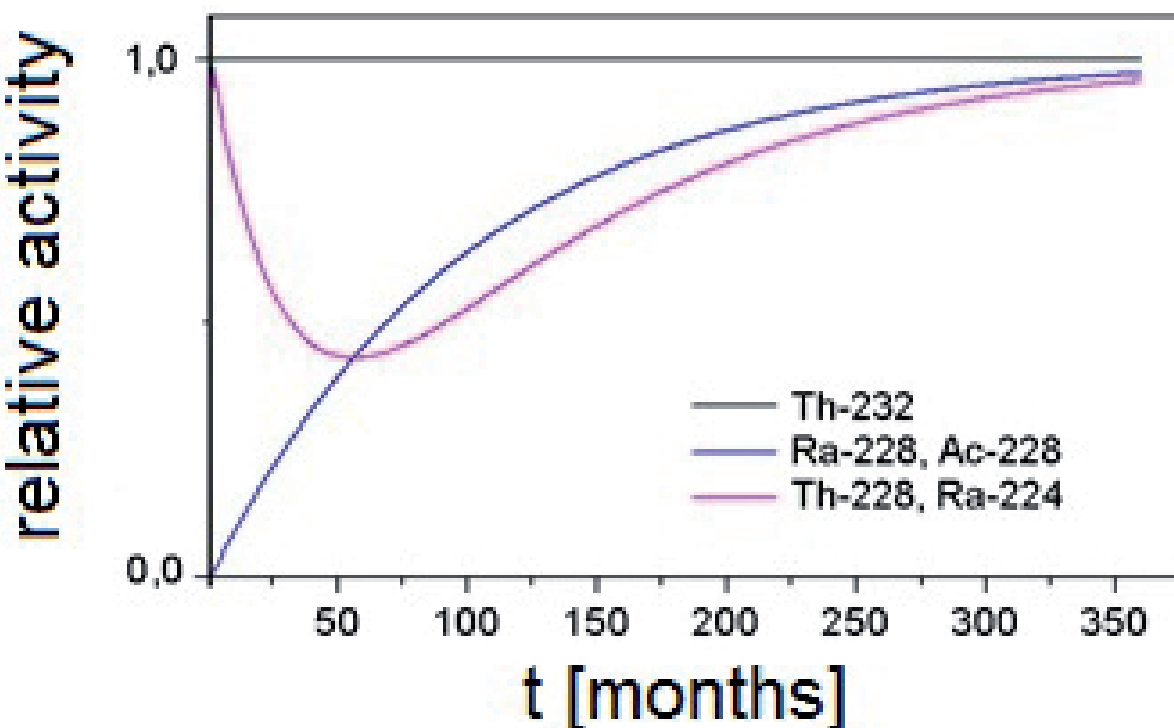
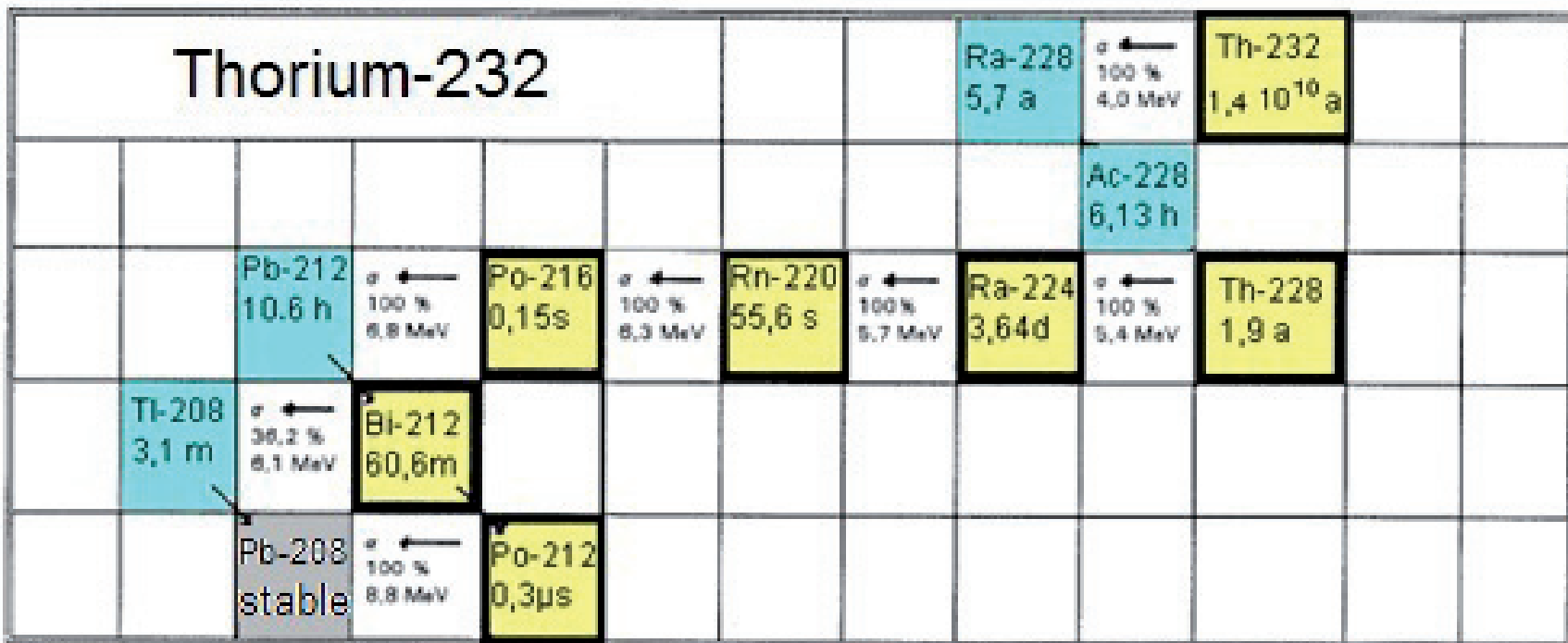
Th-Mg-alloys are no longer used in modern aircraft design.

Doses mainly needed for

- workplaces in collections
- retrospective assessments

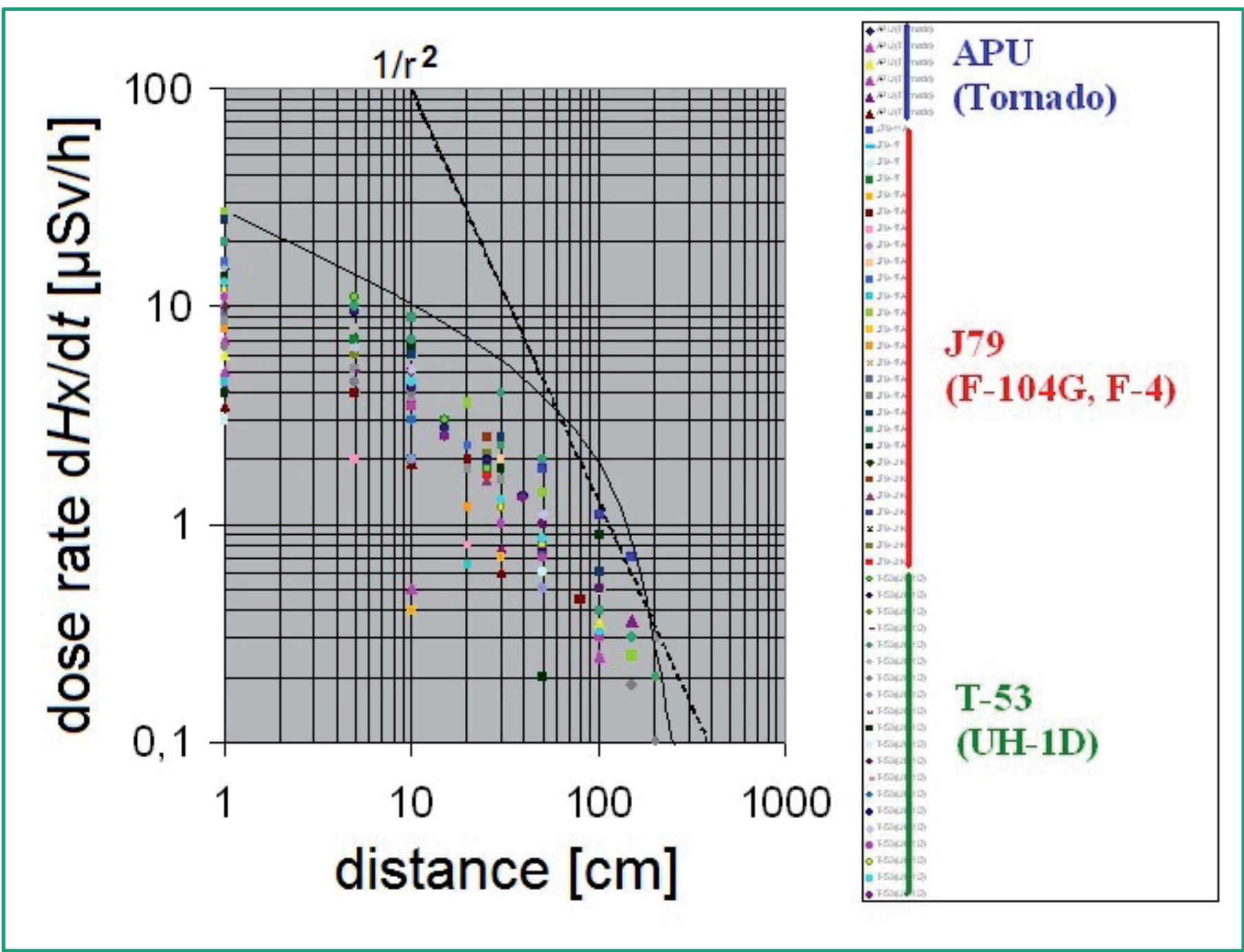
Radiological Properties of Th-232

- Th-232 ($T_{1/2} = 1,4 \text{ E}10 \text{ a}$) decays via 10 daughters (β -, γ -emitters) to Pb-208
- decay daughters dominate dose rate
- dose rate builds up after casting of alloy (chemical separation of non-Th decay daughters)



External Exposure: dose rates:

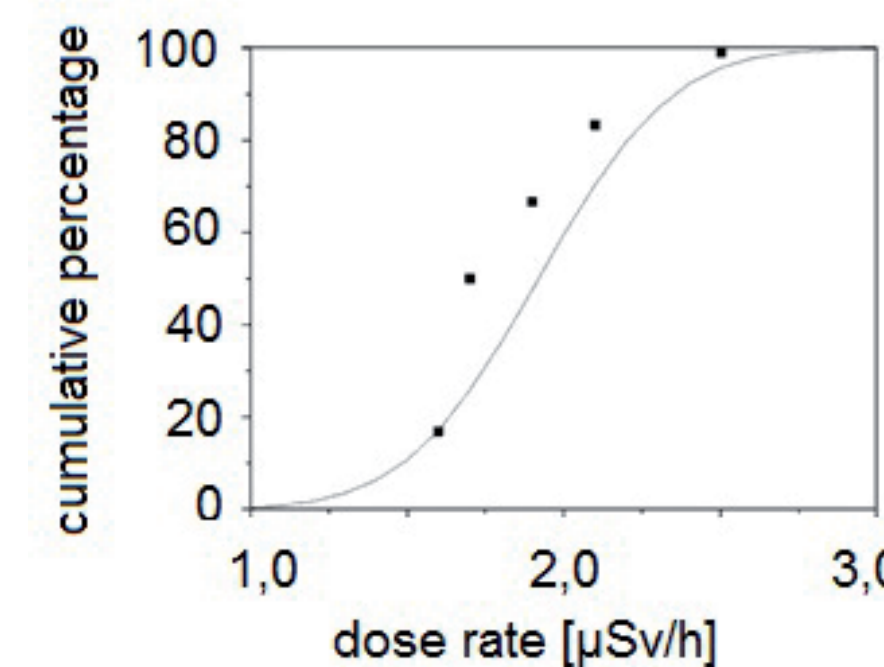
Compilation of dose rate data
obtained as a result of continuous workplace surveillance



- scatter due to
- different positions along engine
 - different ages of alloys
 - different probes

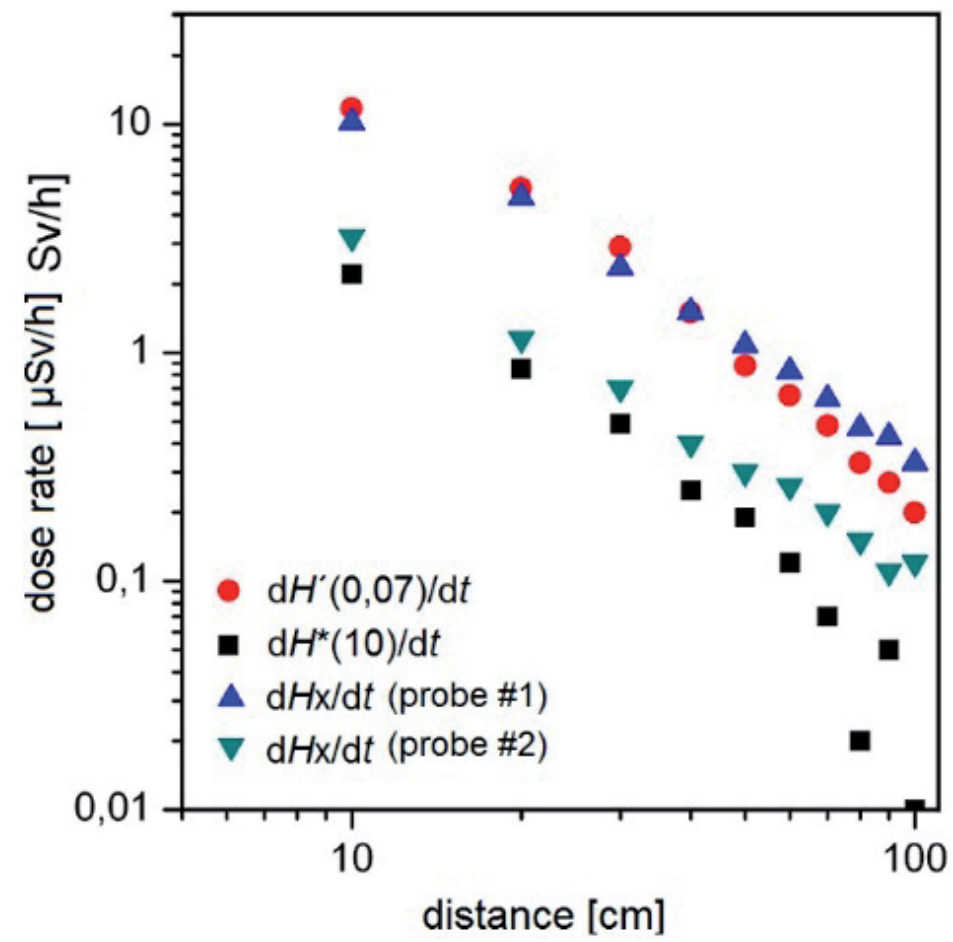
Systematic measurements on
a specific series of engines
show an **uniform distribution**

Example: dose rate at 25 cm distance from J-79 engine



Systematic investigation of dose
quantities $H^*(10)$, $H'(0,07)$ vs. H_x
(recorded in former workplace
Surveillance):

H_x -data do not underestimate $H^*(10)$



Dose rates at different distances
from a gear box (J-79 engine)

Hx-data:
#1: ionization chamber detector
#2: scintillation detector

External exposure: Occupational doses

Max. dose rate ($dH^*(10)/dt$) at 50 cm distance: $2 \mu\text{Sv/h}$

➔ **annual dose to body** (exposure time 4h/d): $\approx 2 \text{ mSv}$

(Exposure time is essential parameter, other assessments yield higher doses [3])

Internal exposure: corrosion products

Grinding/welding not considered here (see e.g. [4]).

- Handling and restauration of engines in collections/museums

- Th-Mg-parts are covered by white corrosion product
- Specific Th-activity corresponds to that ThO_2 .

J-33 engiine kept in collection: White brittle dust on tubes due to corrioion



Inhalation of Th-232 - containing dust is associated with large follow-up doses
(to lung: $1.6\text{E-}4 \text{ Sv/Bq}$, to bone $2.9\text{E-}4 \text{ Sv/Bq}$, effective dose: $2.5\text{E-}5 \text{ Sv/Bq}$ [5])

Acknowledgements:

P. Klemt, M. Röttle: for organizing and performing of the long term workplace surveillance program.

References

- [1] Lutz Strobach, Konstruktionswerkstoff Magnesium: Erwartungen, Probleme, Forschung und Einsatz im deutschen Flugzeugbau von der Mitte des 19. Jahrhunderts bis zum Ende des Zweiten Weltkrieg, Berlin 2016, ISBN-10 3944072731
- [2] Frederic T. Hill: The materials of aircraft construction for designer, user and student of aircraft and aircraft engines 6. Ed. London, 1946 p. 205-211
- [3] T.P Kuipers and A.S. de Koning: Dose Reconstruction for F-104 Starfighter Maintenance Personnel, Feb 2012.
- [4] V. Koukoulou, K. Potiriadis, K. Kehagia: Exposure to thorium caused by the cutting of a turbine engine component.. 1st Hellenic Symposium of Environmental Radioactivity, 23./24.11.2001, Greece ans NORM III Symposium 17.09.2001, Mol, Belgium
- [5] Dosiskoeffizienten bei innerer Strahlenexposition für Einzelpersonen der Bevölkerung, Bundesamt für Strahlenschutz, 2009 (Federal Office for Radiation Protection)



Personal and Environmental Monitoring at the Paul Scherrer Institute using a Radio-Photo Luminescence Dosimetry System

Frank Assenmacher, Eduardo G. Yukihiro, Sabine Mayer

Department of Radiation Safety and Security, Paul Scherrer Institute, 5232 PSI Villigen, Switzerland
Frank.Assenmacher@psi.ch

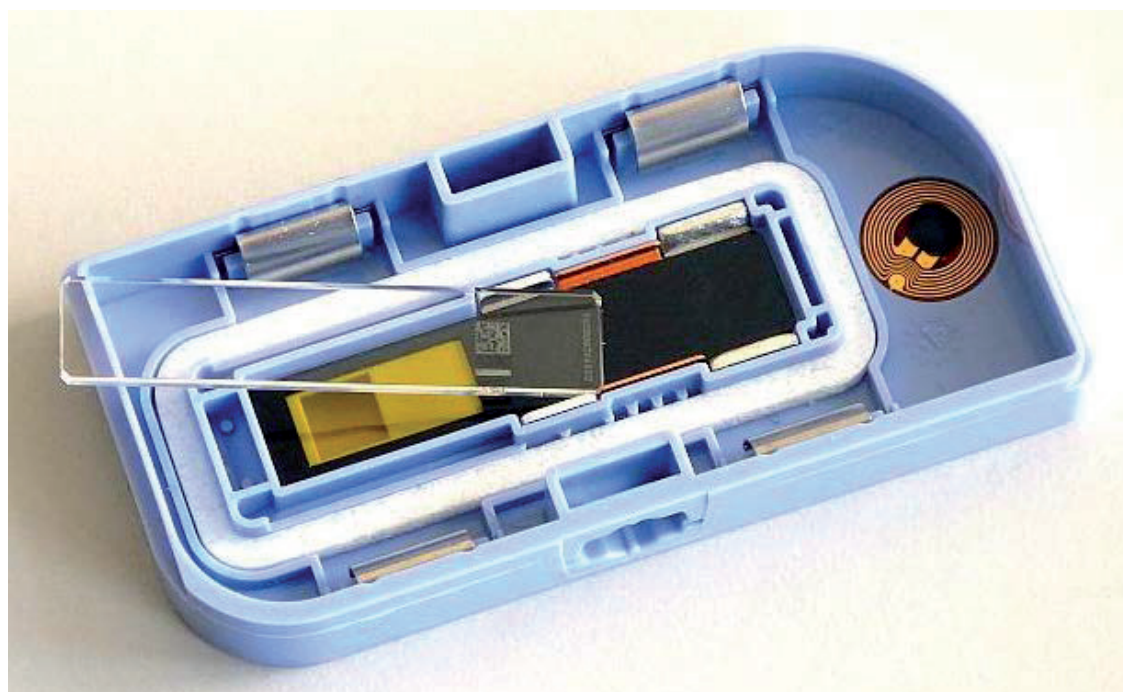
Introduction

The dosimetry service at the Paul Scherrer Institute (PSI) in Switzerland has introduced in 2015 a new dosimetry system for personal and environmental monitoring, based on radio-photo luminescence (RPL) of silver doped phosphate glass. A detailed investigation of the dosimetric properties is given in [1].

In this conference contribution an overview of the collected experience made since its implementation is presented.

Radio-Photo Luminescence Dosimetry System

Manufacturer: Chiyoda Technol, Japan
Detector material: silver doped phosphate glass ($\text{Ag}^+:\text{P}_4\text{O}_{10}$)
Readout: a UV light laser excites radiation induced, stable color centers (Ag^{2+} and Ag^0) and leads to visible light detection
Dosimeter badge: 5 filters and 5 readout areas
Dose quantities: $H_p(10)$, $H_p(0.07)$ (β and γ separately), $H^*(10)$



Intercomparisons Photon Whole Body Dosimeter

Radiation quality	Angle [°]	Intercomparison Organization + Year	$H_p(10)$ Ratio measured / reference	$H_p(0.07)$
N-40	-60	EURADOS 2016	1.18	0.85
N-40	60	EURADOS 2016	1.12	1.08
N-40	0	CH 2015	1.00	1.05
		EURADOS 2016	0.95	1.01
N-80	0	ENSI 2015	1.06	1.10
N-150	-45	EURADOS 2016	0.86	0.88
N-150	45	EURADOS 2016	0.86	0.88
N-150	0	EURADOS 2016	0.87	0.93
N-200	30	CH 2015	0.93	0.94
$^{90}\text{Sr}/^{90}\text{Y}$	0	CH 2016	0.0/0.0	1.00
$^{137}\text{Cs} + ^{90}\text{Sr}/^{90}\text{Y}$	0	EURADOS 2016	0.98	1.00
$^{137}\text{Cs} + \text{N-80}$	0	ENSI 2015	1.01	1.02
^{137}Cs	0	ENSI 2015	0.99	0.99
		CH 2015	1.04	1.04
		CH 2016	1.00	1.00
		CH 2017	1.00	1.00
		EURADOS 2016	0.97	0.97
^{137}Cs	45	CH 2016	1.00	1.00
^{60}Co	0	CH 2016	0.88	0.88
		EURADOS 2016	0.87	0.85

Table of intercomparisons (EURADOS, CH) and approval test (ENSI) results.
CH: Swiss authorities FOPH (Federal Office of Public Health), and ENSI (Swiss Nuclear Safety Inspectorate). EURADOS: intercomparison IC2016ph.

Swiss Environmental Dosimetry Intercomparison

Organized by the secondary standards dosimetry laboratory at PSI in 2016. Three months exposition in ambient environment and irradiation in facility.

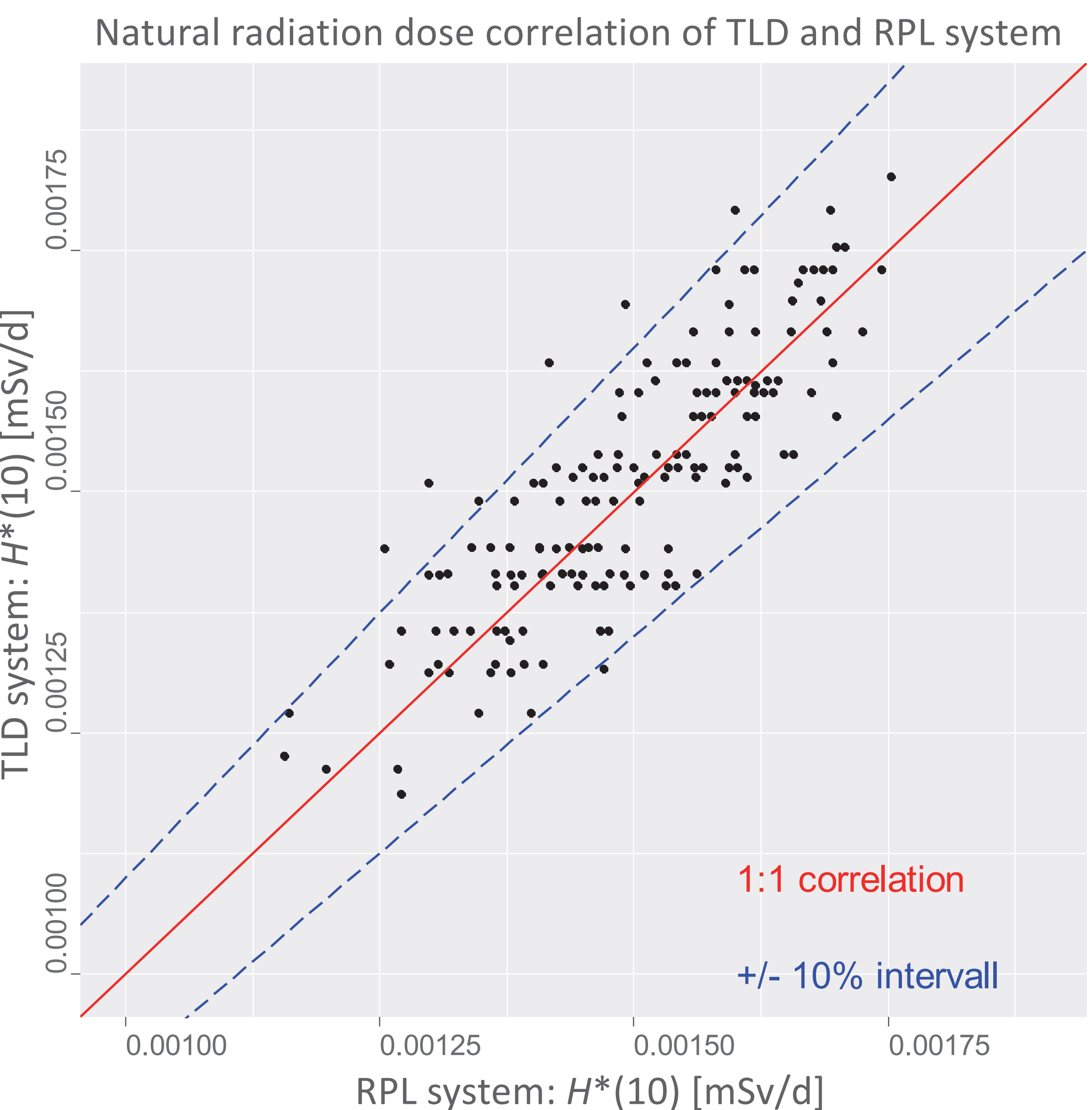
Environment	$H^*(10)$ Ref. Dose [mSv]	Measured [mSv]	Ratio
Laboratory	0.3 +/- 0.01	0.31 +/- 0.06	1.02
	1.7 +/- 0.07	1.64 +/- 0.3	0.96
Natural Radiation (Terrestrial + Cosmic)	0.182 +/- 0.014	0.17 +/- 0.03	0.94

References

[1] Dosimetric properties of a personal dosimetry system based on radio-photoluminescence of silver doped phosphate glass, F. Assenmacher, M. Boschung, E. Hohmann, S. Mayer, Radiation Measurements, Vol 106, 2017, pp 235-241.

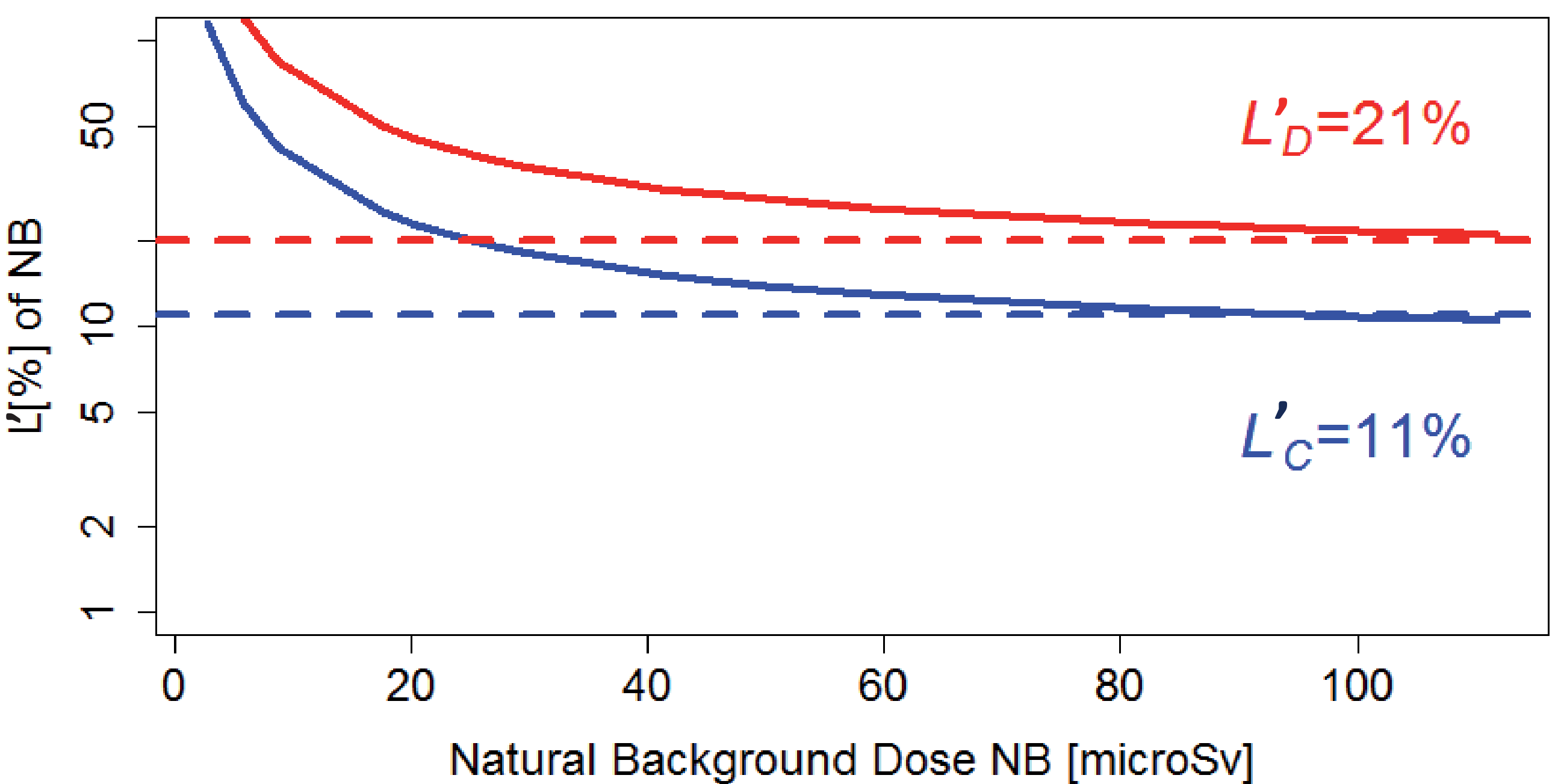
Environmental Dosimetry around PSI

In the greater area around PSI the radiation exposure to the public is monitored. Ideally, only the natural radiation background contributes to the measured doses. Since beginning of 2017 the new RPL system is used in parallel with the established TLD ($\text{Al}_2\text{O}_3:\text{C}$) environmental dosimetry system. The correlation plot compares the dose rates of 35 measurement positions (RPL and TLD) for five quarter periods.



Measurement Uncertainty due to Natural Radiation Background

The individual accumulated dose due to the ubiquitous natural radiation background (NB) is usually not known for each personal dosimeter. An average dose rate can be subtracted but this does not reduce the overall measurement uncertainty. RPL dosimeters have been measured frequently over a year. L_C is the minimum detectable dose avoiding false-positives, and L_D the minimum quantifiable dose avoiding false-negatives. In the plot, L_C and L_D are given in percentage of NB (e.g. $L'_C := L_C / \text{NB} \times 100\%$).



Conclusion

The collected experience since the implementation of the RPL dosimetry system in 2016 shows the good performance in individual and environmental monitoring.

Funding

This work was partially funded by the Swiss Nuclear Safety Inspectorate (contract no. H-101196)



Personal neutron monitoring at the Paul Scherrer Institute

E. G. Yukihara, A. Stabilini, F. Assenmacher, K. Meier and S. Mayer

Department of Radiation Safety and Security, Paul Scherrer Institute, 5232 PSI Villigen, Switzerland

eduardo.yukihara@psi.ch

Abstract

The Paul Scherrer Institute (PSI) carries out personal neutron monitoring services since 1998 using polyallyldiglycol carbonate (PADC) track-etch detectors. Since 2010 this has been done using the commercial system from Track Analysis Systems Ltd. (UK). The design of the dosimeter has been optimised for workplaces around high-energy accelerators, where the neutron energy spectra are dominated by fast neutrons. In addition to the dosimetry of the workers at PSI, the service is also offered to other research institutions in Europe, such as CERN (Switzerland) and DESY (Germany), and via the partner dosimetry services MPA-NRW (Germany), and Seibersdorf Laboratories (Austria). Here we provide an overview of the neutron dosimetry service at PSI, including results of quality assurance tests, e.g. PADC material acceptance tests, as well as the results from the latest intercomparisons.

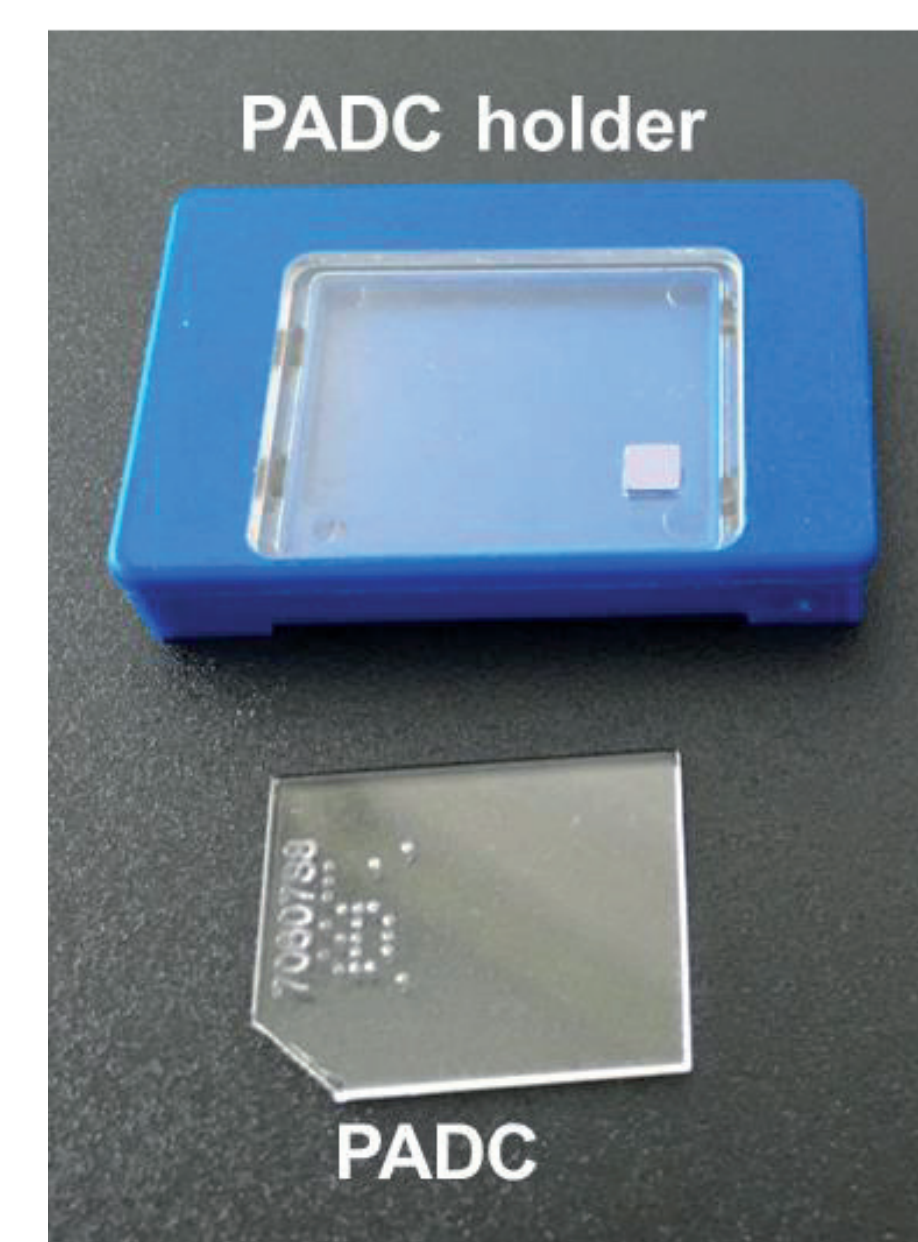


Figure 1: PADC detectors and holder.

The neutron dosimetry system

The system is based on TASTRAK® detectors and the TASLImage system from Track Analysis System Ltd.⁽¹⁾ For every readout period and customer, at least 6 calibration detectors and 6 control detectors (unirradiated) are used.

Table 1: Characteristics of the neutron dosimetry system and detectors used at PSI.

Detectors	TASTRAK® (Track Analysis Systems Ltd.)
Dimensions	20.0 mm × 25.0 mm × 1.5 mm
Converters	Fast n: 2 mm polyamide Thermal n: LiF chip (TLD 600) (optional)
Etching	NaOH 6.25 M - 85 °C - 2h 50min ⁽⁴⁾
Readout	TASLIMAGE™ (Track Analysis Systems Ltd.)
Calibration	²⁴¹ Am-Be

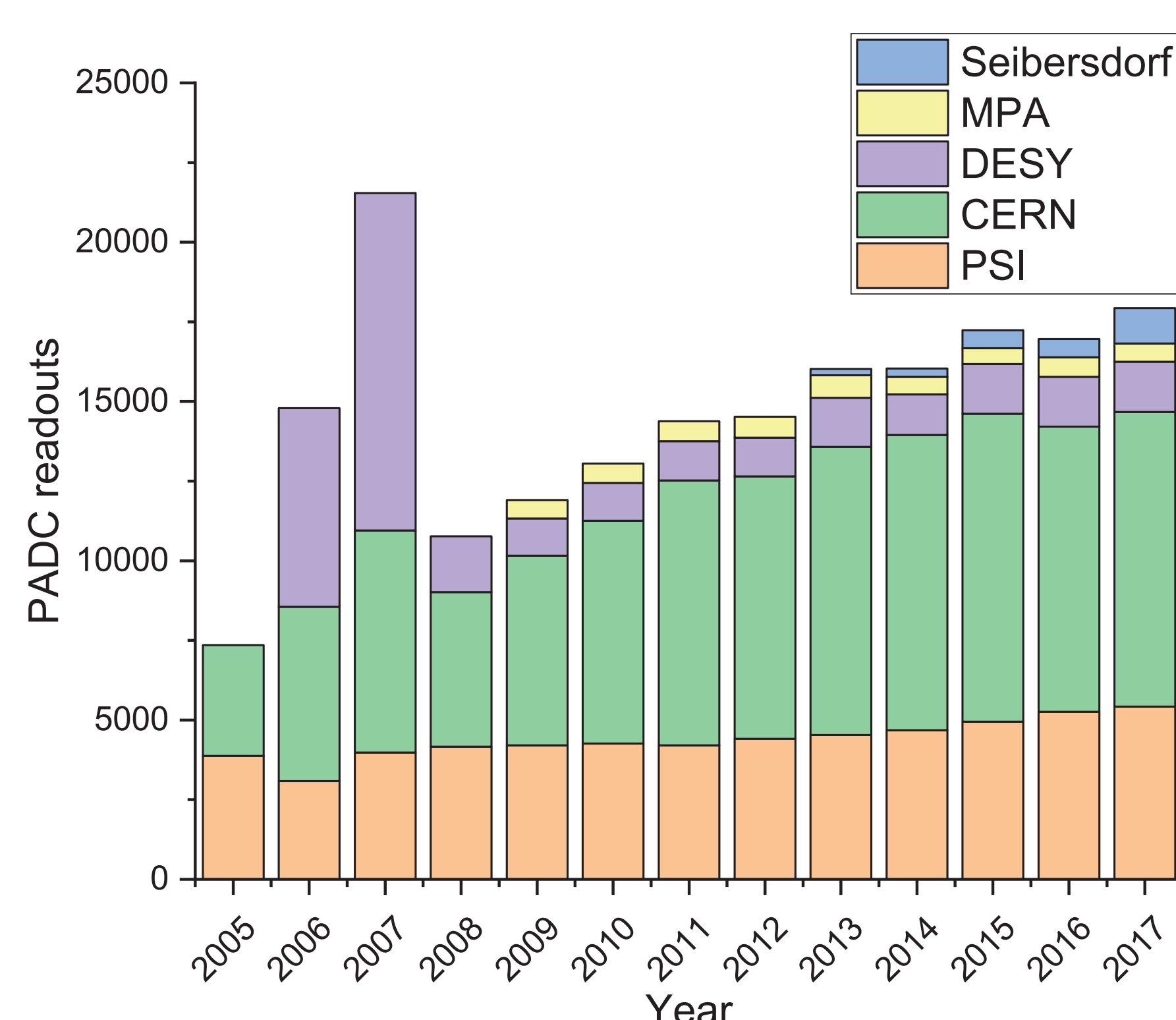


Figure 1: Statistics on PADC readouts at PSI, not counting quality assurance readouts (~30% of the readouts).

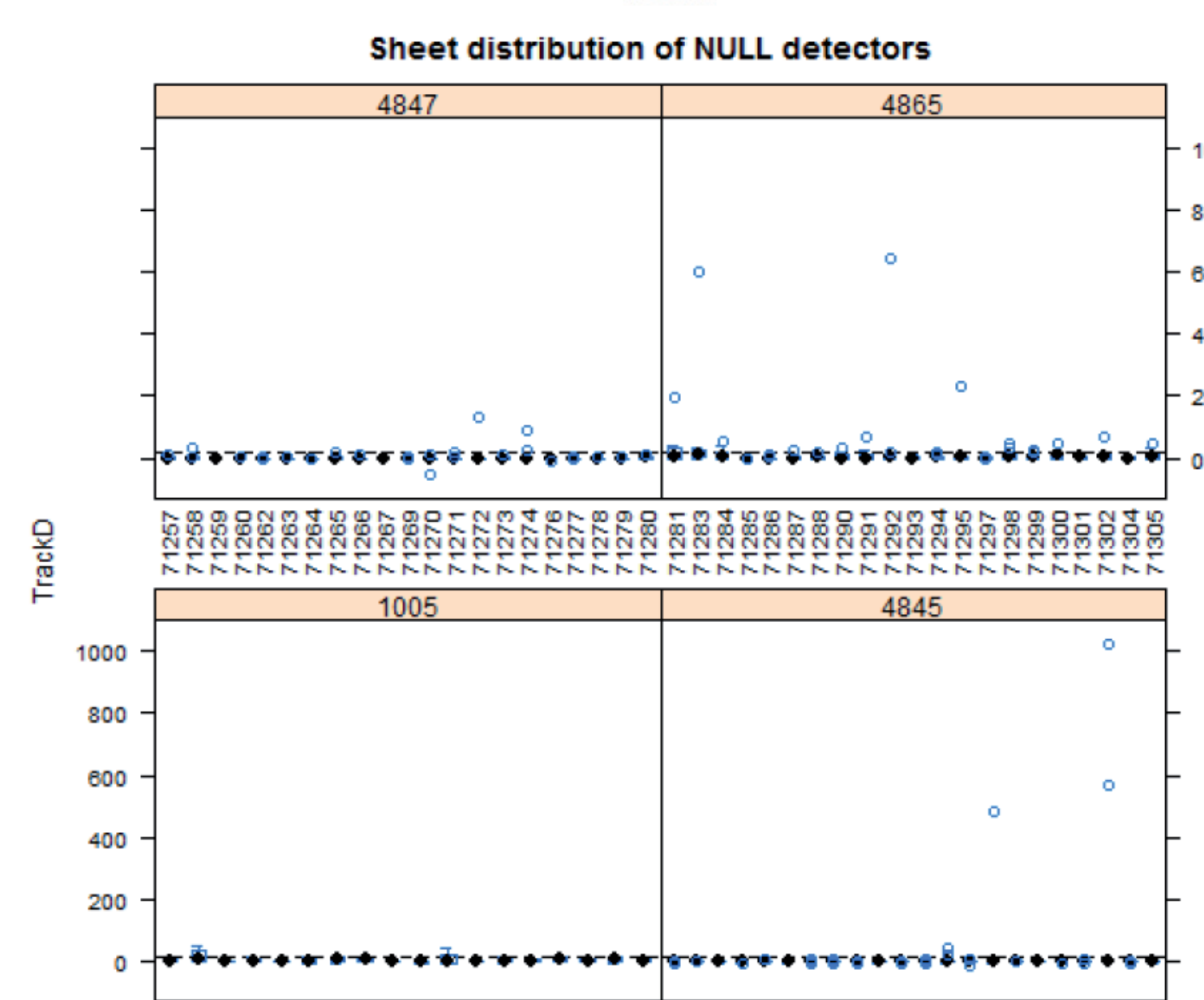
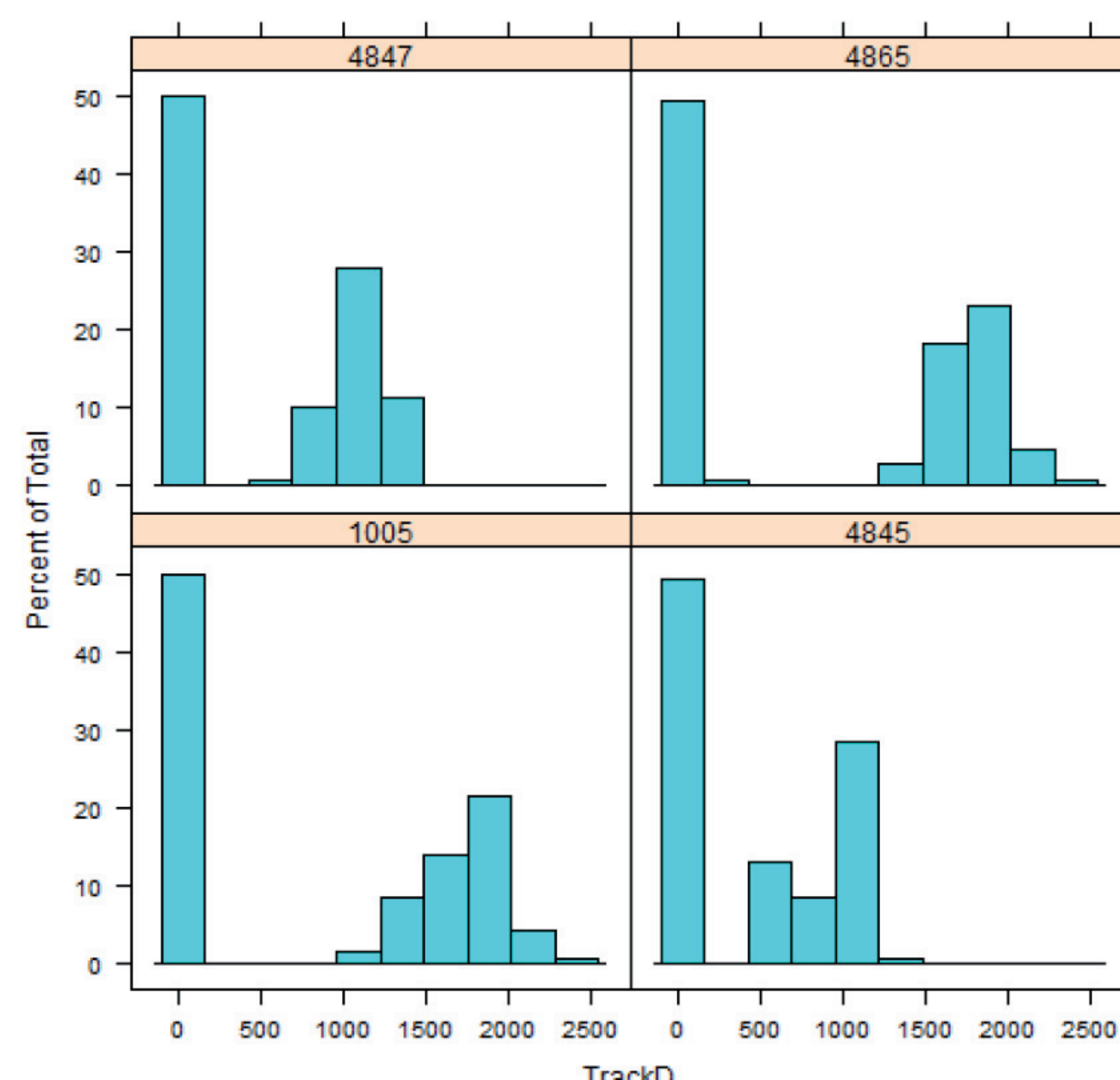


Figure 2: Example of acceptance test results performed at PSI. In this example, only batch 1005 (with the exception of one sheet) was accepted. The others were further investigated and partly rejected.

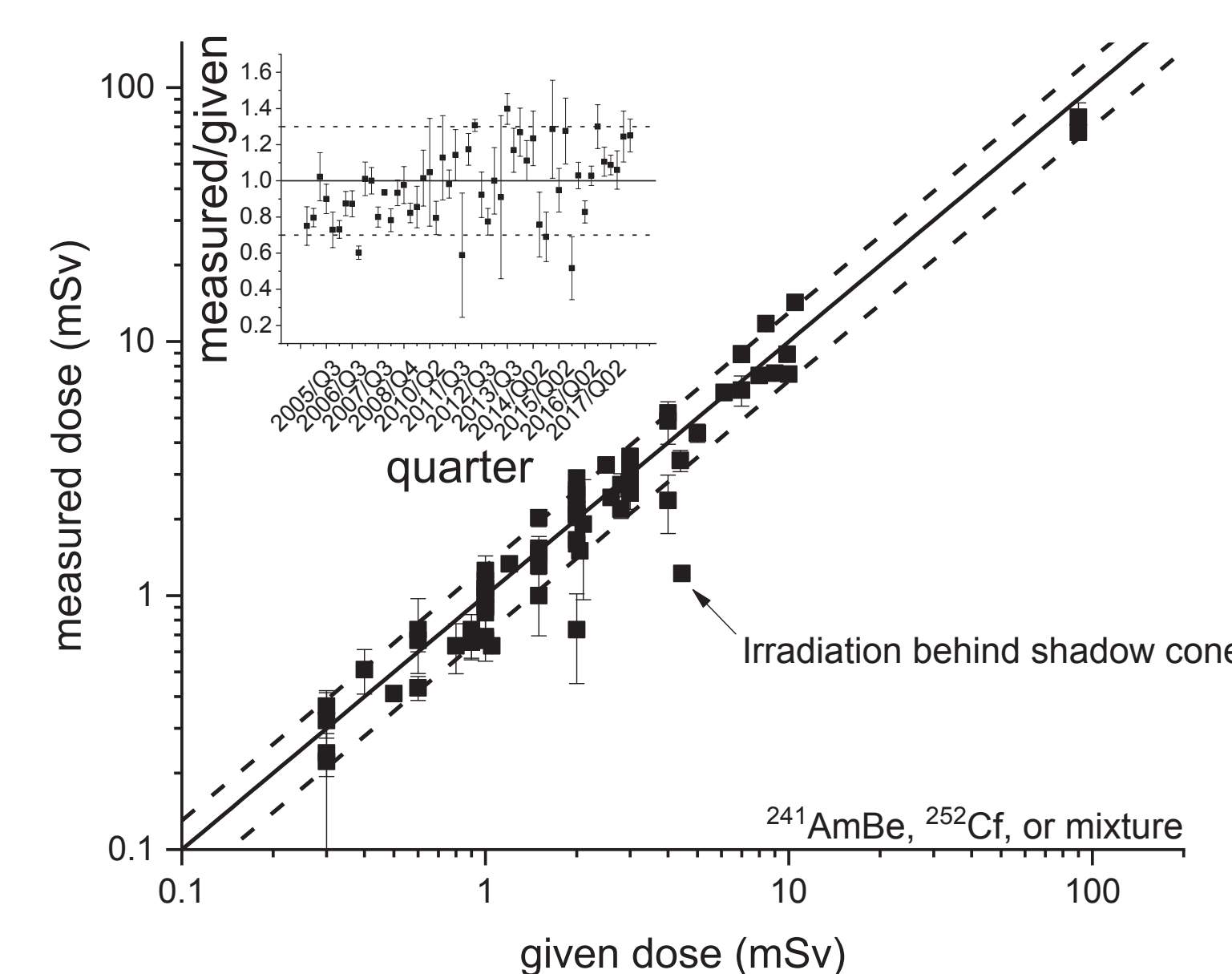


Figure 3: Compilation of blind tests since 2005. The lines indicated the 1:1 trends and $\pm 30\%$ response.

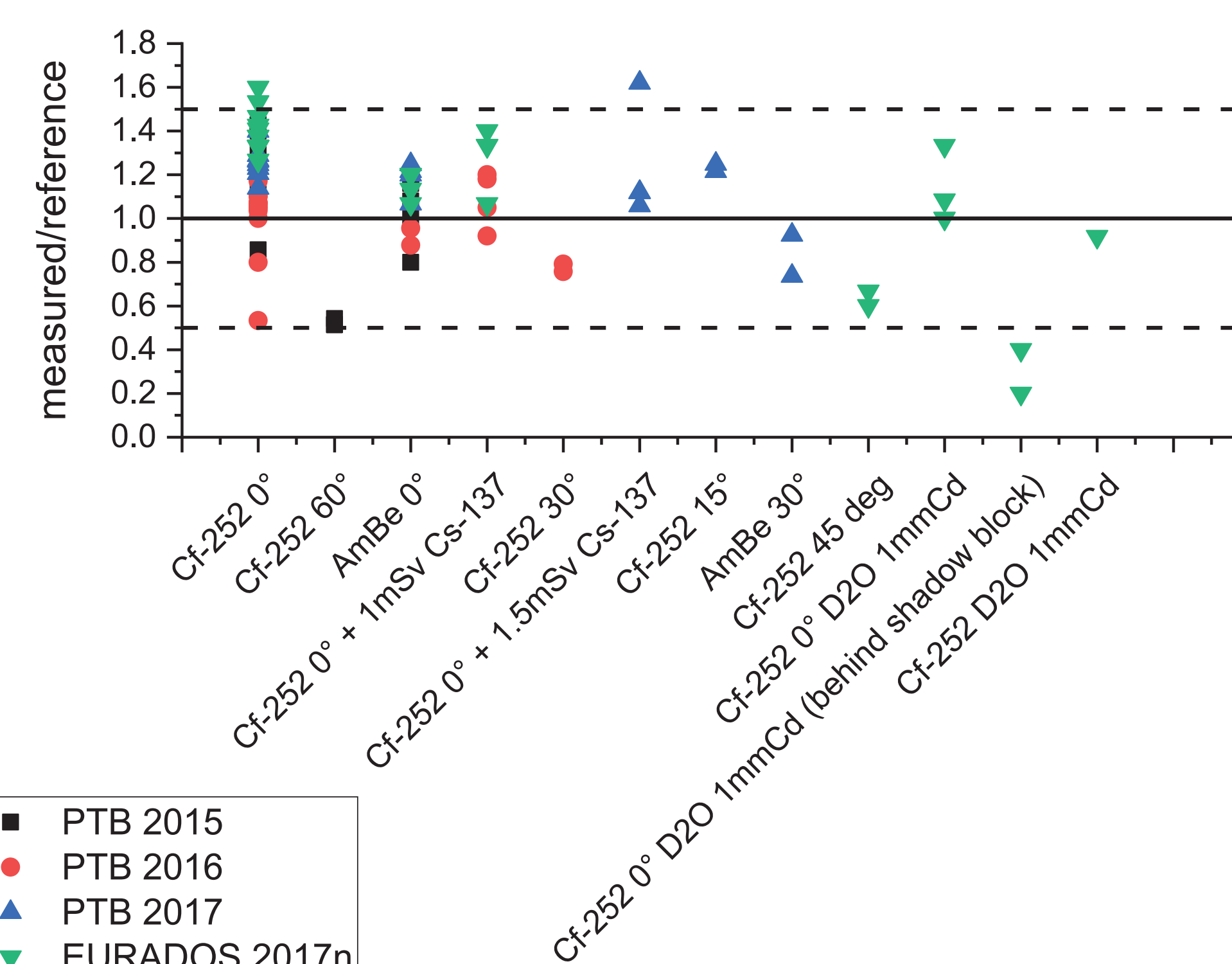


Figure 4: Compilation of intercomparison results from the last three years. The horizontal lines are only a guide.

Conclusions

PSI's neutron dosimetry service has demonstrated each year constant and satisfactory performance in international intercomparisons. This is achieved through rigorous acceptance tests of every sheet of PADC delivered, as well as a continuous monitoring of the performance through blind tests. We also continue to investigate properties of various PADC manufacturers^(2,3) and characterize the properties of the material currently used.

References

- (1) Track Analysis System Ltd (2010). TASLIMAGE Radon and Neutron dosimetry system. Bristol UK.
- (2) Mayer, S. and M. Boschung (2014). "Comparison of different PADC materials for neutron dosimetry." *Radiation Protection Dosimetry* 161(1-4): 104-107.
- (3) Caresana, M., et al. (2017). "Comparison of PADC neutron detectors from different suppliers." *Radiation Protection Dosimetry* in press.
- (4) Assenmacher, F., et al. (2016). "Comparison of different PADC materials and etching conditions for fast neutron dosimetry." *Radiation Protection Dosimetry* 170: 162-167.

Acknowledgements

The authors thank Helga Schröter for the chemical etching of the detectors, the Swiss Nuclear Safety Inspectorate (contract no. H-101196) for the support, and PTB for the opportunity to participate in the intercomparisons.

Radiation Protection assessment of the emission of a d-t Neutron Generator: simulations with MCNP Code and experimental measurements in different operating conditions

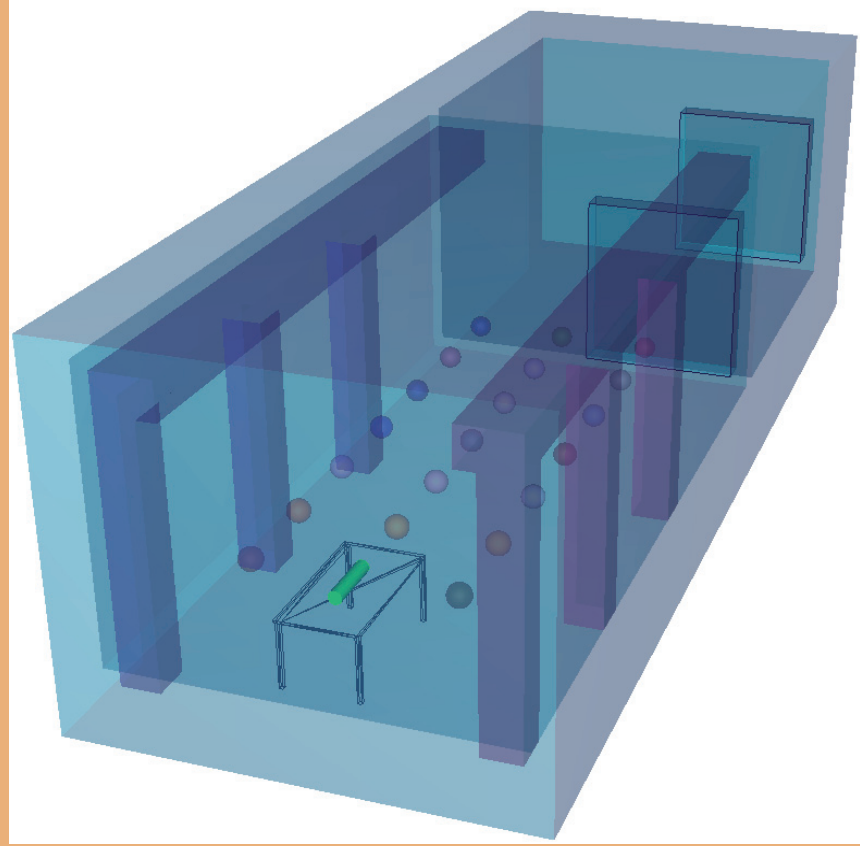
G.M. Contessa¹, N. Cherubini¹, G. Gandolfo², L. Lepore², R. Remetti², S. Sandri¹

1: Italian National Agency for new technologies, energy and sustainable economic development (ENEA), Lungotevere Thaon Di Revel 76, 00196 Rome, Italy
2: University of Rome "Sapienza" – Department of Basic and Applied Sciences for Engineering, Via A. Scarpa 14, 00161 Rome, Italy

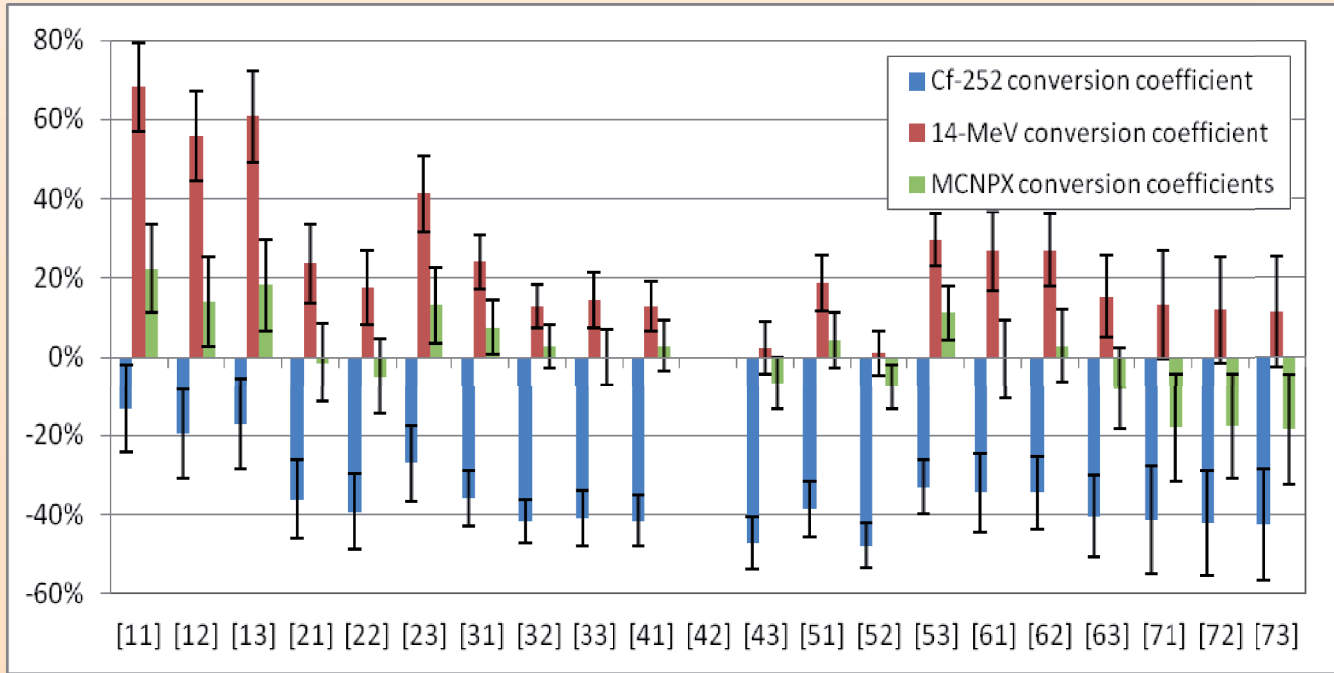
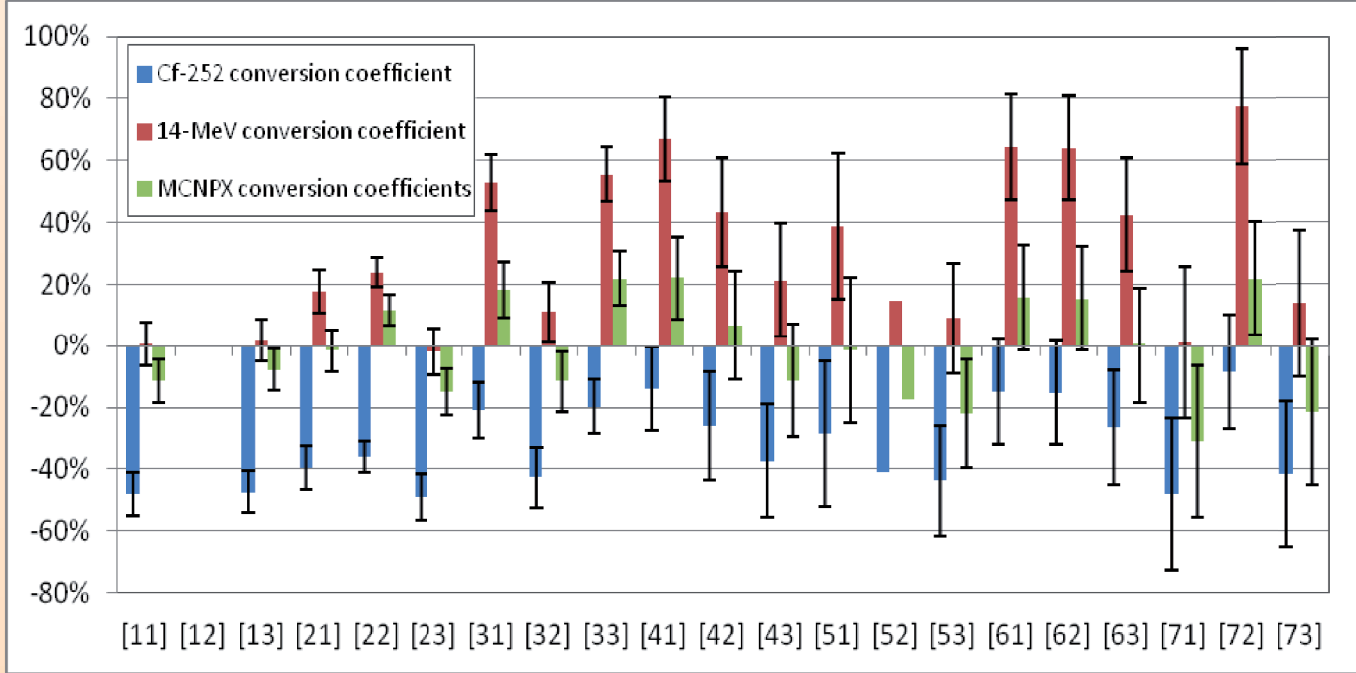
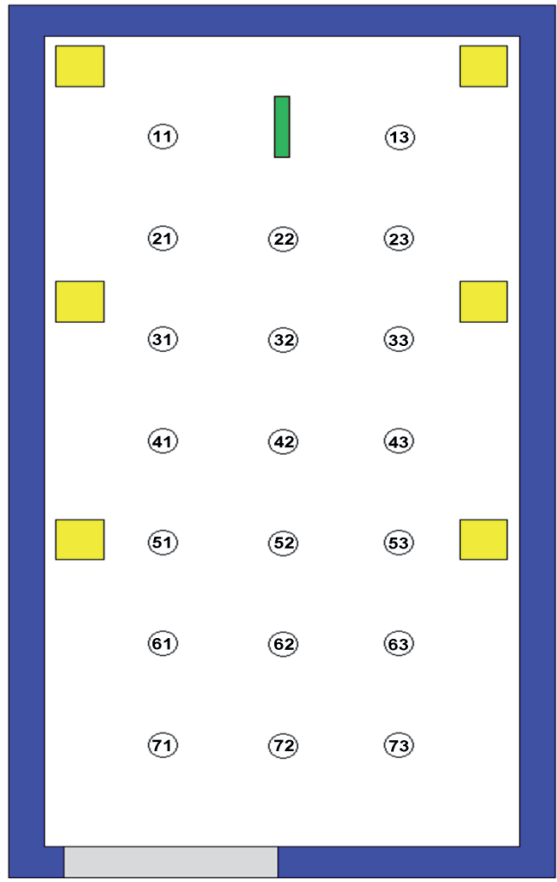
INTRODUCTION

Neutron Generators are one of the most widespread sources of fast neutrons for different kind of analytical applications, ranging from classic activation analysis to the quantitative estimation of the fissile/fertile materials in radioactive wastes packages. When using **portable d-t neutron generators**, determination of Radiation Protection quantities at the point of interest is affected by a series of boundary conditions that could differ from an experimental set-up to another. For instance, neutrons' energy spectrum and flux magnitude could be influenced by irradiation geometries. In order to use neutron dosimeters properly, some considerations on the specific irradiation scenario should be carried out, case by case. In particular, the common assumption of a reference ²⁵²Cf self-fission neutron spectrum for converting measured count rates to dose rates could cause non-conservative results.

EXPERIMENTAL DATA VS MCNPX SIMULATIONS



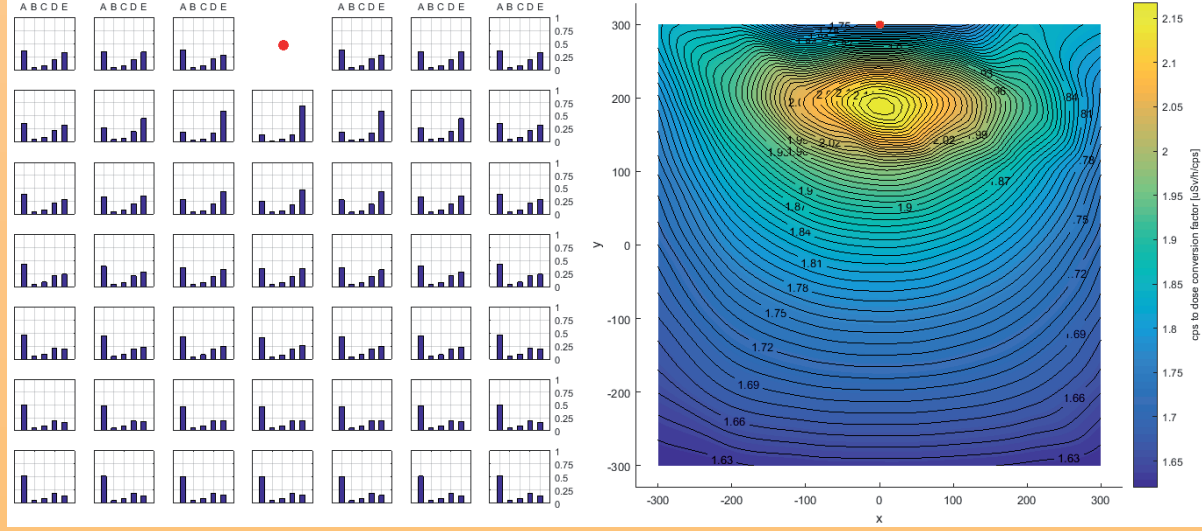
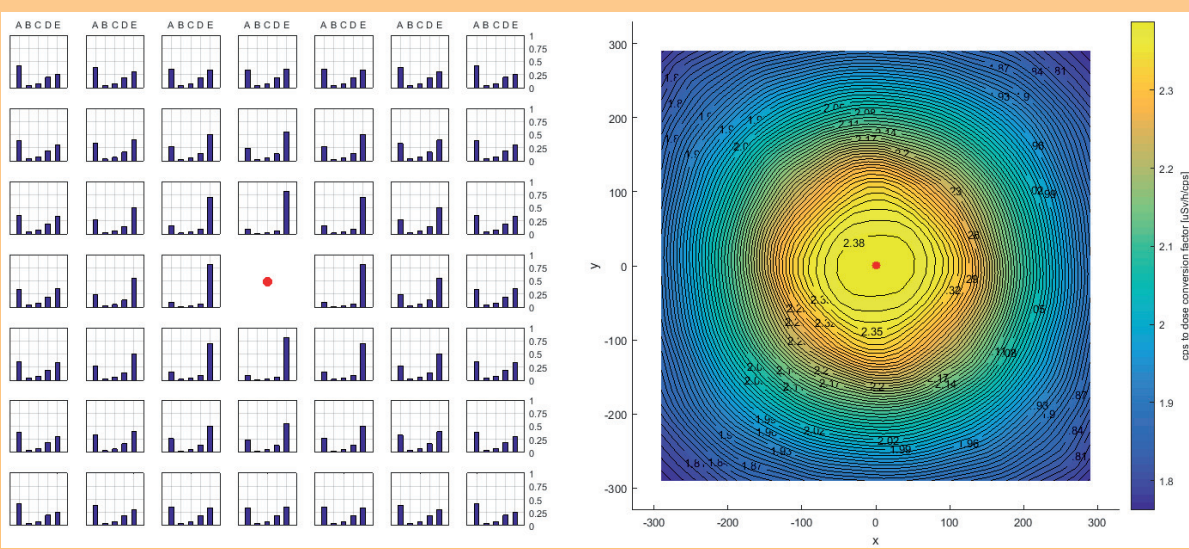
An experimental setup has been arranged inside a '**NEUTRON BUNKER**' hosting a **Thermo Scientific MP-320 neutron generator**. In the bunker's main room 21 positions have been defined: in each one of 20 positions the neutron count rate was measured by **Berthold LB6411 rem-counter**, with the neutron generator at the [1,2] position (i.e. the bottom wall of the neutron bunker) in the first measurement campaign, and at the [4,2] position (i.e. the center of the room) in the second campaign. An accurate model of the building, of the Thermo Scientific MP-320 neutron generator and of the Berthold LB6411 neutron counter have been reproduced by MCNPX. For each measurement the corresponding **MCNPX simulation** was carried out. The purpose was to evaluate the most appropriate **count-rate to dose-rate conversion coefficient** for Berthold LB6411.



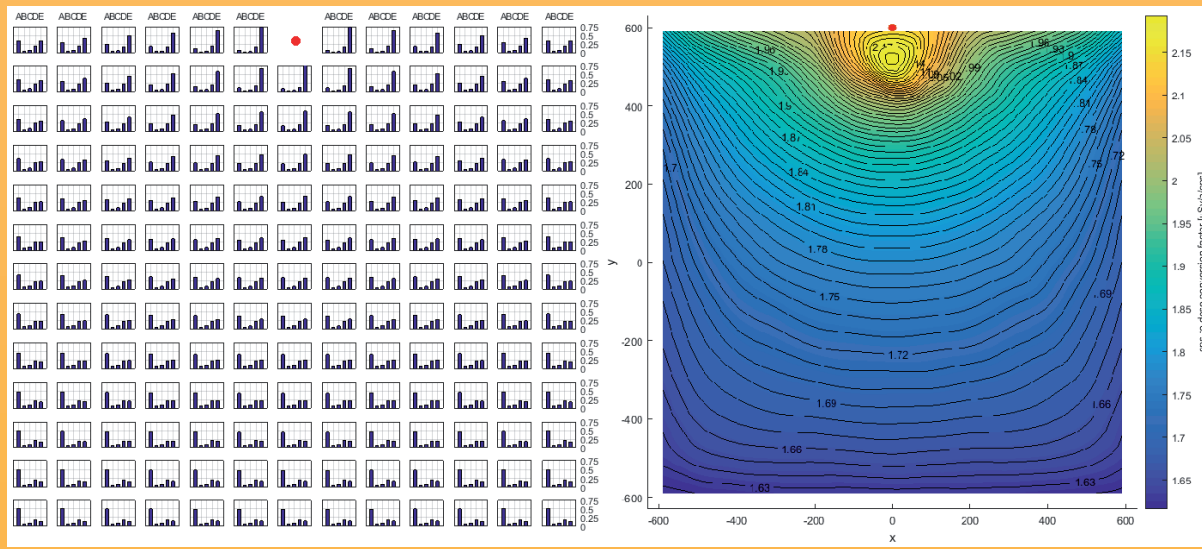
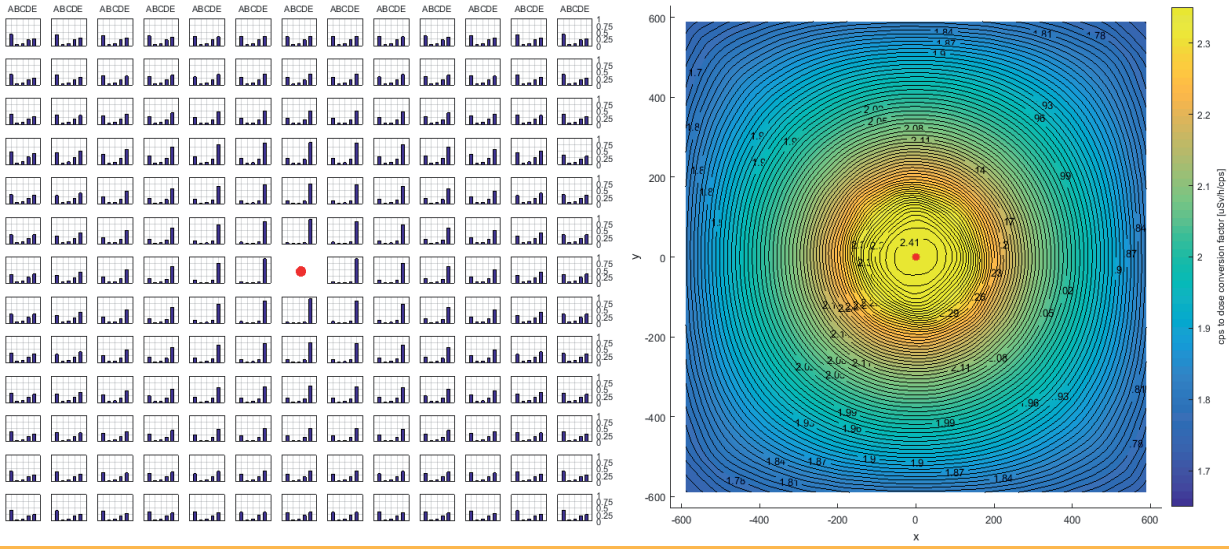
Deviations from Berthold LB6411's dose rates vs. MCNPX dose rates with the neutron generator near a wall (the left) and in central position (right).

SIMULATED SCENARIOS

Having checked a good agreement between experimental and simulated results, MCNPX has been used as a design tool, and four sets of simulations have been carried out for **two bunkers of larger dimensions**:
6.6 m (L) x 6.6 m (W) x 6.6 m (H);
12.6 m (L) x 12.6 m (W) x 12.6 m (H).
1 m²-mesh grid has been used, with 48 and 168 positions evaluated respectively. Two different positions for the neutron generator have been considered, once at room-center, once near a wall. At each position, the response of the Berthold LB6411 detector has been simulated, and the neutron spectrum and the MCNPX-weighted count-rate to dose-rate conversion coefficient for LB6411 have been evaluated.



Large bunker - variation of conversion coefficient vs. position - neutron generator (red dot) at central position (figure on the left) and near a wall (figure on the right).
In each figure on the left simulated neutron spectra vs. spatial position are reported, the letters represent the energy bins from 0.001 eV to 15 MeV. On the right, The MCNPX weighted count-rate to dose-rate conversion factor is represented. The maximum value is 2.39 micro Sv/(h·cps) near the neutron generator, always smaller than the 14 MeV conversion factor value 2.46 micro Sv/(h·cps).



Very large bunker - variation of conversion coefficient vs. position - neutron generator (red dot) at central position (figure on the left) and near a wall (figure on the right).

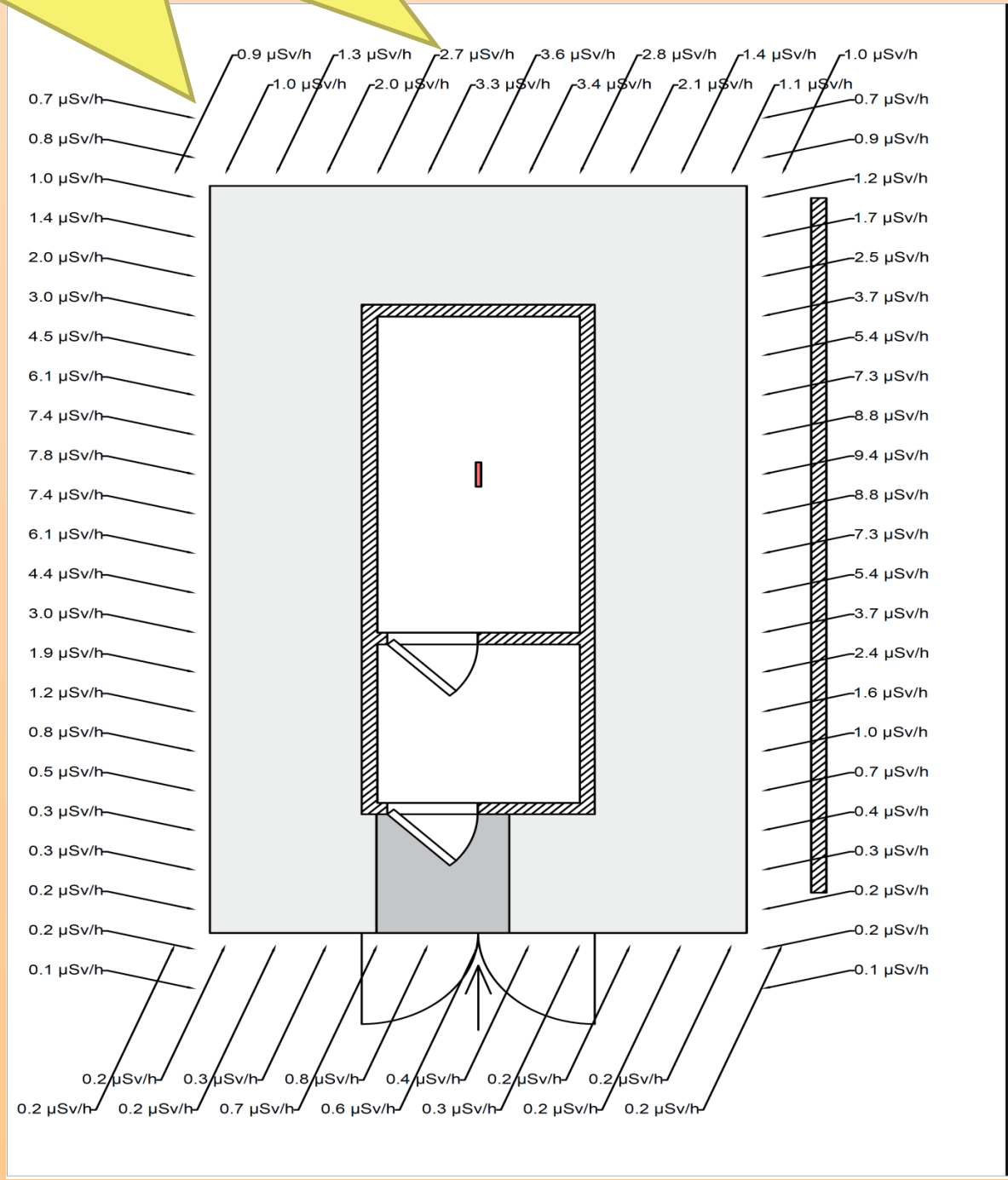
The 14 MeV 'direct-component' (energy range E: 10-15 MeV) is never less than 25% of the total; on the contrary, the 'scattered-component' (energy range A+B+C+D: 10⁻⁹-10 MeV) reaches 75% at maximum. As a conservative assumption, the ratio between the 'scattered-component' and the 'direct-component' is assumed to be 10.

Results show that the default conversion coefficient for LB6411, calibrated as default with the ²⁵²Cf spectrum, should not be used for d-t neutrons' exposure evaluation purposes because, in some cases, it would lead to important underestimations. On the contrary, for an adequate, though conservative, estimate, it is proved that the best solution is to **use the conversion coefficient that assumes a monoenergetic neutron spectrum at 14 MeV**, whatever the environment and geometry of the experimental setup are.

Case study

Exposure evaluations for bunker scenario

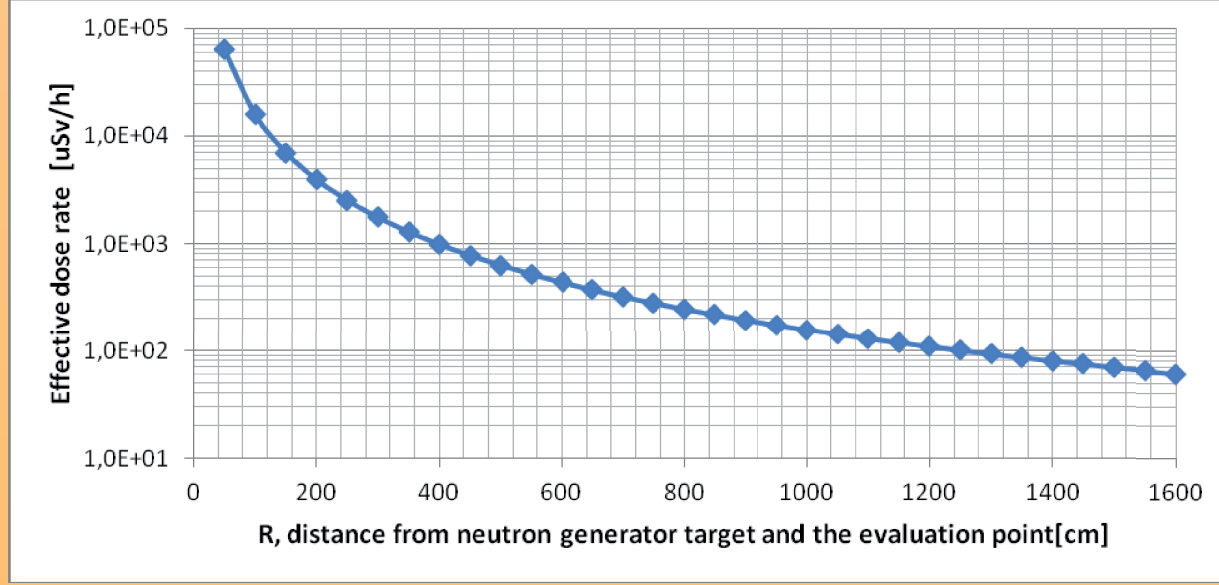
The '**NEUTRON BUNKER**' has been reproduced in the MCNPX code in order to evaluate effective dose rates outside the building. Results are reported in the figure on the right, assuming the maximum neutron generator yield of 10⁸/s. Whatever the selected constraint for the annual effective dose, licensing can be obtained with 30 cm concrete walls as shielding, and by setting appropriate prescriptions to the activities.



From neutron flux to effective dose rate

$$\dot{E} \left[\frac{\mu\text{Sv}}{\text{h}} \right] = \left(\frac{\dot{N}}{4\pi R^2} + 10 \cdot \frac{\dot{N}}{4\pi R^2} \right) \cdot 500 \cdot \frac{3600}{10^6} = 19.8 \cdot \frac{\dot{N}}{4\pi R^2}$$

\dot{E} : effective dose rate (pSv/s);
 \dot{N} : neutron emission by the generator (s⁻¹);
 R : distance from the neutron generator target to the evaluation point (cm);
 CF_{DC} : 'direct-component' conversion factor to effective dose (=500 pSv·cm²);
 SC : 'scattered-component' (=10·('direct-component') - as a conservative assumption).
 CF_{SC} : 'scattered-component' conversion factor to effective dose (=500 pSv·cm²).



Exposure evaluations for OPEN-FIELD scenario

A case study regarding the exposure to d-t neutrons in an open-field geometry is considered. At a distance of R=10 m, the effective dose received by a **worker** engaged for 200 days per year in neutron generator's operations (5 measurement per day) is 5.3 mSv/a. Regarding the **public**, an exclusion zone of radius R=1200 m is obtained with an effective dose constraint of 10 microSv/a and a zone of R=40 m with a constraint of 300 microSv/a.

CONCLUSIONS

Summarizing, in both the experimental campaigns and the four simulated test cases, the Radiation Protection Expert could determine the H*(10) by the Berthold LB6411 rem-counter assuming, as a conservative hypothesis, **the 14 MeV count-rate to dose-rate conversion coefficient**. The outcome has a general value and can be useful if this type of generator has to be used when more accurate evaluations, e.g. by Monte Carlo simulation, are not available, also enabling a more accurate design of experimental activities in different setups. The increasingly widespread use of this type of device for industrial and medical applications makes the results of this work of interest in different situations, especially as a support for the definition of appropriate radiation protection procedures and, in general, for risk analysis.



The Dose Rate Protection System at SwissFEL

Elisa Musto*, Eike Hohmann, Marco Tisi, Albert Fuchs and Sabine Mayer

Department of Radiation Safety and Security, Paul Scherrer Institute (PSI), CH-5232 Villigen PSI, Switzerland

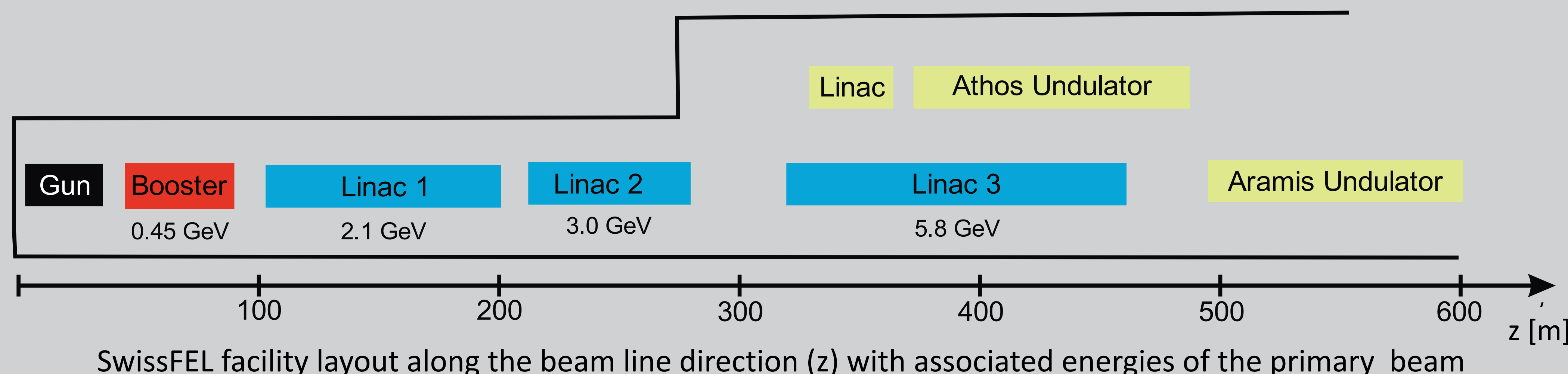
* Elisa.Musto@psi.ch

The Dose Rate Protection System (DRPS) is a safety system built to ensure that the Swiss radiation protection regulations in the surroundings of the Swiss Free Electron Laser (SwissFEL) [1] are respected. Its concept and one exemplary validation measurement are here described.

SwissFEL is the new large research facility at Paul Scherrer Institute (PSI), currently in its commissioning phase. It will produce FEL pulses covering the wavelength range 1 Å to 70 Å (0.1–7 nm).

Design parameters:

- Electron beam energy: 5.8 GeV
- Charge per bunch: 200 pC/pulse
- Repetition rate 100 Hz
- Bunch length: ps



The DRPS @ SwissFEL: motivation

Challenges:

- the SwissFEL facility is integrated in a regional recreation area, partially accessible by the general public;
- the maximum reaction time in case of a major accident scenario (full beam loss) is a few s, otherwise legal limits can be violated.

Pre-studies [2] performed with FLUKA [3] showed that:

- the main contribution to the dose outside the accelerator tunnel comes from secondary neutrons with a high energy component;
- bremsstrahlung photons are mainly peaked in the forward direction.

The DRPS concept

Use extended range neutron dose rate monitors:

- suitable for measurements in pulsed neutron fields;
- suitable to cope with intense photon background;
- placed inside the SwissFEL tunnel.



LUPIN 5401 BF₃-NP PSI
(Else Nuclear)

Shielding characterized in terms of similar configurations or Shielding classes (SC):

- may connect the tunnel to different areas outside of it;
- studied by means of Monte Carlo simulations to derive for each of them the dose attenuation (calibration factor + systematic uncertainties) used by the DRPS.

Data acquisition and evaluation system (DAQE):

- built as safety system, performance level D;
- collects the dose rate readings from the monitoring units;
- averages them over a 4 h time period with a moving window mechanism;
- derives the alarm thresholds for the system;
- if the alarm thresholds are reached, sends a signal to stop beam operation;
- reaction time: < 1s.

Shielding Class & Calibration factor example

Calibration factor (Cf) example for a **ventilation shaft type (SC3, vent_{duct})**:

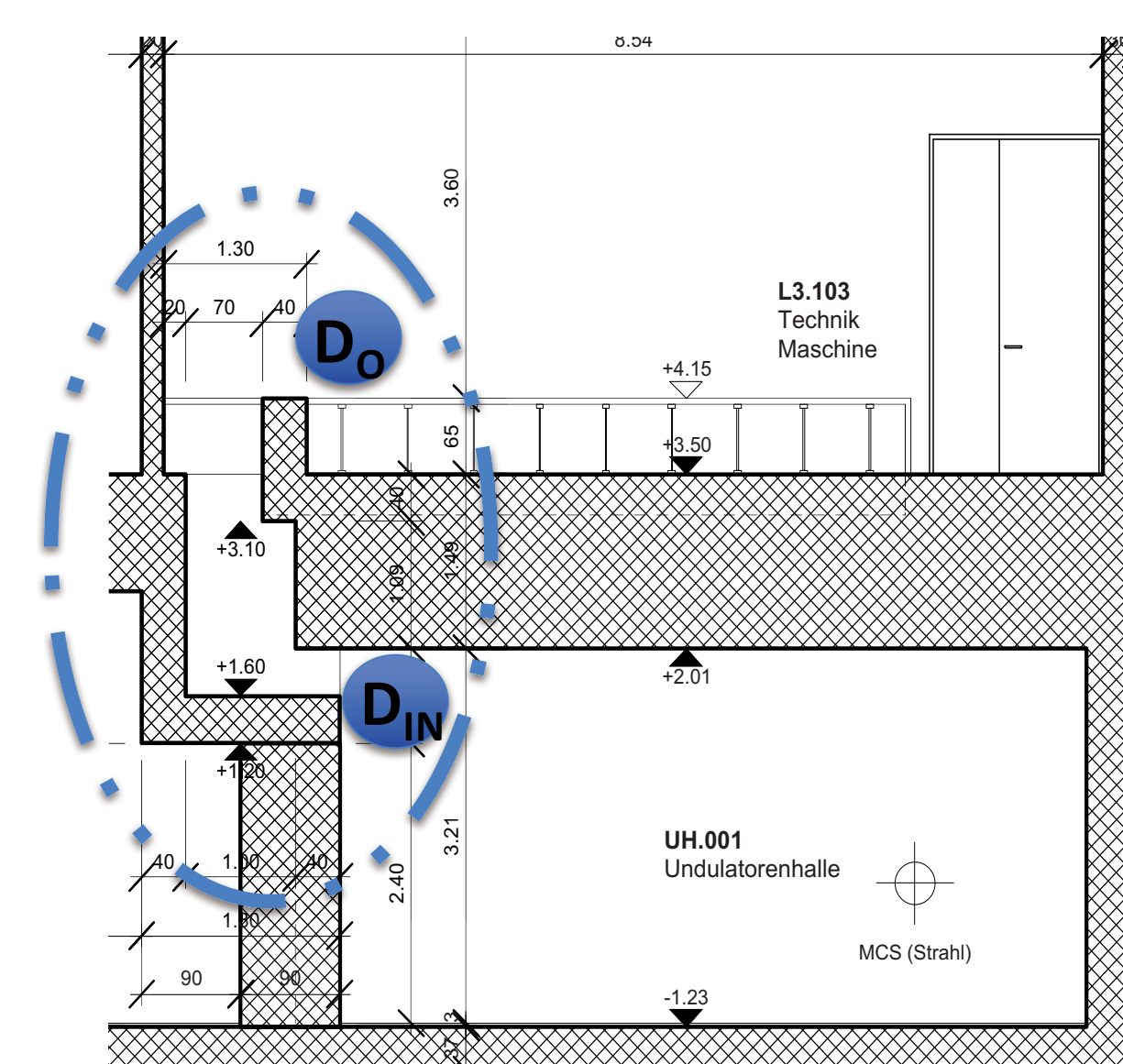
$$Cf(SC3, vent_{duct}) = \frac{D_O}{D_{IN}}$$

D_O = Neutron dose outside the SC

D_{IN} = Neutron inside the tunnel, close to the SC

From simulations:

$$Cf_{sim}(SC3, vent_{duct}) = 1.8 \text{ E-3} \pm 88\% \text{ (sys)}$$



Exemplary measurement setup for validation

Detectors placement

- Outside the tunnel: ✓ 'weakness out'.
- Inside the tunnel: ✓ 'weakness in'; ✓ at 1 m distance to the beam line (max dose).

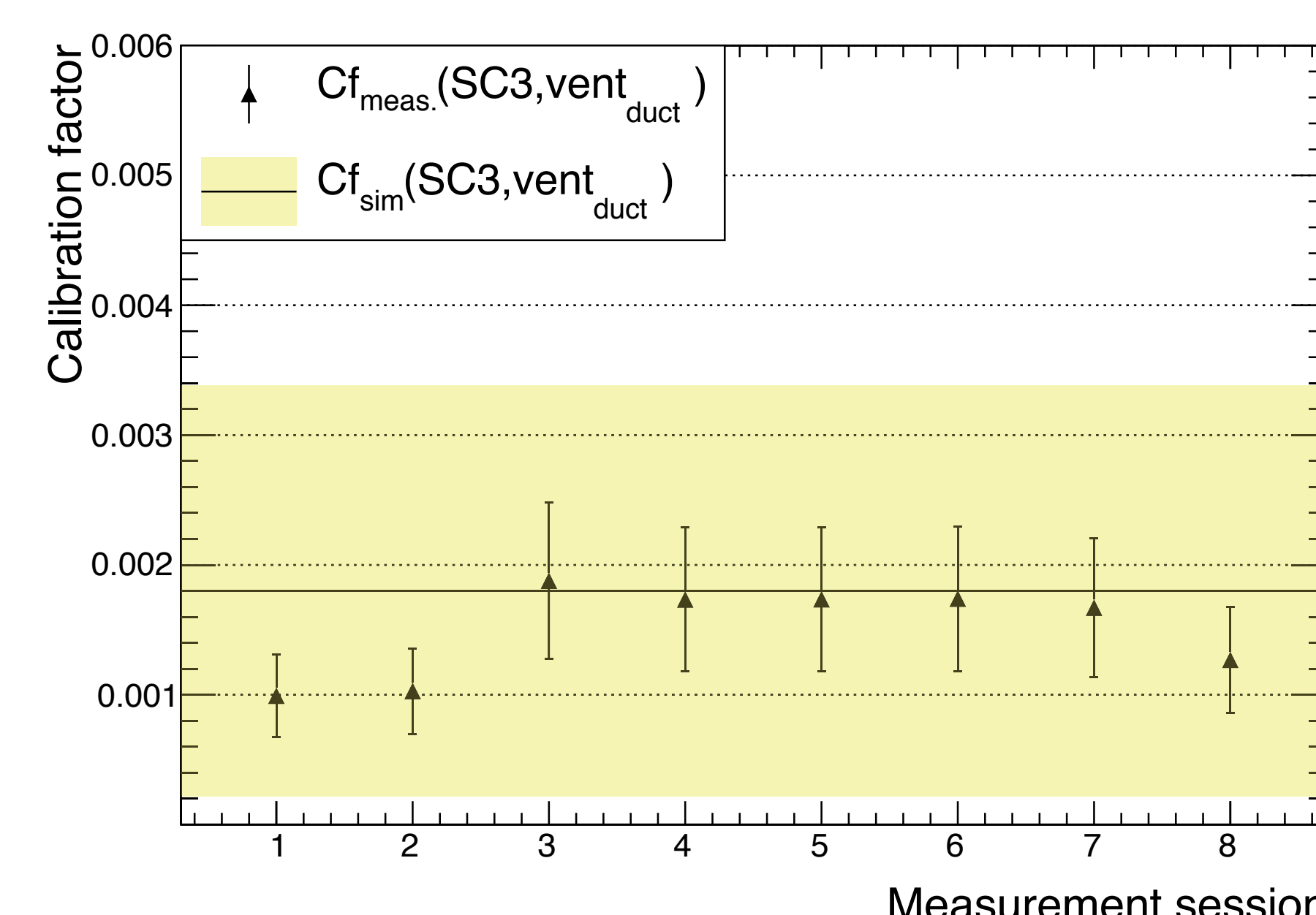


Beam parameters

- maximum charge: Q = 200 pC/pulse;
- maximum energy: E = 2.47 GeV;
- maximum frequency f = 10 Hz.

Cf (SC3, vent_{duct}) obtained from various measurement sessions (featuring different beam configurations/loss points) performed in November and December 2017, compared to the expected value from simulation.

Result



Conclusions

SwissFEL is surveyed by the DRPS. Its commissioning involved measurement campaigns, performed in November and December 2017: the example here presented shows how the measurement's outcome validates the method and calibration assumptions.

References

- [1] R. Ganter (editor), SwissFEL Conceptual design report, <http://www.psi.ch/swissfel/>, (2012).
- [2] E. Hohmann, S. Reiche, A. Fuchs, R. Ganter, F. Le Pimpec, R. Lüscher, S. Mayer, T. Schietinger, PNST V, pp (2013).
- [3] A. Ferrari, P.R. Sala, A. Fasso, and J. Ranft, CERN-2005-10 (2005), INFN/TC_05/11, SLAC-R- 773.

The EURADOS 2017 Intercomparison for Whole Body Neutron Dosimetry

S. Mayer¹, M.-A. Chevallier², E. Fantuzzi³, M. Hajek⁴, M. Luszik-Bhadra⁵, R. Tanner⁶, D. J. Thomas⁷, F. Vanhavere⁸

¹ Paul Scherrer Institute (PSI), Villigen PSI, Switzerland

² Institut de Radioprotection et de Sûreté Nucléaire (IRSN), Fontenay-aux-Roses, France

³ ENEA-Radiation Protection Institute, Bologna (BO), Italy

⁴ International Atomic Energy Agency (IAEA), Vienna, Austria

⁵ Physikalisch-Technische Bundesanstalt (PTB), Braunschweig, Germany

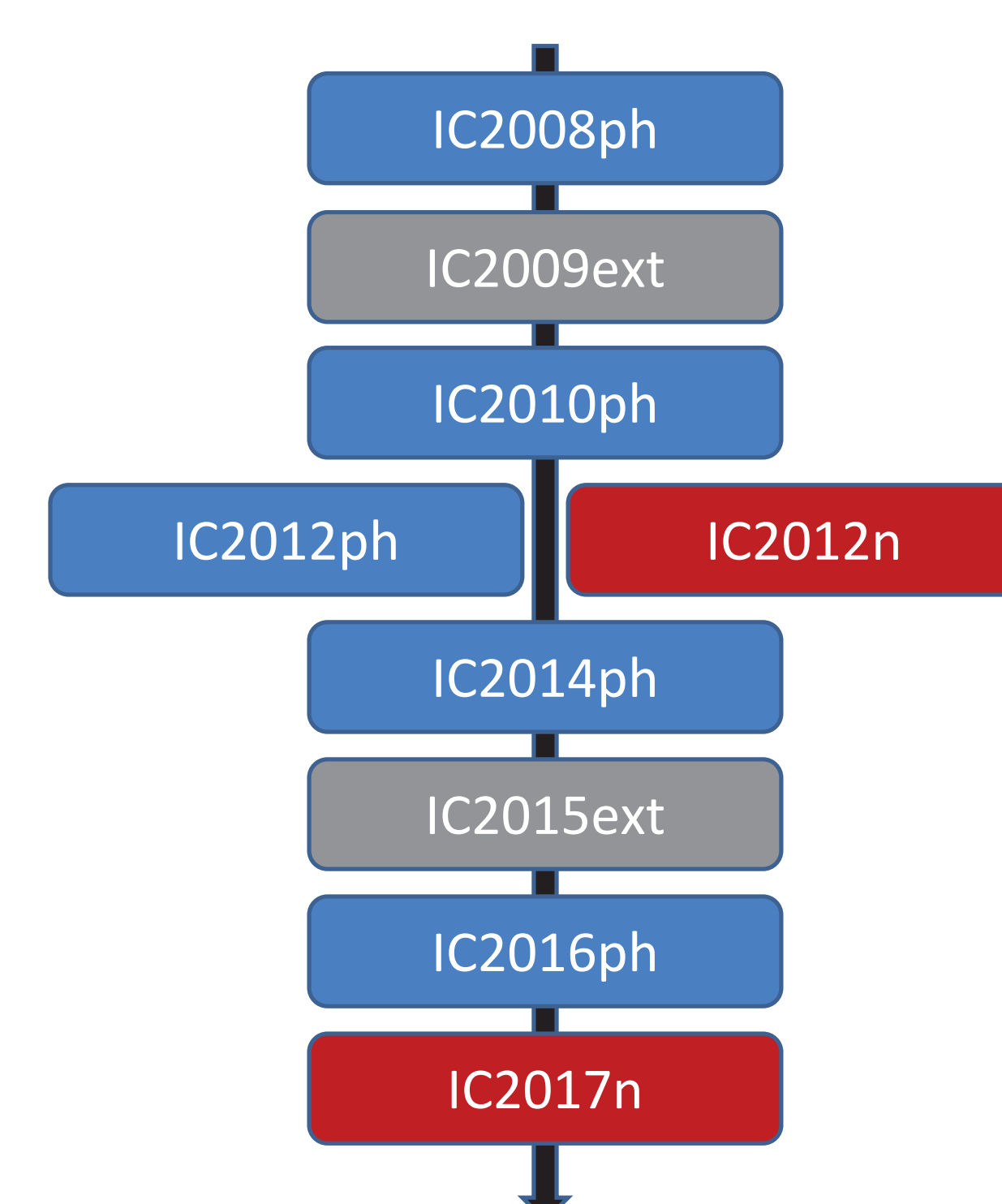
⁶ Public Health England, CRCE, Chilton, UK

⁷ National Physical Laboratory (NPL), Teddington, UK

⁸ SCK•CEN, Belgian Nuclear Research Centre, Mol, Belgium

Abstract

The European Radiation Dosimetry Group (EURADOS) has carried out a number of different intercomparison exercises in the past that qualify as proficiency tests for different dosimetry systems and radiation types. In 2017/2018, the second EURADOS intercomparison for neutron dosimeters (IC2017n) has taken place. The intercomparison concerns the performance of neutron dosimeters intended to measure neutron personal dose equivalent, $H_p(10)$, as provided by individual monitoring services. The neutron dosimeters included in the exercise were restricted to ones routinely used in individual monitoring of occupationally exposed workers. No systems under development were allowed in the intercomparison. The irradiations, which included exposures to neutrons and mixed fields of neutrons and photons as commonly encountered in workplaces, have been performed in accredited irradiation facilities in terms of $H_p(10)$. The energies of the broad neutron spectra used in the intercomparison extended from thermal to several MeV, with different dose values and angles used. Most irradiations have been performed in neutron fields with no additional photon component, over and above that resulting from the neutron-producing process, e.g., photons from a radionuclide neutron source. However, for some fields, an additional photon component had been included.



$H_p(10)$	Source	Number of dosimeters
0.3; 1.5 and 12 mSv	Bare ^{252}Cf source at 0°	4 per dose value
1.5 mSv	Bare ^{252}Cf source at 45°	2
1.2 mSv	D_2O moderated ^{252}Cf source at 0°	4
1.5 mSv	Bare ^{252}Cf source at 0° + 1 mSv ^{137}Cs	4
1 mSv	D_2O moderated ^{252}Cf source behind a shadow block	2
1.5 mSv	Bare AmBe source at 0°	4

Registration and types of dosimeters

Applications were received from 33 participants for 34 dosimetry systems from the following 18 countries:

Austria; Belgium; Brazil; Switzerland; Czech Republic; Germany; Finland; France; United Kingdom; Hungary; India; Italy; Japan; Netherlands; Poland; Romania; Turkey; United States.

The dosimetry systems can be divided into four types:

- *albedo* (14 systems)
- *track* (12 systems)
- *combination* of albedo and track (6 systems)
- *other* (2 systems).

The registration and communication with the participant was established via an on-line platform (IOP). The IOP has turned out to be a practicable tool in previous EURADOS intercomparisons and was therefore adapted for the IC2017n.

What is new compared to IC2012n

IC2017n differs from IC2012n in three main aspects:

1. IC2017n included a one-step procedure for delivering results, not a two-step one as in IC2012n. Additional simplified *a priori* information on the energy distribution was given only to those participants who stated that they need it for evaluation and agree that this information will appear on the “Certificate of Participation”.
2. Some fields of the irradiation plan included an additional photon component.
3. The registration and communication with the participant was established via an on-line platform (IOP).

Conclusion

Exercises such as IC2017n are important for informing the radiation protection community about the present state of the art in neutron dosimetry. They unearth potential difficulties and provide the dosimetry services with opportunities to demonstrate the capabilities of their dosimeters and any recent improvements they have made.



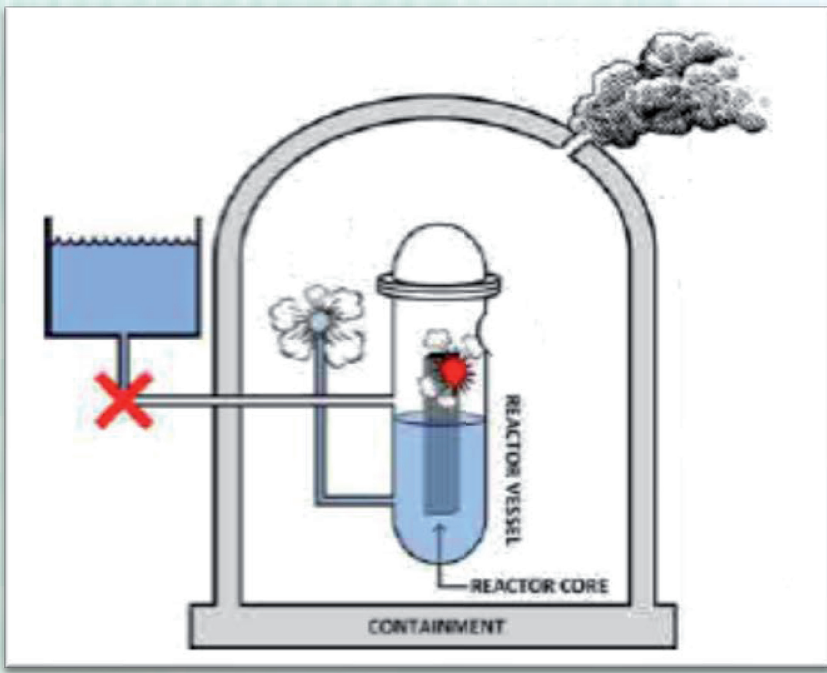
Uncertainty estimation of thyroid activity measurements and its consequences in dose assessment

Anna Pántya, Andor András, Dorottya Jakab, Tamás Pázmándi, Péter Zagvyai
Hungarian Academy of Sciences Centre for Energy Research
E-mail: pantya.anna@energia.mta.hu

Introduction

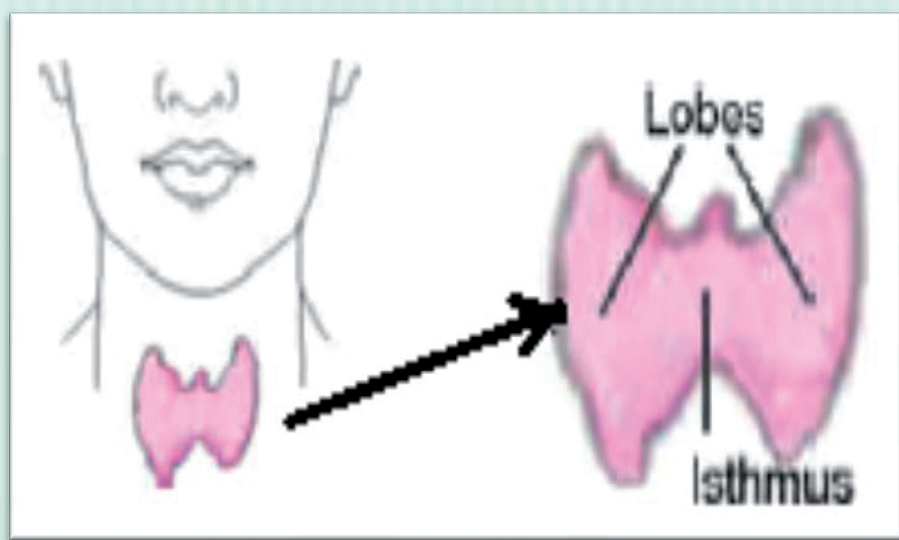
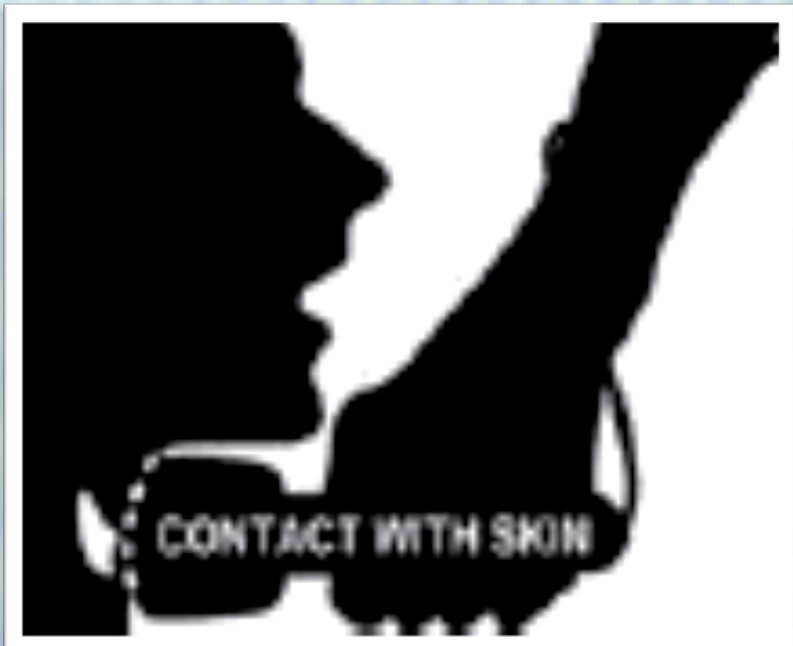
In the case of a nuclear accident, a complex combination and large quantities of radionuclides can get into the air.

It is necessary to observe the members of the population living in the vicinity of the site.

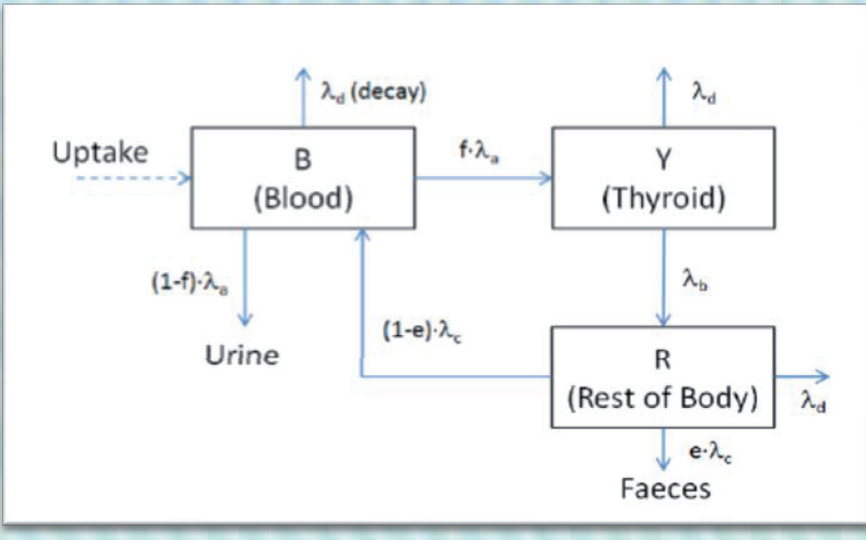


Volatile iodine isotopes may be responsible for the majority of the population's exposure from artificially occurring sources of radiation.

Possible intake of radioiodine in an accident situation: inhalation and ingestion via food chain.



Accumulation of radioiodine in thyroid depends on the availability of stable iodine and the metabolism of ^{131}I in the human body. Intake of stable iodine can be achieved with daily nutrition (e.g. with iodized salt, water, sea food) and also with taking iodine thyroid blocking (ITB) agent before or within few hours after inhalation of radioiodine.



Measurement method and equipment

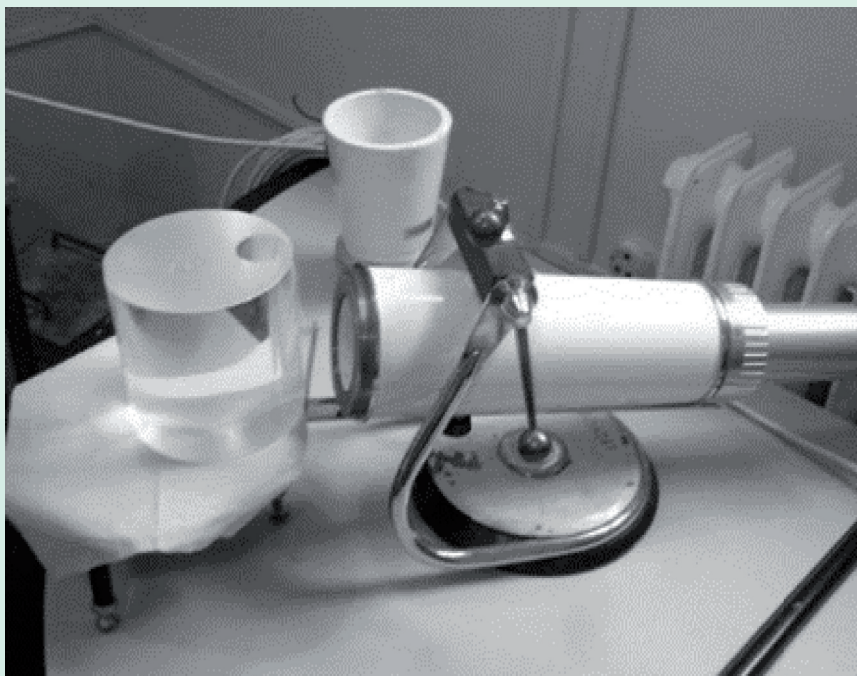
Thyroid activity was measured by lead shielded NaI(Tl) scintillation detector, standing on a vertically adjustable stand for lead shielding, which allows the optimal installation of the equipment.



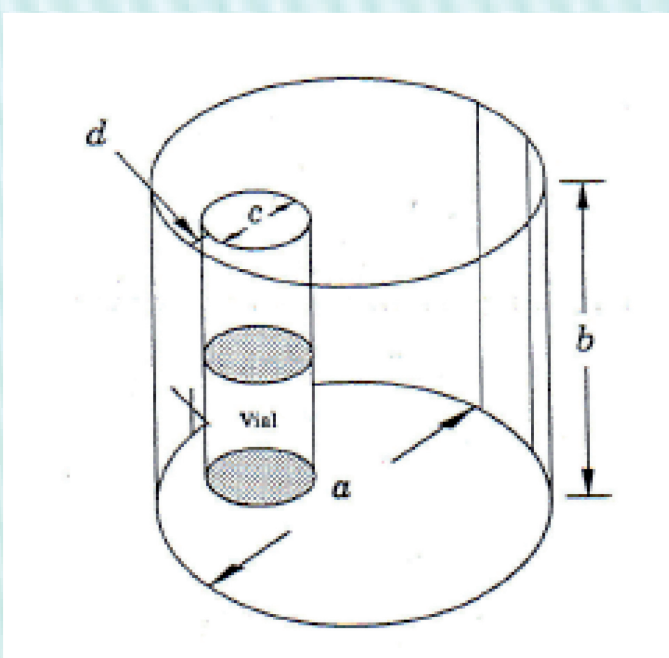
The person to be measured is in the chair and the detector's collimator is directed at the neck towards the position of the thyroid. Measurements were carried out in 3 different measuring position.

Measurment geometry No.	Distance [cm]	Collimator
I.	12.5	Yes
II.	4	Yes
III.	4.5	No

Calibration with different phantoms



For the efficiency calibration ANSI thyroid phantom available at the laboratory was used. This phantom is made of plexi-glass cylinder with a diameter of 150 mm and a height of 146 mm. It has one cavity (20 ml) modeling the thyroid of an adult with 3 calibration sources with different ^{131}I activities.



Vial No.	Activity [Bq]
1	10.3
2	29.4
3	48.5

Vial Name	Height [mm]	Diameter [mm]	Capacity [ml]	Activity [Bq]
5 years	3.2	1.35	3.2	9.09
10 years	5	1.4	7.5	8.02
Adult	5.8	2	19	7.64

A cylinder phantom with a diameter of 130 mm and a height of 120 mm was also used in this project. There were three pair of holes with different sizes in the phantom to imitate the size of the thyroid of 5 and 10 years old children and adults. The activities to be measured were filled in two vials and each vial contained ^{131}I in liquid form.

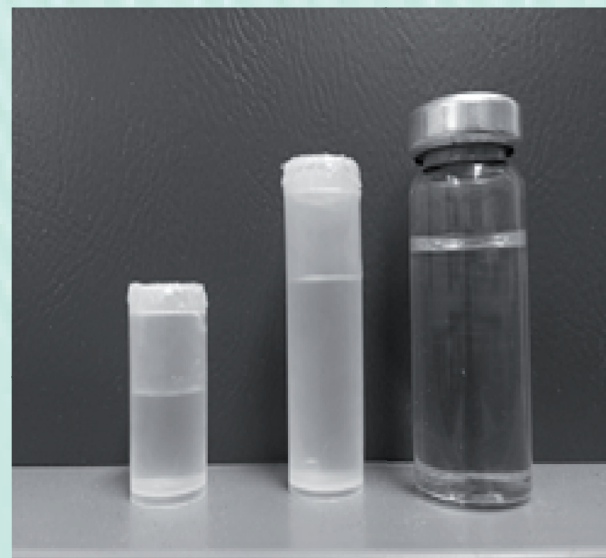


Different phantoms efficiency			
Vial No.	ANSI	Cylinder	Vial Name
1.	2.38	1.98	Adult
2.	2.51		
3.	2.22		

There is about 20% difference between the two different phantom efficiency values.

In the case of the phantom which formation takes into account different thyroid sizes depending on the ages, the efficiencies also show a 20% difference.

Vial Name	Normalized efficiency (to adult)
Adult	1
10 years	1.16
5 years	1.20



Dose estimation

The results of the uncertainty assessments were used in dose estimation calculations with MONDAL 3 code. The results demonstrated that the determination of the uncertainties of dose estimation is a complex process.

The influence of the uncertainties of assumptions such as the date and route of intake as well as the physical and chemical form were also investigated in terms of the accuracy of the final internal dose assessment.

In this study the measured activity was the fixed parameter ($A_m=1000$ Bq), with the variation of the other variables (intake route, elapse time between the intake and measurement, age) it was found that the uncertainty of the dose estimation could reach about 50% level.

Intake route	Absorption type	Time between intake and measurement [days]	Age	Activity of intake [kBq]	Effective dose [μSv]
Inhalation	Type F	1	5 y	11	420
			10 y	11	210
			Adult	12	86
		7	5 y	21	770
			10 y	19	350
			Adult	19	140
Ingestion	f ₁ =1.0	1	5 y	4	400
			10 y	4	210
			Adult	4	87
		7	5 y	7.30	730
			10 y	6.6	340
			Adult	6.5	140

Conclusion

It was stated that the adequate thyroid measurement results are influenced by various parameters e.g. the shape of thyroid, position of the thyroid inside the human body, the distance between the detector and the body surface, and the distribution of the radioactivity within the organ.

References:

- International Atomic Energy Agency: General Safety Requirements Part 7 (2014)
- N. Ishigure, M. Matsumoto, T. Nakano, H. Enomoto „Development of Software for Supporting Internal Dose Estimation” <http://irpaui.irpa.net/pdfs/3a16.pdf> Proc. Symp. IRPA-11, Madrid, 2004. - <http://www.nirs.go.jp/db/anzendb/RPD/mondal3.php>



CENTRE FOR ENERGY RESEARCH
HUNGARIAN ACADEMY OF SCIENCES

5th European IRPA Congress
4 - 8 June 2018
The Hague, The Netherlands

Encouraging Sustainability
in Radiation Protection



5th European IRPA Congress
4 - 8 June 2018
The Hague, The Netherlands

Encouraging Sustainability
in Radiation Protection

